

SIMULATION STUDY OF VOLATILE OIL RESERVOIRS – UNDERSTANDING  
THE RESERVOIR DRIVE MECHANISMS IN CONVENTIONAL AND  
LIQUIDS-RICH UNCONVENTIONAL RESERVOIRS AND ITS EFFECT ON  
LONG TERM DELIVERABILITY

A Dissertation

by

SANDEEP PYARELAL KAUL

Submitted to the Office of Graduate and Professional Studies of  
Texas A&M University  
in partial fulfillment of the requirements for the degree of

DOCTOR OF PHILOSOPHY

Chair of Committee,	Eduardo Gildin
Committee Members,	Akhil Datta-Gupta
	Peter P Valkó
	Prabir Daripa
Head of Department,	A. Daniel Hill

August 2014

Major Subject: Petroleum Engineering

Copyright 2014 Sandeep Pyarelal Kaul

## ABSTRACT

Reservoir simulation studies are the most detailed analysis that can be performed in order to evaluate future performance and remaining reserves of a reservoir, given the in-place volumes. This holds true both for conventional and unconventional reservoirs. The two numbers, in-place volumes and long term deliverability of the reservoir, need to be ascertained with fair amount of accuracy. This is central idea of this dissertation. The overall objectives of the dissertation are outlined in the form of two simulation case studies – one conventional and the other unconventional.

For the conventional reservoir, history matching and subsequent forecasting work becomes a challenging task if limited supporting production data is available and the reservoir is severely depleted. For an offshore, volatile-oil reservoir, added to this challenge was an uncertainty in fluid PVT, where the data clearly suggested presence of condensate, but with black oil properties. The permeability distribution from logs was counterintuitive to the production data from the wells. The reservoir had a structural relief in excess of 1000 ft., most likely having API gradient, but both the API and the GOR data indicated that there were possible errors in measurement. There was uncertainty associated with original oil-water contact also. The production data showed the reservoir to follow primarily a classical solution gas-drive response, but simple material balance analysis proved a weak aquifer effect as well.

The approach followed in simulation was the process of elimination. Pressure match was first achieved, but questions remained about its robustness around the main

sealing fault. GOR was targeted next and several different condensates and one full compositional fluid model of a nearby reservoir were unsuccessfully tested. For matching the historical gas production, a new high condensate yield fluid PVT was used. The idea of another oil-water contact (OWC) was tested in the saddle of the reservoir to account for most likely early water breakthrough in a well there. The secondary gas cap formation and its effects were crucial in achieving satisfactory history match.

The confidence in the history match, as having captured the physics of the flow, led to forecasting scenarios which were not possible with a black oil model. Most of the data was found not to be erroneous. What was needed was judicious data interpretation to achieve satisfactory history match. To produce these kinds of depleted, faulted reservoirs further, a strategy to better manage the evolution of secondary gas cap was of utmost importance.

For the unconventional reservoirs the challenges are equally daunting. The unconventional liquids-rich “shale” reservoirs are made up of shales, siltstones or carbonates. Depending on fracture connectivity, these reservoirs may or may not produce water from aquifers above/below them. Simulation modeling work to estimate reserves for such reservoirs is often restricted to, a well based stimulated rock volume (SRV). Aquifer effects, at the boundary, are often not taken into consideration as water production is insignificant or in some cases non-existent. The in-place volume may not pose as big a challenge for SRV, but the long term deliverability of the wells is affected by the different boundary conditions, which constitutes the natural drive of these reservoirs. Material balance analysis, used for analyzing production data, cannot be

applied here as it is difficult to measure the average reservoir pressure at the well as no tank-like behavior is seen. Decline curve analysis (DCA) and Rate transient analysis (RTA) have limited success for these liquids-rich plays. The former is limited by high shrinkage of volatile oils, which liberate a lot of gas below the bubble point, that might aid or impede long-term well performance. The latter analysis is known to give non-unique solutions under transient conditions.

In order to overcome these limitations a new method is proposed which is based on linear flow regime of these reservoirs. Unlike previous studies where either the matrix alone or the aquifer alone are taken into consideration as source term in the fracture equation, here we take both the matrix and the aquifer as two separate source terms in the fracture equation with two separate interporosity flow parameters, each with slab configuration. The overall performance of the well is dependent on the term,  $\left(\frac{\lambda}{\omega}\right)$ , called as Dual Porosity Proppant Number. For the reservoir, this is defined as volume weighted, dimensionless surface flux transferred from a unit area of matrix to the fracture, per unit matrix volume. As a big picture, this number determines the amount of successful stimulation achieved within the dual porosity reservoir. Based on flow analysis from two different areas, it is possible to reduce the uncertainty associated with RTA alone. One area estimates the aquifer drive and the other estimates the derivative of dimensionless productivity index against time. This derivative of dimensionless productivity index serves dual purpose. It acts as a pressure variable which gives information about the rate of transient-area generation in the reservoir due to drawdown at the well. Hence conventional RTA can be applied. The other purpose is to help

evaluate the long-term well performance since it is part of productivity index. Below the bubble point, the solution gas drive is handled with the help of equivalent Muskat's method for Volatile oil.

Having established the theoretical basis, we then illustrate the effects of various reservoir drives on future performance of such unconventional reservoir. A synthetic field-wide simulation case shows the application and results, which brings out its significance, with and without the use of this method.

The last chapter covers the performance prediction of a horizontal well with transverse fractures without the assumption of linear flow. No detailed analysis of the work is presented.

DEDICATION

June 7, 2004

## ACKNOWLEDGEMENTS

I would like to thank my committee chair, Dr. Eduardo Gildin, and my committee members, Dr. Akhil Datta-Gupta, Dr. Peter Valkó, and Dr. Prabir Daripa, for their guidance and support throughout the course of this research.

Thanks also go to my friends and colleagues, Deepak Chakravarthy, Anu Umachander, Manoj Sarfare, Tarun Grover and the department faculty and staff for making my time at Texas A&M University and at Houston a great experience. I want to extend my thanks to Chevron Corporation for the opportunities I had while working and to all my friends and colleagues there, especially Dr. Anil Ambastha and Dr. Adwait Chawathé whose constant encouragement and efforts have led to successful completion of this very long venture.

Finally, thanks to Aaron, Aritra, Sunita and Dr.Pulin Koul, my sister's family, for their encouragement, patience and love.

## TABLE OF CONTENTS

	Page
ABSTRACT .....	ii
DEDICATION .....	vi
ACKNOWLEDGEMENTS .....	vii
TABLE OF CONTENTS .....	viii
LIST OF FIGURES .....	xii
LIST OF TABLES .....	xvi
<b>CHAPTER I INTRODUCTION AND OVERVIEW .....</b>	<b>1</b>
Introduction .....	1
Conventional versus Unconventional Reservoir .....	3
Role of Hydraulic Fracturing in Unconventional Reservoirs – Problem Description ...	7
Volatile Oil PVT – Its Uniqueness in Comparison to Black – Oil, Retrograde Condensate and Wet Gas PVT .....	13
Objectives of Thesis .....	18
Organization of this Thesis .....	18
<b>CHAPTER II INSIGHTS FROM HISTORY MATCHING AND FORECASTING WORK FOR A STEEPLY-DIPPING, FAULTED VOLATILE OIL CONVENTIONAL RESERVOIR, OFFSHORE NIGERIA .....</b>	<b>21</b>
Introduction .....	21
Reservoir Model Description .....	25
Earth Model .....	25
Dynamic Model .....	28
Challenges Associated with Earth Modeling .....	31
Challenges Associated with Data Measurement Errors .....	33
Identification of Reservoir Drive Mechanisms .....	36
Challenges Associated with PVT Fluid Modeling during History Matching .....	37
Black Oil with Single Bubble Point (No Variation with Depth) .....	39
Condensate (Analog Data) Option and Full Compositional Model .....	40
Final Condensate Model .....	42
Identification of Third Reservoir Drive .....	45
End of History Saturation and Best Case Prediction Scenario .....	46



Conclusions and Recommendations.....	47
<b>CHAPTER III SIMULATION STUDY OF LIQUIDS-RICH, VOLATILE OIL UNCONVENTIONAL RESERVOIR – FOCUS ON RESERVOIR DRIVE MECHANISMS .....</b>	<b>49</b>
Introduction and Stimulated Rock Volume Description .....	49
Matrix Fracture Fluid Exchange .....	51
Matrix Material Balance.....	53
Aquifer Fracture Fluid Exchange .....	57
Concept of Proppant Number – Single Porosity versus Dual Porosity.....	64
Single Porosity Reservoir .....	64
Dual Porosity Reservoir .....	68
Reservoir Drive Mechanisms in Unconventional Reservoir and its Impact .....	71
Full Pseudosteady State Fractured Dual Permeability Dual Mobility Model .....	76
Dimensionless Productivity Index .....	78
Constant Rate Case.....	82
Constant Pressure Case .....	83
Convergence Skin for Horizontal Well.....	85
Summary of Solutions .....	87
Treatment for Solution Gas Drive – Material Balance Method for Volatile Oil Reservoir with Variable Fluid Compressibility .....	89
<b>CHAPTER IV SIMULATION OF UNCONVENTIONAL RESERVOIRS USING MESHLESS METHOD: ACCURATE PERFORMANCE PREDICTION OF DUAL POROSITY RESERVOIRS WITH TRANSVERSE FRACTURES .....</b>	<b>97</b>
Introduction and Objectives of Mathematical Modeling .....	97
The Constant Pressure, Finite Wellbore, Solution of Single Well Centered in Square Drainage Area – Superposition Method Using Transient Constant Rate Radial Solution (Helmy Model).....	98
The Constant Pressure Solution of Single Infinite Conductivity Fracture, Centered in Square Drainage Area – Superposition Method Using Transient Constant Rate Radial Solution .....	101
Fully Penetrating, Single Finite Conductivity Fracture Solution for Vertical Well Using Boundary Element Method – Numerical Generation of Influence Functions ..	104
Constant Rate Case.....	106
Constant Pressure Case .....	110
Partially Penetrating, Single Finite Conductivity Fracture Solution for Vertical Well Using, Partially Penetrating, Finite Wellbore Radial Solution and Boundary Element Method .....	114
Evaluation of Convergence Pressure Drop of Single Transverse Fracture in a Horizontal Well Using Boundary Element Method.....	118
Input Boundary Conditions – Knowns and Unknowns.....	122

Partially Penetrating, Multiple Transverse Finite Conductivity Fracture Solution Using, Partially Penetrating, Finite Wellbore Radial Dual Porosity Solution and Boundary Element Method .....	125
<b>CHAPTER V ANALYSIS, RESULTS AND CONCLUSIONS OF FULL TRANSIENT MATRIX AND AQUIFER UNCONVENTIONAL RESERVOIR MODEL.....</b>	<b>127</b>
Basis for Long Term Deliverability of a Well – The Derivative Analysis .....	127
Proppant Number and Concept of Constant Volume Induced Fracture.....	130
Validation of the Full Transient Model.....	137
Derivative Analysis Using Single Phase Flow Model .....	140
Derivative Analysis Using Two Phase Flow (Aquifer) Model.....	149
Application to Sample Synthetic Field Model .....	153
Analysis of the Results .....	156
Conclusions .....	164
<b>NOMENCLATURE.....</b>	<b>166</b>
<b>REFERENCES .....</b>	<b>177</b>
<b>APPENDIX A: PSEUDOSTEADY STATE DUAL POROSITY MODEL – FORMULATION AND LAPLACE DOMAIN SOLUTION (WARREN &amp; ROOT MODEL) .....</b>	<b>182</b>
<b>APPENDIX B: TRANSIENT DUAL POROSITY MODEL – FORMULATION AND LAPLACE DOMAIN SOLUTION (BELLO MODEL).....</b>	<b>190</b>
<b>APPENDIX C: PSEUDOSTEADY STATE AQUIFER DUAL POROSITY MODEL – FORMULATION AND LAPLACE DOMAIN SOLUTION (LINEAR EQUIVALENT EHLIG-ECONOMIDES AND AYOUB MODEL) .....</b>	<b>199</b>
<b>APPENDIX D: TRANSIENT AQUIFER DUAL POROSITY MODEL – FORMULATION AND LAPLACE DOMAIN SOLUTION (LINEAR EQUIVALENT BOURDET MODEL).....</b>	<b>207</b>
<b>APPENDIX E: FULL PSEUDOSTEADY STATE MATRIX AND AQUIFER FRACTURED DUAL PERMEABILITY DUAL MOBILITY MODEL – FORMULATION AND LAPLACE DOMAIN SOLUTION.....</b>	<b>218</b>
<b>APPENDIX F: TRANSIENT MATRIX FRACTURED DUAL PERMEABILITY DUAL MOBILITY MODEL – FORMULATION AND LAPLACE DOMAIN SOLUTION .....</b>	<b>235</b>

APPENDIX G: TRANSIENT AQUIFER FRACTURED DUAL PERMEABILITY DUAL MOBILITY MODEL – FORMULATION AND LAPLACE DOMAIN SOLUTION .....	254
APPENDIX H: FULL TRANSIENT MATRIX AND AQUIFER FRACTURED DUAL PERMEABILITY DUAL MOBILITY MODEL – FORMULATION AND LAPLACE DOMAIN SOLUTION .....	273

## LIST OF FIGURES

	Page
Figure 1. Water Production Range for Typical Unconventional Well <sup>3</sup> . .....	8
Figure 2. Shale Gas Production Well <sup>3</sup> .....	9
Figure 3. Historical Oil, Water and Gas Production of Bakken Field <sup>5</sup> . .....	10
Figure 4. Historical Oil, Water and Gas Production of Bakken Well <sup>5</sup> .....	10
Figure 5. Historical Gas and Water Production of Eagleford Well <sup>2</sup> . .....	11
Figure 6. Spatial Extent of West Texas Permian Shales <sup>7</sup> .....	12
Figure 7. Phase Envelopes of Hydrocarbon Mixtures <sup>10</sup> .....	13
Figure 8. Typical Phase Envelopes of Volatile Oils Showing Depletion Path. ....	14
Figure 9. Typical Hydrocarbon Fluid Densities in Eagle Ford <sup>12</sup> . .....	17
Figure 10. Stratigraphic Section of Reservoir M. ....	27
Figure 11. Gross Thickness Map.....	27
Figure 12. Upscaled Simulation Model Showing OWCs. ....	29
Figure 13. Upscaled Simulation Model Showing Equilibrium Regions & Possible Communication between Fault Blocks. ....	31
Figure 14. Upscaled Simulation Model Showing OWCs. ....	33
Figure 15. Reservoir GOR Data. ....	34
Figure 16. Reservoir API Data. ....	35
Figure 17. MBAL Model Output to Identify Drive Mechanisms. ....	37
Figure 18. Single Bubble Point Simulation Results for Well#1. ....	39
Figure 19. Single Bubble Point Static Pressure Match for Well#1 and Well#4. ....	40
Figure 20. Condensate Option and Full Compositional Static Pressure Match for Well#1.....	41

Figure 21. Condensate Option Simulation Results for Well#1.....	41
Figure 22. Typical Phase Envelopes. ....	43
Figure 23. Extrapolated Phase Envelope.....	44
Figure 24. History Match Results using Modified PVT Data for Well#1. ....	44
Figure 25. Gravity Segregation Effect in Reservoir M. ....	45
Figure 26. End of History Saturations.....	47
Figure 27. Unconventional Reservoir Having Natural and Transverse Fractures. ....	49
Figure 28. Dual Porosity Mathematical Idealization of Above. ....	49
Figure 29. Single and Various Dual Porosity Reservoir Comparison.....	51
Figure 30. Pseudosteady State Matrix Showing Idealization of the Pressure.....	54
Figure 31. Matrix Pressure Transient as it Travels from $t = 0$ to $t = t$ .....	56
Figure 32. Linear Flow Model for Reservoir and Aquifer. ....	58
Figure 33. The Lumped Parameter Permeable Barrier between Aquifer and Reservoir.....	59
Figure 34. Mathematical Idealization of SRV with Aquifer Support <b>Acw</b> (green) and <b>A</b> (red). ....	74
Figure 35. The Infinite Distribution of Image Wells Required to Simulate the No- flow Condition across the Boundary of a Square Reservoir with Well is Located in the Center.....	99
Figure 36. The Infinite Distribution of Image Wells Required to Simulate the No- flow Condition across the Boundary of a Square Reservoir and a Fracture...	102
Figure 37. Source and Observation Wells for the Generation of Influence Functions. .	105
Figure 38. Mathematical Treatment of Central Well. ....	117
Figure 39. Source Wells and Observation Wells in the Generation.....	123
Figure 40. The Infinite Distribution of Image Wells Required to Simulate the No- flow Condition across the Boundary of a Square Reservoir and Multiple Fracture. ....	125

Figure 41. Matrix Orthogonal Geometries (with different size of matrix blocks but same fracture permeability). .....	133
Figure 42. Matrix Orthogonal Geometries (with same size of matrix blocks but different fracture permeability).....	134
Figure 43. Results of Dimensionless Rate with Single Phase Transient Model for $yeD = 0.559$ and for Different Matrix Geometries as per Bello <sup>9</sup> .....	134
Figure 44. Results of Dimensionless Productivity Index with Single Phase Transient Model for $yeD = 0.559$ and for Case 1. ....	135
Figure 45. Results of Dimensionless Productivity Index with Single Phase Transient Model for $yeD = 0.559$ and for Case 2. ....	135
Figure 46. Validation of Full Transient Model with Bello’s Transient Model (Constant Rate Case). ....	138
Figure 47. Validation of Full Transient Model (dotted) with Bello’s Transient Model (Constant Pressure Case). ....	139
Figure 48. Results with Single Phase Transient Model for $yeD = 1$ as per Bello <sup>9</sup> . ....	141
Figure 49. Results with Single Phase Model for $yeD = 100$ as per Bello <sup>9</sup> .....	141
Figure 50. Reproduction of Rate (solid line) and the Derivative (dotted line) with Single Phase Transient Model for $yeD = 1$ Calculated from Laplace Inversion. ....	144
Figure 51. Reproduction of Constant Rate Derivative from Laplace Solution (solid line) and Constant Pressure Derivative (dotted line) using Material Balance Time with Single Phase Transient Model for $yeD = 1$ . ....	144
Figure 52. Single Phase Derivative Analysis for $yeD = 1$ and $A = Acw$ .....	146
Figure 53. Single Phase Derivative Analysis for $yeD = 1$ and $A = Acw$ .....	146
Figure 54. Single Phase Transient Model $JD$ Results for $yeD = 1$ and $A = Acw$ (Both for Constant Rate and Constant Bottomhole Pressure Case are Shown). ....	148
Figure 55. Single Phase Transient Model $JD\lambda$ Results for $yeD = 1$ and $A = Acw$ (Both for Constant Rate and Constant Bottomhole Pressure Case are Shown). ....	148

Figure 56. Two Phase Derivative Analysis for $yeD = 1$ and $A = Acw$ with $\lambda aq$ . .....	150
Figure 57. Two Phase Derivative Analysis for $yeD = 1$ and $A = Acw$ without $\lambda aq$ . .....	150
Figure 58. Two Phase Transient Model $JD$ Results for $yeD = 1$ and $A = Acw$ (Both for Constant Rate and Constant Bottomhole Pressure Case are Shown). .....	152
Figure 59. Two Phase Transient Model $JD\lambda$ Results for $yeD = 1$ and $A = Acw$ (Both for Constant Rate and Constant Bottomhole Pressure Case are Shown). .....	152
Figure 60. Derivative Analysis for $\kappa f = 0.1, 0.16, 0.25, 0.4$ and $0.63$ , and $yeD = 1$ and $A = Acw$ . .....	153
Figure 61. INTERSECT Output of Major Parameters Used in Simulation Model.....	154
Figure 62. PETREL Input of Major Parameters Used in Simulation Model. ....	154
Figure 63. Unconventional Synthetic Simulation Model in PETREL Showing LGR...155	
Figure 64. Derivative Response in an Infinite Acting Reservoir Showing Radial and Pseudosteady State Flow in the Same Well by Changing Fracture Permeabilities Ten Times. ....	157
Figure 65. Derivative Response in an Infinite Acting Reservoir Showing Bilinear Converts to Linear Flow in the Same Well by Changing Fracture Permeabilities Ten Times. ....	158
Figure 66. Derivative Response in an Infinite Acting Reservoir Showing No Effect on Linear Flow in the Same Well by Changing Fracture Permeabilities Ten Times. ....	159
Figure 67. Derivative Response of a Well With No Flow Boundary Showing Predominantly Linear Flow. ....	160
Figure 68. Productivity Index of above Well from INTERSECT.....	161
Figure 69. Derivative Response of a Well with No Flow Boundary Showing Predominantly Linear Flow and Boundary Effects. ....	162
Figure 70. Derivative Response of a Well With No Flow Boundary Showing Fracture Linear Flow Followed by Matrix Linear Flow.....	163

## LIST OF TABLES

	Page
Table 1. Decline Rates of the Big Three U.S. Shale Oil Plays <sup>1</sup> .....	8
Table 2. Produced Water of Select U.S. Shale Gas Plays <sup>8</sup> .....	12
Table 3. Typical Compositional Mole Percentage of Fluids <sup>10</sup> .....	15
Table 4. Typical Fluid Gravity of Major US Unconventional Plays <sup>2,5,7</sup> .....	17
Table 5. Summary of Original Contacts.....	26
Table 6. Summary of PVT Data.....	38
Table 7. Various Possible Aquifer Drive Mechanisms for Fractured Horizontal Well.....	73
Table 8. Fracture Functions for Solution with Aquifer Support in Linear Dual Porosity.....	87
Table 9. Fracture Functions of Radial/Linear (Aquifer) Dual Porosity Solution.....	88
Table 10. Shape Factors based on Warren & Root Theory <sup>34</sup> .....	132
Table 11. Shape Factors Calculation Dataset as per Bello <sup>9</sup> . .....	136
Table 12. Full Transient Model.....	138



CHAPTER I  
INTRODUCTION AND OVERVIEW

**Introduction**

Conventional and unconventional reservoirs are similar as far as the physics of the fluid flow is concerned. What is vastly different between the two is the economic approach to exploit those reservoirs. This is one of the major reasons which sets them apart.

The general definition of an unconventional reservoir has to be stated first, for the purpose of discussion. This is where we have to rely on the economic approach rather than physics of the fluid flow approach. Unconventional reservoirs are those reservoirs which are very low porosity and permeability and cannot produce economically with the help of natural energy and/or using conventional means of production. These three requirements; porosity, permeability and production with the help of some means other than the natural drive should be present before unconventional reservoir can be exploited economically. From the economic standpoint, they could either produce gas or oil, but the presence of hydraulic fracturing is absolutely important. On the other hand, a conventional reservoir will produce without hydraulic fracturing, on natural drive, but the role of hydraulic fracture in that reservoir is to better the economics further. The point being made here is that hydraulic fracture will be used for unconventional reservoir as an absolute must whereas it may or may not be used for conventional reservoir.

The distinction between unconventional and conventional reservoirs gets fuzzy if only the presence of hydraulic fracturing is used in the definition. From engineering standpoint, we differentiate unconventional reservoirs further on the basis of porosity or permeability. Both these parameters define the physics of fluid flow in any reservoir but strict demarcation is not possible with this criterion alone. From geologic standpoint, low permeability and porosity formations have been defined as shales, siltstones, mudstones, etc. It is not important to go into the geological details, but the fuzziness in differentiating these reservoirs gets mitigated to a large extent if we use these engineering and geological terms in conjunction together with economic criteria. The central focus of this thesis is oil production from both conventional and unconventional reservoirs. Any discussion with respect to gas only reservoirs has not been taken up.

Thus liquids-rich unconventional reservoirs are grouped<sup>1</sup>, keeping in mind all the above viewpoints, into:

1. Shale Oil Reservoirs – These are extremely low porosity and low permeability reservoirs which have predominantly shales and with low sulfur content conventional light oils which are extremely difficult when it comes to extraction.
2. Tight Oil Reservoirs – As compared to above, these reservoirs are slightly better with respect to porosity and permeability but are not ideal reservoirs. Geologically, these are composed of siltstones (mixture of quartz, calcite, etc.) or mudstones (hardened clay) which are still low porosity and permeability.

From a mineral standpoint, the major difference between the above two types of reservoirs is that, for the former, the main mineral (shale) is very fissile whereas the

latter is less brittle. This makes former to break into layers very easily and geologically both the shale and fissures stretch hundreds and thousands of miles. Strictly speaking, there is nothing called pure shale or pure mudstone/siltstone in nature. There is always some shale content associated with any reservoir which could be 100% purity at places, but on a large scale, shales are associated with other sediments. Keeping this geologic limitation in mind, most tight formations, in as far as log data perspective, resemble shale. For that purpose and throughout this thesis, we will refer to all unconventional reservoirs as “shale” reservoirs. This definition is not to be confused with Oil–Shale reservoirs which require the formation be heated and oil extracted out with the help of heating. Generally, these are present at a shallower depth than Shale oil reservoirs.

### **Conventional versus Unconventional Reservoir**

Long term deliverability of any reservoir, conventional or unconventional, boils down to the fact how various forces, responsible for fluid flow, interact with each other. It is important to understand these forces because it is not always possible to have volumetric depletion only (mostly applicable for gas reservoirs). The objective of any reservoir evaluation study and subsequent prediction comes down to assessment of interactions of these natural forces or drive mechanisms. These are:

1. Volumetric Depletion – The fluids are produced because of induced drawdown and without any other natural drive aiding in depletion. Expansion of original fluids, oil or gas or both and/or interstitial water, occurs because of reduction in

pressure. At the same time contraction of reservoir rock skeleton occurs. Generally gas reservoirs exhibit this kind of drive.

2. Solution Gas Drive – This is a fluid PVT driven drive where the liberation and expansion of gas below bubble point results in increased production from the reservoir, if effectively managed.
3. Gravitational Drive – Usually associated with the geology of reservoir and its structure such as dip or net thickness of the reservoir being so great that the lighter fluids separate and occupy upper parts of the reservoir whereas the heavier fluids settle down to the bottom. This is often referred to as gravity segregation.
4. Gas Cap Drive – Produced because of the relative volume of gas is bigger than oil in the reservoir and typically associated with reservoirs having initial pressure close to saturation pressure. A good example would be when the average reservoir pressure goes below the bubble point early in the producing life of the reservoir, the expansion energy of the gas is driving factor for production.
5. Aquifer Drive – Conventional oil reservoirs are rarely without water drive. Water is always present in sedimentary deposits and aids in production (from kerogen) and migration of oil in a marine setting. In cases where this drive is altogether absent is the big reservoirs of Central Asia, which are carbonate in origin. Although volumetrically carbonate reservoirs are bigger than their sedimentary counterparts, the latter are more prolific in numbers.

The above are the principal natural drive mechanisms of the conventional reservoirs and sometimes a combination of any two is generally referred to as a combination drive. In this thesis we will take up the case of three simultaneous reservoir drive mechanisms.

Reservoir data interpretation, using material balance, forms the backbone of understanding these drive mechanisms. Geologic models are built and are then calibrated with the help of the available production and pressure data. This process is called history-matching or model calibration. Since geological model represents the best guess of how the reservoir looks like, it often needs to be modified on dynamic (engineering) side to achieve a satisfactory history match. This is the reason multipliers are applied to change largely the permeability field. The urge to apply multipliers to porosity field is generally desisted because it affects the in-place volumes. This is the most common way out. There are certain situations when any amount of changes of the permeability field does not help in achieving history match. As a result, a simulation engineer has to reassess the approach and play around not only with the rock properties, such as porosity and permeabilities, but instead test various fluid properties such as PVT data, rock compaction data, etc. as well. This makes it an advanced history matching exercise because most of the times all operators, mitigate the uncertainty in PVT data, by strict quality control methods during the initial life of the reservoir. Also the reservoir have been cored enough to have an idea of compressibility of reservoir rocks. For this dissertation, the conventional reservoir part is dedicated to history matching and prediction performance of an offshore Nigerian reservoir which had very limited pressure data and only basic PVT data.

Liquids-rich unconventional reservoirs will also exhibit all the above drive mechanisms. The only restriction being the time of economic life of the reservoir being evaluated since in unconventional reservoirs transient lasts very long. The length of transient depends on magnitude of low permeability, which means for a particular average permeability the transient does not reach the boundary. Also, since the permeability is low, the amount of depletion achieved may not be enough to bring down the pressure below the bubble point. Also we cannot rule out the presence of solution gas drive altogether. But in order to study solution gas drive we have to put detailed PVT information in our models, both above and below bubble point. This scenario is not possible when dimensionless variables are used.

Gravity does play a part only in a limited sense, as for example, some of the operators have tried producing horizontal wells with toe up rather than heel down with encouraging results. This topic is not covered in the thesis.

This leaves us with aquifer drive mechanism for these reservoirs. We have to state one obvious major assumption we have made in this thesis. Aquifer water does not enter the reservoir. This assumption is valid since fluids do not move/invade that easily in such low permeabilities. The fractures, both natural and hydraulic, provide good connectivity throughout the reservoir. If single phase is assumed in the reservoir, the obvious question is how any aquifer drive would affect these reservoirs? The short answer is if we assume a small control volume (Stimulated Rock Volume – SRV) around a hydraulically fractured well that is being depleted and subject to no flow (pseudosteady state) boundaries or aquifer around it, then all interactions of these with

the reservoir determines long term well performance. Also, this aquifer can be in pseudosteady state or transient condition and may be present above or below the reservoir.

Before we turn away from this topic, it is necessary to put in a word of caution. When we talk about transient aquifer boundary, the intuitive assumption is that the boundary is moving, as it does in a conventional reservoir. The only problem here is this cannot be achieved in an unconventional reservoir. The assumption which is made in this thesis with regards to transient aquifer boundary condition is that the unconventional reservoir is surrounded, above or below as the case maybe, with a conventional reservoir which has good permeability. In order to achieve transient effect the water saturation rapidly changes outside the lower or the upper boundary. This assumption leaves intact the single phase oil within the SRV but at the same time takes into account realistically the aquifer effect. It will be discussed in detail in subsequent chapter of this thesis.

### **Role of Hydraulic Fracturing in Unconventional Reservoirs – Problem Description**

There are no direct references to reservoir drive mechanisms in the literature for unconventional reservoirs. Part of the challenge is associated with this fact is that the reporting of water production in the literature has been next to nothing. For liquids-rich plays, Bakken, Eagleford and Permian are considered to be the biggest reservoirs<sup>1</sup> in US, given in Table 1. It also gives their oil decline rates for initial five year period.

**Table 1.** Decline Rates of the Big Three U.S. Shale Oil Plays<sup>1</sup>.

Play	Year 1	Year 2	Year 3	Year 4	Year 5
Bakken-Three Forks	43%	35%	30%	20%	20%
Eagle Ford	55%	40%	30%	20%	20%
Permian Basin	50%	40%	30%	20%	20%

NOTE: Year 1 decline is calculated as the average production during the 12th month of production vs. IP30 daily production. Subsequent yearly decline rates are calculated against the last month of the previous year daily average production. After Year 5, I assumed a flat 7 percent annual decline.

A general insight to the amount of water being produced by unconventional reservoirs can be had from a few sources such as a SPE paper by Li Fan *et al.*<sup>2</sup>, IHS report by Gay *et al.*<sup>3</sup>. Figure 1, from Gay *et al.*<sup>3</sup>, gives an idea of the percentage of water being produced throughout the life of the well in unconventional reservoir.

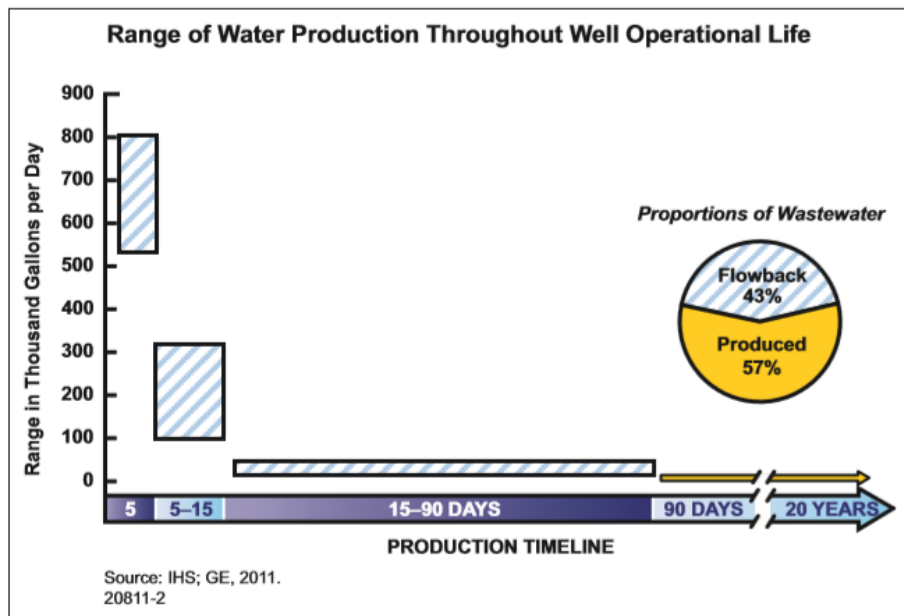


**Figure 1.** Water Production Range for Typical Unconventional Well<sup>3</sup>.



As is clear from the figure, approximately 40% of wastewater is produced in 0.5% of the well's operational life. This is the result of fracture flowback. The remaining 60% is produced during the remaining 20 years of operation. It is this water which needs to be evaluated from the perspective of drive mechanism, although it might be minimal, but water-cut will be high. For the hydraulically fractured unconventional well, the presence of water effects the long term deliverability. Figure 2 shows the shale basins<sup>4</sup> and associated aquifers in US.

Sources, like company's investor presentation<sup>5</sup>, suggest that Bakken horizontal wells do produce water during its operational lifetime as shown in figure 3 and figure 4. But for Eagleford reservoir, it becomes difficult to demonstrate any water production because most operators do not see any water production in their wells.

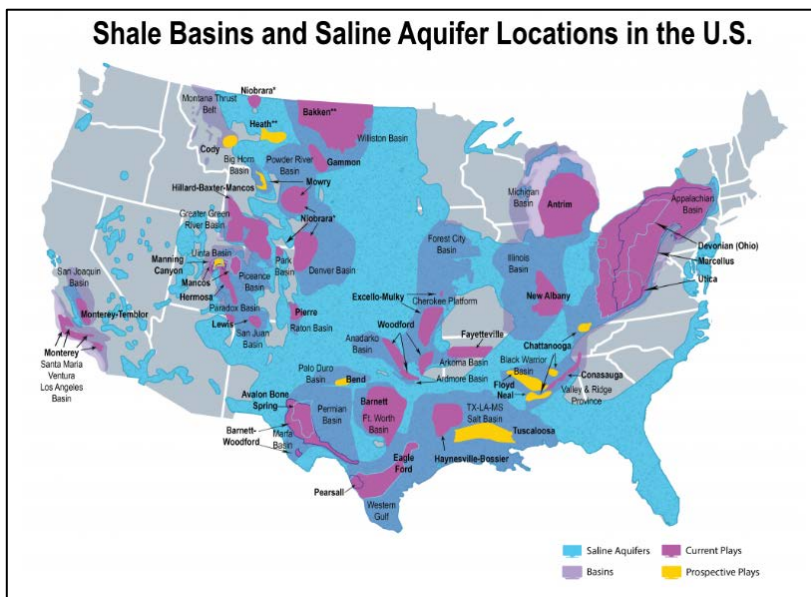


**Figure 2. Shale Gas Production Well<sup>3</sup>.**

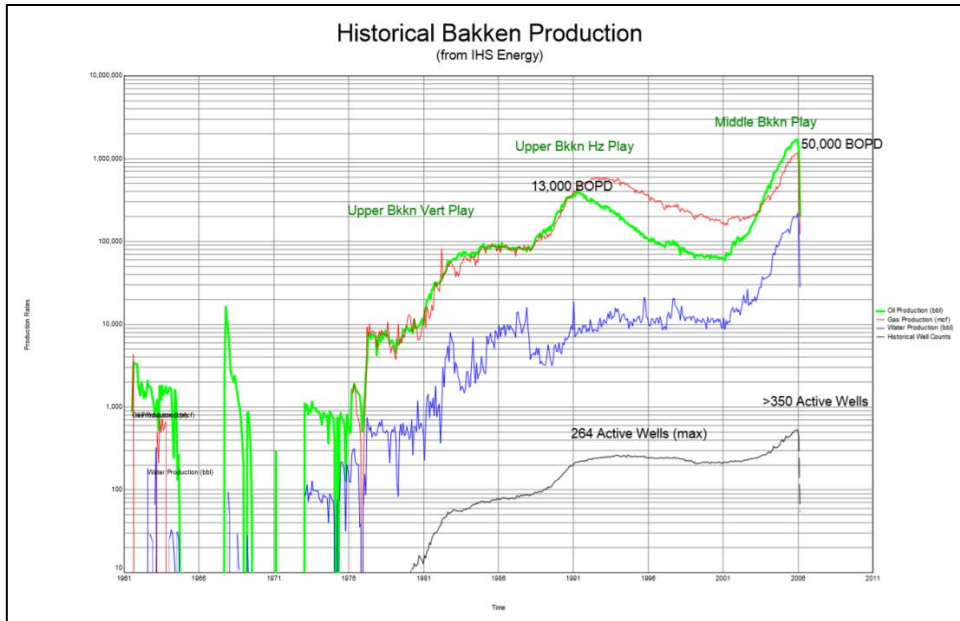


**Figure 3.** Historical Oil, Water and Gas Production of Bakken Field<sup>5</sup>.

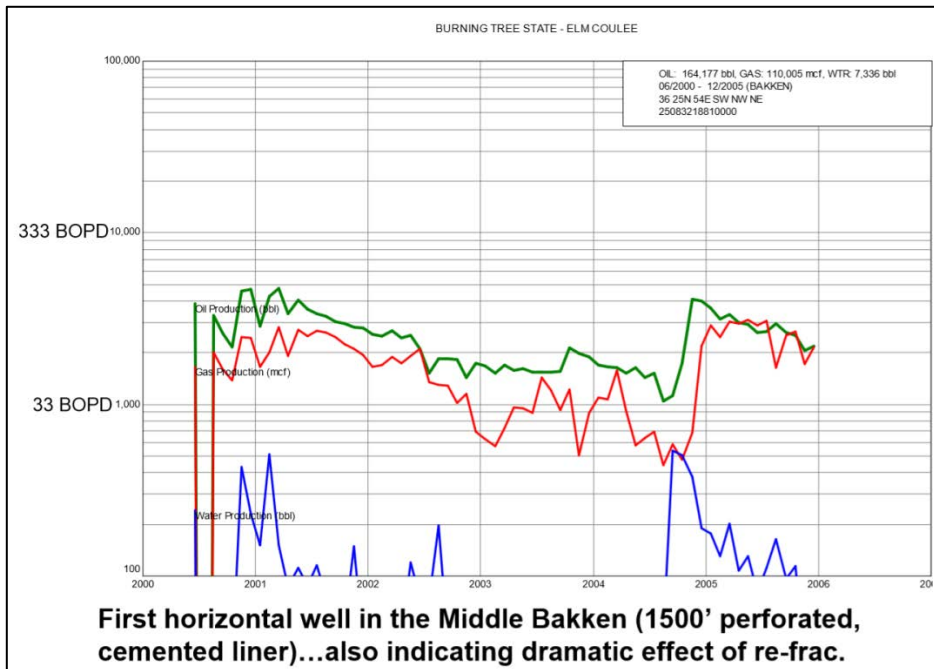
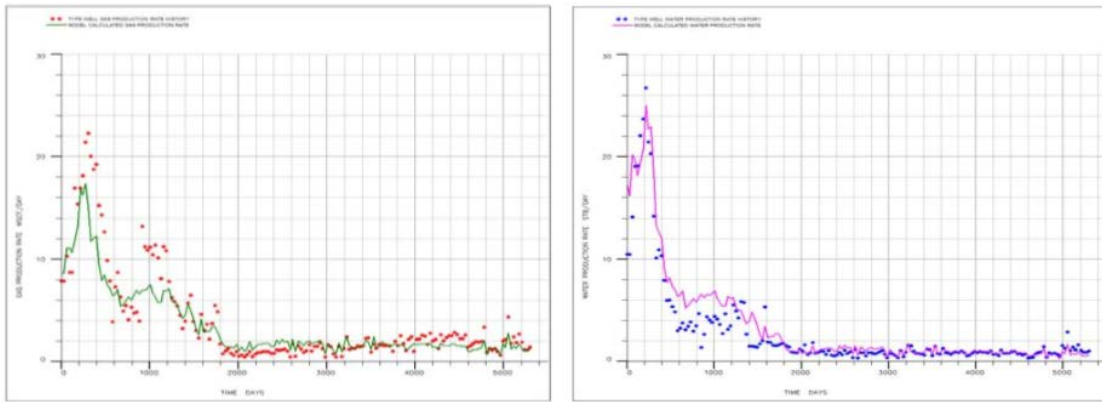


**Figure 4.** Historical Oil, Water and Gas Production of Bakken Well<sup>5</sup>.



(a) Gas Production

(b) Water Production

**Figure 5.** Historical Gas and Water Production of Eagleford Well<sup>2</sup>.

In Eagleford reservoir there is no water production, which does not mean that water is all together absent. Li Fan *et al.*<sup>2</sup> do show history matching carried out for an Eagleford well producing oil, gas and water as shown in figure 5. As pointed out previously, there is nothing called ‘shale-only’ reservoir and in South Texas predominantly marine shale are interlaid with, quartz and carbonates<sup>6</sup>. It is common to expect Eagleford to be underlain by Woodbine sandstone in East Texas. As a result of this, wells produce ‘produced water’. This is more common and may not be confused with the flowback water produced just after of hydraulic fracturing operations. Bottom line, the unconventional reservoir maybe underlain/overlain by formation(s) containing predominantly water. This suggests water may be produced during the lifetime of these hydraulically fractured wells. Also shale play may not be predominantly shale at all. This is particularly common in Permian shale reservoirs, such as Cline shale play in West Texas that ranks among these emerging plays. The Cline shale has been recognized

by some as the fourth leg of the Permian-aged Wolfcamp shale (Wolfcamp D). The Wolfcamp is broken down into A, B, and C intervals based on variations in lithology throughout the formation as shown in figure 6 from investor presentation given by Schepel<sup>6</sup>. These are actually carbonate reservoirs.

Although shale gas reservoirs are not the focus of this thesis, Table 2 from investor presentation given by Craft<sup>8</sup>, shows produced water from these gas plays.

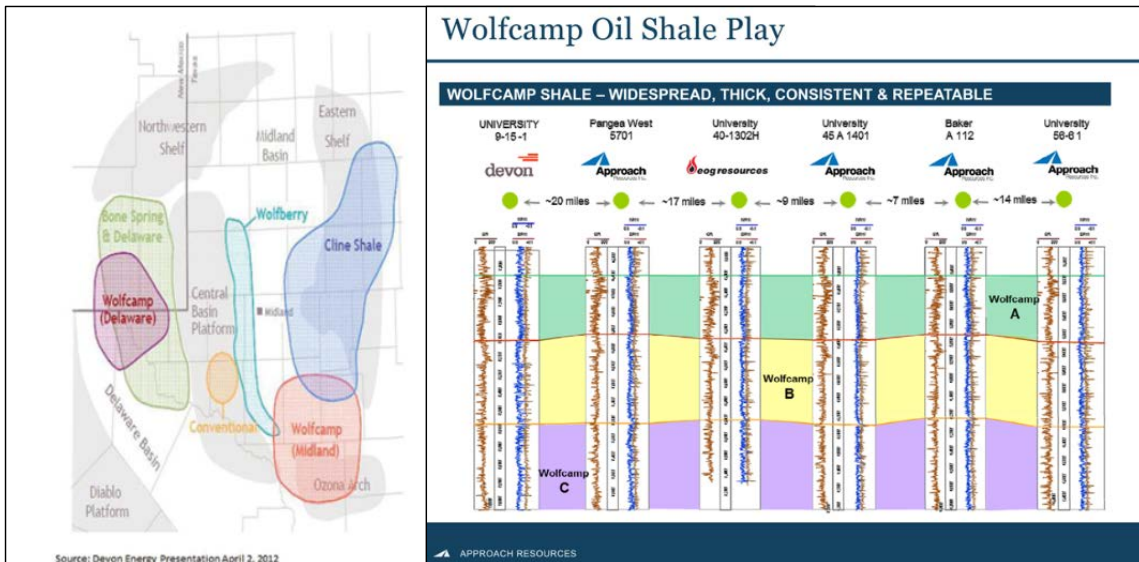


**Figure 6.** Spatial Extent of West Texas Permian Shales<sup>7</sup>.

**Table 2.** Produced Water of Select U.S. Shale Gas Plays<sup>8</sup>.

PRODUCED WATER BY US SHALE PLAY		
Shale	Initial water production (first 10 days) (gal/well)	Long-term water production
Barnett	500,000-600,000	High (>1,000 gal/ MMcf)
Fayetteville	500,000-600,000	Moderate (200-1,000 gal/MMcf)
Marcellus	500,000-600,000	Low (<200 gal/ MMcf)
Haynesville	250,000	Moderate(200-1,000 gal/MMcf)

Source: Data from Chesapeake Energy.

As a big picture of the problem, solutions as presented by Bello<sup>9</sup> when extended to liquids-rich plays with aquifers, would not correctly predict long – term deliverability of wells. This is because of more than one boundary conditions act on the reservoir (reservoir drive mechanism) which determine the rate of average pressure decline.

### **Volatile Oil PVT – Its Uniqueness in Comparison to Black – Oil, Retrograde Condensate and Wet Gas PVT**

Volatile oil is a unique reservoir fluid as compared to all others. In order to point out this difference, we have to state an important point, that both black oil and volatile oil are liquids at reservoir temperature initially (bubble point system) whereas retrograde condensate and wet gas are gas at initial temperature (dew point system). figure 7, that

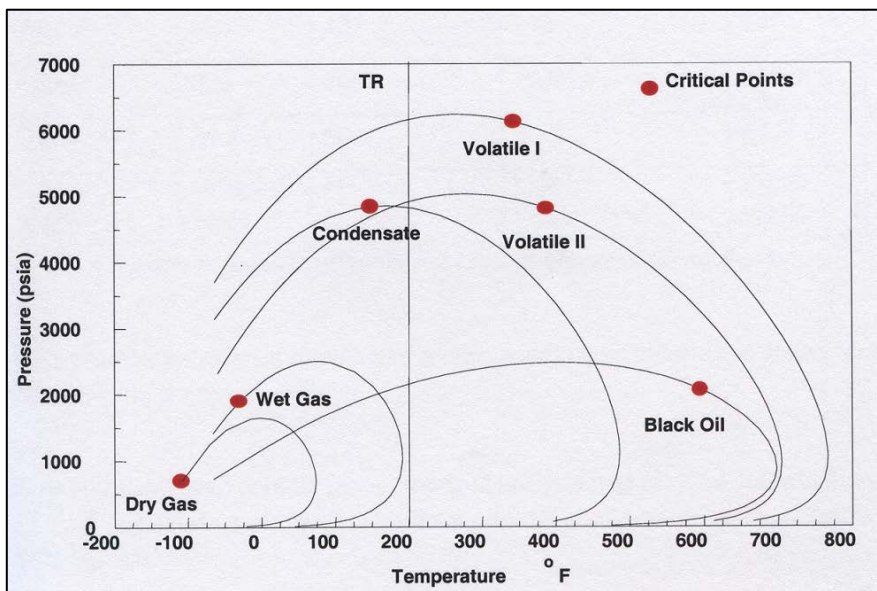


**Figure 7.** Phase Envelopes of Hydrocarbon Mixtures<sup>10</sup>.

is after Barrufet<sup>10</sup>, shows phase envelopes with hydrocarbon mixtures with same components but with different proportions. The implication of the different sizes is apparent if we compare it with information in basic phase envelope, shown in figure 8. Once the pressure decreases below the bubble point due to depletion in the reservoir, the gradient of the percentage liquid lines are very sharp (due to high volatility) below the bubble point line. This results in the volatile oils liberating a large amount of gas for a very little pressure drop below the bubble point. Large amount of gas in the reservoir supplies energy (solution gas/gas cap drive) to the liquids in the reservoir. If the geological structure of the reservoir cannot

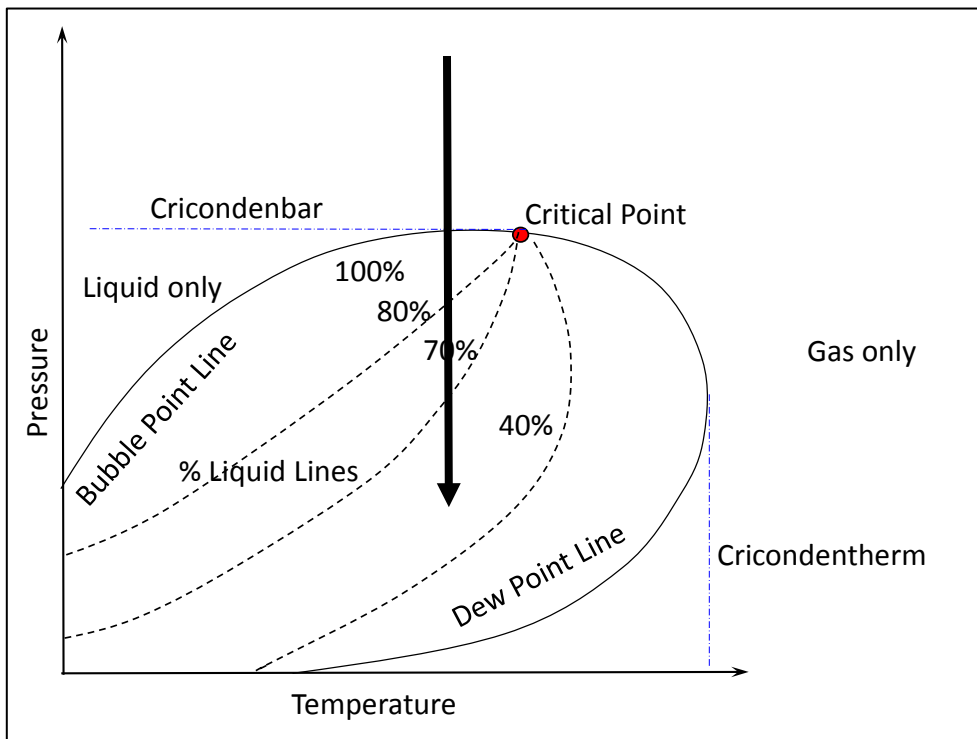


**Figure 8.** Typical Phase Envelopes of Volatile Oils Showing Depletion Path.

accommodate huge gas liberation then the gas cap drive becomes a good virtual gas injection. The underlying assumption in this statement is that permeability is sufficiently high (considering conventional reservoir) to allow fast depletion and drag the pressure below the bubble point fast or alternatively, the production period is sufficiently large that the reservoir is below bubble point for greater part of its productive life. In unconventional reservoir, if we are

**Table 3.** Typical Compositional Mole Percentage of Fluids<sup>10</sup>.

<b>Component</b>	<b>Black Oil</b>	<b>Volatile Oil</b>	<b>Retrograde Condensate</b>	<b>Wet Gas</b>
C <sub>1</sub>	48.83	63.36	87.07	95.85
C <sub>2</sub>	2.75	7.52	4.39	2.67
C <sub>3</sub>	1.93	4.74	2.29	0.34
C <sub>4</sub>	1.6	4.12	1.74	0.52
C <sub>5</sub>	1.15	3.97	0.83	0.08
C <sub>6</sub>	1.59	3.38	0.60	0.12
C <sub>7+</sub>	42.15	12.91	3.80	0.42
MW of C <sub>7+</sub>	225	181	112	157
GOR (scf/stb)	625	2,000	18,200	105,000
°API	34.3	50.1	60.8	54.7
Color	Greenish Black	Light Orange	Light Straw	Water White

in nano-darcy range then the average reservoir pressure does not get depleted much (especially below bubble point) and we will consider gas cap drive altogether absent for them.

As opposed to this, gas condensate conventional reservoirs, have gas at initial temperature or pressure. Here usually, when the reservoir pressure goes below the dew point, 'retrograde effect' kicks in which results in liquid drop-off. If the dip of the reservoir is sufficiently high or the geological structure is huge, it results in heavier hydrocarbon components settling downdip of the structure. This results in setting up of the API gradient.

The differentiation between volatile oil and retrograde condensate is very well defined.  $C_{7+}$  fraction need to be greater than 12.5% for volatile oil. If it is below this value then the hydrocarbon system behaves as condensate. This can be seen from Table 3. Such kind of strict demarcation is not present between black oil and volatile oil. For the hydrocarbon system to be classified as black oil, as per McCain<sup>11</sup>, the following criteria must be met:

- Oil formation volume factor has to be less than 2.0 rb/stb (low shrinkage oil).
- Initial GOR should be less than 2,000 scf/stb.
- $C_{7+}$  fraction should be greater than 30%.
- Density should be less than 45°.

Not all criteria are met when classifying black oil, hence it becomes difficult to identify the hydrocarbon system in the absence of any reliable PVT data.



Wet gas never forms liquids in the reservoir but some liquid drop off may occur at separator. Initial GOR values in excess of 100,000 scf/stb are considered as wet gas. As seen from figure 7, wet gas phase envelope is very small in comparison to others. Table 4 gives the idea of the fluids gravities of three major unconventional reservoirs in US (figure 9). No attempt is made to account for variation in PVT for small pore spaces.

**Table 4.** Typical Fluid Gravity of Major US Unconventional Plays<sup>2,5,7</sup>.

Plays	<sup>o</sup> API
Bakken – Three Forks	40 <sup>o</sup> – 45 <sup>o</sup> (Mountrail County)
Eagle Ford (Oil to Condensate Window)	31 <sup>o</sup> – 59 <sup>o</sup>
Permian Basin (Wolfcamp)	38 <sup>o</sup> – 42 <sup>o</sup> (Cline Shale) / 40 <sup>o</sup> – 43 <sup>o</sup> (Rest)

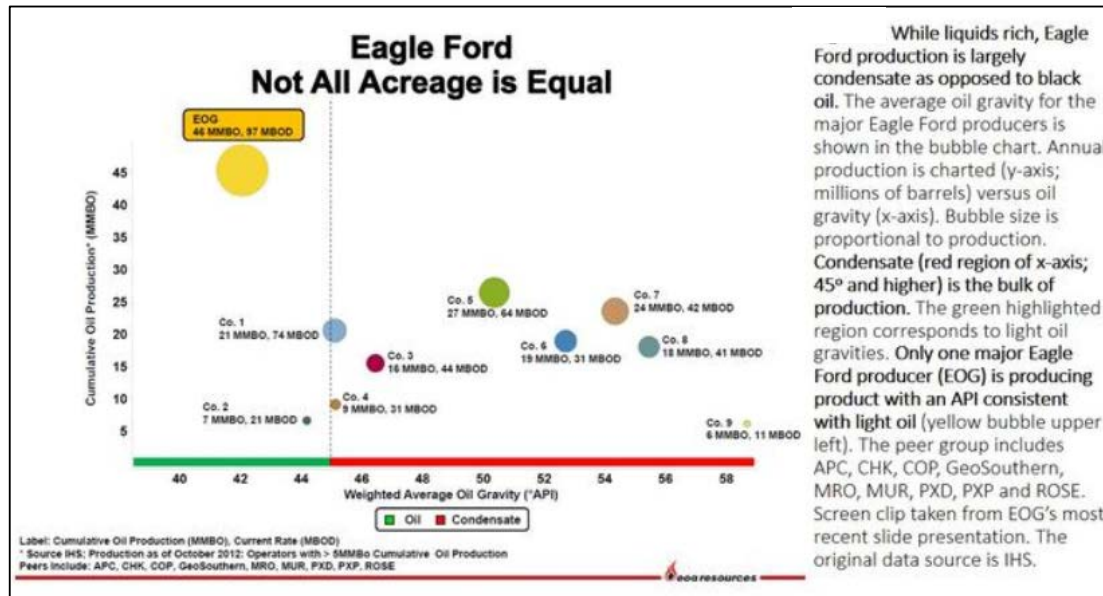


**Figure 9.** Typical Hydrocarbon Fluid Densities in Eagle Ford<sup>12</sup>.

## **Objectives of Thesis**

This thesis has the following objectives:

1. Study conventional volatile oil (light-oil) reservoir, such as Reservoir M in offshore Nigeria, to evaluate long term deliverability based on study of reservoir drive mechanisms.
2. To develop mathematical model of unconventional volatile oil (light-oil) reservoir to evaluate long term deliverability based on reservoir drive mechanisms and with constant fracture volume (Proppant Number) concept:
  - a. Assuming linear flow for multi-stage hydraulically fractured dual porosity model.
  - b. Using superposition and radial flow solutions to arrive at multi-stage hydraulically fractured dual porosity solution.
3. Verification of the linear flow for multi-stage hydraulically fractured dual porosity model using synthetic case.

## **Organization of this Thesis**

The proposed chapter wise outline of the thesis is:

- Chapter I – Introduction
  - Conventional and Unconventional Reservoirs with emphasis on the natural drive mechanisms which effect the long term deliverability.
  - Role of Hydraulic Fracturing in Unconventional Reservoirs to highlight the importance of water production and hence aquifer support on long

term performance of hydraulically fractured unconventional well. The presence of water bearing formation outside the shale formation can result in a different depletion of average reservoir pressure in comparison to pure volumetric depletion (without aquifer support).

- Role of PVT both in conventional and unconventional reservoirs without going into the variation in PVT in small pore spaces. Since operators of unconventional reservoirs go after NGLs, these wells are mostly have light oil as reservoir fluids.
- Chapter II – Insights from History Matching and Forecasting Work for a Steeply – Dipping, Faulted Volatile Oil Conventional Reservoir, Offshore Nigeria.
  - Describes the history matching and forecasting work for conventional Reservoir M in offshore Nigeria.
- Chapter III – Simulation Study of Liquids – Rich, Volatile Oil Unconventional Reservoir – Focus on Reservoir Drive Mechanisms.
  - Discusses the mathematical derivation of hydraulically fractured horizontal well in presence of aquifer and linear flow dual porosity reservoirs.
  - Extends the concept of Proppant Number to dual porosity.
  - Discusses Dimensionless Productivity Index.
  - Show the applicability of the method in a simulation model.

- Chapter IV – Simulation of Unconventional Reservoirs using Meshless Method: Accurate Performance Prediction of Dual Porosity Reservoir with Transverse Fractures.
  - Discusses the use of method of images (principle of superposition) on radial flow solution to derive the constant rate and constant pressure solutions with following scenarios:
    - Fully penetrating, single infinite conductive fracture at the center of square drainage area.
    - Fully penetrating, single finite conductivity fracture using BEM.
    - Partially penetrating, single finite conductive fracture.
    - Partially penetrating, single transverse finite conductive fracture.
    - Partially penetrating, multiple transverse finite conductivity fracture in a horizontal well.
  - Verify the results.
- Chapter V – Results of unconventional reservoir study and Conclusions.

## CHAPTER II

### INSIGHTS FROM HISTORY MATCHING AND FORECASTING WORK FOR A STEEPLY-DIPPING, FAULTED VOLATILE OIL CONVENTIONAL RESERVOIR, OFFSHORE NIGERIA \*

#### **Introduction**

Reservoir M is the deeper producing reservoir of a field in offshore Nigeria which has been continuously on production since Oct. 1980 (~33 yrs). The field is a complexly faulted, collapsed rollover anticline and is saddle separated from one of the biggest fields in Chevron's portfolio in Nigeria. Its proximity to that big reservoir has resulted in the pressure effects being felt in shallow sands suggesting that the regional aquifer is common to both the reservoirs. The structure of this reservoir is having a dip of around 1000 ft. from crest to the spill point. The crestal well of this reservoir has produced for the largest period in the life of the reservoir. In all, nine fault blocks have been identified and developed. Some faults are known to be leaky, resulting in fluid communication.

Around the end of 2011, the asset decided to evaluate waterflood (WF) opportunity for all mature fields. Based on decline curve analysis, Reservoir M was identified as a possible WF candidate. The reservoir was already pressure depleted by

---

\* Reprinted with permission from "Insights From History Matching and Forecasting Work for a Steeply-Dipping, Faulted Volatile Oil Conventional Reservoir, Offshore Nigeria" by Sandeep P. Kaul, Anil Kumar Ambastha, Vincent Eme, Jefferson Louis Creek. 2013 ATCE Proceedings, SPE 166452, Copyright 2013, Society of Petroleum Engineers.

67% from initial pressure and seemed to have no upside. As per good reservoir management strategy, majority of fields are further developed, beyond primary Earth model was constructed and history match undertaken to ascertain if there was a value in further producing the reservoir under repressurization/waterflooding (WF).

At a high level, the objective of history-matching exercise is to better understand the reservoir behavior. This is usually associated with taking a closer look at the drive mechanisms of a given reservoir. Conventional wisdom does require performing a classical material balance (MBAL) study, as shown by Dake<sup>13</sup>, Kabir *et al.*<sup>14</sup>, Pletcher<sup>15</sup>, Esor<sup>16</sup>, etc. which gives a quick insight into the drive energies of the reservoir, but such course is seldom taken. Part of the problem is the number of wells, which then becomes large, making the MBAL model itself unwieldy. Coupled with this is the large data management problem which discourages the practitioner to use this method. For these huge cases (multi-million cell models), there are large number of papers in literature highlighting the various approaches and techniques that can be used to solve the problem such as that by Williams *et al.*<sup>17</sup>, Ambastha *et al.*<sup>18</sup>, etc. to name a few. But the underlying basis of all these deterministic approaches is that the simulation engineer is provided with very reliable data inputs. A detailed model then captures the reservoir performance.

Also since history matching has a non-unique solution; stochastic approaches like Experimental Design together with Assisted History Matching (AHM) techniques have been found to be very powerful tools. A few prominent papers which show the application of these techniques are Hoffmann *et al.*<sup>19</sup>, Emanuel and Milliken<sup>20</sup>, King *et*

*al.*<sup>21</sup>, etc. These approaches try to capture complex reservoir performance by changing input parameter ranges and going ahead with a suite of reservoir models to get to most probable reservoir performance.

Majority of above history-matching techniques are centered on the modification of static parameters such as porosity, permeability, transmissibilities, compartmentalization, etc. Challenge and complexity in history matching comes from understanding complex reservoir behaviors which are not easily apparent based on the available data. As a result, various possible reservoir behaviors may not get investigated within the current normal practice of using available softwares and therefore, associated drives may or may not make it under the microscope of the simulation engineer. Bartlett *et al.*<sup>22</sup> describe the challenges associated with Atlantis, a reservoir in Gulf of Mexico, which started with being simple but after development drilling and initial production performance showed extensive faulting, baffles and presence of perched water. Availability of drilling, seismic and other additional reliable data helped in a better reservoir development plan. The restricted aquifer support was supplemented by water injection for better reservoir management. An improved understanding of reservoir connectivities was also achieved. Although the reservoir was geologically more complex, there was no surprise in identifying the reservoir drive mechanisms which determined the performance.

Surprises are often associated when there is interaction of multiple reservoir drive mechanisms in a complex reservoir architecture aided by gravity. One of these one-off approaches is modeling gravity segregation drive. Although it is possible to

demonstrate it with the MBAL method, as done by Ambastha and Aziz<sup>23</sup>, it can elude the engineer if sufficient attention is not paid. A full-field compositional simulation study by Ypma<sup>24</sup> was performed on Statfjord reservoir to know the role of compositional effects during secondary, gravity-stable nitrogen injection. The overall conclusions are similar to this study as gas condensates formed near the top of the reservoir and volatile oils got accumulated downdip of the structure. But what sets this work apart from Statfjord study is the critical thinking associated with arriving at this gravity-segregation scenario, without the aid of any commercial history-match tool or extensive phase-behavior experiments performed before simulation. We did not have any fluid characterization report to begin with. Alternatively, commercial material balance software, like *MBAL*<sup>TM25</sup> model, may help in identifying these complex drive interactions, but would require advanced model setup using equation of state option and/or pore volume variation with depth. Also, initially we did not make a concerted effort to identify this drive as all PVT models did not generate a big enough secondary gas cap, the driving force behind gravity segregation drive in our model. Instead, water from the main aquifer broke through in the wells producing a strong water drive. The identification of three reservoir drives, which were present in this reservoir, became apparent in the simulation model after improved PVT model was used. This is not to suggest that we did not realize the huge dip making an impact, but all the initial results were either inherently inconsistent or did not go along with what MBAL model was predicting.



## **Reservoir Model Description**

The reservoir has five penetrations in all. Out of these five penetrations, three wells have been active with one well, Well#1, producing for 28 years continuously before being shut down for high GOR in 2008. Well#4 is still producing in the field at a very low rate and Well#5 was shut down on account of high BS&W after five years of production. Well#2 and Well#3 were not brought online because the intent was to produce oil and these wells were suspected to produce gas and hence never perforated.

### *Earth Model*

This reservoir represents reworked shoreface deposits located within the clastic nearshore depositional environment. The stratigraphic section of the field is shown in figure 10 with all the five penetrations. To put this in a better perspective, the gross thickness map, figure 11, is also shown. It shows that thickness is increasing from southwest, where it is the lowest, to northeast, where it is the highest. The other main features of this earth model are highlighted in the following:

- Reservoir M is a reworked shoreface deposit formed via the winnowing of deltaic deposit by wave and current action.
- Reworking is more prominent in NW as evidenced by serrated log character.
- It consists of two stratigraphic lobes separated by ~5ft thick, shale interval.
- Lower lobe is a thicker, overall coarsening upwards progradational sequence.
- Upper Lobe is a thinner, overall fining upwards retrogradational sequence.

Taking into account relevant G&G uncertainties, low, mid and high static models were constructed. The original oil-in-place was an uncertainty and gave a wide range to probabilistic volumetric estimates. The original static fluid contacts were by far the biggest uncertainty. The final contact ranges are given in the Table 5. The main points which need to be highlighted are:

- OGOC uncertainty was approximately 69 ft.
- OOWC uncertainty was approximately 621 ft. Production data suggests OOWC may be closer to the maximum closing contour.
- No additional data available to narrow the current band of uncertainty (No MDT availability and low seismic data quality which needed re-processing. Amplitude extractions were not definitive).
- Low and High case OGOC & OOWC scenarios used to generate probabilistic volumetric estimates.

**Table 5.** Summary of Original Contacts.

	Low	Mid	High
OGOC	-6474'ss		-6386'ss (Crest Of Structure)
OOWC	-6859'ss		-7480'ss (Max. Closing Contour)

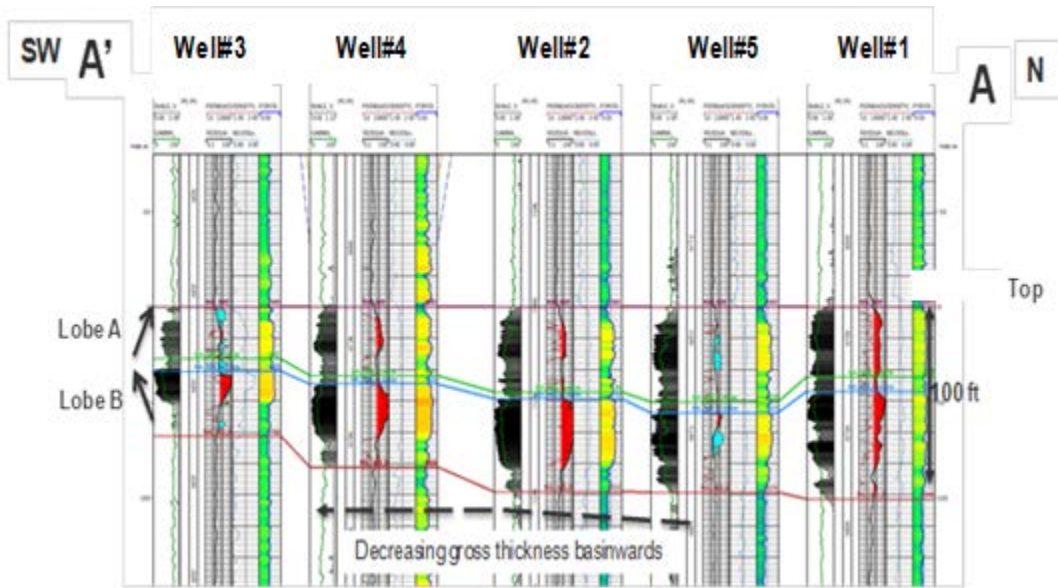


**Figure 10.** Stratigraphic Section of Reservoir M.

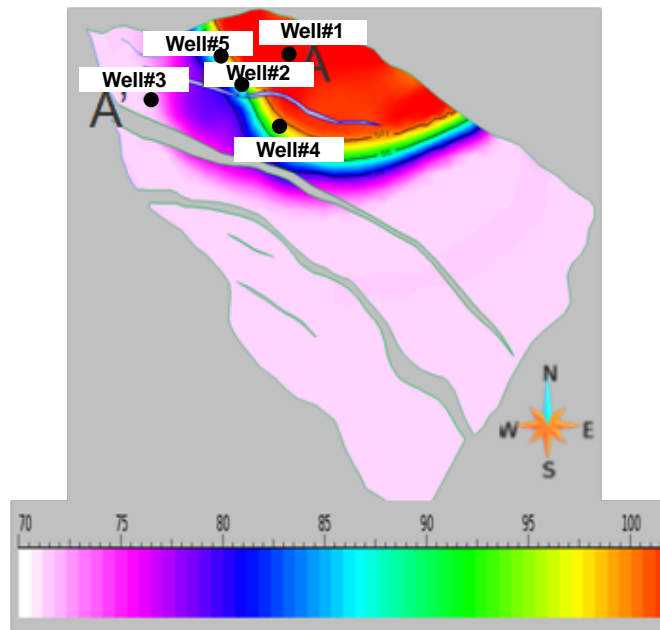


**Figure 11.** Gross Thickness Map.

Booked volumes to date were based on a previous Simulation Study (OOWC sensitization done to achieve result). Additionally, the static parameters uncertainty analysis, done on the original oil-in-place (OOIP), suggested that OOWC was the single biggest hitter. This information was very important, as far as dynamic modeling is concerned. It resulted in two different scenarios: first scenario having 3 different OOWCs (Black Oil PVT used) and the second scenario with two different OOWCs (Volatile Oil PVT used). At this stage, there was no consensus on which particular PVT model could be used since there was no fluid characterization report available for the reservoir. PVT model choice caused the original oil-in-place (OOIP) estimates of dynamic model to be different from that of the static model. The structure has the least impact and hence it was taken out of dynamic uncertainty analysis to reduce scenarios for dynamic modeling.

### *Dynamic Model*

Before upscaling, the fine-scale static model had cell size dimensions of 50 ft × 50 ft × 2 ft with total grid blocks of 100 × 100 × 72 having 373,104 active cells. It was upscaled in X and Y directions only to cell size of 100 ft × 100 ft × 2 ft with total blocks of 50 × 50 × 72 having 89,568 active cells.

For the purpose of identifying unique features of this reservoir, for discussion purposes and from CPU run time stand point, the upscaled grid was divided into 5 different regions as per the following:

- Region 1 – The saddle near Well#5 to account for OWC1

- Region 2 – The fault block for Well#1.
- Region 3 – The fault block for Well#4 to account for OWC2.
- Region 4 – Aquifer Region (Deactivated).
- Region 5 – Aquifer Region (Deactivated).

Region 4 and Region 5 were deactivated to speed up the run time. The coarse scale model with OWCs is shown in figure 12 and region numbers are shown in figure 13.

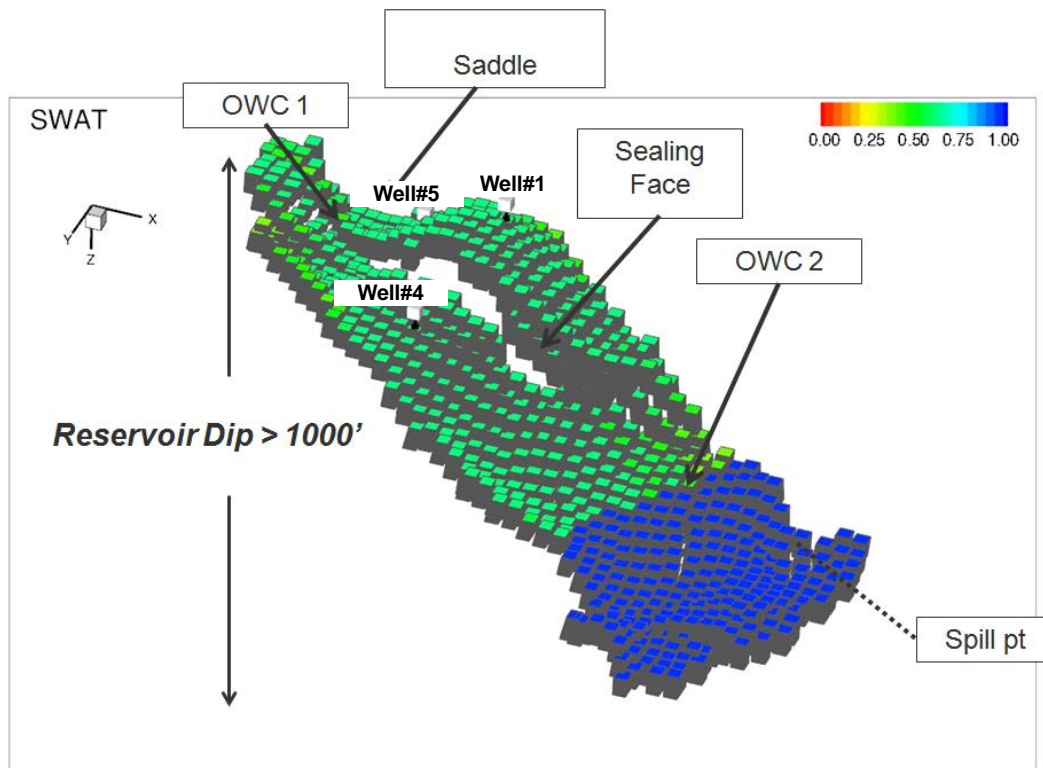


**Figure 12.** Upscaled Simulation Model Showing OWCs.

The model has an aquifer which is common to Region2 and Region3. Region1 (saddle region) is in pressure communication with Region3 through the oil zone. The motivation for having an oil-water contact in saddle was based on water cut production data for Well#5 which showed a value greater than 50% from first month of production. Also water showed up in Well#1 after Well#5 was shut down. Completions in Well#5 also came to be of questionable integrity, adding to the list of uncertainties in the reservoir.

Another uncertainty was difference in pressures between Region1, Region2 with that of Region3. If the single well test value for Region 3 was to be believed, then there was a pressure differential of ~600 psi. A lot of conclusions cannot be derived from a single data point, but the fact remained that the fault was sealing in hydrocarbon area. If the fault remained fully communicable, the gas movement became uncontrollable between Region1 and Region 3. The data did not suggest pressure equalization and in the presence of gas, sealing had to be present. Figure 13 also shows the possible fault communication scenarios which were considered.

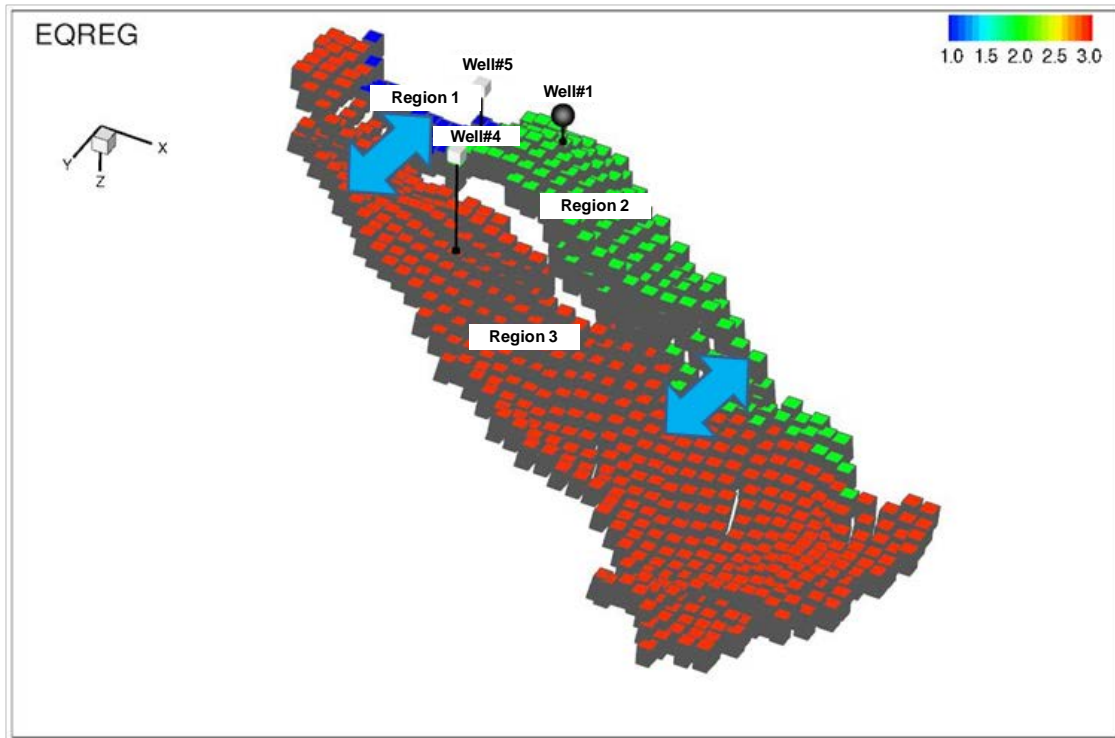


**Figure 13.** Upscaled Simulation Model Showing Equilibrium Regions & Possible Communication between Fault Blocks.

### **Challenges Associated with Earth Modeling**

The immediate challenge at the onset of history-match process was the inability to have Well#1 produce at the required historical oil constraint. The basic history-matching exercise was dictated by it. With the existing earth model parameters, the reservoir pore volume around Well#1 had to be increased to ensure that historical oil rate constraint was met. The pore volume multiplier of 1.5 was used, which was deemed to be unacceptable. A closer look at the problem revealed that the reason for this was associated with the porosity, which showed average porosity values around Well#1 to be

depressed. This is also illustrated in figure 10 where this information is displayed as light green color. The bright yellow color as seen in the figure represents higher porosity values. The production data showed that this particular well, with varying oil rate, had produced uninterrupted for 28 years. As the static information could not be verified from seismic data, owing to its low quality, it was decided to change the geological setting in the reservoir based on production data. Keeping the porosity-permeability transform constant, the geological trend of the reservoir was revised so as to help meet the oil rate constraint during history matching. The exact reason for going against the information provided by logs could not be arrived at. The well in question was the first penetration in the reservoir and the fact that the logging tools could have been of early 1980 era was the only justification which seemed plausible. This resulted in two scenarios where, more than likely, either the logging tools were unable to pick up correct porosity or the tool may have had a calibration problem. In conclusion, the production data overrode the information that was provided by the logs. Figure 14 shows the changes to the values of porosity incorporated to the earth model as represented through the Kh sum maps (keeping the same porosity-permeability transform).



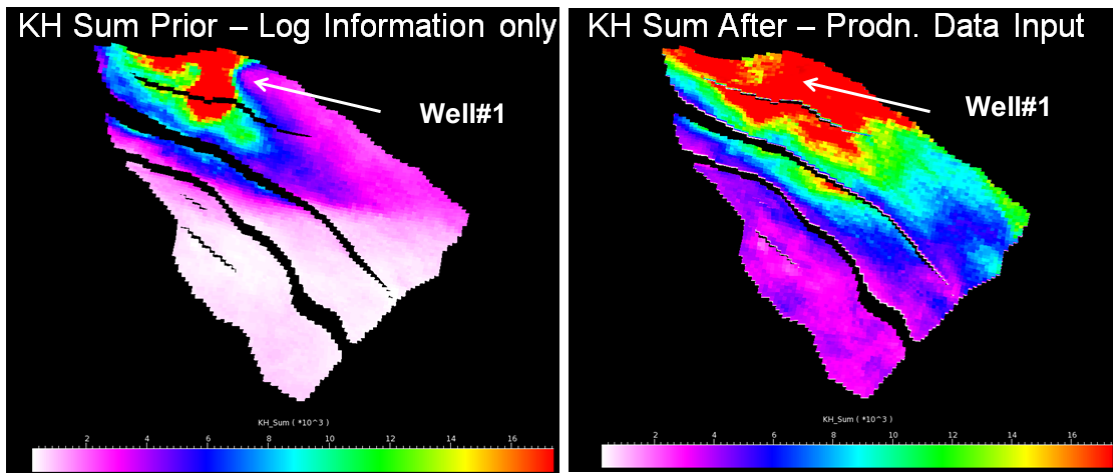


**Figure 14.** Upscaled Simulation Model Showing OWCs.

### Challenges Associated with Data Measurement Errors

The producing GOR and the API data were also analyzed and are shown in figure 15 and figure 16, respectively. The data suggests that the  $R_{si} = 770$  scf/STB (initial GOR) remains constant for two years for Well#1, before the reservoir goes below the bubble-point pressure and producing GOR starts to increase. Initial GOR value, allowing for errors in measurement in the field, indicates that it is a black-oil system as suggested by McCain<sup>11</sup>. Since gas measurements are the least accurate in the field, the GOR measurement integrity also came to be questioned.

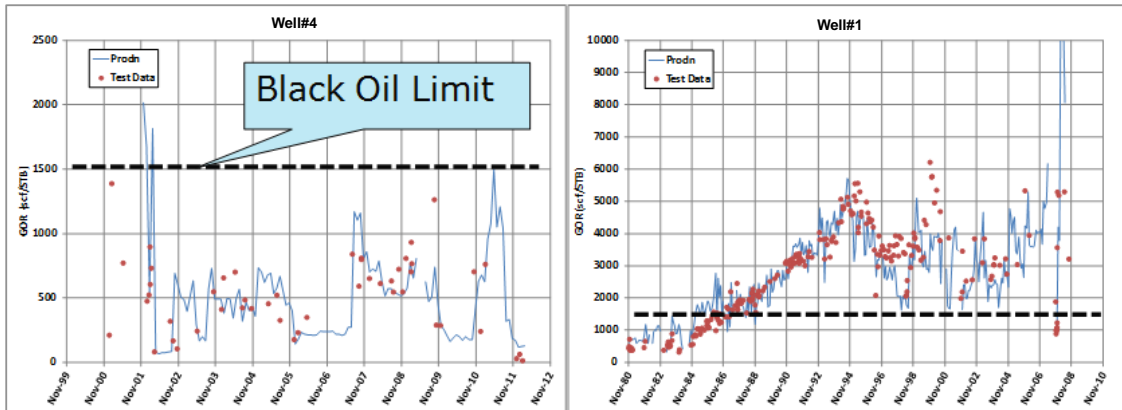


**Figure 15.** Reservoir GOR Data.

Communication between fault blocks also needed revisiting. Well#4 was brought on production after ~20 years of reservoir life and still saw  $R_{si}$  which was below the 1500 scf/STB line (black-oil limit). This reinforced the idea of fault being sealing in the hydrocarbon area. Initially, this motivated us to try black-oil as the reservoir fluid. A similar parallel can be drawn when API data was analyzed and shown in figure 16. The API of the crestal well, Well#1, has remained constant at 42° API (volatile oil range), whereas the other two wells have varying API. This is especially true for Well#4 which was brought into production after ~20 years and produces at 32° API for the first 2 years and API data for Well#5 had a range from 28° API to 46° API. The reservoir was clearly having volatile oil, but at the same time exhibiting black-oil properties. As would have been customary under the circumstances, there were two distinct lines of opinion; one which suggested that there were huge measurement errors in API data and the other

suggesting caution so as not to miss any vital information which the reservoir data was trying to suggest.

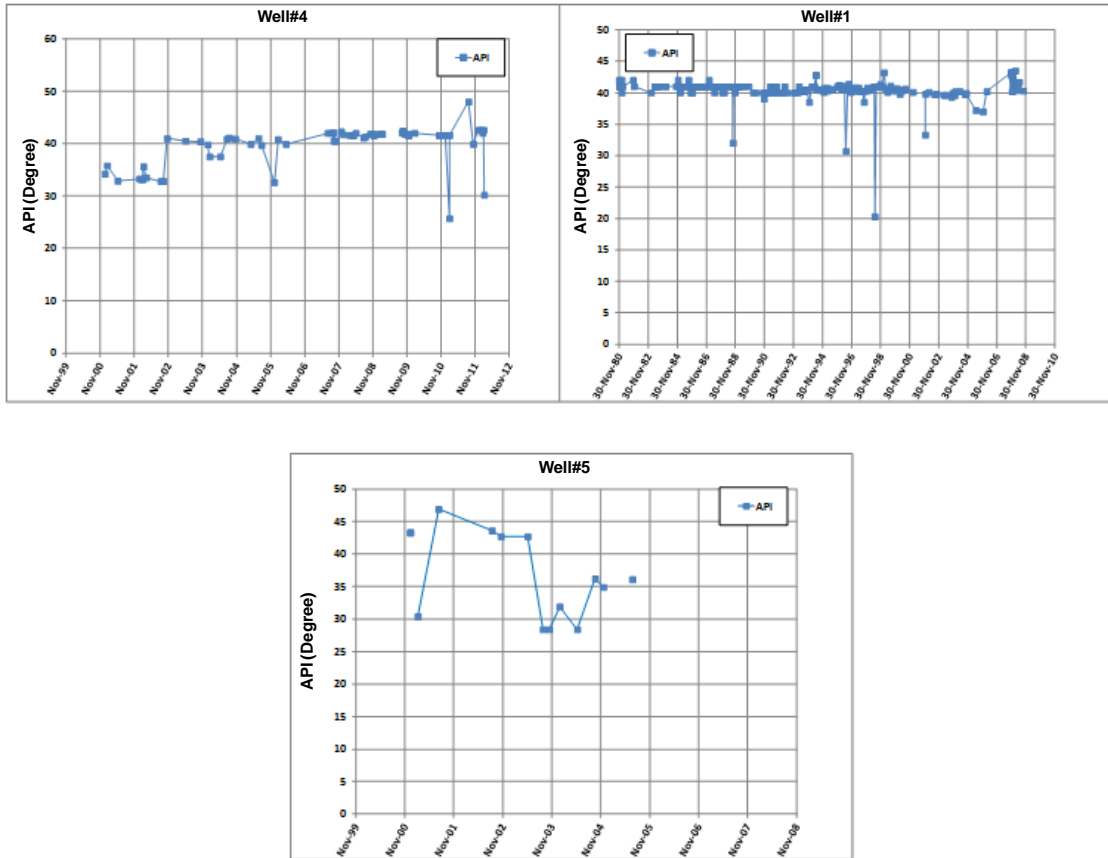


**Figure 16.** Reservoir API Data.

## Identification of Reservoir Drive Mechanisms

The production data analysis was carried out with material balance (MBAL model) to understand the various drive mechanisms and the effect of aquifer. As mentioned previously, the look at the pattern of GOR production led us to believe that the reservoir was following the classical solution-gas drive. This was the first drive of the reservoir and has been explained very well in Dake's book<sup>13</sup>. The second drive mechanism was the water influx and the results of this analysis are shown in figure 17. The unique feature of this MBAL model output, which mathematically calculates drive indices and shown in the figure, is that the water influx energy is decreasing in time. Water influx usually follows a pattern of being ever increasing once breakthrough is achieved in the reservoir. This is a sign of a weak water drive. Campbell<sup>27</sup> plot also supported this hypothesis. Also, the best fit Havlena-Odeh<sup>28</sup> plot, given the error in the fit, suggested no upward revision in the original oil-in-place.

Apart from the fact that there was a dip of around ~1000 ft from the crest to the spill point in the reservoir, impact of a weak water drive was not very clear at this point in time of the history-matching exercise.

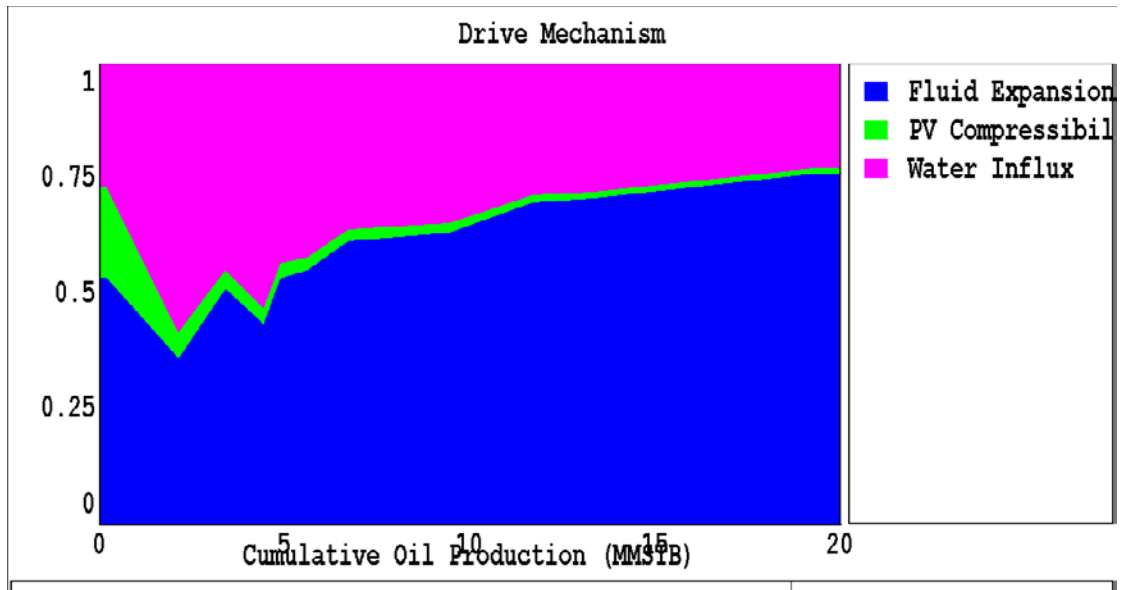


**Figure 17.** MBAL Model Output to Identify Drive Mechanisms.

### **Challenges Associated with PVT Fluid Modeling during History Matching**

This was the biggest simulation challenge. The data indicated borderline black-oil fluid, but in strict theoretical sense, it was Volatile oil. With Well#1 as the benchmark, following scenarios were tried in history-match exercise:

1. Black Oil with single bubble point (no variation with depth)
2. Black Oil with variable bubble point with depth
3. Black Oil with single bubble point and  $k_v/k_h$  Ratio = 0.3
4. Condensate (Analog Data) Option and Full Compositional Model
5. Final Condensate Model

For brevity, this chapter carries detailed discussions about scenarios #1, #4 and #5 only. The most important point to be noted was that for all the three black oil models, the historical oil production constraint was only honored with OOIP which were more than 20% higher than that proposed by MBAL model. Also, all these black oil models had to have three OWCs to match water breakthrough at the wells and were repeatedly giving strong water drive signature. In-house program was used to generate the relevant black-oil PVT data. The base PVT with which simulation was attempted, to begin with, is shown in Table 6.

**Table 6.** Summary of PVT Data

<b>Reservoir Properties</b>			
	Initial Pressure	2,949	psia
	Reservoir Temperature	218	°F
	Datum	6775	ft TVDSS
<b>Oil Properties</b>			
	Oil API Gravity	42	Degree
	Initial Solution GOR	770	scf/STB
	Bubble Point Pressure	2,500	psia

*Black Oil with Single Bubble Point (No Variation with Depth)*

This was the first attempt in history matching. Initial GOR of 770 scf/STB was chosen in fault block of Well#1. The simulation result of this attempt is shown in figure 18. The GOR match for the whole history period, especially 1996-2002, for Well#1 was very poor. The gas production, as shown, tracks historical values early in the life of the well, but once the pressure goes below the bubble point, gas production is unable to keep up and follows a flat profile. This is seen in the GOR figure. The pressure match is shown in figure 19.

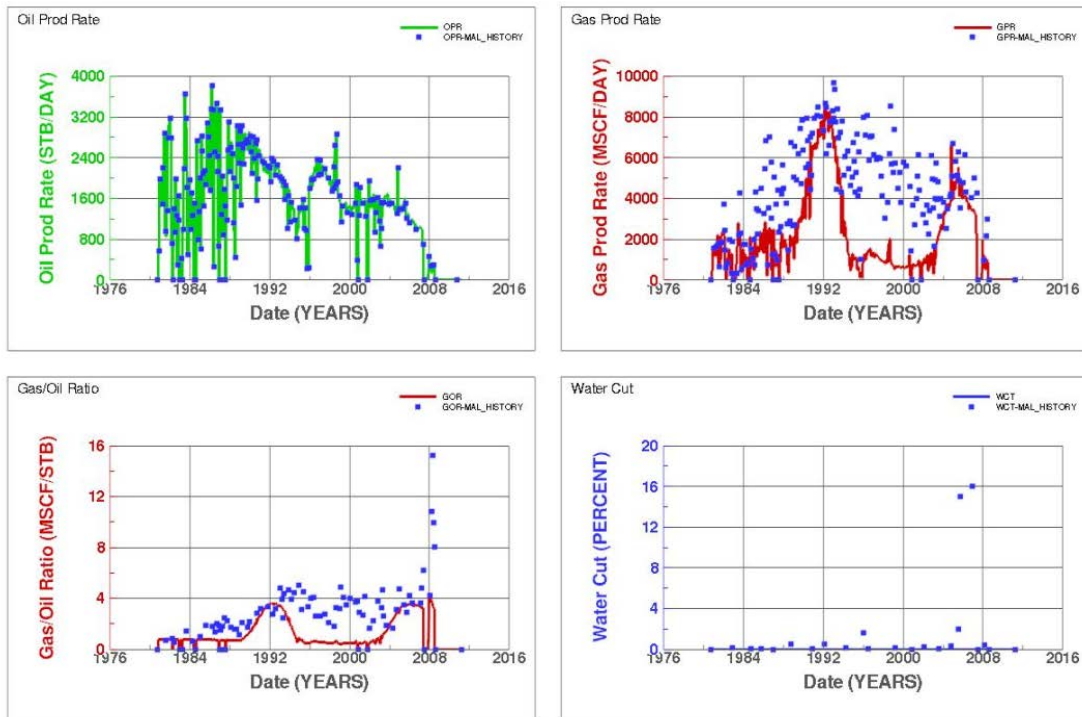


**Figure 18.** Single Bubble Point Simulation Results for Well#1.

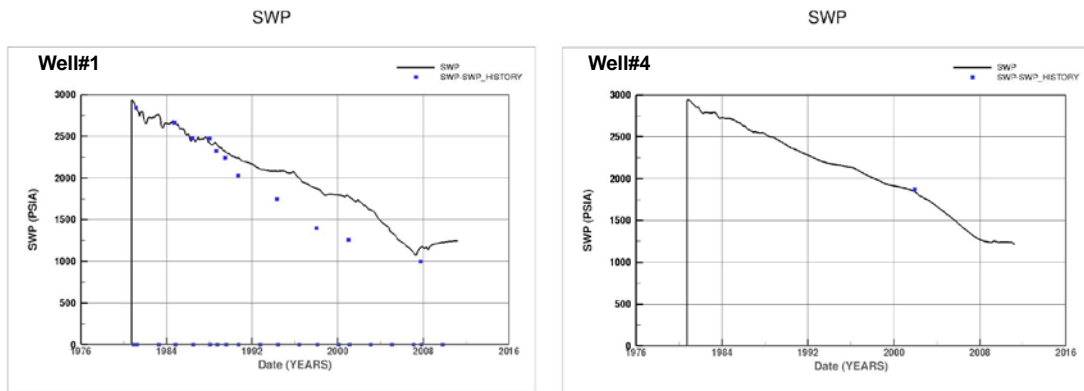


**Figure 19.** Single Bubble Point Static Pressure Match for Well#1 and Well#4.

*Condensate (Analog Data) Option and Full Compositional Model*

In CHEARS<sup>®</sup>, Chevron’s in-house reservoir simulator, condensate option was activated and an Analog PVT (Condensate Yield,  $R_L$ , of 35 STB/MMscf,  $API = 35^\circ$ ) was used. This PVT model was attempted to see whether any further improvement in GOR could be possible. A 4-component full compositional model was also attempted to see whether that would help. Figure 19 and figure 20 shows the results of static well pressure for both these analog condensate and full compositional models. The condensate model gave a good pressure match, but the full compositional model died after it ran for the first 5 years of history. GOR match (shown in figure 21 for condensate model only) was somewhat better than the black-oil model. The biggest reservation for using these two models was the OOIP, which was too optimistic than the runs with the black-oil PVT. Both these options were eventually abandoned.



### SWP

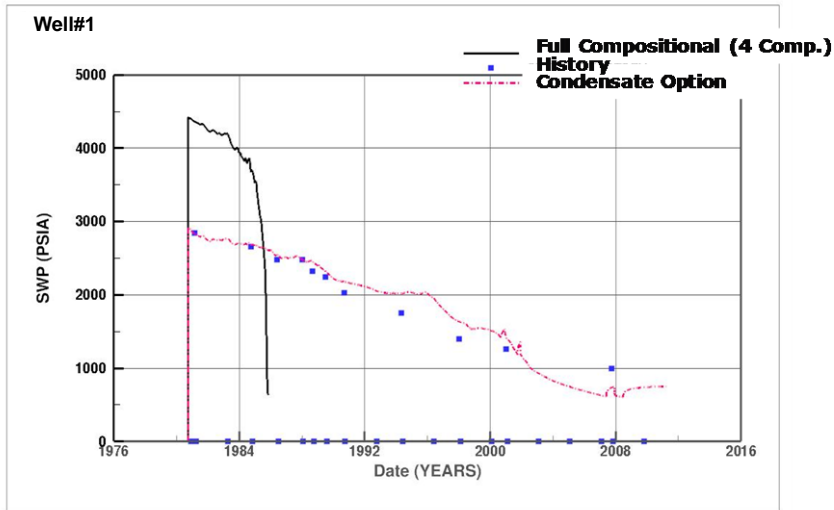


**Figure 20.** Condensate Option and Full Compositional Static Pressure Match for Well#1.

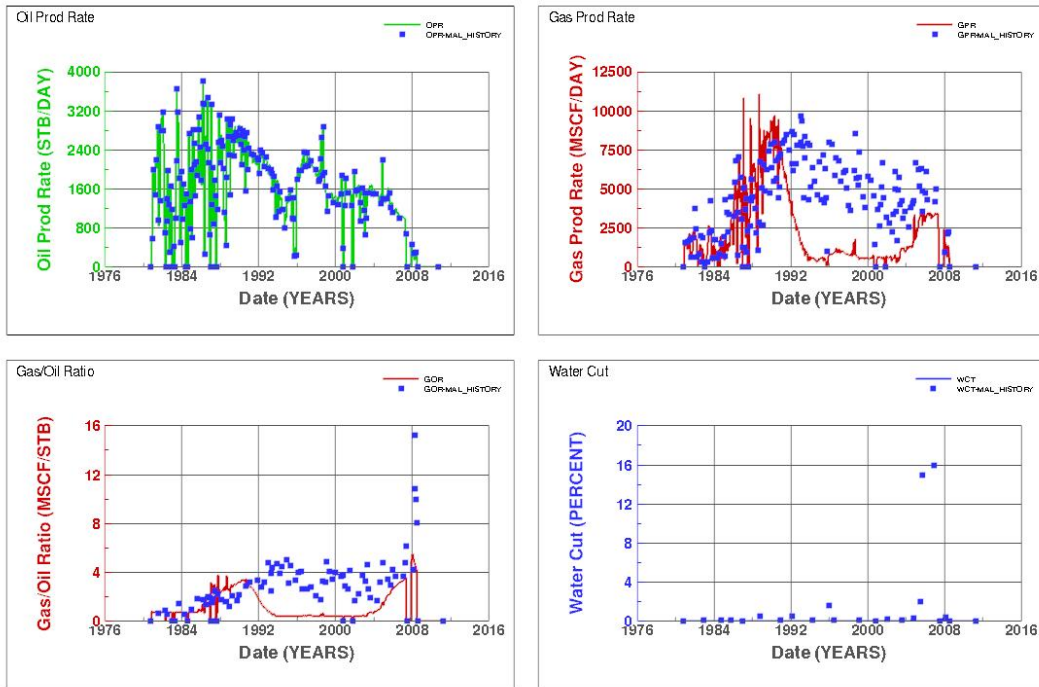


**Figure 21.** Condensate Option Simulation Results for Well#1.

### *Final Condensate Model*

Since the GOR match had improved using analog condensate model, it was decided to modify this existing PVT so that simulation could produce more gas. The basis of change was API of 66° (volatile oil) measured at the facility. The modified PVT was created out of analog data ( $R_L$  of 35 STB/MMscf, API = 35°) and was modified to  $R_L$  of 75 STB/MMscf at 3000 psi dew-point pressure, API = 62°.

To understand what was happening in the reservoir, it is important to turn to the basics of PVT analysis. Figure 22 shows the phase envelope of various reservoir fluids. Theoretically, volatile oils have the largest phase envelope. What this means is that a condensate model may fit into a volatile oil envelope, but the possibility of black oil fitting into volatile oil envelope was very slim. This is because the envelope for black oil is very constricted in comparison to volatile oil. This was the major reason why black-oil models were failing to produce the required gas rate or match GOR.

## CPCP<sup>®17</sup> Manual

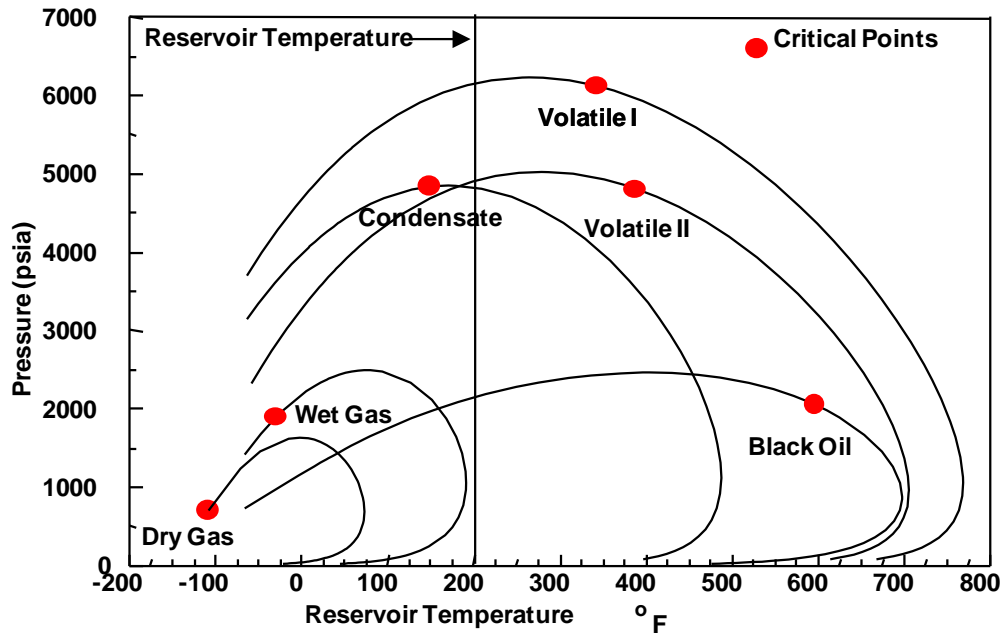


**Figure 22.** Typical Phase Envelopes.

What made the modified condensate model (extrapolated envelope) to work was the gradient of the liquid lines which would have been similar to the actual volatile oil envelope, had a fluid characterization report been available. This is shown in figure 23. As a result of this, the history-match results obtained were very satisfactory as shown in figure 24. The key message which needs highlighting is that all this was achieved without the use of any permeability or PV multiplier.

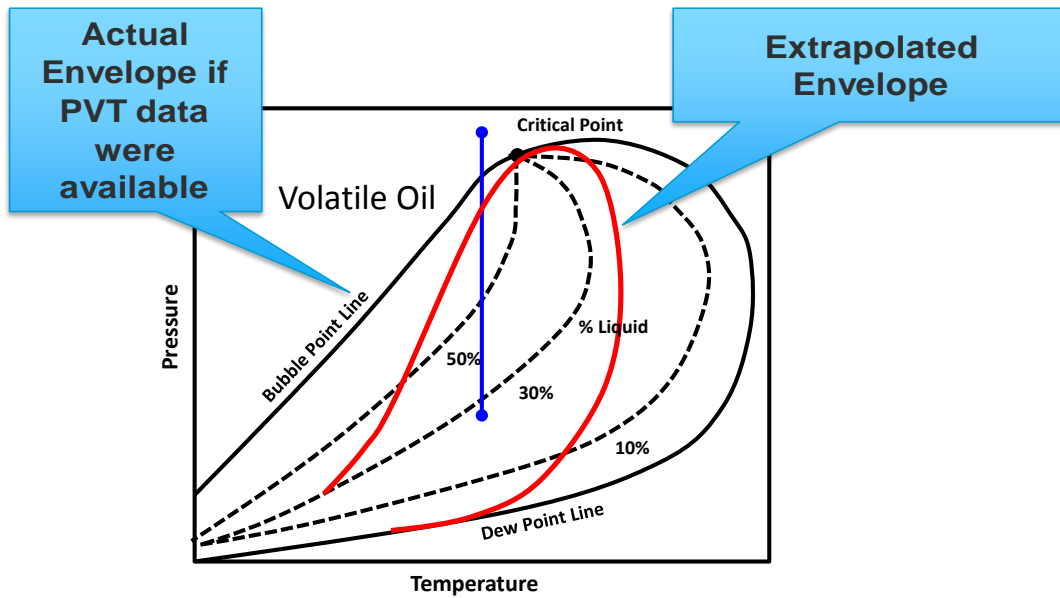


Figure 23. Extrapolated Phase Envelope.

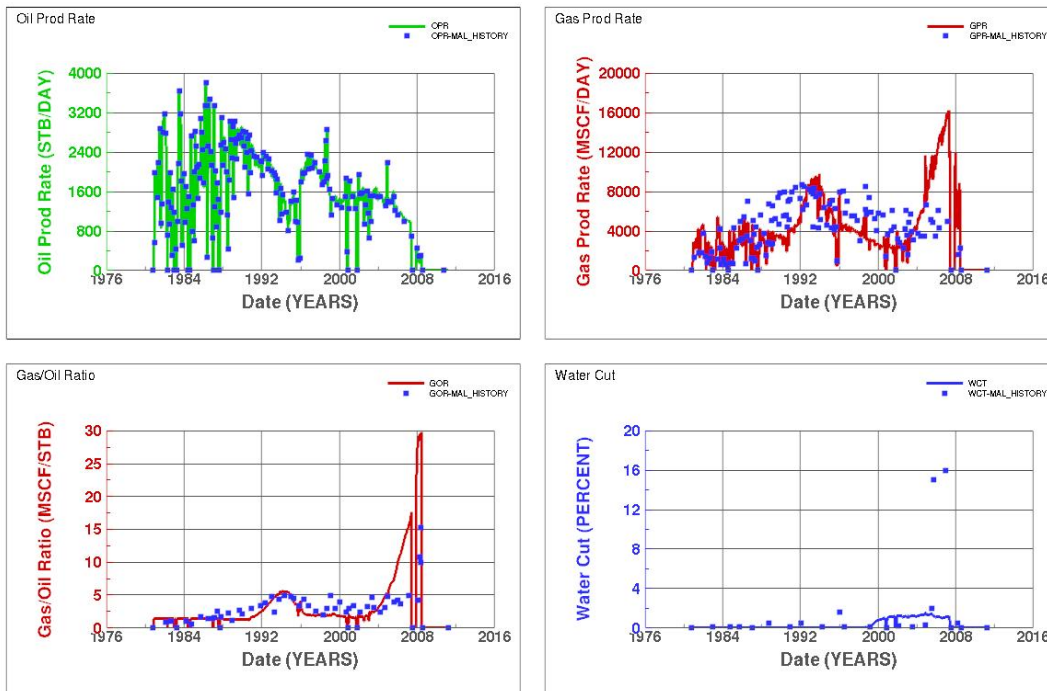
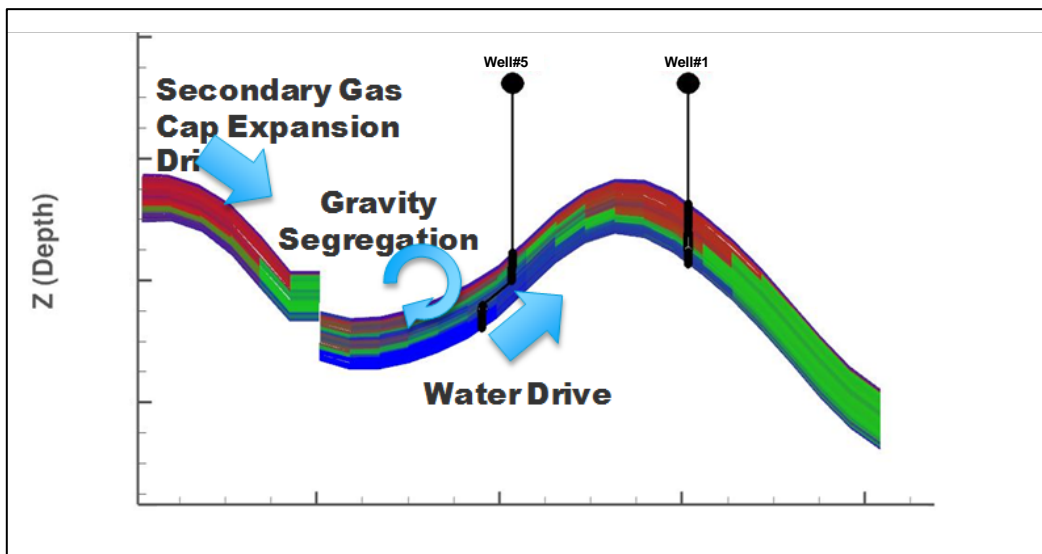


Figure 24. History Match Results using Modified PVT Data for Well#1.

### Identification of Third Reservoir Drive

It is worthwhile to pause here and go into the details of how the reservoir was behaving. This was the main reason for the robustness of the history match process. Gravity segregation played an important part in the overall performance of the reservoir. Figure 25 illustrates the effect of this drive.



**Figure 25.** Gravity Segregation Effect in Reservoir M.

The saddle was the place where all the action was taking place as shown in figure 25. The crestal well, Well#1, was continuously stripping the reservoir of all the lighter components. This resulted in the formation of secondary gas cap, formed in the structurally higher parts of the reservoir and acted as a piston drive (similar to gravity-stable gas injection). This drove both the oil and water closer to Well#1. But the water

underrode the oil in the saddle and the gas overrode that same oil. This led to a churning effect of the entire three-phase system in the saddle area. As a result, the API gravity went from being a very light oil of 47° API to heavy fraction oil of 28° API (see figure 16 for API data). This gave us confidence in the history-match model as having captured the physics of fluid flow. This scenario was not possible with the black-oil or analog condensate PVT. Again, for both black-oil and condensate models, the main aquifer was active instead of the aquifer in the saddle, resulting in a very strong water drive and producing inadequate history match.

#### **End of History Saturation and Best Case Prediction Scenario**

As expected for a solution gas-drive reservoir with significant gravity segregation, an analysis of all the layers of the simulation model revealed the oil saturation to be concentrated on the downdip portion of the structure (see Figure 26). It was just a matter of putting a well in this area which fetched additional reserves. Gas lift had to be used to sustain production in the new development well. To have the best case prediction scenario, it became apparent that the evolution of the secondary gas cap had to be in a controlled manner. Also, the main aquifer was not the main drive in the reservoir, which was in line with the MBAL model predicting a weak water drive. Thus the water drive energy came from the fault leakage / water accumulation in the saddle. Out of the many prediction scenarios being evaluated, none gave a better result than the one in which Well#5, a producer, was converted to injector and was responsible for

slowing the expansion of the secondary gas cap. This yielded an incremental reserve of 8 MMSTBO, while maintaining the same original oil-in-place as all the previous studies.

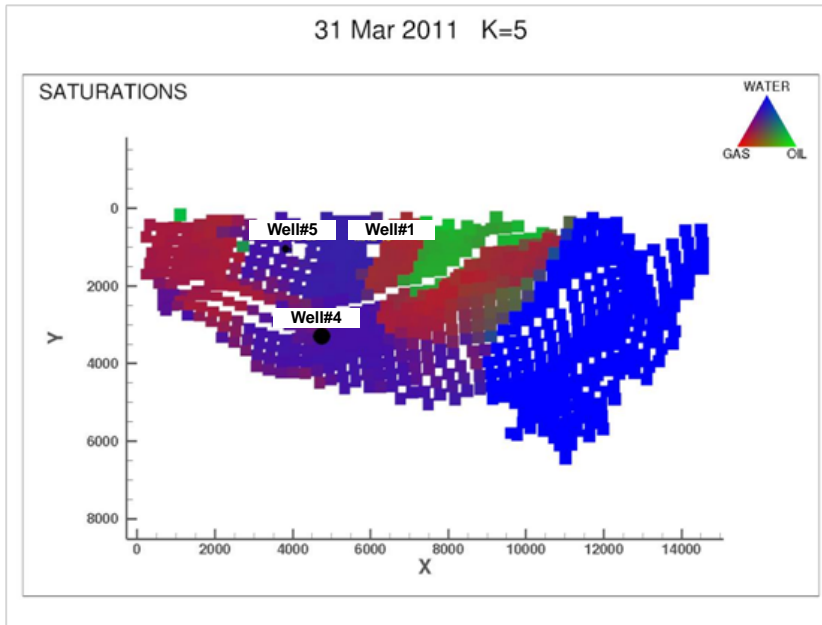


**Figure 26.** End of History Saturations.

### Conclusions and Recommendations

As a result, the following conclusions and recommendations were arrived at:

1. In a brown field development, with good judgment, most forms of data were honored and to the maximum possible extent. It was a given that there were errors in data measurement, but these errors could not be consistently wrong for a long period of time. The drastic variation of API held a lot of information in the end and proved this point.
2. Generally, two drive mechanisms can be present in any reservoir and are more

common. Sometimes these drives can be induced to efficiently produce the reservoir. Alternatively, these drive mechanisms maybe apparent in commercial tools, like *MBAL*<sup>™</sup>, model which have a theoretical basis of showing them. What becomes more challenging is to identify the drives that are outside the general scope of these commercial softwares. This requires more critical thinking and forces one to study and understand the impact they create on reservoir performance.

3. There was a very subtle difference between fault leakage and presence of small aquifer. In this simulation study, we could not arrive at a definitive conclusion early on. The only way the idea got implemented eventually in the simulation model was by incorporating oil-water contact in the saddle area. All these challenges encountered broke the myth that only large reservoirs are the ones which are most complicated.
4. Repressurization during water flood in this reservoir would yield good results only when each drive of the reservoir was identified and steps taken to mitigate the downside associated with each one of them. For this reservoir, controlled expansion of secondary gas cap was the only viable option, knowing that the reservoir is severely pressure-depleted.
5. Team approach for such simulation studies is a given, but what makes it successful is the iterative process amongst various disciplines during history matching. This was seen in this study when use of production data was favored over well log data.



## CHAPTER III

### SIMULATION STUDY OF LIQUIDS-RICH, VOLATILE OIL UNCONVENTIONAL RESERVOIR – FOCUS ON RESERVOIR DRIVE MECHANISMS

#### Introduction and Stimulated Rock Volume Description

All unconventional reservoirs need to be stimulated so that they can produce at economical rates. As a result of this stimulation of the unconventional reservoir, the traditional bi-winged hydraulic fracture, may not be formed. Based on the micro-seismic

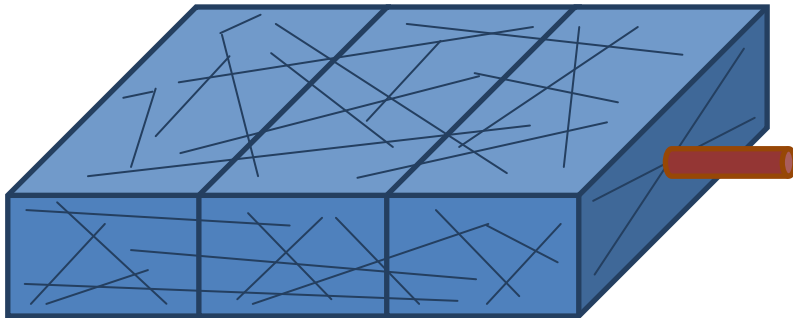


**Figure 27.** Unconventional Reservoir Having Natural and Transverse Fractures.

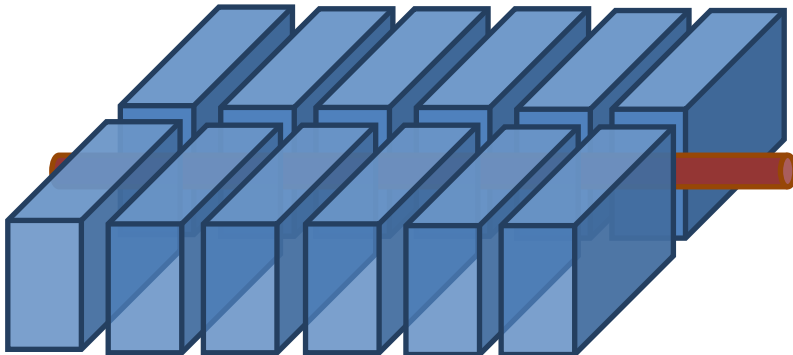


**Figure 28.** Dual Porosity Mathematical Idealization of Above.

data and its mapping, as a result of the fracturing process, dendric fracture swarms are formed instead and these are mathematically modeled best as dual porosity reservoirs. This means that there is a matrix domain which feeds into the fracture domain. The physical reservoir is as shown in the figure 27 whereas the idealized mathematical version is shown in figure 28. Since the matrix is very low permeability, only the stimulated part of the whole reservoir is taken into consideration. For the purpose of our mathematical modeling, this extends upto the fracture half-length, as represented in the figure above, and is called Stimulated Rock Volume (SRV). The fluid flow in these kind of highly anisotropic reservoirs exhibit predominantly linear flow regime. For a dual porosity system it is adequate to represent this regime with slab geometry as shown (1D linear flow only). The horizontal well is assumed to be infinite conductivity, the SRV length equal to the length of the horizontal well and with the convergence effect of the fluid flow accounted for additionally.

The SRV also acts as a control volume which forms the basis of defining the bulk properties. For a dual porosity system, the matrix and the fracture are not described by their intrinsic properties. The bulk properties, such as porosity and permeability, are obtained from intrinsic properties as:

$$\varphi_{mb} = \left( \frac{V_{rm}}{V_{rf+rm}} \right) \varphi_m \dots\dots\dots(3-1)$$

$$k_{mb} = \left( \frac{V_{rm}}{V_{rf+rm}} \right) k_m \dots\dots\dots(3-2)$$

The dimensionless storativity,  $\omega$ , and interporosity flow parameter,  $\lambda$ , are:

$$\omega = \left( \frac{\varphi_{fb} c_f}{\varphi_{fb} c_f + \varphi_{mb} c_m} \right) \dots\dots\dots(3-3)$$

$$\lambda = \left( \frac{\alpha k_{mb} A_{cw}}{k_{fb}} \right) \dots\dots\dots(3-4)$$

Where  $\alpha$  is the matrix-fracture shape function which is dictated by the geometry of the block.  $c_f$  and  $c_m$  are the compressibilities of the fracture and matrix respectively.  $\lambda$ , is based on area,  $A_{cw}$ , rather than,  $r_w^2$ , for an unconventional reservoir with linear flow.

### Matrix Fracture Fluid Exchange

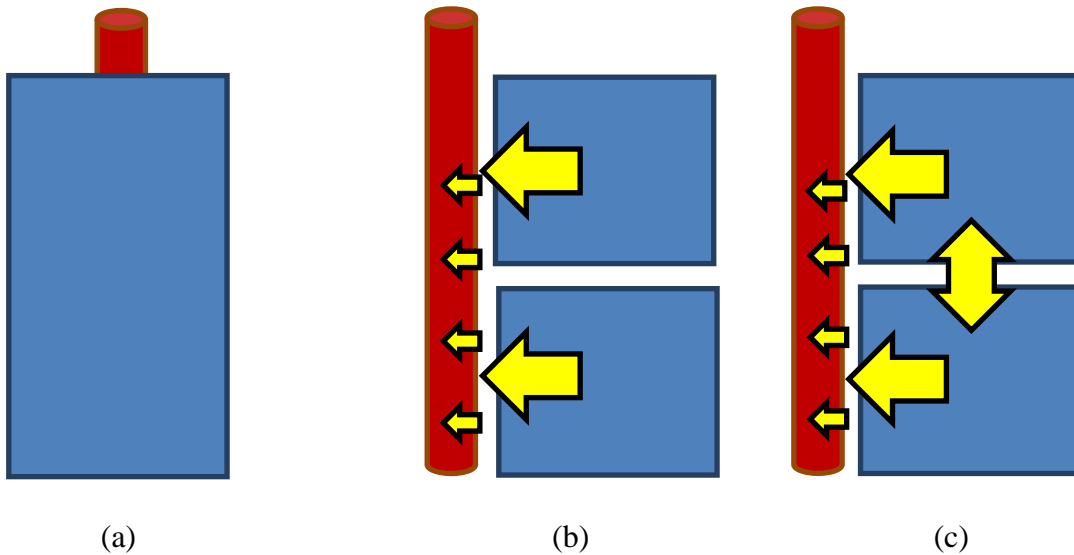


**Figure 29.** Single and Various Dual Porosity Reservoir Comparison.

The basic premise of dual porosity reservoir is that the oil is in the matrix whereas the fracture system is present to connect it to the wellbore. Based on this fact, natural fracture reservoirs, in comparison to single porosity (as shown in figure 29(a)), are classified as:

- (a) Dual Porosity – Matrix communicates with the wellbore through the fracture only figure 29(b).
- (b) Dual Permeability – Matrix communicates with the wellbore as well as with others figure 29(c).

Simply stated the naturally fractured reservoirs have got two boundaries which have got an important bearing as to how these reservoirs are going to produce. These are:

1. Boundary demarcating the matrix blocks.
2. Boundary demarcating the edge of the reservoir.

In Warren and Root model<sup>29</sup>, the most common of the dual porosity mathematical idealizations for naturally fractured reservoirs, first boundary goes into the geometric term represented by as the shape function. The other, boundary of the SRV, then sets the second boundary for an unconventional reservoir. This makes the study of unconventional reservoir different from conventional reservoir as it is assumed that the reservoir beyond the SRV does not contribute significantly for the whole production period, assumed to be 20-30 years.

For the purpose of this research we will assume that an SRV behaves like a dual porosity system rather than a dual permeability system. This is based on the fact that the

size and the magnitude of permeability of the matrix block is not big enough for dual permeability effect to make a significant contribution.

*Matrix Material Balance*

In order to solve for a dual porosity, the ideal way would be to discretize the fracture and the matrix separately with a computational mesh. This is not possible in practice because the level of detailed information required for building such a mesh is not always available. Though it is possible to discretize the matrix with average parameters, as is done using MINC<sup>30</sup> method, the most common method used is the lumped-parameter model. Warren and Root model is based on this method where the underlying assumption is that the matrix is treated as a source/sink in the fracture discretized element. The strength of the source/sink is proportional to the potential difference between the local fracture and the average matrix pressure. At this point it is sufficient to say that average matrix pressure can be evaluated keeping in mind the first boundary, which is the matrix block boundary itself, as mentioned earlier. The resultant conditions are:

- (a) Pseudosteady state – Warren and Root theory is based on this assumption.
- (b) Transient – the pressure transient has not felt the effect of the boundary.

The general representation of diffusivity equation for the fracture takes the form:

$$\nabla \cdot \left( \frac{k_{rf}}{\mu} \nabla p_{rf} \right) = \left( \varphi_{rf} c_{rf} \right) \frac{\partial p_{rf}}{\partial t} + \sigma_{rm} + \sigma_{aq} \quad \dots\dots\dots(3-5)$$

where the last two terms in the above equation are referred to as the source terms and are included in the fracture equation only in dual porosity formulation. The gravitational term is neglected in the above equation.

(a) Pseudosteady state Matrix: Warren and Root (lumped-parameter approach) model assumes that, the pressure gradient of the fluid within the matrix varies linearly rather than a parabolic (typical) profile, shown in figure 30 as:

$$\left. \frac{dp_{rm}}{dz} \right|_{z=h_m/2} = \beta \frac{(\overline{p_{rm}} - p_{rf})}{h_{rm}/2} \dots\dots\dots(3-6)$$

Here  $\beta = 3$  represents the lumped parameter equation constant for the slab geometry drained from a single face of the slab.

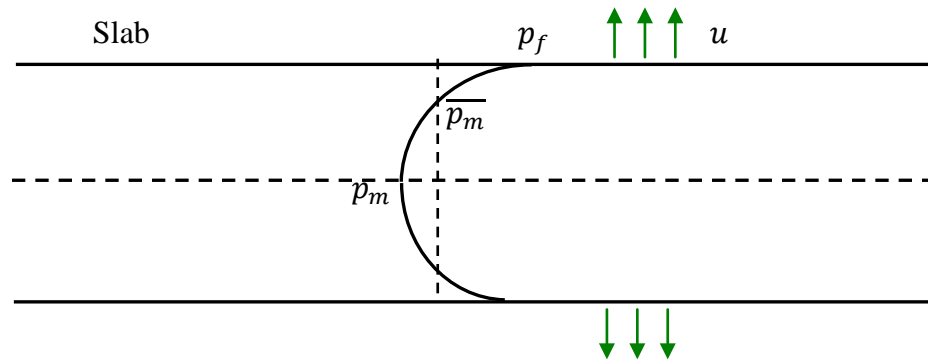


**Figure 30.** Pseudosteady State Matrix Showing Idealization of the Pressure.

Thus the flux (surface flow per unit area of the matrix fracture interface) at the surface is:

$$u = \frac{k_{rm}}{\mu} \left. \frac{dp_{rm}}{dz} \right|_{z=h_{rm}/2} = \frac{6 k_{rm}}{\mu} \frac{(\overline{p_{rm}} - p_{rf})}{h_{rm}} \dots\dots\dots(3-7)$$

In order to preserve the linearity of the fracture equation, eqn.(3-5), the total flow rate is expressed in terms of the flow per unit matrix volume as:

$$\sigma_{rm} = \left( \frac{Area}{Vol.} \right) u = \left( \frac{2}{h_{rm}} \right) \frac{dp_{rm}}{dz} \Big|_{z=h_{rm}/2} \dots\dots\dots(3-8)$$

$$\sigma_{rm} = \left( \frac{2}{h_{rm}} \right) \frac{(2 \times 3) k_{rm} (\overline{p_{rm}} - p_{rf})}{\mu h_{rm}} = \left( \frac{12}{h_{rm}^2} \right) \frac{k_{rm}}{\mu} (\overline{p_{rm}} - p_{rf}) \dots\dots\dots(3-9)$$

$$\sigma_{rm} = \alpha \frac{k_{rm}}{\mu} (\overline{p_{rm}} - p_{rf}) \dots\dots\dots(3-10a)$$

$$\sigma_{rmf} = \sigma_{rm} A_{cw} = \lambda_{rmf} (\overline{p_{rm}} - p_{rf}) \dots\dots\dots(3-10b)$$

Where  $\alpha = \left( \frac{12}{h_{rm}^2} \right) \dots\dots\dots(3-11a)$

And,  $\lambda_{rmf} = \alpha \left( \frac{k_{rm}}{k_{rf}} \right) A_{cw} \dots\dots\dots(3-11b)$

Here  $\alpha$  is the shape factor for the slab and converts the flow rate to flow per unit matrix volume and  $\lambda_{rmf}$  is the interporosity flow parameter after algebraic rearrangement of fracture equation is done to make it dimensionless. Also,  $\sigma_{rmf}$  is the source term (after algebraic manipulation of fracture equation) assuming single phase flow. For matchstick (cylinder, n = 2) and cube (sphere, n = 3) is:

$$\alpha = \frac{4n(n+2)}{h_{rm}^2} \dots\dots\dots(3-12)$$

(b) Transient Matrix: The underlying assumption of pseudosteady state Warren and Root model is not true under transient state. The solution of transient matrix was first put forth by deSwan<sup>31</sup> and by Kazemi<sup>32</sup> (slab). Similar to Warren and Root model, Kazemi's model allows for all the flow regimes, transient, late transient and pseudosteady state.

For the slab matrix, the diffusivity equation is:

$$\nabla \cdot \left( \frac{k_{rm}}{\mu} \nabla p_{rm} \right) = (\phi_{rm} c_{rm}) \frac{\partial p_{rm}}{\partial t} \dots \dots \dots (3-13)$$

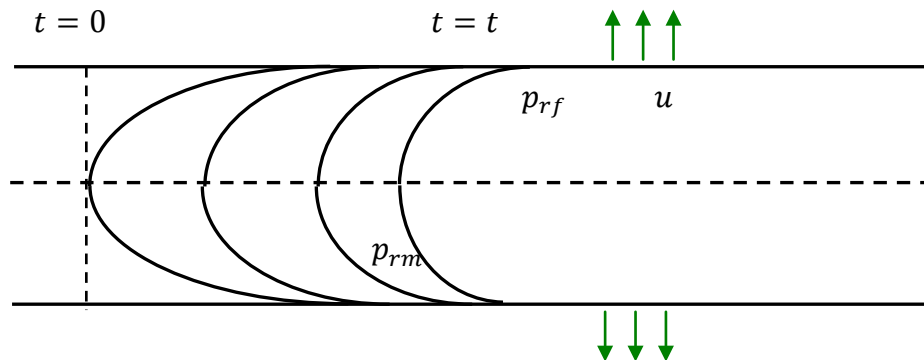


**Figure 31.** Matrix Pressure Transient as it Travels from  $t = 0$  to  $t = t$ .

The initial and boundary conditions are:

Initial Condition:  $p_{rm}(z, t = 0) = p_i$

Inner Boundary Condition:  $\frac{\partial p_{rm}}{\partial z} \Big|_{z=0} = 0$  for all  $t$

Outer Boundary Condition:  $p_{rm} \Big|_{z=\frac{h_m}{2}} = p_f$  for all  $t$



Again, the flux (surface flow per unit area of the matrix fracture interface, figure 31) at the surface of the slab is given by:

$$u = \frac{q}{A} \Big|_{interface} = \frac{k_m}{\mu} \frac{dp_m}{dz} \Big|_{z=h_m/2} \dots\dots\dots(3-14)$$

and in order to preserve the linearity of the fracture equation the total flow rate is expressed in terms of the flow per unit matrix volume as:

$$\sigma_m = \left( \frac{Area}{Vol.} \right) u = \left( \frac{2}{h_m} \right) \frac{dp_m}{dz} \Big|_{z=h_m/2} \dots\dots\dots(3-15)$$

For the transient solution this is solved in such a way that the formulation of  $\alpha$  and  $\lambda$  is common to both pseudosteady state and transient (refer Appendices).

### **Aquifer Fracture Fluid Exchange**

Although the above section relates the transfer of fluid between the matrix and the fracture, a similar method can be used for two phase aquifer (matrix) and the reservoir (fracture) flow. Hence the name Dual Porosity (Fracture-Aquifer), Dual Mobility (Oil-Water) Model. As the aquifer is not in communication with the well it is a limiting form of this Dual Permeability Model (two layer model). For all purposes, this is a limited aquifer which means its size is comparable to that of the reservoir. It acts like matrix. This method is similar to one proposed by Ehlig-Economides and Ayoub<sup>33</sup> (dual

permeability case – two layer commingled production, single perforated layer, figure 32(a)) based on radial diffusivity equation. This model is based on linear flow with

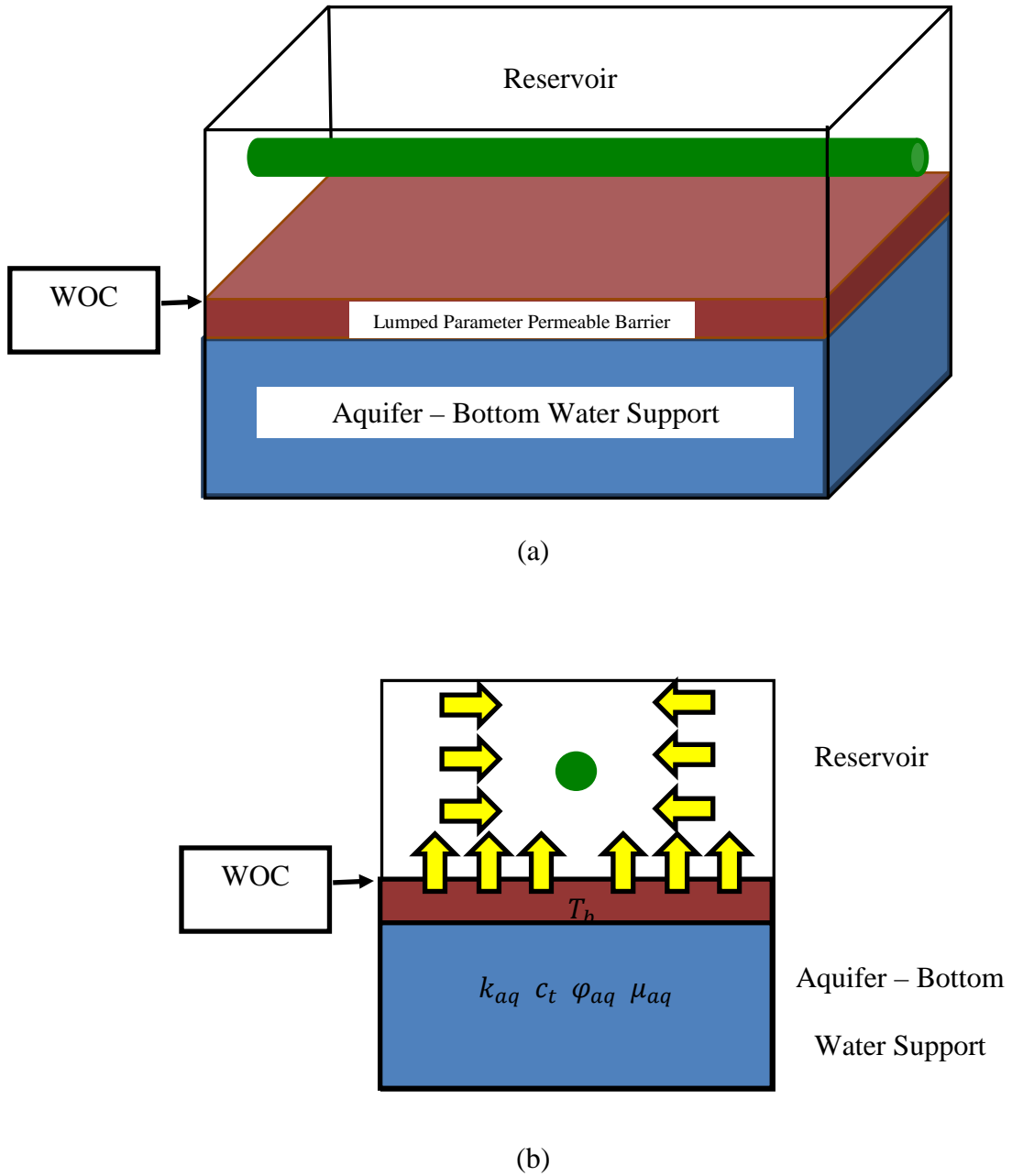


**Figure 32.** Linear Flow Model for Reservoir and Aquifer.

aquifer at the bottom layer and production happening from top layer (flow is unidirectional for aquifer and bidirectional for oil in case of slab formulation). The direction of the linear flow is described in the figure 32(b). The notation and outline of this section is similar to that used by Stewart<sup>34</sup>.

As it is a dual porosity (limiting dual permeability) model the fluid flow occurs in the fracture (top layer) and eqn.(3-5) is the governing differential equation. Both the matrix and the aquifer are treated as source terms which are represented in that equation with the underlying assumption that water-oil contact (WOC) does not move. This is a fair assumption for unconventional reservoir.

The main difference is the way matrix source term is accounted for in the fracture equation (as elaborated in the previous section). Here the lumped parameter effective (permeable) barrier is introduced, between the reservoir and the aquifer. This approach helps is in quantifying the crossflow in terms of barrier and aquifer properties.

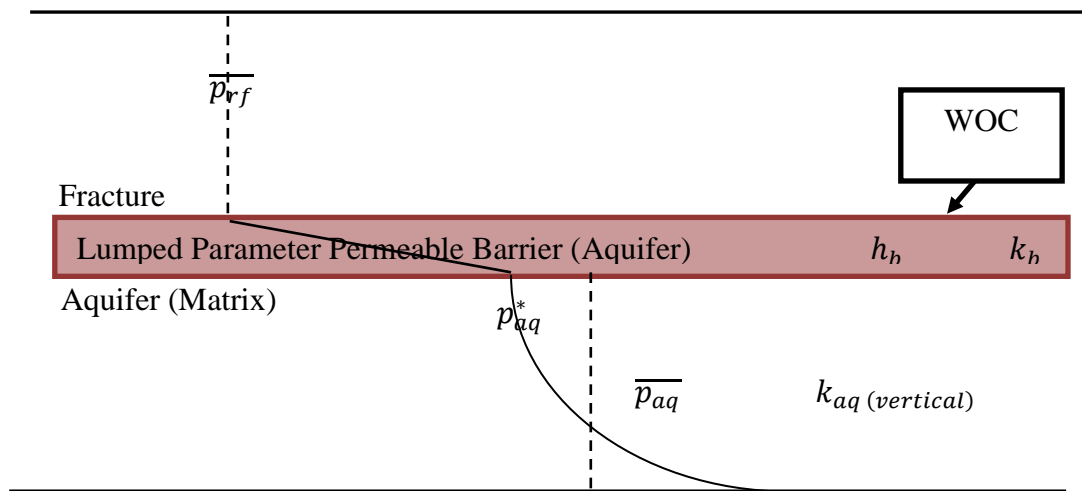


**Figure 33.** The Lumped Parameter Permeable Barrier between Aquifer and Reservoir.

The implied meaning of the barrier is that the reservoir (fracture), as shown in figure 33, can be in pseudosteady state or transient with aquifer, which itself either could be in pseudosteady state or transient. Simply stated, the reservoir (fracture) flow regime can be different from the flow regime of the aquifer. Since only reservoir (fracture) is perforated, both of these act as a single unit and most parameters are combination of variables. Also this barrier has negligible storage capacity and, again, the fluid exchange only happens through top face of aquifer.

(a) Pseudosteady state Aquifer: As stated earlier, this means WOC does not move.

The crossflow flux between the barrier and the aquifer (for simplicity assume single phase flow) is given by:

$$u = \frac{k_b}{\mu_{aq}} \frac{(p_{aq}^* - \bar{p}_{rf})}{h_b} = \beta \frac{k_{aq}}{\mu_{aq}} \frac{(\bar{p}_{aq} - p_{aq}^*)}{h_{aq}} \dots\dots\dots (3-15)$$

For two phase flow, see Appendix. Eliminating  $p_{aq}^*$  from the above equation we get:

$$u = \frac{(\bar{p}_{aq} - \bar{p}_{rf})}{\frac{1}{\left(\frac{k_b}{\mu_{aq} h_b}\right)} + \frac{1}{\left(\frac{\beta k_{aq}}{\mu_{aq} h_{aq}}\right)}} = \frac{\left(\frac{k_b}{\mu_{aq} h_b}\right)}{1 + \left(\frac{k_b h_{aq}}{\beta k_{aq} h_b}\right)} (\bar{p}_{aq} - \bar{p}_{rf}) = \frac{(T_b)_{eff}}{\mu_{aq}} (\bar{p}_{aq} - \bar{p}_{rf}) \dots\dots (3-16)$$

Where,

$$(T_b)_{eff} = \frac{\left(\frac{k_b}{h_b}\right)}{1 + \left(\frac{k_b h_{aq}}{\beta k_{aq} h_b}\right)} = \left[ \frac{T_b}{1 + \left(\frac{T_b h_{aq}}{\beta k_{aq}}\right)} \right] = \left[ \frac{1}{\frac{1}{T_b} + \left(\frac{h_{aq}}{\beta k_{aq}}\right)} \right] \dots\dots\dots (3-17)$$

$$T_b = \frac{k_b}{h_b} \dots\dots\dots(3-18)$$

Here  $\beta = 3$  and  $\frac{1}{T_b}$  is called the lumped parameter barrier resistance which can now be assumed very small (as compared to the second term in denominator). In order to preserve the linearity of the fracture equation, eqn.(3-5), the total flow rate for the aquifer is expressed in terms of the flow per unit aquifer volume and is similar to eqn.(3-10), as:

$$\sigma_a = \underline{\alpha} \left( \frac{k_{aq}}{\mu_{aq}} \right) (\overline{p}_{aq} - \overline{p}_{rf}) \dots\dots\dots(3-19a)$$

$$\sigma_{aq} = \sigma_a A_{cw} = \lambda_{aqf} (\overline{p}_{aq} - \overline{p}_{rf}) \dots\dots\dots(3-19b)$$

Here,  $\underline{\alpha}$ , is the aquifer-fracture shape function. From eqn.(3-16) and eqn.(3-19):

$$\underline{\alpha} = \frac{(T_b)_{eff}}{k_{aq}} \dots\dots\dots(3-20)$$

And, 
$$\lambda_{aqf} = \underline{\alpha} \left( \frac{k_{aq}}{k_{rf}} \right) A_{cw} = \left( \frac{(T_b)_{eff}}{k_{rf}} \right) A_{cw} \dots\dots\dots(3-21)$$

(b) Transient Aquifer: By definition transient aquifer means that the WOC is moving. The dual mobility model, which forms the basis of this reservoir-aquifer model, is not designed to handle relative permeability effects due to change in

saturation in the oil (reservoir) zone. The assumption being made here is the aquifer will move only the distance equal to the thickness of lumped parameter effective (permeable) barrier for the life of the well. This assumption is being made to as realistically capture the effect of bottom water as possible. Again, the barrier has negligible storage capacity and zero resistance (it is incorporated mathematically in the transient model through eqn.(3-23b)).

We start with the diffusivity equation, for the slab matrix, as:

$$\nabla \cdot \left( \frac{k_{aq}}{\mu_{aq}} \nabla p_{aq} \right) = (\varphi_{aq} c_{aq}) \frac{\partial p_{aq}}{\partial t} \dots\dots\dots (3-22)$$

The gravitational term is neglected. The initial and boundary conditions are:

Initial Condition:  $p_{aq}(z, t = 0) = p_i$

Inner Boundary Condition:  $\left. \frac{\partial p_{aq}}{\partial z} \right|_{z=0} = 0$  for all t

Outer Boundary Condition:  $p_{aq}|_{z=h_{aq}} = p_f$  for all t

Again, the flux (surface flow per unit area of the matrix fracture interface) at the surface of the slab is given by (for simplicity we are not accounting for two phase flow between matrix and aquifer here):

$$u = \frac{k_{aq}}{\mu} \left. \frac{\partial p_{aq}}{\partial z} \right|_{z=h_m} \dots\dots\dots (3-23a)$$

Here: 
$$k_{aq} = \frac{(h_a+h_b)}{\left(\frac{h_b}{k_b} + \frac{h_a}{k_a}\right)} (h_a \gg h_b, k_b \gg k_a) \dots\dots\dots(3-23b)$$

and in order to preserve the linearity of the fracture equation the total flow rate is expressed in terms of the flow per unit matrix volume (with flow from one surface only) as:

$$\sigma_{aq} = \left(\frac{Area}{Vol.}\right) u = \left(\frac{1}{h_{aq}}\right) \left[\frac{k_{aq}}{\mu} \frac{\partial p_{aq}}{\partial z} \Big|_{z=h_m}\right] \dots\dots\dots(3-24)$$

For the transient solution the governing differential equation is solved in such a way that it results in  $\underline{\alpha}$  that is common to pseudosteady state formulation (refer Appendices for details of single phase and two phase flow). The final form for single phase flow is:

$$\sigma_{aq} = \left(\frac{1}{h_m^2}\right) \frac{k_{aq} A_{cw}}{k_{fb}} \frac{\partial p_{aqD}}{\partial z_D} \Big|_{z_D=1} = \left(\frac{\lambda_{aq}}{12}\right) \frac{\partial p_{aqD}}{\partial z_D} \Big|_{z_D=1} \dots\dots\dots(3-25)$$

$$\lambda_{aq} = \left(\frac{12}{h_{aq}^2}\right) \frac{k_{aq} A_{cw}}{k_{fb}} \dots\dots\dots(3-26)$$

$$\underline{\alpha} = \left(\frac{1}{h_m^2}\right) \dots\dots\dots(3-27)$$

## Concept of Proppant Number – Single Porosity versus Dual Porosity

Effectiveness of any stimulation operation is judged by the amount of stimulation achieved. The implied meaning here is achieve an optimal propped volume in the reservoir. This propped volume is directly responsible for the performance of the well in the reservoir. It will be discussed next and how the idea is extended to dual porosity taken thereafter.

### *Single Porosity Reservoir*

For these kind of reservoirs, the well performance using constant propped volume concept, has been extensively documented by Oligney *et al*<sup>35</sup>, Valko<sup>36</sup>, Amini<sup>37</sup>, etc. to name a few. This section describes the gist of that constant propped volume concept.

Any fracture formed in the reservoir has got two competing dimensions fighting for the same resource if the volume of the reservoir is fixed. The best way to formulate the problem (maximize the deliverability of the reservoir) is to make the formulation in the form of dimensionless variables. Two important parameters are, the penetration ratio,  $I_x$ , and the dimensionless fracture conductivity,  $C_{fD}$ .

$$I_x = \frac{2 x_f}{x_e} \dots\dots\dots (3-28)$$

$$C_{fD} = \frac{k_f w}{k x_f} \dots\dots\dots (3-29)$$



Having a fixed volume of reservoir (permeability,  $k$ ) and with fixed amount of proppant (which fixes the propped volume) together with the knowledge of proppant properties (e.g proppant permeability,  $k_f$ ), this concept states that there only one way of maximizing production for the well. This is based on knowing the dimensionless Proppant Number,  $N_p|_{S\varphi}$ , for a given  $C_{fD}$ . Specifically it states there is only one value of dimensionless fracture conductivity,  $C_{fD}$ , for a given Proppant Number,  $N_p|_{S\varphi}$ , which will give maximum dimensionless productivity,  $J_D$ . The Proppant Number is defined as the permeability weighted fraction of the volume of fracture,  $V_f$ , with the volume of the reservoir,  $V$ , and is defined as:

$$N_p|_{S\varphi} = \left(\frac{2k_f}{k}\right) \left(\frac{V_f}{V}\right) \dots\dots\dots(3-30)$$

Also expressed as:

$$N_p|_{S\varphi} = \frac{4k_f x_f w}{k x_e^2} = I_x^2 C_{fD} \dots\dots\dots(3-31)$$

To simplify the process of selecting the optimum fracture Romero<sup>38</sup> has constructed graphs of  $J_D$  versus  $C_{fD}$  for different  $N_p|_{S\varphi}$  values.

If we were to analyze what eqn.(3-31) essentially does, we have to start with approximate solution of linear flow of a finite conductivity hydraulically fractured well at the center of the fracture as given by Raghavan<sup>39</sup>. The reservoir width is  $2x_f$  and

extends to infinity in the direction perpendicular to the fracture surface and the governing differential equation of fluid flow in Laplace domain is:

$$\frac{d^2 \overline{p}_{fD}}{dx_D^2} - \left( \frac{2}{C_{fD}\sqrt{s}} + \frac{1}{\eta_{fD}} \right) s \overline{p}_{fD} = 0 \dots\dots\dots(3-32)$$

where  $s$  is the Laplace space variable and  $\eta_{fD}$  is the dimensionless diffusivity ratio as:

$$\eta_{fD} = \frac{\eta_f}{\eta} = \frac{\varphi_f c_f k}{\varphi c k_f} \dots\dots\dots(3-33)$$

It is important to realize that apart from this differential equation, eqn.(3-31), being subjected to a boundary condition and initial condition, it is also subjected to the outer boundary condition that the reservoir is bound at  $y_D \rightarrow \infty$ . For a low or very low permeability reservoir this implies that the pressure away from the fracture in the reservoir would be approaching initial pressure at some finite distance  $y_D \neq \infty$ . Assuming that distance to be  $y$  and on rearranging eqn.(3-32) we get:

$$\frac{d^2 \overline{p}_{fD}}{dx_D^2} - 2 \left( \frac{1}{C_{fD}\sqrt{s}} + \frac{1}{2} Np \left( \frac{V}{V_f} \right)^2 \right) s \overline{p}_{fD} = 0$$

$$\frac{d^2 \overline{p}_{fD}}{dx_D^2} - 2 \left( \frac{1}{C_{fD}\sqrt{s}} + \frac{1}{2} Np \left( \frac{y}{w} \times \frac{x}{x_f} \times \frac{h}{h} \right)^2 \right) s \overline{p}_{fD} = 0$$

As this equation is one dimensional and independent of  $y$ , and  $\frac{y}{w}$  acts as constant, yields:

$$\frac{d^2 \overline{p_{fD}}}{dx_D^2} - 2 \left( \frac{1}{C_{fD} \sqrt{s}} + \text{Const.} \frac{N_p |s \varphi}{l_x^2} \right) s \overline{p_{fD}} = 0 \dots\dots\dots (3-34)$$

and is of the form:

$$\frac{d^2 \overline{p_{fD}}}{dx_D^2} - sf(s) \overline{p_{fD}} = 0 \dots\dots\dots (3-35)$$

where,

$$f(s) = 2 \left( \frac{1}{C_{fD} \sqrt{s}} + \text{Const.} \frac{N_p |s \varphi}{l_x^2} \right) \dots\dots\dots (3-36)$$

is the fracture function. This implies eqn.(3-36), together with eqn.(3-31), forms a constant (one variable) coefficient linear differential equation inside the Laplace domain. This shows Proppant Number essentially a variable of the differential equation, the solution of which gives the value of  $J_D$ . Alternatively, eqn.(3-36) can be expressed in terms of the dimensionless reservoir fracture fluid exchange term, the dimensionless fracture conductivity  $C_{fD}$ . This idea will now be useful in describing Proppant Number in dual porosity well performance and will be helpful in extending to it.

*Dual Porosity Reservoir*

For dual porosity reservoir, under transient and hydraulically fractured horizontal well in a low permeability reservoir, the governing differential equation for linear flow is given by Bello. The pseudosteady version, in the Laplace domain, is given as (See Appendix for details):

$$\frac{\partial^2 \overline{p}_{fD}}{\partial x_D^2} - sf(s)\overline{p}_{fD} = 0 \dots\dots\dots(3-37)$$

Where,

$$f(s) = \frac{\omega(1-\omega)s+\lambda}{(1-\omega)s+\lambda} \dots\dots\dots(3-38)$$

is called fracture function and is same to Warren and Root model. Eqn.(3-38) is be rearranged as:

$$f(s) = \frac{1+s\left(\frac{\omega}{\lambda}\right) - s\omega\left(\frac{\omega}{\lambda}\right)}{1+\frac{s}{\omega}\left(\frac{\omega}{\lambda}\right) - s\left(\frac{\omega}{\lambda}\right)} \dots\dots\dots(3-39)$$

Here  $\lambda$  is the dimensionless interporosity flow parameter (pseudosteady state),

$$\lambda = \alpha A_{cw} \frac{k_{mb}}{k_{fb}} \dots\dots\dots(3-40)$$

And  $\omega$  is the dimensionless storativity coefficient,

$$\omega = \frac{\varphi_{fb} c_f}{(\varphi c_t)_{m+f}} \dots\dots\dots(3-41)$$

Here  $A_{cw}$  is the area of cross-section of the reservoir at the horizontal well,  $\alpha$ , is the pseudosteady state shape function which is a geometric term and takes into account the surface area responsible for the fluid exchange to occur between the matrix and the fracture,  $k_{mb}$ ,  $k_{fb}$ , are the bulk volume adjusted permeabilities of the matrix and fracture block,  $\varphi_{fb}$ ,  $\varphi$ , are the bulk volume adjusted pore volumes.

Just as in eqn.(3-35),  $f(s)$ , the fracture function depends on a single parameter  $\left(\frac{\lambda}{\omega}\right)$ . Again just as in single porosity, this  $f(s)$  term is essentially based mainly on interporosity fluid exchange term,  $\lambda$ , which captures the physics of the flow between matrix and the fracture. In comparison,  $\omega$ , is a pure number which gives the ratio of the volume of fracture to the total volume. But when it is combined with  $\lambda$  it becomes a permeability weighted ratio of volume of fracture to the total volume of the reservoir, which is Proppant Number for dual porosity reservoirs. In order to have direct proportionality (rather than inverse proportionality) with interporosity flow parameter, we define it as:

$$\frac{1}{N_p|_{D\varphi}} = \left(\frac{\omega}{\lambda}\right) = \left(\frac{k_{fb}}{\alpha A_{cw} k_{mb}}\right) \left(\frac{V_f}{V}\right) \dots\dots\dots (3-42)$$

This Dual Porosity Proppant Number is defined as volume weighted, dimensionless surface flux transferred from a unit area of matrix to the fracture, per unit matrix volume. It is used for pseudosteady state and transient models in the present form (although  $\lambda$  has

different formulations for transient, by many authors). As it is not the same as its single porosity counterpart, there are two important points which need to be mentioned here:

1. This formulation has the permeability of the matrix block as well as the shape factor which specifies the surface area needed for the fluid exchange to occur. The shape factor can be constant/vary and the permeability of matrix block can remain constant/vary and the resultant Proppant Number can be the same. Throughout this entire study we are assuming shape factor for slab which corresponds to linear flow between the matrix and fracture.
2. If we are drawing a parallel with single porosity scenario, one cannot exclusively define dimensionless fracture conductivity  $C_{fD}$  in a dual porosity case. Firstly, there are natural fractures present which means ideally we will have to define  $C_{fD}$  for both natural and hydraulic fractures. This is not practical or even possible. Secondly here, for the SRV, the length of the fracture(s) generated is always equal to the width of the reservoir which means  $I_x = 1$ . If we were to generalize this means,  $\lambda$ , has the essential elements of  $C_{fD}$ , both for natural as well as hydraulic, when it comes to dual porosity reservoirs. But in a strict sense, eqn.(3-31) cannot be used as a definition of Proppant Number for dual porosity models.

## **Reservoir Drive Mechanisms in Unconventional Reservoir and its Impact**

Based on the previous sections we can know that there are essentially two kinds of boundary conditions – pseudosteady state and transient. If we assume that the reservoir (the SRV in this case) is not subjected to any other boundary condition then the reservoir is under volumetric depletion. For the SRV if there is an aquifer underlying it, then we can have various combinations of these boundary conditions, the interactions of which lead to different reservoir performance that are classified as drive of the reservoir. The idea here is that, unlike conventional reservoirs where water-oil contact (WOC) can be present within the reservoir, for unconventional reservoir no such WOC is envisaged. The unconventional reservoir thickness is small and it is being supported by a limited aquifer. Since shales are supposed to be source rocks of conventional reservoirs, the simplest of the mathematical models which can be constructed is the one where it lies over a formation that has water. The big picture scenario is that the long term deliverability of these reservoirs (SRVs) changes from that of pure volumetric depletion. If all other rock and fluid parameters, such as permeability, viscosity, etc., are known then the measure of long term deliverability is the variation of Dimensionless Productivity Index,  $J_D$ , with time. Thus the volumetric depletion case forms one of the limiting cases where the aquifer is assumed to be zero. The presence of ‘Bottom Water’ drive, which can either be pseudosteady state or transient, has its own effect which can be classified as ‘weak’ or ‘strong’ depending on mobility,  $\left(\frac{k_{aq}h_{aq}}{\mu_{aq}}\right)$ , value of the aquifer.

Hence we have:

1. Volumetric Depletion – Underlying aquifer is altogether absent.
2. Weak Bottom Water Drive – If  $\mu_{rf} < \mu_{aq}$  then mobility of the oil in the reservoir is greater than the mobility of water in the fracture,  $\left(\frac{k_{rf}h_{rf}}{\mu_{rf}}\right) > \left(\frac{k_{aq}h_{aq}}{\mu_{aq}}\right)$ , then the bottom water has a weak water drive. The aquifer can be pseudosteady state or transient.
3. Strong Bottom Water Drive – If  $\mu_{rf} > \mu_{aq}$  then mobility of the oil in the reservoir is less than the mobility of water in the fracture,  $\left(\frac{k_{rf}h_{rf}}{\mu_{rf}}\right) < \left(\frac{k_{aq}h_{aq}}{\mu_{aq}}\right)$ , then the bottom water has a strong water drive. Again, the aquifer can be pseudosteady state or transient.
4. Infinite (Steady State) Aquifer – If  $\left(\frac{k_{rf}h_{rf}}{\mu_{rf}}\right) \ll \left(\frac{k_{aq}h_{aq}}{\mu_{aq}}\right)$  that happens if  $h_{rf} \ll h_{aq}$  and implies  $\kappa_f \rightarrow 0$ . This is not covered as a topic as it is the limiting case of strong water drive.

The important point to be noted here is that the magnitude of  $kh$  will also determine whether a strong or a weak water drive is present. This is where it impacts the long term deliverability of the reservoir. The presence of water may not appear significant at first or the fractured horizontal well may not produce water at all but it will make its presence felt during the productive life of the well. Thus, in the end it can be said the aquifer (bottom water), can be in pseudosteady state or transient, which has to



be combined with the rock ( $k$ ) or ( $h$ ) parameters and the fluid parameter ( $\mu$ ), to know the drive of the reservoir. Pictorially this is shown in figure 32(b), and in Table 7 as:

**Table 7.** Various Possible Aquifer Drive Mechanisms for Fractured Horizontal Well.

Boundary Condition	Pseudosteady State		Transient	
	Reservoir			
Fracture	Weak ✓	Strong ✓	Weak ✓	Strong ✓
Aquifer	Strong ✓	Weak ✓	Strong ✓	Weak ✓

Based on Table 7 we have four different models to incorporate these boundary conditions and the reservoir drive mechanisms, which are incorporated with the help of the parameters in eqn.(3-43) and eqn.(3-44) and their relative magnitude with each other. An important point which needs to be discussed here are the two areas,  $A_{cw}$ , and ,  $A$ . The former is responsible for the dimensionless pressure response whereas the latter is responsible for dimensionless productivity index calculations, to be discussed in subsequent section.

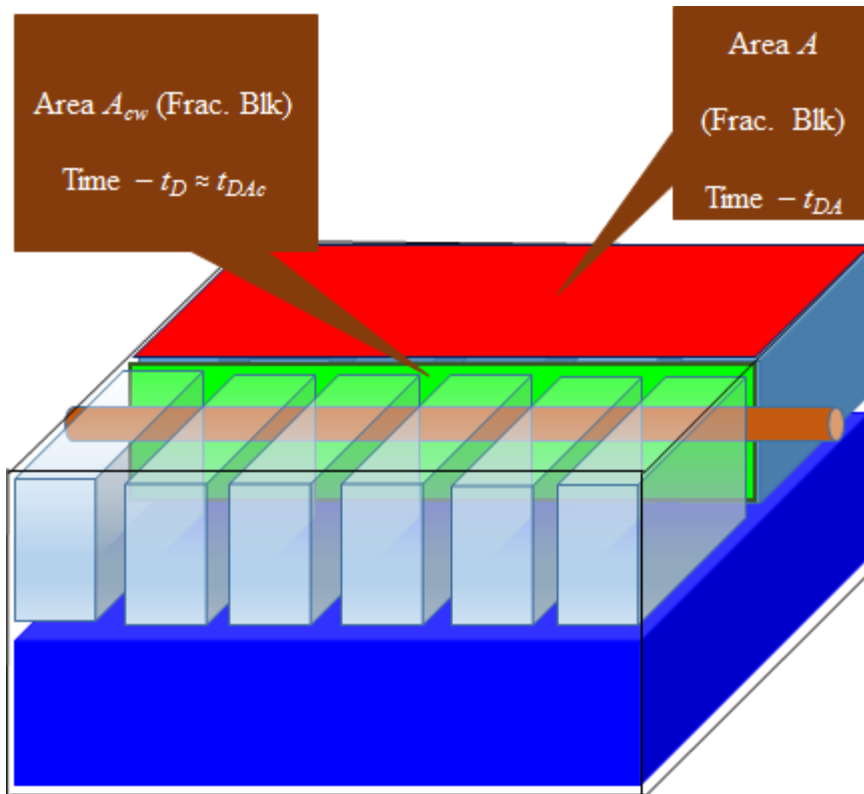


**Figure 34.** Mathematical Idealization of SRV with Aquifer Support  $A_{cw}$  (green) and  $A$  (red).

$$\kappa_{raq} = \left( \frac{\frac{k_{aq} h_{aq}}{\mu_{aq}}}{\frac{k_{rf} h_{rf}}{\mu_{rf}} + \frac{k_{rm} h_{rm}}{\mu_{rm}}} \right) \dots\dots\dots(3-43)$$

$$\kappa_{rf} = \left( \frac{\frac{k_{rf} h_{rf}}{\mu_{rf}}}{\frac{k_{rf} h_{rf}}{\mu_{rf}} + \frac{k_{rm} h_{rm}}{\mu_{rm}}} \right) \dots\dots\dots(3-44)$$

The other various parameters are defined as:

$$\omega_{rf} = \frac{\varphi_{rm} h_{rm}}{\varphi_{rf} h_{rf} + \varphi_{rm} h_{rm}} = 1 - \omega_{rm} \dots\dots\dots(3-45)$$

$$\omega_{raq} = \frac{\varphi_{aq} h_{aq}}{\varphi_{rf} h_{rf} + \varphi_{rm} h_{rm}} \dots\dots\dots(3-46)$$

$$t_D = \left( \frac{\left( \frac{k_{fb} h_{fb}}{\mu_{fb}} + \frac{k_{aq} h_{aq}}{\mu_{aq}} \right) t}{(\varphi_{fb} h_{fb} + \varphi_{aq} h_{aq}) c_f A_{cw}} \right) \dots\dots\dots(3-47)$$

Again, an important point to be noted here is that the governing differential equation of fluid flow in Laplace domain is based on the vertical area of flow,  $A_{cw}$ , into the horizontal well and the associated dimensionless time is,  $t_D$ , whereas for the dimensionless productivity index calculations are based on the horizontal area,  $A$ , as in figure 34, and the corresponding time is,  $t_{DA}$ , (mathematically defined in a later section).

All analytical solutions are derived under the following assumptions:

- a) Both the reservoir and matrix together with reservoir and aquifer have linear flow. The shape of the matrix is slab (linear) and not matchstick (cylindrical) or cube (sphere).
- b) Both the horizontal well and the transverse fractures are fully penetrating in a closed rectangular reservoir producing at constant rate. Both natural fractures as well as hydraulic fractures are present.
- c) The hydraulic fractures do not drain beyond the boundary of the rectangular reservoir.

- d) Flow is towards the center of the rectangular reservoir (SRV).
- e) The linear model is modified to incorporate the convergence skin for the fluid draining into the horizontal well.
- f) Each medium (reservoir and aquifer) is assumed to be homogeneous and isotropic and fluid from aquifer does not mix with that of the fracture.
- g) The average pressure of the reservoir (SRV) does not go below the bubble-point. It is possible that some gas might get liberated around the fractures which can be considered to be minimal.

The complete derivations of Laplace domain solutions are given in Appendix C (pseudosteady state) and Appendix D (Transient). The real domain solutions can be obtained by inverting using GWR algorithm<sup>40</sup>. The Warren & Root (pseudosteady state) model for linear flow is presented in Appendix A whereas Bello (linear transient flow) model is presented in Appendix B. No explanation is given in either of the topics as relevant literature is assumed to be familiar with the reference material.

#### *Full Pseudosteady State Fractured Dual Permeability Dual Mobility Model*

As mentioned earlier in this chapter, we have used dual permeability (two-layer model with cross-flow) and no perforation (horizontal well is in the upper layer) in the bottom layer. Since we are dealing with two different fluids hence it is a dual mobility model.

As shown in figure 34, (with fracture block outlined), the reservoir part itself is dual porosity model which has got its own shape function,  $\alpha$ , and interporosity flow

parameter,  $\lambda_{rmf}$ . The aquifer is connected with the fracture block only with a different shape factor,  $\underline{\alpha}$ , and its own interporosity flow parameter,  $\lambda_{aqf}$ . Mathematically they are:

$$\alpha = \left( \frac{12}{h_{rm}^2} \right) \dots\dots\dots (3-11a)$$

And, 
$$\lambda_{rmf} = \alpha \left( \frac{k_{rm}}{k_{rf}} \right) A_{cw} \dots\dots\dots (3-11b)$$

$$\underline{\alpha} = \frac{(T_b)_{eff}}{k_{aq}} \dots\dots\dots (3-20)$$

And, 
$$\lambda_{aqf} = \underline{\alpha} \left( \frac{k_{aq}}{k_{rf}} \right) A_{cw} = \left( \frac{(T_b)_{eff}}{k_{rf}} \right) A_{cw} \dots\dots\dots (3-21)$$

The fracture function for this case (see Appendix E) is given by:

$$f(s) = \left[ \left( \frac{\omega_{aq}}{\kappa_f} \right) + \lambda \left( \frac{(1-\omega)(\Lambda) \left( \frac{\kappa_{fb}}{\kappa_f} \right)}{(1-\omega)(\Lambda) \left( \frac{\kappa_{fb}}{\kappa_f} \right) s + \lambda} \right) + \left( \frac{\lambda_{aq}}{\kappa_f} \right) \left( \frac{(1-\omega_{aq})}{(1-\omega_{aq})s + \lambda_{aq}} \right) \right] \dots\dots\dots (3-48)$$

The constant rate and constant pressure solutions are attributed to El-Bambi<sup>41</sup>, are reproduced here:

$$\overline{p}_{wrfD} = \frac{2\pi}{s\sqrt{sf(s)}} \frac{\cosh(x_{De}\sqrt{sf(s)})}{\sinh(x_{De}\sqrt{sf(s)})} = \frac{2\pi}{s\sqrt{sf(s)}} \frac{1+\exp(-2y_{De}\sqrt{sf(s)})}{1-\exp(-2y_{De}\sqrt{sf(s)})} \dots\dots (3-49)$$

$$\overline{q}_{wrfD} = \frac{\sqrt{sf(s)}}{2\pi s} \frac{\sinh(x_{De}\sqrt{sf(s)})}{\cosh(x_{De}\sqrt{sf(s)})} = \frac{\sqrt{sf(s)}}{2\pi s} \frac{1-\exp(-2y_{De}\sqrt{sf(s)})}{1+\exp(-2y_{De}\sqrt{sf(s)})} \dots\dots (3-50)$$

The solution is then obtained by inverting into the real domain using GWR algorithm<sup>40</sup>.

### Dimensionless Productivity Index

Productivity index is defined as the total liquid flow rate produced for a unit pressure drawdown. For single phase flow, productivity index is given by:

$$J = \frac{q}{(\bar{p} - p_{wf})} \dots\dots\dots (3-51)$$

where  $q$  is the flowrate,  $\bar{p}$  is the average reservoir pressure and  $p_{wf}$  is the bottomhole flowing pressure. This value should be constant for a well producing at constant rate and under pseudosteady state condition. The more important implied meaning of this equation is that the boundaries of the reservoir are clearly defined for constant productivity index. Conversely, if the well is flowing under boundary dominated flow, the flowrate is variable, but productivity index is constant. Again, constant productivity index for the boundary dominated flow will only happen in presence of boundaries of the reservoir.

But in both cases, there is a preceding flow period, during which time there is transient flow. Strictly speaking there is no productivity index defined in conventional reservoirs for this flow period as it is variable. The transient period is sufficient small in comparison to either pseudosteady state flow or the boundary dominated flow. In unconventional reservoirs, the transient regime might be the only flow regime in the reservoir. If the conventional reservoir is under pseudosteady state or boundary dominated state then any decline in productivity index is attributed to damage to completion or non-reservoir related mechanical problems. Conversely, the productivity

index during transient and in an unconventional reservoir is still defined by eqn.(3-51), but its value depends on the time. The time associated with when the bottomhole measurement was made (for pseudosteady state case) or the time associated with the rate measurement was carried out (for boundary dominated case) determines the value of productivity index.

Dimensionless productivity index,  $J_D$ , is the geometric part (drainage area) of the productivity index and is defined in terms of that productivity index as:

$$J = \left( \frac{2\pi k h}{\mu B} \right) J_D \dots\dots\dots (3-52)$$

For a single phase the radial flow well deliverability equation, in terms of productivity index, transforms to:

$$J = \left( \frac{2\pi k h}{\alpha_1 \mu B} \right) \left[ \frac{1}{\ln\left(\frac{r_e}{r_w}\right) - \frac{3}{4} + s} \right] \dots\dots\dots (3-53)$$

$$J_D = \left( \frac{1}{\ln\left(\frac{r_e}{r_w}\right) - \frac{3}{4} + s} \right) \dots\dots\dots (3-54)$$

Assuming there is no damage or stimulation the skin,  $s = 0$ , vanishes and then the remaining terms are dependent on the geometry of the reservoir only.

It is not always possible to get a closed form solution of dimensionless productivity index,  $J_D$ , for all scenarios. This is especially true for a horizontal well with transverse hydraulic fractures (as described in this thesis). In order to calculate average reservoir pressure and hence calculate  $J_D$  on the basis of constant compressibility, we make an assumption that the average reservoir pressure never goes below bubble point. This is a valid assumption in most of the liquids-rich unconventional reservoirs, both under volumetric depletion (assigned life of 20 – 30 yrs.). The derivation is in Appendix (The equivalent Muskat method, takes into account variable compressibility is covered later).

Let, 
$$q_D = \frac{1}{2\pi} \left( \frac{\alpha_1 q B \mu}{k \sqrt{A_{cw}} (p_i - p_{wf})} \right) = \frac{1}{2\pi} \left[ \frac{q B \mu}{(0.001127) k \sqrt{A_{cw}} (p_i - p_{wf})} \right] \dots\dots\dots (3-55)$$

$$t_D = \frac{0.00633 k t}{\varphi \mu c_t A_{cw}} = \frac{5.615 (0.001127) k t}{\varphi \mu c_t A_{cw}} \dots\dots\dots (3-56)$$

Combining the above two equations we have:

$$q_D t_D = \frac{1}{2\pi} \left[ \frac{q B \mu}{(0.001127) k \sqrt{A_{cw}} (p_i - p_{wf})} \right] \left( \frac{5.615 (0.001127) k t}{\varphi \mu c_t A_{cw}} \right) = \frac{5.615}{2\pi} \left[ \frac{q B t}{\varphi c_t A_{cw} \sqrt{A_{cw}} (p_i - p_{wf})} \right]$$



Hence,

$$N_{pD} = q_D t_D = \frac{5.615}{2\pi} \left[ \frac{q B t}{\varphi c_t A_{cw} \sqrt{A_{cw}} (p_i - p_{wf})} \right] = \frac{0.8936 N_p B}{\varphi c_t A_{cw} \sqrt{A_{cw}} (p_i - p_{wf})} \dots\dots (3-57)$$

Also, equation of compressibility is given by:

$$c_t = - \left( \frac{1}{V} \right) \left( \frac{\Delta p}{\Delta V} \right) \dots\dots\dots (3-58)$$

Here:

$$V = \varphi A \sqrt{A_{cw}}$$

$$\Delta p = p_i - \overline{p_{Av}}$$

Which when applied to the above compressibility equation results in:

$$\frac{1}{\varphi c_t A \sqrt{A_{cw}}} = \left( \frac{\Delta p}{\Delta V} \right) \dots\dots\dots (3-59)$$

But,

$$\Delta V = N_p B \text{ (bbls)}$$

$$\Delta p = \left( \frac{\Delta V}{\varphi c_t A \sqrt{A_{cw}}} \right) = \left( \frac{5.615 N_p B}{\varphi c_t A \sqrt{A_{cw}}} \right) \dots\dots\dots (3-60)$$

*Constant Rate Case*

Since Eqn.(3-51) is valid for both pseudosteady state and boundary dominated flow cases, we can also write it as:

$$J = \frac{q}{(p_i - p_{wf}) - (p_i - \overline{p_{Av}})} \dots\dots\dots(3-61)$$

$$\left( \frac{\alpha_1 \mu B}{2\pi k \sqrt{A_{cw}}} \right) J = \frac{q}{\left( \frac{2\pi k \sqrt{A_{cw}}}{\alpha_1 \mu B} \right) (p_i - p_{wf}) - \left( \frac{2\pi k \sqrt{A_{cw}}}{\alpha_1 \mu B} \right) (p_i - \overline{p_{Av}})} \dots\dots\dots(3-62)$$

$$J_D = \frac{1}{(p_D - \overline{p_{AvD}})} \dots\dots\dots(3-63)$$

Where,

$$p_D = \frac{2\pi}{\alpha_1} \left[ \frac{k \sqrt{A_{cw}} (p_i - p_{wf})}{q B \mu} \right] \dots\dots\dots(3-64)$$

$$\overline{p_{AvD}} = \frac{2\pi}{\alpha_1} \left[ \frac{k \sqrt{A_{cw}} (p_i - \overline{p_{Av}})}{q B \mu} \right]$$

We know,

$$\Delta p = \left( \frac{\Delta V}{\varphi c_t A \sqrt{A_{cw}}} \right) = \left( \frac{5.615 N_p B}{\varphi c_t A \sqrt{A_{cw}}} \right) \dots\dots\dots(3-65)$$

Or, multiplying both sides, we have:

$$\frac{2\pi}{\alpha_1} \left[ \frac{k \sqrt{A_{cw}}}{q B \mu} (p_i - \overline{p_{Av}}) \right] = \frac{2\pi}{\alpha_1} \left[ \frac{k \sqrt{A_{cw}}}{q B \mu} \left( \frac{5.615 q B t}{\varphi c_t A \sqrt{A_{cw}}} \right) \right]$$

$$\overline{p_{AvD}} = \frac{2\pi}{\alpha_1} \left( \frac{5.615 k t}{\varphi \mu c_t A} \right) \dots\dots\dots (3-66)$$

$$\overline{p_{AvD}} = 2\pi t_{DA} \dots\dots\dots (3-67)$$

Where,

$$t_{DA} = \frac{5.615}{\alpha_1} \left( \frac{k t}{\varphi \mu c_t A} \right) = \frac{0.00633 k t}{\varphi \mu c_t A} \dots\dots\dots (3-68)$$

Substituting back in dimensionless productivity equation:

$$J_D = \frac{1}{(p_D - 2\pi t_{DA})} \dots\dots\dots (3-69)$$

*Constant Pressure Case*

For this case, dimensionless rate is defined as:

$$\frac{1}{q_D} = \frac{2\pi}{\alpha_1} \left[ \frac{k \sqrt{A_{cw}} (p_i - p_{wf})}{q B \mu} \right] \dots\dots\dots (3-70)$$

Again,

$$N_{pD} = \frac{5.615}{2\pi} \left[ \frac{N_p B}{\varphi c_t A_{cw} \sqrt{A_{cw}} (p_i - p_{wf})} \right] \dots\dots\dots (3-71)$$

This can be rearranged as:

$$N_p B = \frac{2\pi N_{pD}}{5.615} \varphi c_t A_{cw} \sqrt{A_{cw}} (p_i - p_{wf}) \dots\dots\dots (3-72)$$

Combining the two equations:

$$\left(\frac{\varphi c_t A \sqrt{A_{cw}}}{5.615}\right) \Delta p = \frac{2\pi N_{pD}}{5.615} \varphi c_t A_{cw} \sqrt{A_{cw}} (p_i - p_{wf}) \dots \dots \dots (3-73)$$

$$\Delta p = \frac{2\pi N_{pD}}{(A/A_{cw})} (p_i - p_{wf})$$

$$\Delta p = \frac{2\pi N_{pD}}{A_D} (p_i - p_{wf}) \dots \dots \dots (3-74)$$

Multiplying both sides:

$$\frac{2\pi}{\alpha_1} \left[ \frac{k \sqrt{A_{cw}}}{q B \mu} (p_i - \bar{p}_{Av}) \right] = \frac{2\pi N_{pD}}{A_D} \left( \frac{2\pi}{\alpha_1} \right) \left[ \frac{k \sqrt{A_{cw}}}{q B \mu} (p_i - p_{wf}) \right] \dots \dots \dots (3-75)$$

$$\frac{1}{q_{AvD}} = \left( \frac{2\pi N_{pD}}{A_D} \right) \frac{1}{q_D} \dots \dots \dots (3-76)$$

Here,

$$\frac{1}{q_{AvD}} = \frac{2\pi}{\alpha_1} \left[ \frac{k \sqrt{A_{cw}}}{q B \mu} (p_i - \bar{p}_{Av}) \right] \dots \dots \dots (3-77)$$

Substituting this back:

$$J = \frac{q}{(p_i - p_{wf}) - (p_i - \bar{p}_{Av})} \dots \dots \dots (3-78)$$

$$\left(\frac{\alpha_1 \mu B}{2\pi k \sqrt{A_w}}\right) J = \frac{q}{\left(\frac{2\pi k \sqrt{A_w}}{\alpha_1 \mu B}\right)(p_i - p_{wf}) - \left(\frac{2\pi k \sqrt{A_w}}{\alpha_1 \mu B}\right)(p_i - \bar{p}_{Av})} \dots\dots\dots (3-79)$$

$$J_D = \frac{1}{\left(\frac{1}{q_D} - \frac{1}{q_{AvD}}\right)} \dots\dots\dots (3-80)$$

$$J_D = \frac{q_D}{\left[1 - \left(\frac{2\pi N p_D}{A_D}\right)\right]} \dots\dots\dots (3-81)$$

### Convergence Skin for Horizontal Well

We start with the method outlined by Bello<sup>9</sup>. He has proposed the distortion of linear to radial around the horizontal wellbore given by Lichtenberger<sup>42</sup> and reproduced here as:

$$s_h = -\ln \left[ \left( \frac{\pi r_w}{h} \right) \left( 1 + \sqrt{\frac{k_v}{k_h}} \right) \sin \left( \frac{\pi d_z}{h} \right) \right] \dots\dots\dots (3-82)$$

where,  $d_z$ , is the nearest horizontal boundary,  $h$ , is the height of the reservoir and  $k_v$  and  $k_h$  are the vertical and horizontal permeabilities. In terms of linear values it is:

$$s_{hcw} = \left( \frac{\sqrt{A_{cw}}}{L_w} \right) s_h \dots\dots\dots (3-83)$$

where,  $L_w$ , is the length of the horizontal well. Inside the Laplace domain, the above equation is treated as an additional pressure drop according to the following relation (constant rate case):

$$\overline{p}_{Ds} = \overline{p}_D + \left( \frac{2\pi s_{hcw}}{s} \right) \dots\dots\dots(3-84)$$

And for constant pressure case as:

$$\overline{q}_{Ds} = \frac{1}{s^2 \overline{p}_{Ds}} \dots\dots\dots(3-85)$$

## Summary of Solutions

**Table 8.** Fracture Functions for Solution with Aquifer Support in Linear Dual Porosity.

Model	Fracture function, $f(s)$
Full Pseudosteady State Matrix and Aquifer Fractured Dual Permeability Model (Appendix E)	$f(s) = \left[ \left( \frac{\omega_{aq}}{\kappa_f} \right) + \left( \frac{\left( \frac{\lambda}{\omega} \right) (1 - \omega) (\Lambda) \left( \frac{\kappa_{fb}}{\kappa_f} \right)}{\left( \frac{1 - \omega}{\omega} \right) (\Lambda) \left( \frac{\kappa_{fb}}{\kappa_f} \right) s + \left( \frac{\lambda}{\omega} \right)} \right) \right. \\ \left. + \left( \frac{\lambda_{aq}}{\kappa_f} \right) \left( \frac{(1 - \omega_{aq})}{(1 - \omega_{aq})s + \lambda_{aq}} \right) \right]$
Transient Matrix Fractured Dual Permeability Model (Appendix F)	$f(s) = \omega \left[ \left( \frac{\omega_{aq}}{\omega \kappa_f} \right) + \left( \frac{1}{3s} \right) \left( \frac{\lambda}{\omega} \right) \sqrt{3s \left( \frac{1 - \omega}{\omega} \right) (\Lambda) \left( \frac{\kappa_{fb}}{\kappa_f} \right) \left( \frac{\omega}{\lambda} \right)} \right. \\ \left. \times \tanh \left( \sqrt{3s \left( \frac{1 - \omega}{\omega} \right) (\Lambda) \left( \frac{\kappa_{fb}}{\kappa_f} \right) \left( \frac{\omega}{\lambda} \right)} \right) \right] \\ + \left( \frac{\lambda_{aq}}{\kappa_f} \right) \left\{ \frac{(1 - \omega_{aq})}{(1 - \omega_{aq})s + \lambda_{aq}} \right\}$
Transient Aquifer Fractured Dual Permeability Model (Appendix G)	$f(s) \\ = \left[ \left( \frac{\omega_{aq}}{\kappa_f} \right) + \left( \frac{\left( \frac{\lambda}{\omega} \right) (1 - \omega) (\Lambda) \left( \frac{\kappa_{fb}}{\kappa_f} \right)}{\left( \frac{1 - \omega}{\omega} \right) (\Lambda) \left( \frac{\kappa_{fb}}{\kappa_f} \right) s + \left( \frac{\lambda}{\omega} \right)} \right) \right. \\ \left. + \left( \frac{\lambda_{aq}}{12 s \kappa_f} \right) \sqrt{s \left( \frac{12(1 - \omega_{aq})}{\lambda_{aq}(1 - \kappa_f)} \right)} \tanh \left( \sqrt{s \left( \frac{12(1 - \omega_{aq})}{\lambda_{aq}(1 - \kappa_f)} \right)} \right) \right]$
Full Transient Matrix and Aquifer Fractured Dual Permeability Model (Appendix H)	$f(s) \\ = \omega \left[ \left( \frac{\omega_{aq}}{\omega \kappa_f} \right) + \left( \frac{1}{3s} \right) \left( \frac{\lambda}{\omega} \right) \sqrt{3s \left( \frac{1 - \omega}{\omega} \right) (\Lambda) \left( \frac{\kappa_{fb}}{\kappa_f} \right) \left( \frac{\omega}{\lambda} \right)} \right. \\ \left. \times \tanh \left( \sqrt{3s \left( \frac{1 - \omega}{\omega} \right) (\Lambda) \left( \frac{\kappa_{fb}}{\kappa_f} \right) \left( \frac{\omega}{\lambda} \right)} \right) \right] \\ + \left( \frac{\lambda_{aq}}{12 s \kappa_f} \right) \sqrt{s \left( \frac{12(1 - \omega_{aq})}{\lambda_{aq}(1 - \kappa_f)} \right)} \tanh \left( \sqrt{s \left( \frac{12(1 - \omega_{aq})}{\lambda_{aq}(1 - \kappa_f)} \right)} \right)$

**Table 9.** Fracture Functions of Radial/Linear (Aquifer) Dual Porosity Solution.

<p>Warren and Root Dual Porosity Pseudosteady State Model (Appendix A)</p>	$f(s) = \frac{1 + s \left(\frac{\omega}{\lambda}\right) - s \omega \left(\frac{\omega}{\lambda}\right)}{1 + \frac{s}{\omega} \left(\frac{\omega}{\lambda}\right) - s \left(\frac{\omega}{\lambda}\right)}$
<p>Bello Transient Dual Porosity Linear Flow Model (Appendix B)</p>	$f(s) = \omega \left[ 1 + \left(\frac{1}{3s}\right) \left(\frac{\lambda}{\omega}\right) \sqrt{3s \left(\frac{1-\omega}{\omega}\right) \left(\frac{\omega}{\lambda}\right)} \tanh \left( \sqrt{3s \left(\frac{1-\omega}{\omega}\right) \left(\frac{\omega}{\lambda}\right)} \right) \right]$
<p>Equivalent Linear Ehlig- Economides and Ayoub Pseudosteady State Aquifer (Appendix C)</p>	$f(s) = \frac{\omega_{aq}(1 - \omega_{aq})s + \lambda_{aq}}{\kappa_{fb}[(1 - \omega_{aq})s + \lambda_{aq}]}$
<p>Equivalent Linear Bourdet Transient Aquifer (Appendix D)</p>	$f(s) = \omega_{aq} + \frac{\lambda_{aq}}{12s} \sqrt{s \frac{12(1 - \omega_{aq})}{\lambda_{aq}}} \tanh \left( \sqrt{s \frac{12(1 - \omega_{aq})}{\lambda_{aq}}} \right)$



## Treatment for Solution Gas Drive – Material Balance Method for Volatile Oil

### Reservoir with Variable Fluid Compressibility

This method involves combined use of Muskat<sup>43</sup> material balance method (MBE) method and Walsh<sup>44</sup> formulation for volatized oil-gas ratio in these reservoirs. The difference between having an aquifer drive reservoir as opposed to solution gas drive or gas cap drive reservoir is that, for the former, boundary conditions need to be changed in order to arrive at a solution whereas, in the latter other drive reservoirs, we have to solve a non-linear partial differential equation. This is because by changing PVT properties we are changing these pressure dependent variables. To keep the linear form of the equation, we have to calculate these inputs prior to solving (implicit calculation) the equation. Since, our assumption is that the water does not invade the reservoir, converting results of aquifer drive solution to solution gas drive solution amounts to applying a correction. Again, the dimensionless productivity index equations for constant rate and constant pressure, for our reference, are:

$$J_D = \frac{1}{(p_D - \bar{p}_{AvD})} \dots\dots\dots (3-63)$$

$$J_D = \frac{q_D}{\left[1 - \left(\frac{2\pi N p_D}{A_D}\right)\right]} \dots\dots\dots (3-79)$$

These are dependent on following dimensionless variables, for constant rate case:

$$p_D = \frac{2\pi}{\alpha_1} \left[ \frac{k \sqrt{A_{cw}} (p_i - p_{wf})}{q B \mu} \right] \dots\dots\dots (3-64)$$

$$\overline{p_{AvD}} = \frac{2\pi}{\alpha_1} \left[ \frac{k \sqrt{A_{cw}} (p_i - \overline{p_{Av}})}{q B \mu} \right]$$

$$\overline{p_{AvD}} = \frac{2\pi}{\alpha_1} \left( \frac{5.615 k t}{\varphi \mu c_t A} \right) \dots\dots\dots (3-66)$$

$$\overline{p_{AvD}} = 2\pi t_{DA} \dots\dots\dots (3-67)$$

Where,

$$t_{DA} = \frac{5.615}{\alpha_1} \left( \frac{k t}{\varphi \mu c_t A} \right) = \frac{0.00633 k t}{\varphi \mu c_t A} \dots\dots\dots (3-68)$$

For constant pressure case, they are:

$$\frac{1}{q_D} = \frac{2\pi}{\alpha_1} \left[ \frac{k \sqrt{A_{cw}} (p_i - p_{wf})}{q B \mu} \right] \dots\dots\dots (3-70)$$

$$N_{pD} = \frac{5.615}{2\pi} \left[ \frac{N_p B}{\varphi c_t A_{cw} \sqrt{A_{cw}} (p_i - p_{wf})} \right] \dots\dots\dots (3-71)$$

Also,

$$\frac{1}{q_{AvD}} = \frac{2\pi}{\alpha_1} \left[ \frac{k \sqrt{A_{cw}}}{q B \mu} (p_i - \overline{p_{Av}}) \right] \dots\dots\dots (3-77)$$

These variables,  $\mu, B$  are pressure dependent for each phase and  $c_t$ , which is also saturation dependent and have to be known in advance (implicit variables). Also, since we are solving a multiphase problem, the oil and gas in the reservoir (water exists only in residual form) have to be handled independently, especially below the bubble point.

Based on Perrine and Martin<sup>45</sup> diffusivity equation for multiphase flow, we define the following for this multiphase flow:

$$S_g + S_o + S_{wc} = 1 \dots\dots\dots(3-86)$$

$$\lambda_t = \lambda_g + \lambda_o + \lambda_w = \frac{k_g}{\mu_g} + \frac{k_o}{\mu_o} + \frac{k_w}{\mu_w} \dots\dots\dots(3-87)$$

$$c_t = S_g c_g + S_o c_o + S_{cw} c_w + c_f \dots\dots\dots(3-88)$$

Below the bubble point, we have:

$$c_o = -\frac{1}{B_o} \left( \frac{dB_o}{dp} - \frac{dR_{so}}{dp} B_g \right) \dots\dots\dots(3-89a)$$

$$c_g = -\frac{1}{B_g} \left( \frac{dB_g}{dp} \right) \dots\dots\dots(3-89b)$$

We modified the Muskat<sup>43</sup> material balance method to account for the effect of volatilized oil-gas ratio. This follows from generalized material balance equation of Walsh<sup>42</sup>. For simplicity, the underlying assumption for the method outlined here, is either the volatile oil reservoir is above the bubble point or is right at it at the start of depletion (reservoir initial gas cap calculations are more involved). Let,  $V_p$ , be the pore volume. Then the stock tank barrels of remaining oil,  $N_r$ , in the reservoir is:

$$N_r = V_p \left( \frac{S_o}{B_o} + \frac{S_g R_v}{B_g} \right) (STB) \dots\dots\dots(3-90)$$

Differentiating with respect to pressure gives:

$$\frac{dN_r}{dp} = V_p \left( \frac{1}{B_o} \frac{dS_o}{dp} - \frac{S_o}{B_o^2} \frac{dB_o}{dp} + \frac{R_v}{B_g} \frac{dS_g}{dp} - \frac{R_v S_g}{B_g^2} \frac{dB_g}{dp} + \frac{S_g}{B_g} \frac{dR_v}{dp} \right) \dots\dots\dots (3-91)$$

The gas remaining in the reservoir,  $G_r$  free and dissolved, is:

$$G_r = V_p \left( \frac{R_{so} S_o}{B_o} + \frac{(1-S_o-S_{wc})}{B_g} \right) (scf) \dots\dots\dots (3-92)$$

Differentiating with respect to pressure gives:

$$\frac{dG_r}{dp} = V_p \left( \frac{R_{so}}{B_o} \frac{dS_o}{dp} + \frac{S_o}{B_o} \frac{dR_{so}}{dp} - \frac{R_{so} S_o}{B_o^2} \frac{dB_o}{dp} - \frac{1}{B_g} \frac{dS_o}{dp} - \frac{(1-S_o-S_{wc})}{B_g^2} \frac{dB_g}{dp} \right) \dots\dots\dots (3-93)$$

If the reservoir pressure is dropping at the rate,  $\frac{dp}{dt}$ , then the producing gas-oil ratio is:

$$R_p = \left( \frac{dG_r/dp}{dN_r/dp} \right) \dots\dots\dots (3-94)$$

Substituting eqn.(3-91) and eqn.(3-93) into eqn.(3-94), we get:

$$R_p = \frac{\frac{R_{sO}dS_o}{B_o dp} + \frac{S_o dR_{sO}}{B_o dp} - \frac{R_{sO}S_o dB_o}{B_o^2 dp} - \frac{1}{B_g} \frac{dS_o}{dp} - \frac{(1-S_o-S_{wc})dB_g}{B_g^2 dp}}{\frac{1}{B_o} \frac{dS_o}{dp} - \frac{S_o dB_o}{B_o^2 dp} + \frac{R_v dS_g}{B_g dp} - \frac{R_v S_g dB_g}{B_g^2 dp} + \frac{S_g dR_v}{B_g dp}} \dots\dots\dots (3-95)$$

Producing gas-oil ratio is also expressed as:

$$R_p = R_{sO} + \left( \frac{k_g/\mu_g B_o}{k_o/\mu_o B_g} \right) (scf/STB) \dots\dots\dots (3-96)$$

Combining eqn.(3-95) and eqn.(3-96) we have:

$$\frac{dS_o}{dp} = \frac{\left( \frac{S_o B_g}{B_o} \right) \left[ \frac{dR_{sO}}{dp} \right] + \left( \frac{k_g/\mu_g}{k_o/\mu_o} \right) \left( \frac{S_o}{B_o} \right) \left[ \frac{dB_o}{dp} \right] - \left( \frac{1-S_o-S_{wc}}{B_g} \right) \left[ 1 - R_v \left( R_{sO} + \left( \frac{k_g/\mu_g}{k_o/\mu_o} \right) \left( \frac{B_o}{B_g} \right) \right) \right] \left[ \frac{dB_g}{dp} \right]}{1 + \left( \frac{k_g/\mu_g}{k_o/\mu_o} \right)} - \frac{\left[ R_{sO} + \left( \frac{k_g/\mu_g}{k_o/\mu_o} \right) \left( \frac{B_o}{B_g} \right) \right] \left( R_v \left[ \frac{dS_g}{dp} \right] + S_g \left[ \frac{dR_v}{dp} \right] \right)}{1 + \left( \frac{k_g/\mu_g}{k_o/\mu_o} \right)} \dots\dots (3-97)$$

It is clear from eqn.(3-97) that the saturation of oil depends on the change in the saturation of the gas as well, since oil drops out of volatile oil. If that volatilized oil-gas ratio is considered to be zero,  $R_v = 0$ , then the equation reduces to Muskat's eqn. given by:

$$\frac{dS_o}{dp} = \frac{\left( \frac{S_o B_g}{B_o} \right) \left[ \frac{dR_{sO}}{dp} \right] + \left( \frac{k_g/\mu_g}{k_o/\mu_o} \right) \left( \frac{S_o}{B_o} \right) \left[ \frac{dB_o}{dp} \right] - \left\{ \frac{(1-S_o-S_{wc})}{B_g} \right\} \left[ \frac{dB_g}{dp} \right]}{1 + \left( \frac{k_g/\mu_g}{k_o/\mu_o} \right)} \dots\dots\dots (3-98a)$$

$$\frac{\Delta S_o}{\Delta p} = \frac{S_o X(p) + S_o \left(\frac{k_g}{k_o}\right) Y(p) - (1 - S_o - S_{wc}) Z(p)}{1 + \left(\frac{k_g/\mu_g}{k_o/\mu_o}\right)} \dots\dots\dots (3-98b)$$

Where for Muskat's equation, these terms primarily depend on PVT properties, are:

$$X(p) = \left(\frac{B_g}{B_o}\right) \left[\frac{dR_{so}}{dp}\right] \dots\dots\dots (3-99a)$$

$$Y(p) = \left(\frac{1}{B_o}\right) \left(\frac{\mu_o}{\mu_g}\right) \left[\frac{dB_o}{dp}\right] \dots\dots\dots (3-99b)$$

$$Z(p) = \left(\frac{1}{B_g}\right) \left[\frac{dB_g}{dp}\right] = -B_g \left[\frac{d(1/B_g)}{dp}\right] \dots\dots\dots (3-99c)$$

For eqn.(3-97) these terms are defined as:

$$X(p) = \left(\frac{B_g}{B_o}\right) \left[\frac{dR_{so}}{dp}\right] \dots\dots\dots (3-100a)$$

$$Y(p) = \left(\frac{1}{B_o}\right) \left(\frac{k_g/\mu_g}{k_o/\mu_o}\right) \left[\frac{dB_o}{dp}\right] \dots\dots\dots (3-100b)$$

$$Z(p) = \left(\frac{1}{B_g}\right) \left[1 - R_v \left(R_{so} + \left(\frac{k_g/\mu_g}{k_o/\mu_o}\right) \left(\frac{B_o}{B_g}\right)\right)\right] \left[\frac{dB_g}{dp}\right] \dots\dots\dots (3-100c)$$

$$= -B_g \left[1 - R_v \left(R_{so} + \left(\frac{k_g/\mu_g}{k_o/\mu_o}\right) \left(\frac{B_o}{B_g}\right)\right)\right] \left[\frac{d(1/B_g)}{dp}\right] \dots\dots\dots (3-100c)$$

$$W(p) = \left[R_{so} + \left(\frac{k_g/\mu_g}{k_o/\mu_o}\right) \left(\frac{B_o}{B_g}\right)\right] \dots\dots\dots (3-100d)$$

Thus eqn.(3-97) reduces to a simplified form:

$$\frac{\Delta S_o}{\Delta p} = \frac{S_o X(p) + S_o Y(p) - (1 - S_o - S_{wc}) Z(p) + W(p) \left( R_v \left[ \frac{\Delta S_g}{\Delta p} \right] + S_g \left[ \frac{dR_v}{dp} \right] \right)}{1 + \left( \frac{k_g / \mu_g}{k_o / \mu_o} \right)} \dots\dots\dots (3-101)$$

Here is the step by step outline of proposed method for a reservoir at bubble-point:

Step 1. Select a future reservoir pressure  $p_2$  below the initial (current) reservoir pressure  $p_1$  ( $p_2$  can be obtained from Laplace space solution after inversion) and obtain the necessary PVT data. Assume that the cumulative oil production has increased to  $N_{p2}$ .  $G_{p1}$  are set equal to zero at the initial reservoir pressure, i.e., bubble-point pressure.

Step 2. Plot  $k_{ro}$  and  $k_{rg}$  versus gas saturation. Plot  $R_{so}$ ,  $R_v$ ,  $B_o$  and  $(1/B_g)$  versus pressure and determine the derivatives  $\frac{dB_o}{dp}$ ,  $\frac{dR_{so}}{dp}$ ,  $\frac{dR_v}{dp}$  and  $\frac{d(1/B_g)}{dp}$ .

Step 3. Calculate the cumulative gas production  $G_{p2}$  by the MBE:

$$G_{p2} = N \left[ (R_{si} - R_s) - \frac{B_{oi} - B_o}{B_g} \right] - N_{p2} \left[ \frac{B_o}{B_g} - R_s \right] \dots\dots\dots (3-102)$$

Step 4. Calculate the oil and gas saturation (no attempt is made to quantify volatilized oil drop-out) at the assumed cumulative oil production  $N_{p2}$  using the equations:

$$S_o = (1 - S_{wc}) \left[ 1 - \frac{N_{p2}}{N} \right] \left( \frac{B_o}{B_{oi}} \right)$$

$$S_g = 1 - S_o - S_{wc}$$

Step 5. Calculate the pressure and saturation dependent variables  $X(p), Y(p), Z(p)$  and  $W(p)$ .

Step 6. Solve the eqn.(3-101) for  $\frac{\Delta S_o}{\Delta p}$  with saturation  $S_{o1}$  and  $S_{g1}$  at  $p_1$ , with  $\Delta p$  being the difference with initial pressure.

Step 7. Determine the oil and gas saturation,  $S_{o2}$  and  $S_{g2}$ , at  $p_2$  from:

$$S_{o2} = S_{o1} - (p_1 - p_2) \left( \frac{\Delta S_o}{\Delta p} \right)$$

$$S_{g2} = 1 - S_{o2} - S_{wc}$$

Step 8. Recalculate  $\frac{\Delta S_o}{\Delta p}$  using  $S_{o2}$  and  $S_{g2}$ , at  $p_2$ .

Step 9. Calculate the average value  $\left( \frac{\Delta S_o}{\Delta p} \right)_{avg}$  for the two pressures  $p_1$  and  $p_2$ .

Step 10. Recalculate  $(S_{o2})_{avg}$  at  $p_2$  from:

$$(S_{o2})_{avg} = S_{o1} - (p_1 - p_2) \left( \frac{\Delta S_o}{\Delta p} \right)_{avg}$$

$$S_{g2} = 1 - S_{o2} - S_{wc}$$

This value of  $S_{o2}$  and  $S_{g2}$  becomes the input for next time step.

Step 11. Solve for cumulative oil production using eqn.(3-103) and cumulative gas production using eqn.(3-102). Repeat step 5 to step 10 with pressure drops from Laplace space solution after inversion.

$$N_{p2} = N \left[ 1 - \left( \frac{B_o}{B_g} \right) \left( \frac{S_o}{1-S_{wc}} \right) \right] \dots\dots\dots(3-103)$$

Thus in the end, for constant rate case,  $\overline{p_{AvD}}$  can be recalculated for each time step as will the values for  $q_D$  and  $N_{pD}$ , for constant pressure case, in calculating  $J_D$ .



## CHAPTER IV

### SIMULATION OF UNCONVENTIONAL RESERVOIRS USING MESHLESS METHOD: ACCURATE PERFORMANCE PREDICTION OF DUAL POROSITY RESERVOIRS WITH TRANSVERSE FRACTURES

#### **Introduction and Objectives of Mathematical Modeling**

Closed form solution of a single finite conductivity hydraulic fracture for boundary dominated flow is a challenging problem. The usual course available is to solve this problem numerically in a simulator which has got limitations on how finely gridded the fracture cells can be to arrive at an accurate solution. Apart from the challenge of assigning the number of possible grid blocks which can slow the solution process down drastically, the contrast in permeability between the fracture and the reservoir lead to convergence errors that are significant enough under multiphase flow (present in single phase flow as well) and have the potential of bringing the execution process to a very slow pace. The big picture is that even if we allow sufficient time for the problem to be executed numerically the accuracy of the solution is always in doubt.

The way around it is to use semi-analytical solutions. As a research tool, they are better suited than their numerical counterparts because of high degree of accuracy of closed form solutions available inside the Laplace domain, although these also suffer from slow speed of execution as a real domain solution is sought.

The objective of this chapter is to numerically combine the simple semi-analytical Laplace domain solution(s) using superposition method based on the idea of

Matthew, Bronze & Haselbrok<sup>46</sup> and then obtain the real domain solution by (again) numerical inversion. Helmy & Wattenbager<sup>47</sup> applied this method to determine shape factors for various reservoir shapes flowing under boundary dominated flow. We will use this method to find solutions for complex well geometries like a horizontal well with several transverse fractures.

**The Constant Pressure, Finite Wellbore, Solution of Single Well Centered in Square Drainage Area – Superposition Method Using Transient Constant Rate Radial Solution (Helmy Model)**

This section describes the details of process of superposition using method of images in Laplace domain to obtain solution of a single well under transient and boundary dominated flow. Consider a single radial well. We start with the constant rate solution. With the help of superposition we create reservoir boundaries (for square drainage area) and using Van Everdingen & Hurst<sup>48</sup> methodology we generate the constant pressure solution as an end result of superposition of all the constant rate solutions. The starting point is the constant rate transient, finite wellbore, solution for a single well in Laplace domain as:

$$\overline{p}_D(r_D, u) = \frac{K_0(r_D, \sqrt{u})}{u^{\frac{3}{2}} K_1(\sqrt{u})} \dots\dots\dots (4-1)$$

Using method of images, so as to insert boundaries around the producing well, the solution of superposition problem is carried out in Laplace domain space. The final result can be had after reverting back to real domain. Figure 35 gives the methodology used to arrive at the solution in the Laplace domain space and the previous section outline the mathematics behind it. Theoretically, we need an infinite number of image wells to arrive at a solution, but practically this is not possible and the solution is generated with finite number of image wells, with the assumption that the error between the two solutions is negligible.

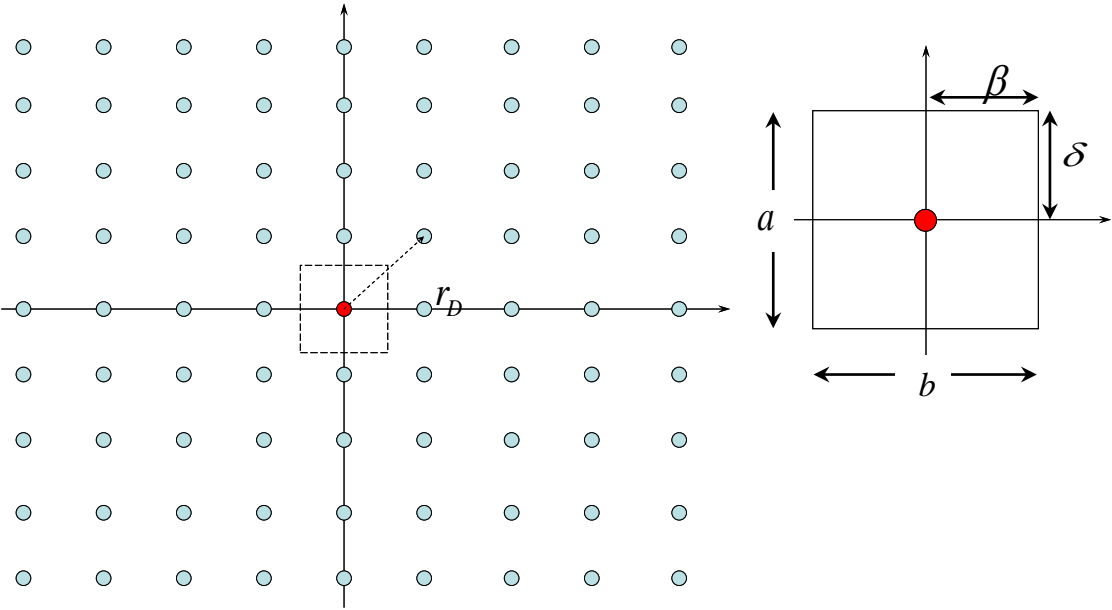


**Figure 35.** The Infinite Distribution of Image Wells Required to Simulate the No-flow Condition across the Boundary of a Square Reservoir with Well is Located in the Center.

Mathematically, as stated earlier, for a well centered in a square drainage are we

have:

$$\overline{p}_D(r_D, u) = \frac{K_0(r_D, \sqrt{u})}{u^{\frac{3}{2}} K_1(\sqrt{u})} + \sum_{j=1}^{\infty} \frac{K_0(r_{Dj}, \sqrt{u})}{u^{\frac{3}{2}} K_1(\sqrt{u})} \dots\dots\dots (4-2)$$

where the summation term take the following form:

$$\sum_{j=1}^{\infty} \frac{K_0(r_{Dj}, \sqrt{u})}{u^{\frac{3}{2}} K_1(\sqrt{u})} = \sum_{\substack{m=-\infty \\ n=-\infty}}^{\substack{m=\infty \\ n=\infty}} \frac{K_0(r_{D1}, \sqrt{u})}{u^{\frac{3}{2}} K_1(\sqrt{u})} + \frac{K_0(r_{D2}, \sqrt{u})}{u^{\frac{3}{2}} K_1(\sqrt{u})} + \frac{K_0(r_{D3}, \sqrt{u})}{u^{\frac{3}{2}} K_1(\sqrt{u})} + \frac{K_0(r_{D4}, \sqrt{u})}{u^{\frac{3}{2}} K_1(\sqrt{u})} \dots\dots\dots (4-3)$$

Here both  $m$  and  $n$  are not simultaneously zero. From figure 35 we have:

$$r_{D1} = \frac{\sqrt{(2ma)^2 + (2nb)^2}}{r_w} \dots\dots\dots (4-4a)$$

$$r_{D2} = \frac{\sqrt{(2(m+\delta)a)^2 + (2nb)^2}}{r_w} \dots\dots\dots (4-4b)$$

$$r_{D3} = \frac{\sqrt{(2ma)^2 + (2(n+\beta)b)^2}}{r_w} \dots\dots\dots (4-4c)$$

$$r_{D4} = \frac{\sqrt{(2(m+\delta)a)^2 + (2(n+\beta)b)^2}}{r_w} \dots\dots\dots (4-4d)$$

The final real domain solution for boundary dominated flow is obtained by inversion using GWR subroutine<sup>40</sup> as per the method outlined by van-Everdingen and Hurst<sup>48</sup> as:

$$\bar{q}_D = \frac{1}{u^2 \bar{p}_D(r_D, u)} \dots\dots\dots(4-5)$$

**The Constant Pressure Solution of Single Infinite Conductivity Fracture, Centered in Square Drainage Area – Superposition Method Using Transient Constant Rate Radial Solution**

This section describes the details of process of superposition using method of images in generating an infinite conductivity fracture as a series of off-centered wells. The method is split into three step process:

1. Helmy’s method as a template to describe a well at the center of square drainage area to get constant rate and constant pressure solutions.
2. With the constant rate solution, repeat the step by moving the well off–center along the length of the fracture in the square drainage area and then superposing them on the earlier model generated in step 1. This is the infinite conductivity fracture solution. It is inverted to real domain solution.
3. Use boundary element method (similar to Romero’s<sup>38</sup> method) for the solution for finite conductivity fracture using solution from step 2. Repeat the process with constant pressure solution.

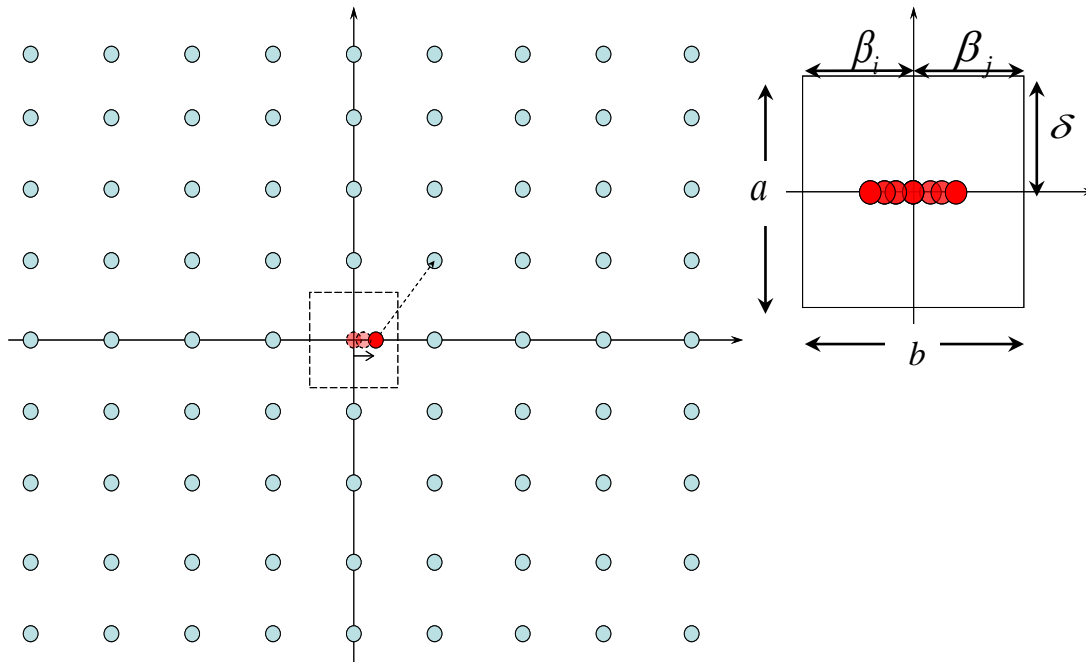


**Figure 36.** The Infinite Distribution of Image Wells Required to Simulate the No-flow Condition across the Boundary of a Square Reservoir and a Fracture.

The way we have to set up the superposition algorithm is to generate a specific number of off center wells (source wells, theoretically,  $n_w \rightarrow \infty$ ) which will be placed along the full fracture length, figure 36, and the whole process gets repeated for each off centered well. Like the previous expression, only the interwell distances change in magnitude as:

$$r_{D1} = \frac{\sqrt{(2ma)^2 + (2nb)^2}}{r_w} \dots\dots\dots (4-5a)$$

$$r_{D2} = \frac{\sqrt{(2(m + \delta)a)^2 + (2nb)^2}}{r_w} \dots\dots\dots(4-5b)$$

For  $n < 0$

$$r_{D3i} = \frac{\sqrt{(2ma)^2 + (2(n + \beta_i)b)^2}}{r_w} \dots\dots\dots(4-5c)$$

For  $n > 0$

$$r_{D3j} = \frac{\sqrt{(2ma)^2 + (2(n + \beta_j)b)^2}}{r_w} \dots\dots\dots(4-5d)$$

For  $n < 0$

$$r_{D4i} = \frac{\sqrt{(2(m + \delta)a)^2 + (2(n + \beta_i)b)^2}}{r_w} \dots\dots\dots(4-5e)$$

For  $n > 0$

$$r_{D4j} = \frac{\sqrt{(2(m + \delta)a)^2 + (2(n + \beta_j)b)^2}}{r_w} \dots\dots\dots(4-5f)$$

From eqn.(16) and from eqn.(17), we have:

$$\left[ \sum_{j=1}^{\infty} \left( \frac{K_0(r_{Dj}, \sqrt{u})}{u^{\frac{3}{2}} K_1(\sqrt{u})} \right) \right]_{n_w \rightarrow \infty} = \left[ \sum_{\substack{m=-\infty \\ n=-\infty}}^{\substack{m=\infty \\ n=\infty}} \left( \frac{K_0(r_{D1}, \sqrt{u})}{u^{\frac{3}{2}} K_1(\sqrt{u})} + \frac{K_0(r_{D2}, \sqrt{u})}{u^{\frac{3}{2}} K_1(\sqrt{u})} + \frac{K_0(r_{D3}, \sqrt{u})}{u^{\frac{3}{2}} K_1(\sqrt{u})} + \frac{K_0(r_{D4}, \sqrt{u})}{u^{\frac{3}{2}} K_1(\sqrt{u})} \right) \right]_{n_w \rightarrow \infty} \dots\dots\dots(4-6)$$

Thus the Laplace domain solution of pressure drop at a well operating at constant rate is:

$$\overline{p_D}(r_D, u) = \left( \frac{K_0(r_D, \sqrt{u})}{u^{\frac{3}{2}} K_1(\sqrt{u})} \right) + \left[ \sum_{j=1}^{\infty} \left( \frac{K_0(r_{Dj}, \sqrt{u})}{u^{\frac{3}{2}} K_1(\sqrt{u})} \right) \right]_{n_w \rightarrow \infty} \dots\dots\dots (4-7)$$

The constant pressure solution was then derived as per the method outlined earlier using van-Everdingen and Hurst<sup>48</sup> approach as:

$$\overline{q_D} = \frac{1}{u^2 \overline{p_D}(r_D, u)} \dots\dots\dots (4-8)$$

$$\overline{N_{pD}} = \frac{1}{u^3 \overline{p_D}(r_D, u)} \dots\dots\dots (4-9)$$

This gives the rate and cumulative production of an infinitely conductive fracture under boundary dominated flow condition which is at the center in a square drainage area. The real domain solution is obtained by numerically inversion using GWR subroutine<sup>40</sup>.

**Fully Penetrating, Single Finite Conductivity Fracture Solution for Vertical Well Using Boundary Element Method – Numerical Generation of Influence Functions**

This method is similar to Romero’s method but differs in formulation used to generate influence function. Conventionally, influence function is generated from closed form solutions in boundary element method. Instead of using Ozkan’s<sup>49</sup> pseudosteady state formulation, superposition of radial solutions in Laplace domain is carried out to imitating a bounded infinite fracture which then generate the required influence functions. After inversion, boundary element method is used to arrive at a solution.



We divide the full fracture wing of length,  $2x_f$ , into  $n_w$  segments of equal length as shown in figure 37. The source well is placed at the center of each segment and is represented by the solid line in figure 37 and we place observation wells at the end of the other segments represented by the dashed line in the figure. Thus the distance between the two source points, represented by subscript  $w$ , is double the distance between a source point and an observation point, represented by the subscript  $o$ .

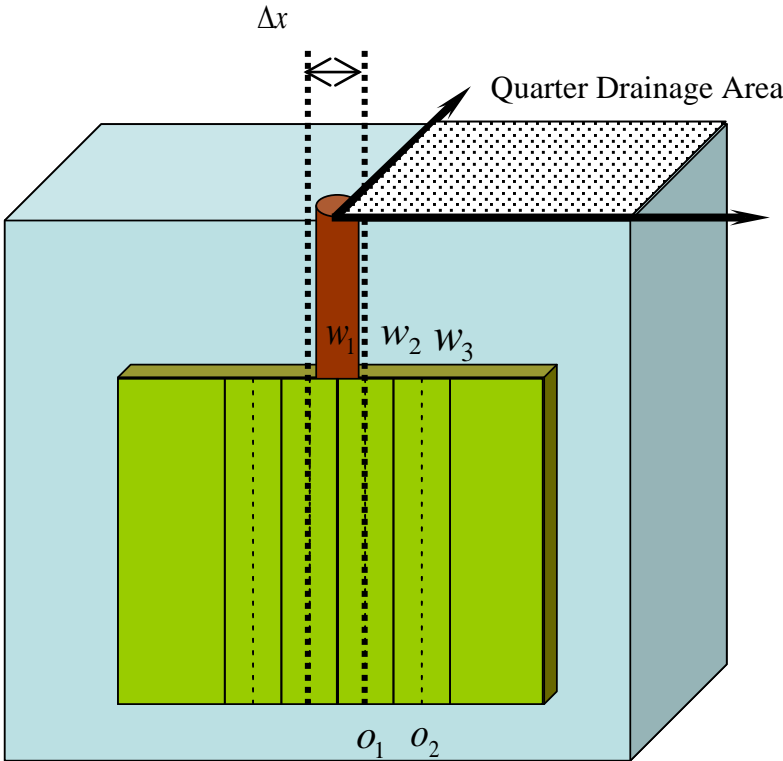


**Figure 37.** Source and Observation Wells for the Generation of Influence Functions.

*Constant Rate Case*

Consider only quarter of the drainage area as shown. Although the figure shows only two source wells (not counting the well  $w_1$  itself) & 2 observation wells on the right hand side of the fracture, assume that there are 4 source and 4 observation wells.

When the observation points are 1 – 2 & the influence of source wells at point 2, 3, and 4 on them within the half of the fracture length is:

$$\Delta p_{f,1-2} = \bar{p} - p_{w,1-2} = \frac{2\alpha_1\mu B}{k_f h w} [q_2(x_{o2} - x_{o1}) + q_3(x_{o2} - x_{o1}) + q_4(x_{o2} - x_{o1})] \dots\dots\dots(4-9)$$

Using Darcy law the above can also be expressed as pressure drops, called influence functions, within the reservoir with respect to average reservoir pressure for the same observation points 1 – 2 and the source wells at 2, 3 and 4 as:

$$\Delta p_{R,1-2} = \bar{p} - p_{w,1-2} = \frac{\alpha_1\mu B}{2\pi k_f h} \left[ q_1 L^{-1} \left( \sum \frac{K_0(r_{Dq_{1-2i}}, \sqrt{u})}{u^{\frac{3}{2}} K_1(\sqrt{u})} \right) + q_2 L^{-1} \left( \sum \frac{K_0(r_{Dq_{1-2i}}, \sqrt{u})}{u^{\frac{3}{2}} K_1(\sqrt{u})} \right) + q_3 L^{-1} \left( \sum \frac{K_0(r_{Dq_{1-2i}}, \sqrt{u})}{u^{\frac{3}{2}} K_1(\sqrt{u})} \right) + q_4 L^{-1} \left( \sum \frac{K_0(r_{Dq_{1-2i}}, \sqrt{u})}{u^{\frac{3}{2}} K_1(\sqrt{u})} \right) \right] \dots\dots(4-10)$$

where  $r_{Dq_i}$  represents the distance between given two observation well for different positions of the source wells and  $q_i$  is production from each of those source wells.

Since the fluid flows from the reservoir into the fracture, the pressure drop in the reservoir is equal to the pressure drop in the fracture, at the fracture face, as:

$$\Delta p_f = \Delta p_R \dots\dots\dots(4-11)$$

Or equating eqn.(4-9) and eqn.(4-10), we have:

$$\frac{\alpha_1 \mu B}{2\pi k_f h} \left[ q_1 L^{-1} \left( \sum \frac{K_0(r_{Dq(1-2)1}, \sqrt{u})}{u^{\frac{3}{2}} K_1(\sqrt{u})} \right) + q_2 L^{-1} \left( \sum \frac{K_0(r_{Dq(1-2)2}, \sqrt{u})}{u^{\frac{3}{2}} K_1(\sqrt{u})} \right) + q_3 L^{-1} \left( \sum \frac{K_0(r_{Dq(1-2)3}, \sqrt{u})}{u^{\frac{3}{2}} K_1(\sqrt{u})} \right) + q_4 L^{-1} \left( \sum \frac{K_0(r_{Dq(1-2)4}, \sqrt{u})}{u^{\frac{3}{2}} K_1(\sqrt{u})} \right) \right] =$$

$$= \frac{2\alpha_1 \mu B}{k_f h w} [q_2(x_{o2} - x_{o1}) + q_3(x_{o2} - x_{o1}) + q_4(x_{o2} - x_{o1})]$$

On rearranging:

$$\left[ q_1 L^{-1} \left( \sum \frac{K_0(r_{Dq(1-2)1}, \sqrt{u})}{u^{\frac{3}{2}} K_1(\sqrt{u})} \right) + q_2 L^{-1} \left( \sum \frac{K_0(r_{Dq(1-2)2}, \sqrt{u})}{u^{\frac{3}{2}} K_1(\sqrt{u})} \right) + q_3 L^{-1} \left( \sum \frac{K_0(r_{Dq(1-2)3}, \sqrt{u})}{u^{\frac{3}{2}} K_1(\sqrt{u})} \right) + q_4 L^{-1} \left( \sum \frac{K_0(r_{Dq(1-2)4}, \sqrt{u})}{u^{\frac{3}{2}} K_1(\sqrt{u})} \right) \right] =$$

$$= \frac{4\pi k}{k_f w} [q_2(x_{o2} - x_{o1}) + q_3(x_{o2} - x_{o1}) + q_4(x_{o2} - x_{o1})] \dots (4-11)$$

On multiplying with  $x_f$ :

$$\left[ q_1 L^{-1} \left( \sum \frac{K_0(r_{Dq(1-2)1}, \sqrt{u})}{u^{\frac{3}{2}} K_1(\sqrt{u})} \right) + q_2 L^{-1} \left( \sum \frac{K_0(r_{Dq(1-2)2}, \sqrt{u})}{u^{\frac{3}{2}} K_1(\sqrt{u})} \right) + q_3 L^{-1} \left( \sum \frac{K_0(r_{Dq(1-2)3}, \sqrt{u})}{u^{\frac{3}{2}} K_1(\sqrt{u})} \right) + q_4 L^{-1} \left( \sum \frac{K_0(r_{Dq(1-2)4}, \sqrt{u})}{u^{\frac{3}{2}} K_1(\sqrt{u})} \right) \right] =$$

$$= \frac{4\pi}{C_{fD} x_f} [q_2(x_{o2} - x_{o1}) + q_3(x_{o2} - x_{o1}) + q_4(x_{o2} - x_{o1})] \dots (4-12)$$

But penetration ratio is given by:

$$I_x = \frac{2x_f}{x_e} \dots (3-28)$$

Dimensionless fracture conductivity,  $C_{fD}$ , is given by:

$$C_{fD} = \frac{k_f w}{k x_f} \dots\dots\dots (3-29)$$

And dimensionless production rate,  $q_D$ , is given by:

$$q_D = \frac{q B \mu}{2\pi k h} (\bar{p} - p_{wf}) \dots\dots\dots (4-13)$$

Thus the final equation for solution at observation point 1 – 2 with source wells at 2, 3, and 4 is:

$$\left[ \begin{array}{l} q_{D1} L^{-1} \left( \sum \frac{K_0(r_{Dq(1-2)1}, \sqrt{u})}{u^{\frac{3}{2}} K_1(\sqrt{u})} \right) \\ + q_{D2} L^{-1} \left( \sum \frac{K_0(r_{Dq(1-2)2}, \sqrt{u})}{u^{\frac{3}{2}} K_1(\sqrt{u})} \right) - \frac{4\pi}{C_{fD} I_x} q_{D2} (x_{o2} - x_{o1}) \\ + q_{D3} L^{-1} \left( \sum \frac{K_0(r_{Dq(1-2)3}, \sqrt{u})}{u^{\frac{3}{2}} K_1(\sqrt{u})} \right) - \frac{4\pi}{C_{fD} I_x} q_{D3} (x_{o2} - x_{o1}) \\ + q_{D4} L^{-1} \left( \sum \frac{K_0(r_{Dq(1-2)4}, \sqrt{u})}{u^{\frac{3}{2}} K_1(\sqrt{u})} \right) - \frac{4\pi}{C_{fD} I_x} q_{D4} (x_{o2} - x_{o1}) \end{array} \right] = 0 \dots\dots\dots (4-14)$$

Similarly, for observation points 1 – 3 and 1 – 4, the resulting equations are:

$$\left[ \begin{array}{l} q_{D1} L^{-1} \left( \sum \frac{K_0(r_{Dq(1-3)1}, \sqrt{u})}{u^{\frac{3}{2}} K_1(\sqrt{u})} \right) \\ + q_{D2} L^{-1} \left( \sum \frac{K_0(r_{Dq(1-3)2}, \sqrt{u})}{u^{\frac{3}{2}} K_1(\sqrt{u})} \right) - \frac{4\pi}{C_{fD} I_x} q_{D2} (x_{o2} - x_{o1}) \\ + q_{D3} L^{-1} \left( \sum \frac{K_0(r_{Dq(1-3)3}, \sqrt{u})}{u^{\frac{3}{2}} K_1(\sqrt{u})} \right) - \frac{4\pi}{C_{fD} I_x} q_{D3} (x_{o3} - x_{o1}) \\ + q_{D4} L^{-1} \left( \sum \frac{K_0(r_{Dq(1-3)4}, \sqrt{u})}{u^{\frac{3}{2}} K_1(\sqrt{u})} \right) - \frac{4\pi}{C_{fD} I_x} q_{D4} (x_{o3} - x_{o1}) \end{array} \right] = 0 \dots\dots\dots (4-15)$$

$$\left[ \begin{array}{l} q_{D1}L^{-1} \left( \sum \frac{K_0(r_{Dq(1-1)1}, \sqrt{u})}{u^{\frac{3}{2}}K_1(\sqrt{u})} \right) \\ + q_{D2}L^{-1} \left( \sum \frac{K_0(r_{Dq(1-1)2}, \sqrt{u})}{u^{\frac{3}{2}}K_1(\sqrt{u})} \right) - \frac{4\pi}{C_{\rho}I_x} q_{D2}(x_{o2} - x_{o1}) \\ + q_{D3}L^{-1} \left( \sum \frac{K_0(r_{Dq(1-1)3}, \sqrt{u})}{u^{\frac{3}{2}}K_1(\sqrt{u})} \right) - \frac{4\pi}{C_{\rho}I_x} q_{D3}(x_{o3} - x_{o1}) \\ + q_{D4}L^{-1} \left( \sum \frac{K_0(r_{Dq(1-1)4}, \sqrt{u})}{u^{\frac{3}{2}}K_1(\sqrt{u})} \right) - \frac{4\pi}{C_{\rho}I_x} q_{D4}(x_{o4} - x_{o1}) \end{array} \right] = 0 \quad \dots\dots\dots(4-16)$$

To complete the system of linear equations, we equate these systems of equation for unit pressure drop at the well:

$$q_{D1}L^{-1} \left( \sum \frac{K_0(r_{Dq(1-1)1}, \sqrt{u})}{u^{\frac{3}{2}}K_1(\sqrt{u})} \right) + q_{D2}L^{-1} \left( \sum \frac{K_0(r_{Dq(1-1)2}, \sqrt{u})}{u^{\frac{3}{2}}K_1(\sqrt{u})} \right) + q_{D3}L^{-1} \left( \sum \frac{K_0(r_{Dq(1-1)3}, \sqrt{u})}{u^{\frac{3}{2}}K_1(\sqrt{u})} \right) + q_{D4}L^{-1} \left( \sum \frac{K_0(r_{Dq(1-1)4}, \sqrt{u})}{u^{\frac{3}{2}}K_1(\sqrt{u})} \right) = 1 \quad \dots\dots\dots(4-17)$$

The first term in the above equation is measured with respect to wellbore radius since  $K_0(r_{Dq(1-1)1}, \sqrt{u}) \rightarrow \infty$  as  $r_{Dq(1-1)1} \rightarrow 0$ . The complete system of equations can be expressed in matrix form as:

$$A x = d \quad \dots\dots\dots(4-18)$$

Where, A, is a matrix given by:

$$\left[ \begin{array}{cccc} \text{(1)} & \text{(2)} & \text{(3)} & \text{(4)} \\ \text{(1)} & L^{-1} \left( \sum \frac{K_0(r_{Dq(1-1)1}, \sqrt{u})}{u^{\frac{3}{2}}K_1(\sqrt{u})} \right) & L^{-1} \left( \sum \frac{K_0(r_{Dq(1-1)3}, \sqrt{u})}{u^{\frac{3}{2}}K_1(\sqrt{u})} \right) & L^{-1} \left( \sum \frac{K_0(r_{Dq(1-1)4}, \sqrt{u})}{u^{\frac{3}{2}}K_1(\sqrt{u})} \right) \\ \text{(2)} & L^{-1} \left( \sum \frac{K_0(r_{Dq(1-1)2}, \sqrt{u})}{u^{\frac{3}{2}}K_1(\sqrt{u})} \right) - \frac{4\pi}{C_{\rho}I_x} (x_{o2} - x_{o1}) & L^{-1} \left( \sum \frac{K_0(r_{Dq(1-1)3}, \sqrt{u})}{u^{\frac{3}{2}}K_1(\sqrt{u})} \right) - \frac{4\pi}{C_{\rho}I_x} (x_{o2} - x_{o1}) & L^{-1} \left( \sum \frac{K_0(r_{Dq(1-1)4}, \sqrt{u})}{u^{\frac{3}{2}}K_1(\sqrt{u})} \right) - \frac{4\pi}{C_{\rho}I_x} (x_{o2} - x_{o1}) \\ \text{(3)} & L^{-1} \left( \sum \frac{K_0(r_{Dq(1-1)2}, \sqrt{u})}{u^{\frac{3}{2}}K_1(\sqrt{u})} \right) - \frac{4\pi}{C_{\rho}I_x} (x_{o2} - x_{o1}) & L^{-1} \left( \sum \frac{K_0(r_{Dq(1-1)3}, \sqrt{u})}{u^{\frac{3}{2}}K_1(\sqrt{u})} \right) - \frac{4\pi}{C_{\rho}I_x} (x_{o3} - x_{o1}) & L^{-1} \left( \sum \frac{K_0(r_{Dq(1-1)4}, \sqrt{u})}{u^{\frac{3}{2}}K_1(\sqrt{u})} \right) - \frac{4\pi}{C_{\rho}I_x} (x_{o3} - x_{o1}) \\ \text{(4)} & L^{-1} \left( \sum \frac{K_0(r_{Dq(1-1)2}, \sqrt{u})}{u^{\frac{3}{2}}K_1(\sqrt{u})} \right) - \frac{4\pi}{C_{\rho}I_x} (x_{o2} - x_{o1}) & L^{-1} \left( \sum \frac{K_0(r_{Dq(1-1)3}, \sqrt{u})}{u^{\frac{3}{2}}K_1(\sqrt{u})} \right) - \frac{4\pi}{C_{\rho}I_x} (x_{o3} - x_{o1}) & L^{-1} \left( \sum \frac{K_0(r_{Dq(1-1)4}, \sqrt{u})}{u^{\frac{3}{2}}K_1(\sqrt{u})} \right) - \frac{4\pi}{C_{\rho}I_x} (x_{o4} - x_{o1}) \end{array} \right] \dots\dots\dots(4-19)$$

$x$  , is a vector given by:

$$x = \begin{bmatrix} q_{D1} \\ q_{D2} \\ q_{D3} \\ q_{D4} \end{bmatrix} \dots\dots\dots (4-20)$$

$d$  , is a vector given by:

$$d = \begin{bmatrix} 1 \\ 0 \\ 0 \\ 0 \end{bmatrix} \dots\dots\dots (4-21)$$

The dimensionless productivity index for total reservoir is derived from,  $x$  , vector as:

$$J_D = 4 \sum_{i=1}^4 q_{Di} \dots\dots\dots (4-22)$$

*Constant Pressure Case*

Repeating the same process in the previous section, the Darcy law based derivation for the fracture for the observation points at 1 – 2 with the influence of source wells at point 2, 3, and 4 on them along the fracture half-length is:

$$\Delta \bar{P}_{f\_CPress,1-2} = \frac{2\alpha_1 \mu B}{k_f h w} [q_{2\_CPress} (x_{o2} - x_{o1}) + q_{3\_CPress} (x_{o2} - x_{o1}) + q_{4\_CPress} (x_{o2} - x_{o1})] \dots\dots\dots (4-23)$$

Since the fracture is producing at constant pressure we can also be expressed as pressure drops in the reservoir, called influence functions, for the same observation points 1 – 2 and the source wells at 2, 3 and 4 as:

$$\Delta p_{R\_CPress,1-2} = \frac{\alpha_1 \mu B}{2\pi k_f h} \left[ q_{1\_CPress} L^{-1} \left( \sum \frac{1}{q_{Dq_{(1-2)1\_CPress}}} \right) + q_{2\_CPress} L^{-1} \left( \sum \frac{1}{q_{Dq_{(1-2)2\_CPress}}} \right) + q_{3\_CPress} L^{-1} \left( \sum \frac{1}{q_{Dq_{(1-2)3\_CPress}}} \right) + q_{4\_CPress} L^{-1} \left( \sum \frac{1}{q_{Dq_{(1-2)4\_CPress}}} \right) \right]$$

And using eqn.(4-8) we convert this inverse Laplace rate (reciprocal) variables in the above equation to inverse Laplace pressure variables as:

$$\Delta p_{R\_CPress,1-2} = \frac{\alpha_1 \mu B}{2\pi k_f h} \left[ q_{1\_CPress} L^{-1} \left( \sum \frac{K_0(r_{Dq_{(1-2)1}}, \sqrt{u})}{u^{\frac{3}{2}} K_1(\sqrt{u})} \right) + q_{2\_CPress} L^{-1} \left( \sum \frac{K_0(r_{Dq_{(1-2)2}}, \sqrt{u})}{u^{\frac{3}{2}} K_1(\sqrt{u})} \right) + q_{3\_CPress} L^{-1} \left( \sum \frac{K_0(r_{Dq_{(1-2)3}}, \sqrt{u})}{u^{\frac{3}{2}} K_1(\sqrt{u})} \right) + q_{4\_CPress} L^{-1} \left( \sum \frac{K_0(r_{Dq_{(1-2)4}}, \sqrt{u})}{u^{\frac{3}{2}} K_1(\sqrt{u})} \right) \right] \dots (4-24)$$

It is important to note that the inverse Laplace constant pressure variable above is the same as that the inverse Laplace constant rate variable. Here, again,  $r_{Dq_i}$  represents the distance between given two observation well for different positions of the source wells and  $q_{i\_CPress}$  is production from each of those source wells at constant pressure. Since the fluid flows from the reservoir into the fracture, the pressure drop in the reservoir is equal to the pressure drop in the fracture, at the fracture face, as:

$$\Delta p_{f\_CPress} = \Delta p_{R\_CPress} \dots \dots \dots (4-25)$$

Going according to the same lines as the previous section we have:

$$\left[ q_{1\_CPress} L^{-1} \left( \sum \frac{K_0 (r_{Dq(1-2)1}, \sqrt{u})}{u^{\frac{3}{2}} K_1(\sqrt{u})} \right) + q_{2\_CPress} L^{-1} \left( \sum \frac{K_0 (r_{Dq(1-2)2}, \sqrt{u})}{u^{\frac{3}{2}} K_1(\sqrt{u})} \right) + q_{3\_CPress} L^{-1} \left( \sum \frac{K_0 (r_{Dq(1-2)3}, \sqrt{u})}{u^{\frac{3}{2}} K_1(\sqrt{u})} \right) + q_{4\_CPress} L^{-1} \left( \sum \frac{K_0 (r_{Dq(1-2)4}, \sqrt{u})}{u^{\frac{3}{2}} K_1(\sqrt{u})} \right) \right] =$$

$$= \frac{4\pi k}{k_f w} [q_{2\_CPress} (x_{o2} - x_{o1}) + q_{3\_CPress} (x_{o2} - x_{o1}) + q_{4\_CPress} (x_{o2} - x_{o1})] \dots\dots\dots (4-26)$$

On multiplying with  $x_f$ :

$$\left[ q_{1\_CPress} L^{-1} \left( \sum \frac{K_0 (r_{Dq(1-2)1}, \sqrt{u})}{u^{\frac{3}{2}} K_1(\sqrt{u})} \right) + q_{2\_CPress} L^{-1} \left( \sum \frac{K_0 (r_{Dq(1-2)2}, \sqrt{u})}{u^{\frac{3}{2}} K_1(\sqrt{u})} \right) + q_{3\_CPress} L^{-1} \left( \sum \frac{K_0 (r_{Dq(1-2)3}, \sqrt{u})}{u^{\frac{3}{2}} K_1(\sqrt{u})} \right) + q_{4\_CPress} L^{-1} \left( \sum \frac{K_0 (r_{Dq(1-2)4}, \sqrt{u})}{u^{\frac{3}{2}} K_1(\sqrt{u})} \right) \right] =$$

$$= \frac{4\pi}{C_{jD} x_f} [q_{2\_CPress} (x_{o2} - x_{o1}) + q_{3\_CPress} (x_{o2} - x_{o1}) + q_{4\_CPress} (x_{o2} - x_{o1})] \dots\dots\dots (4-27)$$

To complete the system of linear equations, we equate the summation of pressure drops at the real well at the end of fracture due to source wells being at various points to a unit pressure drop at that real well (definition of productivity index):

$$q_{D1\_CPress} L^{-1} \left( \sum \frac{K_0 (r_{Dq(1-1)1}, \sqrt{u})}{u^{\frac{3}{2}} K_1(\sqrt{u})} \right) + q_{D2\_CPress} L^{-1} \left( \sum \frac{K_0 (r_{Dq(1-1)2}, \sqrt{u})}{u^{\frac{3}{2}} K_1(\sqrt{u})} \right) + q_{D3\_CPress} L^{-1} \left( \sum \frac{K_0 (r_{Dq(1-1)3}, \sqrt{u})}{u^{\frac{3}{2}} K_1(\sqrt{u})} \right) + q_{D4\_CPress} L^{-1} \left( \sum \frac{K_0 (r_{Dq(1-1)4}, \sqrt{u})}{u^{\frac{3}{2}} K_1(\sqrt{u})} \right) = 1 \dots\dots\dots (4-28)$$

The complete system of equations can again be expressed in matrix form as:

$$A x_{CPress} = d_{CPress} \dots\dots\dots (4-29)$$



Here,  $A$ , is a matrix which is exactly same for constant rate case and is given by:

$$\begin{bmatrix} (1) & L^{-1} \left( \sum \frac{K_0(r_{D_{01-210}}, \sqrt{u})}{u^{\frac{3}{2}} K_1(\sqrt{u})} \right) & L^{-1} \left( \sum \frac{K_0(r_{D_{01-212}}, \sqrt{u})}{u^{\frac{3}{2}} K_1(\sqrt{u})} \right) & L^{-1} \left( \sum \frac{K_0(r_{D_{01-213}}, \sqrt{u})}{u^{\frac{3}{2}} K_1(\sqrt{u})} \right) & L^{-1} \left( \sum \frac{K_0(r_{D_{01-214}}, \sqrt{u})}{u^{\frac{3}{2}} K_1(\sqrt{u})} \right) \\ (2) & L^{-1} \left( \sum \frac{K_0(r_{D_{01-210}}, \sqrt{u})}{u^{\frac{3}{2}} K_1(\sqrt{u})} \right) & L^{-1} \left( \sum \frac{K_0(r_{D_{01-212}}, \sqrt{u})}{u^{\frac{3}{2}} K_1(\sqrt{u})} \right) - \frac{4\pi}{C_{\beta D} I_s} (x_{v2} - x_{v1}) & L^{-1} \left( \sum \frac{K_0(r_{D_{01-213}}, \sqrt{u})}{u^{\frac{3}{2}} K_1(\sqrt{u})} \right) - \frac{4\pi}{C_{\beta D} I_s} (x_{v2} - x_{v1}) & L^{-1} \left( \sum \frac{K_0(r_{D_{01-214}}, \sqrt{u})}{u^{\frac{3}{2}} K_1(\sqrt{u})} \right) - \frac{4\pi}{C_{\beta D} I_s} (x_{v2} - x_{v1}) \\ (3) & L^{-1} \left( \sum \frac{K_0(r_{D_{01-210}}, \sqrt{u})}{u^{\frac{3}{2}} K_1(\sqrt{u})} \right) & L^{-1} \left( \sum \frac{K_0(r_{D_{01-212}}, \sqrt{u})}{u^{\frac{3}{2}} K_1(\sqrt{u})} \right) - \frac{4\pi}{C_{\beta D} I_s} (x_{v2} - x_{v1}) & L^{-1} \left( \sum \frac{K_0(r_{D_{01-213}}, \sqrt{u})}{u^{\frac{3}{2}} K_1(\sqrt{u})} \right) - \frac{4\pi}{C_{\beta D} I_s} (x_{v3} - x_{v1}) & L^{-1} \left( \sum \frac{K_0(r_{D_{01-214}}, \sqrt{u})}{u^{\frac{3}{2}} K_1(\sqrt{u})} \right) - \frac{4\pi}{C_{\beta D} I_s} (x_{v3} - x_{v1}) \\ (4) & L^{-1} \left( \sum \frac{K_0(r_{D_{01-210}}, \sqrt{u})}{u^{\frac{3}{2}} K_1(\sqrt{u})} \right) & L^{-1} \left( \sum \frac{K_0(r_{D_{01-212}}, \sqrt{u})}{u^{\frac{3}{2}} K_1(\sqrt{u})} \right) - \frac{4\pi}{C_{\beta D} I_s} (x_{v2} - x_{v1}) & L^{-1} \left( \sum \frac{K_0(r_{D_{01-213}}, \sqrt{u})}{u^{\frac{3}{2}} K_1(\sqrt{u})} \right) - \frac{4\pi}{C_{\beta D} I_s} (x_{v3} - x_{v1}) & L^{-1} \left( \sum \frac{K_0(r_{D_{01-214}}, \sqrt{u})}{u^{\frac{3}{2}} K_1(\sqrt{u})} \right) - \frac{4\pi}{C_{\beta D} I_s} (x_{v4} - x_{v1}) \end{bmatrix}$$

$x_{CPress}$ , is a solution vector. It is multiplied and divided by the corresponding constant rate values from eqn.(4-21) and is:

$$x_{CPress} = \begin{bmatrix} q_{D1\_CPress} \\ q_{D2\_CPress} \\ q_{D3\_CPress} \\ q_{D4\_CPress} \end{bmatrix} = \begin{bmatrix} \left( \frac{q_{D1\_CPress}}{q_{D1}} \right) q_{D1} \\ \left( \frac{q_{D2\_CPress}}{q_{D2}} \right) q_{D2} \\ \left( \frac{q_{D3\_CPress}}{q_{D3}} \right) q_{D3} \\ \left( \frac{q_{D4\_CPress}}{q_{D4}} \right) q_{D4} \end{bmatrix}$$

$d_{CPress}$ , is a vector given by:

$$d_{CPress} = \begin{bmatrix} 1 \\ 0 \\ 0 \\ 0 \end{bmatrix}$$

The problem get reduced to a constant rate one with the exception of scaling of the constant pressure dimensionless well rates. The dimensionless productivity index for total reservoir is derived from,  $X_{CPress}$ , vector as:

$$J_{D\_CPress} = 4 \sum_{i=1}^4 \left( \frac{q_{Di\_CPress}}{q_{Di}} \right) q_{Di} \dots\dots\dots(4-30)$$

**Partially Penetrating, Single Finite Conductivity Fracture Solution for Vertical Well Using, Partially Penetrating, Finite Wellbore Radial Solution and Boundary Element Method**

We start by using, for a vertical well, pressure drop given by continuous point source solution (forming an equivalent line source solution) for a well in infinite reservoir, as given by Ozkan<sup>49</sup> is:

$$\Delta \bar{p}(r_D, u) = \frac{\tilde{q} \mu h}{2\pi k L h_D s} K_0(r_D, \sqrt{u}) \dots\dots\dots(4-31)$$

Where the point source flow rate,  $\tilde{q}$ , is summed up to give the line source term (STB) as:

$$q = \tilde{q} h B$$

$s$  and  $u$  are the Laplace space variables and,

$$h_D = \frac{h}{L} \sqrt{\frac{k}{k_z}}$$

If converted to dimensionless form, this solution will transform into well-known line source solution as:

$$\overline{p}_D(r_D, u) = \frac{1}{u} K_0(r_D, \sqrt{u}) \dots\dots\dots (4-32)$$

If wellbore radius is also taken into consideration then the equivalent finite wellbore (cylindrical source) solution, given in the text (and is repeated here), is:

$$\overline{p}_D(r_D, u) = \frac{K_0(r_D, \sqrt{u})}{u^{\frac{3}{2}} K_1(\sqrt{u})} \dots\dots\dots (4-33)$$

For a partially penetrating vertical well, pressure drop given by continuous point source solution (forming an equivalent line source solution) in an infinite reservoir, is:

$$\Delta \overline{p}(r_D, u) = \frac{\tilde{q} \mu h}{2\pi k L h_D s} K_0(r_D, \sqrt{u}) + \frac{2\tilde{q} \mu h}{\pi^2 k L h_D s} \sum_{n=1}^{\infty} \left[ \left( \frac{1}{n} \right) K_0(r_D \varepsilon_n) \sin \left( n \pi \frac{h_w}{2h} \right) \cos \left( n \pi \frac{z_w}{h} \right) \cos \left( n \pi \frac{z}{h} \right) \right] \dots\dots (4-34)$$

Where, once again, the point source flow rate,  $\tilde{q}$ , is summed up to give the line source term (STB) as:

$$q = \tilde{q} h_w B \dots\dots\dots (4-35)$$

$s$  and  $u$  are the Laplace space variables and various other variable are:

$$h_D = \frac{h_w}{L} \sqrt{\frac{k}{k_z}} \dots\dots\dots(4-36)$$

$$\varepsilon_n = \sqrt{u + \frac{n^2 \pi^2}{h_D^2}} \dots\dots\dots(4-37)$$

$z_w$  and  $z$  are the variables in the  $z$ -direction, where the integration is carried out from

$z_w - \frac{h_w}{2}$  to  $z_w + \frac{h_w}{2}$ , and  $h_w$  is the open interval. If  $h_w = h$ , it implies fully

penetrating vertical line source well. By analogy, the dimensionless form for line source solution, is:

$$\overline{p}_D(r_D, u) = \frac{1}{u} K_0(r_D, \sqrt{u}) + \left(\frac{4}{\pi}\right) \left(\frac{h}{h_w}\right) \left(\frac{1}{u}\right) \sum_{n=1}^{\infty} \left[ \left(\frac{1}{n}\right) K_0(r_D \varepsilon_n) \sin\left(n \pi \frac{h_w}{2h}\right) \cos\left(n \pi \frac{z_w}{h}\right) \cos\left(n \pi \frac{z}{h}\right) \right] \dots\dots\dots(4-38)$$

If wellbore radius is also taken into consideration then, by analogy, the equivalent finite wellbore (cylindrical source) solution will be:

$$\overline{p}_{D-pp}(r_D, u) = \frac{K_0(r_D, \sqrt{u})}{u^{\frac{3}{2}} K_1(r_D, \sqrt{u})} + \left(\frac{4}{\pi}\right) \left(\frac{h}{h_w}\right) \sum_{z=z_w-\frac{h_w}{2}}^{z_w+\frac{h_w}{2}} \sum_{n=1}^{\infty} \left[ \left(\frac{1}{n}\right) \left(\frac{K_0(r_D \varepsilon_n)}{u^{\frac{3}{2}} K_1(r_D, \sqrt{u})}\right) \sin\left(n \pi \frac{h_w}{2h}\right) \cos\left(n \pi \frac{z_w}{h}\right) \cos\left(n \pi \frac{z}{h}\right) \right] \dots\dots\dots(4-39)$$

The second summation aggregates the solution along the cylindrical source in the vertical direction. This solution is then used in the superposition process, with everything else remaining same from the radial solution discussed previously, as:

$$\left[ \sum_{j=1}^{\infty} \left( \frac{K_0(r_{Dj}, \sqrt{u})}{u^{\frac{3}{2}} K_1(\sqrt{u})} \right) \right]_{n_w \rightarrow \infty} = \left[ \sum_{\substack{m=-\infty \\ n=-\infty}}^{m=\infty \\ n=\infty} \left( P_{D-pp} + \frac{K_0(r_{D2}, \sqrt{u})}{u^{\frac{3}{2}} K_1(\sqrt{u})} + \frac{K_0(r_{D3}, \sqrt{u})}{u^{\frac{3}{2}} K_1(\sqrt{u})} + \frac{K_0(r_{D4}, \sqrt{u})}{u^{\frac{3}{2}} K_1(\sqrt{u})} \right) \right]_{n_w \rightarrow \infty} \quad \text{..(4-40)}$$

Thus the Laplace domain solution of dimensionless pressure for a constant rate is:

$$\overline{p}_D(r_D, u) = \left( \frac{K_0(r_D, \sqrt{u})}{u^{\frac{3}{2}} K_1(\sqrt{u})} \right) + \left[ \sum_{j=1}^{\infty} \left( \frac{K_0(r_{Dj}, \sqrt{u})}{u^{\frac{3}{2}} K_1(\sqrt{u})} \right) \right]_{n_w \rightarrow \infty} \quad \text{.....(4-41)}$$

The way it is implement in the algorithm is shown in the figure 38 below.

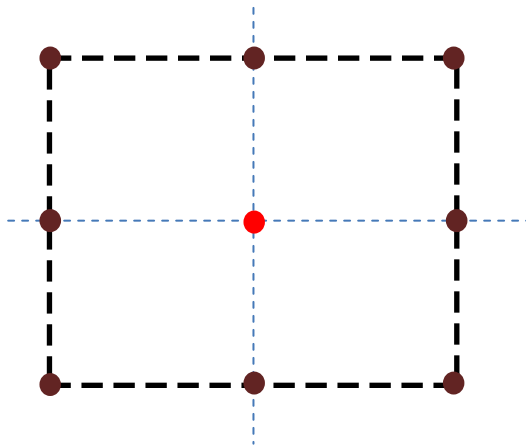


**Figure 38.** Mathematical Treatment of Central Well.

The full penetration radial solution (brown wells – all other except central one) are still used to form the boundaries but the partial penetrating well solution (central red well), in Laplace domain and given by eqn.(4-41), is used as the basis of superposition to arrive at the solution of partially penetrating fracture. This is the solution of infinitely conductive, partially penetrating fracture. The process of generation of influence function for boundary element method is repeated to generate the solution of finite conductivity partially penetrating fracture. Both constant rate and constant pressure solution can be evaluated. Use of earlier method is envisaged.

**Evaluation of Convergence Pressure Drop of Single Transverse Fracture in a  
Horizontal Well Using Boundary Element Method**

This section gives the big picture of boundary element method (BEM) using constant boundary elements. Refer to Katsikadelis<sup>50</sup> for an exhaustive explanation. We start with the *divergence theorem of Gauss* as:

$$\int_{\Omega} \nabla \cdot u \, d\Omega = \int_{\Gamma} u \cdot n \, ds \dots\dots\dots(4-42)$$

This converts the domain integral (represented on the LHS of the equation) on a domain  $\Omega$  to a line integral (represented on the RHS of the equation) at the boundary  $\Gamma$ .

Specifically, for BEM, we use *Green’s second identity* that is more suited for numerical implementation. This is given by:

$$\int_{\Omega} (v \nabla^2 u - u \nabla^2 v) d\Omega = \int_{\Gamma} \left( v \frac{\partial u}{\partial n} - u \frac{\partial v}{\partial n} \right) ds \dots\dots\dots(4-43)$$

Here in this case  $u$  is the unknown variable and  $v$  is a known variable. In order for  $v$  to be known, the solution needs to be twice differentiable (This condition also applies to  $u$ ). For this reason we chose Dirac delta function which has a density at any point  $Q(\xi, \eta)$ , with the source present at  $P(x, y)$ , mathematically expressed as:

$$f(Q) = \delta(Q - P) \dots\dots\dots(4-44)$$

Thus,  $v$  satisfies the Laplace equation:

$$\nabla^2 v = \delta(Q - P) \dots\dots\dots(4-45)$$

The fundamental solution of this equation, used in BEM method in terms of polar coordinates, is given by:

$$v = \left( \frac{1}{2\pi} \right) \ln r \dots\dots\dots(4-46)$$

For the unknown variable  $u$ , we derive the solution of the Laplace equation:

$$\nabla^2 u = 0 \dots\dots\dots(4-47)$$

for the general boundary conditions:

$$u = \bar{u} \text{ on } \Gamma_1 \dots\dots\dots(4-48)$$

$$\frac{\partial u}{\partial n} = \bar{u}_n \text{ on } \Gamma_2 \dots\dots\dots(4-49)$$

as proposed below. By applying *Green's second identity* for the functions  $u$  and  $v$  that satisfy the above Laplace equation as:

$$u(P) = \int_{\Omega} u(Q) \delta(Q-P) d\Omega_Q = -\int_{\Gamma} \left[ v(q,P) \frac{\partial u(q)}{\partial n_q} - u(q) \frac{\partial v(q,P)}{\partial n_q} \right] ds_q \dots\dots\dots(4-50)$$

Here the points inside the domain are expressed as upper case letters whereas the points on the boundary are expressed as lower case letters. The above equation for a smooth boundary is given by:

$$\frac{1}{2} u(P) = -\int_{\Gamma} \left[ v(q,P) \frac{\partial u(q)}{\partial n_q} - u(q) \frac{\partial v(q,P)}{\partial n_q} \right] ds_q \dots\dots\dots(4-51)$$

The discretized form of this equation, for  $N$  constant elements, is given by:

$$\frac{1}{2} u^i = -\sum_{j=1}^N \int_{\Gamma_j} v(p_i, q) \frac{\partial u(q)}{\partial n_q} ds_q + \sum_{j=1}^N \int_{\Gamma_j} u(q) \frac{\partial v(p_i, q)}{\partial n_q} ds_q \dots\dots\dots(4-52)$$

Rearranging and rewriting in terms of *influence coefficients*, we have:



$$-\frac{1}{2}u^i + \sum_{j=1}^N \left( \int_{\Gamma_j} \frac{\partial v}{\partial n_q} ds_q \right) u^j = \sum_{j=1}^N \left( \int_{\Gamma_j} v ds_q \right) u_n^j \dots\dots\dots(4-53)$$

which can be expressed in a general form:

$$\sum_{j=1}^N H_{ij} u^j = \sum_{j=1}^N G_{ij} u_n^j \dots\dots\dots(4-54)$$

$$[H]\{u\} = [G]\{u_n\} \dots\dots\dots(4-55)$$

$$\begin{bmatrix} [H_{11}] & [H_{12}] \end{bmatrix} \begin{Bmatrix} \{u\}_1 \\ \{u\}_2 \end{Bmatrix} = \begin{bmatrix} [G_{11}] & [G_{12}] \end{bmatrix} \begin{Bmatrix} \{u_n\}_1 \\ \{u_n\}_2 \end{Bmatrix} \dots\dots\dots(4-56)$$

$\{u\}_1$  and  $\{u_n\}_2$  are the known variables and  $\{u_n\}_1$  and  $\{u\}_2$  are the unknown variables.

If we were to rearrange the above matrix so that all the knowns are on the RHS and all the unknowns are on the LHS, we will have:

$$\begin{bmatrix} [H_{12}] & - [G_{11}] \end{bmatrix} \begin{Bmatrix} \{u\}_2 \\ \{u_n\}_1 \end{Bmatrix} = \begin{bmatrix} - [H_{11}]\{u\}_1 & + [G_{12}]\{u_n\}_2 \end{bmatrix} \dots\dots\dots(4-57)$$

$$[A] \{X\} = \{B\} \dots\dots\dots(4-58)$$

which can be solved for the unknown vector,  $X$ , which is the solution. Important point to consider here is that both for the known vector,  $B$ , and the unknown vector,  $X$ , we need the value of either the principal variable or its derivative at the boundary.

*Input Boundary Conditions – Knowns and Unknowns*

The key to numerically solving this problem is to account for the known boundary conditions. To evaluate these, we rely on the method proposed by Brown<sup>51</sup> and reproduced here. We start by considering the flow from the tip of the fracture to the wellbore at the end of the same fracture. We have from the Darcy’s law (assuming the flow is in  $x$ -direction):

$$v = \left( \frac{k_f}{\mu} \right) \nabla p \dots\dots\dots(4-59)$$

$$v_x = - \left( \frac{k_f}{\mu} \right) \left( \frac{\partial p_f}{\partial x} \right)_{x=0} \dots\dots\dots(4-60)$$

This volumetric velocity is calculated at the end of the fracture,  $x_d = 0$ , having the dimensions equal to the width,  $w$ , and height,  $h$ . The flow rate is computed using the surface integral of the above equation and the flow rate is equal to quarter of total flow into the fracture being modeled and that the fracture is bi-winged.

$$\int_0^{w/2} \int_0^{w/2} v_x \partial y \partial z = - \left( \frac{k_f}{\mu} \right) \int_0^{w/2} \int_0^{w/2} \left( \frac{\partial p_f}{\partial x} \right)_{x=0} \partial y \partial z \dots\dots\dots(4-61)$$

Which results in:

$$\frac{q_f}{8} = - \left( \frac{k_f}{\mu} \right) \left( \frac{w}{2} \right) \left( \frac{h}{2} \right) \left( \frac{\Delta p_f}{\Delta x} \right)_{x=0} \dots\dots\dots(4-62)$$

Converting the above equation into dimensionless form we have:

$$1 = - \left( \frac{k_f w B}{\pi k x_f} \right) \left( \frac{\Delta p_{fD}}{\Delta x_D} \right)_{x_D=0} \dots\dots\dots(4-63)$$

But,

$$C_{fD} = - \left( \frac{k_f w}{k x_f} \right) \dots\dots\dots(3-29)$$

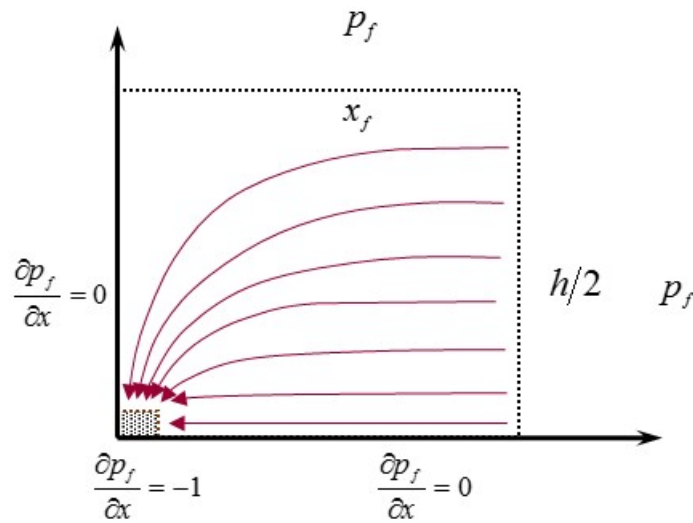


**Figure 39.** Source Wells and Observation Wells in the Generation.

Thus the eqn.(4-63) in terms of reservoir barrels is:

$$\left( \frac{\Delta p_{fD}}{\Delta x_D} \right)_{x_D=0} = - \left( \frac{\pi}{C_{fD}} \right) \dots\dots\dots(4-64)$$

In this equation the solution at the wellbore represents the flow entering the fracture at  $\Delta x_D = 1$ . At the boundary, the flow is subjected to the following constraint:

$$\Delta p_{JD} = \Delta p_{RD} \dots\dots\dots(4-65)$$

which means that the dimensionless pressure drop just inside and the outside (reservoir) of the fracture should be equal. This pressure continuity, at the boundary, is important.

Combining these two equations, we arrive at the overall constraint which, all known pressure values at the boundary are subjected to, and is given by eqn.(4-58). The majority of the known pressure values are along the top of the quarter section of the fracture as in figure 39 and the pressures generated by the superposition process are then multiplied by eqn.(4-64) to give the known boundary values. The derivatives of all boundary terms on the fracture are given by:

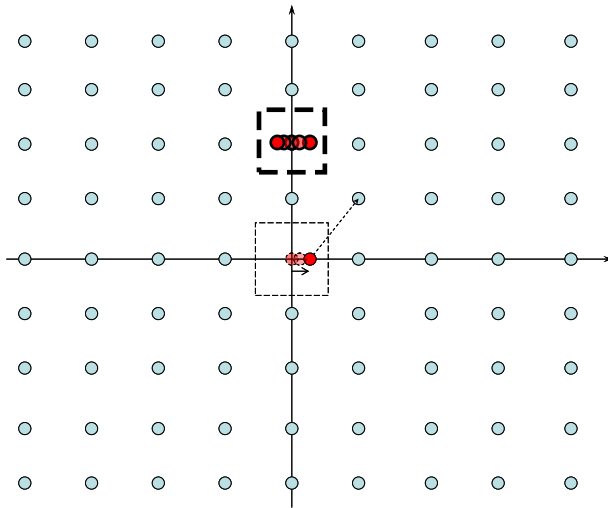
$$\frac{\partial p_{JD}}{\partial x_D} = -1 \dots\dots\dots(4-66)$$

Figure 39 shows the way the boundary conditions are entered in the BEM solution. It is quarter of the whole transverse fracture with the horizontal well being represented by a square at the bottom left corner. The dimension of square is equal to that of the well which means the diagonal of the square is equal to radius of the well. The no flow condition, for the left side and the bottom boundary, is created by having the derivative on the two sides to be equal to zero which comes out of symmetry. The top and the right boundary are subjected to the known primary variable which is pressure in this case but subject to constraint outlined by eqn.(4-61).

## Partially Penetrating, Multiple Transverse Finite Conductivity Fracture Solution Using, Partially Penetrating, Finite Wellbore Radial Dual Porosity Solution and Boundary Element Method

The method is outlined in five steps:

1. Use the previous Helmy's method to describe a well at the center of square drainage area to get constant rate and constant pressure solutions.
2. With the constant rate solution, repeat the step by moving the well off-center along the length of the fracture in the square drainage area. This is the infinite conductivity fracture solution. Invert it into real domain solution.
3. Use boundary element method (similar to Romero's<sup>38</sup> method) for the solution for finite conductivity fracture using solution from step 2.
4. Calculate the convergence pressure drop using BEM outlined previously.
5. Repeat step 3 for each transverse fracture treated independently, figure 40.



**Figure 40.** The Infinite Distribution of Image Wells Required to Simulate the No-flow Condition across the Boundary of a Square Reservoir and Multiple Fracture.

Mathematically, it means solving independently the matrices and adding the result as:

$$\begin{array}{r} A x = d \quad Fracture \ 1 \\ + \\ A x = d \quad Fracture \ 2 \\ + \quad \dots\dots\dots(4-67) \\ \cdot \\ \cdot \\ A x = d \quad Fracture \ n \end{array}$$

Dual porosity effect is incorporated using eqn.(3-38) in the radial solution.

## CHAPTER V

### ANALYSIS, RESULTS AND CONCLUSIONS OF FULL TRANSIENT MATRIX AND AQUIFER UNCONVENTIONAL RESERVOIR MODEL

Although all four solutions are outlined in the Appendices E through H, the emphasis is on the full transient model only given by Appendix H. This model has the capability of reproducing results of early transient, late transient and pseudosteady state conditions both for the matrix and the aquifer.

#### **Basis for Long Term Deliverability of a Well – The Derivative Analysis**

The dimensionless productivity index as outlined in earlier chapters, for both constant rate case and constant pressure cases, are given by:

Constant Rate Case:

$$J_D = \frac{1}{(p_D - \bar{p}_{AvD})} \dots \dots \dots (3-63)$$

$$J_D = \frac{1}{(p_D - 2\pi t_{DA})} \dots \dots \dots (3-69)$$

Constant Pressure Case:

$$J_D = \frac{1}{\left(\frac{1}{q_D} - \frac{1}{q_{AvD}}\right)} \dots \dots \dots (3-80)$$

$$J_D = \frac{q_D}{\left[1 - \left(\frac{2\pi N p_D}{A_D}\right)\right]} \dots \dots \dots (3-81)$$

The above equations, for further understanding, are rewritten as:

Constant Rate Case:

$$\left(\frac{1}{J_D}\right) = p_D - 2\pi t_{DA} \dots\dots\dots(5-1)$$

Constant Pressure Case:

$$\left(\frac{1}{J_D}\right) = \frac{1}{q_D} \left[1 - \left(\frac{2\pi N_{pD}}{A_D}\right)\right] \dots\dots\dots(5-2)$$

Taking the logarithmic derivative of both sides of the above equations, we have:

Constant Rate Case:

$$\frac{d}{d(\ln t_D)} \left(\frac{1}{J_D}\right) = \frac{dp_D}{d(\ln t_D)} - 2\pi \frac{dt_{DA}}{d(\ln t_D)} \dots\dots\dots(5-3)$$

Constant Pressure Case:

$$\frac{d}{d(\ln t_D)} \left(\frac{1}{J_D}\right) = \frac{d}{d(\ln t_D)} \left(\frac{1}{q_D}\right) - \left(\frac{2\pi}{A_D}\right) \frac{d}{d(\ln t_D)} \left(\frac{N_{pD}}{q_D}\right) \dots\dots\dots(5-4)$$

Here,

$$t_{DAc} = t_D = \frac{0.00633 k t}{\varphi \mu c_t A_{cw}} = \frac{5.615 (0.001127) k t}{\varphi \mu c_t A_{cw}} \dots\dots\dots(3-56)$$

$$t_{DA} = \frac{5.615}{\alpha_1} \left(\frac{k t}{\varphi \mu c_t A}\right) = \frac{0.00633 k t}{\varphi \mu c_t A} \dots\dots\dots(3-68)$$



Combining the two eqn.(3-56) and eqn.(3-68) gives:

$$t_{DA} = \left(\frac{t_D}{A_D}\right) \dots\dots\dots (5-5)$$

And we know,

$$N_{pD} = q_D t_D \dots\dots\dots (5-6a)$$

$$A_D = \frac{A}{A_{cw}} \dots\dots\dots (5-6b)$$

Hence for both cases and from eqn.(5-5) and eqn.(5-6), we have:

Constant Rate Case:

$$\frac{d}{d(\ln t_D)} \left(\frac{1}{J_D}\right) = \frac{dp_D}{d(\ln t_D)} - \left(\frac{2\pi}{A_D}\right) \frac{dt_D}{d(\ln t_D)} \dots\dots\dots (5-7)$$

Constant Pressure Case:

$$\frac{d}{d(\ln t_D)} \left(\frac{1}{J_D}\right) = \frac{d}{d(\ln t_D)} \left(\frac{1}{q_D}\right) - \left(\frac{2\pi}{A_D}\right) \frac{dt_D}{d(\ln t_D)} \dots\dots\dots (5-8)$$

which reduces to and is written as an equation of straight line (log-log plot) for linear model (bilinear or linear flow only):

Constant Rate Case:

$$\frac{d}{d(\ln t_D)} \left(\frac{1}{J_D}\right) = \frac{dp_D}{d(\ln t_D)} - \left(\frac{2\pi}{A_D}\right) t_D \dots\dots\dots (5-9)$$

Constant Pressure Case:

$$\frac{d}{d(\ln t_D)} \left(\frac{1}{J_D}\right) = \frac{d}{d(\ln t_D)} \left(\frac{1}{q_D}\right) - \left(\frac{2\pi}{A_D}\right) t_D \dots\dots\dots (5-10)$$

There is an important point which needs attention here. The area,  $A_D$ , is known ( $A_D = 1$  for all cases in this thesis). Also since the flow is bilinear or linear (for the former it will be quarter slope whereas for the latter it will be half slope on a log-log plot), then overall solution in time is an equation of line with two slopes. The eqn.(5-9) and eqn.(5-10) have been deliberately left in this form in order to exploit the constant slope values which are only possible with the logarithmic derivative.

### Proppant Number and Concept of Constant Volume Induced Fracture

As per definition, the source terms are given by volumetric average as:

$$\sigma_{mf} = \sigma_m \left( \frac{V_m}{V_{f+m}} \right) = \alpha \left( \frac{k}{\mu} \right)_{mb} \left. \frac{\partial p_m}{\partial z} \right|_{z=h_{mb}/2} \dots\dots\dots(5-11)$$

Where a similar volumetric averaging is done on permeability as:

$$\left( \frac{k}{\mu} \right)_{mb} = \frac{k_m}{\mu_m} \left( \frac{V_m}{V_{f+m}} \right) \approx \frac{k_m}{\mu_m} (1 - \omega) \dots\dots\dots(5-12)$$

Hence,

$$k_{mb} \approx k_m (1 - \omega) \dots\dots\dots(5-13)$$

Here the permeability is the parameter which gets averaged and not the fluid viscosity.

Also, by definition we have:

$$\phi_{mb} = \left( \frac{V_m}{V_{f+m}} \right) \phi_m \dots\dots\dots(5-14)$$

$$\omega = \frac{\phi_{fb}c_f}{\phi_{fb}c_f + \phi_{mb}c_m} \approx \left( \frac{V_f}{V_{f+m}} \right) \dots\dots\dots(5-15)$$

recalling the interporosity flow parameter is given by:

$$\lambda_{rmf} = \lambda = \alpha \left( \frac{k_{mb}}{k_{rf}} \right) A_{cw} \dots\dots\dots(3-11)$$

Analyzing the above equations, for a dual porosity unconventional reservoir, the effect of hydraulic fracturing results in increasing the propped part of the fracture as opposed to the non-proppant propped part (including the natural fractures). Increasing the propped part increases  $\omega$  and there is simultaneous decrease of average reservoir permeability,  $k_{mb}$  based on eqn.(5-13), which in turn decreases  $\lambda_{rmf}$ . As a result there is a net change of the dual porosity proppant number  $\left( \frac{\lambda}{\omega} \right)$ . This is based on slab configuration assumption. The value of the dual porosity proppant number can be further changed by changing two components within  $\lambda_{rmf}$ :

1. Changing the shape factor, keeping the permeability unchanged. The various shape factors are given in Table 10.
2. Changing the permeability, keeping shape factor unchanged. There is a limit to this increase for any  $\lambda_{rmf}$ .

**Table 10.** Shape Factors based on Warren & Root Theory<sup>34</sup>

Flow Element Model	Number of Fracture Planes ( $n$ )	Value of PSS Lumped Parameter ( $\beta$ )	Surface Area to Volume ratio ( $\frac{2n}{h_m}$ )	Warren & Root Shape Factors ( $\sigma$ )
Linear (Slab)	1	6	$2/h_m$	$12/h_m^2$
Cylindrical (Matchstick)	2	8	$4/h_m$	$32/h_m^2$
Spherical (Cube)	3	10	$6/h_m$	$60/h_m^2$

Here  $h_m$  is the characteristic length. A constant volume fracture having a same area/volume ratio, (surface area of matrix to the matrix volume, refer figure 41) but different matrix configuration (characteristic length) that are in the proportion 1:2:3 (1-D, 2-D and 3-D respectively), will exhibit the same transient response. This is Case 1 and constant volume refers to the same volume of proppant pumped across different configurations but also refers to exactly the same area/volume ratio as well. To state this differently, in a dual porosity reservoir if the induced hydraulic fracture, for Case 1 only, creates matrix blocks of 1D, 2D or 3D configuration so that they have the same area/volume ratio, then all these three different hydraulic fractures will exhibit the same transient response.

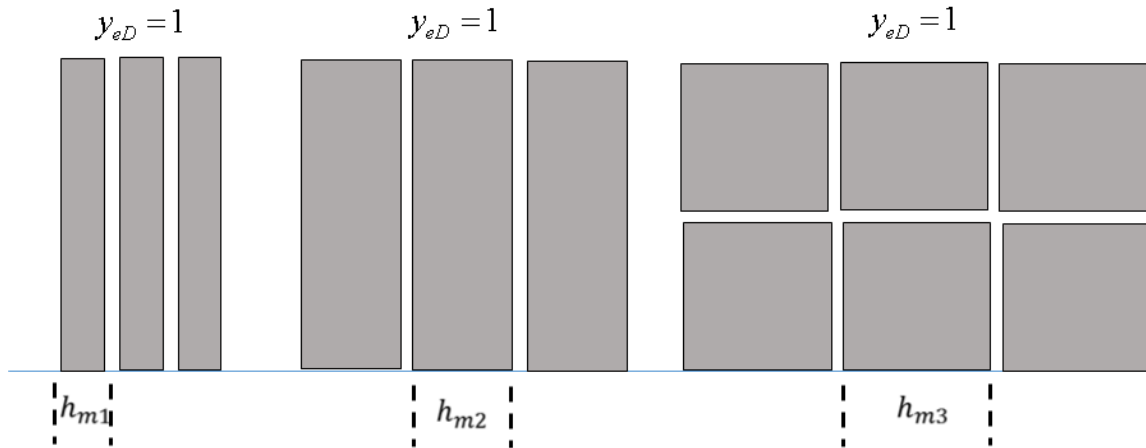


**Figure 41.** Matrix Orthogonal Geometries (with different size of matrix blocks but same fracture permeability).

Conversely, a constant volume fracture with exactly the same dimension (characteristic length) but across different configurations, 1D, 2D and 3D as referred in figure 42, which have different area/volume ratio but the ratio of matrix to fracture permeability values are such that their product with shape factor are in the proportion 1:2:3, (1-D, 2-D and 3-D respectively), will also exhibit the same transient response. This is Case 2. It is only when the boundary effects (boundary dominated or pseudosteady state flow) makes their presence felt that the solutions depart from each other in both these cases. The results are shown by Bello<sup>9</sup> in his dissertation and are reproduced in figure 43 and the results of dimensionless productivity index are shown in figure 44 and figure 45. For both Case 1 and Case 2, results are the same. The data set is shown in Table 11.

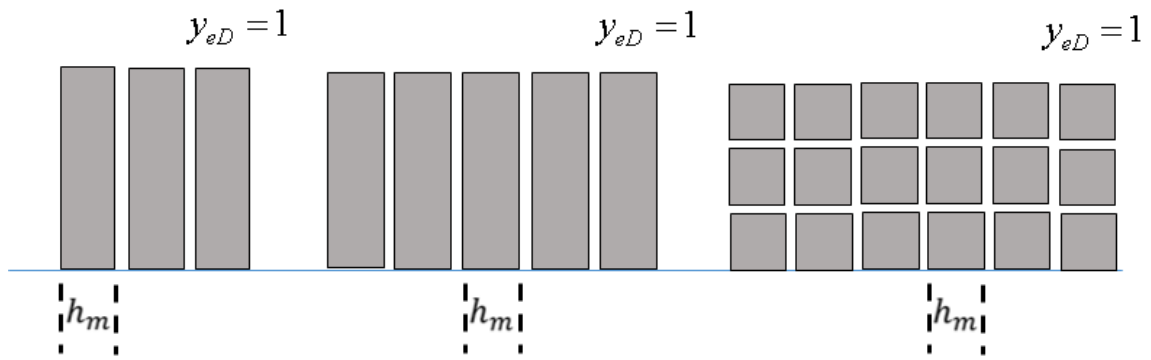


**Figure 42.** Matrix Orthogonal Geometries (with same size of matrix blocks but different fracture permeability).

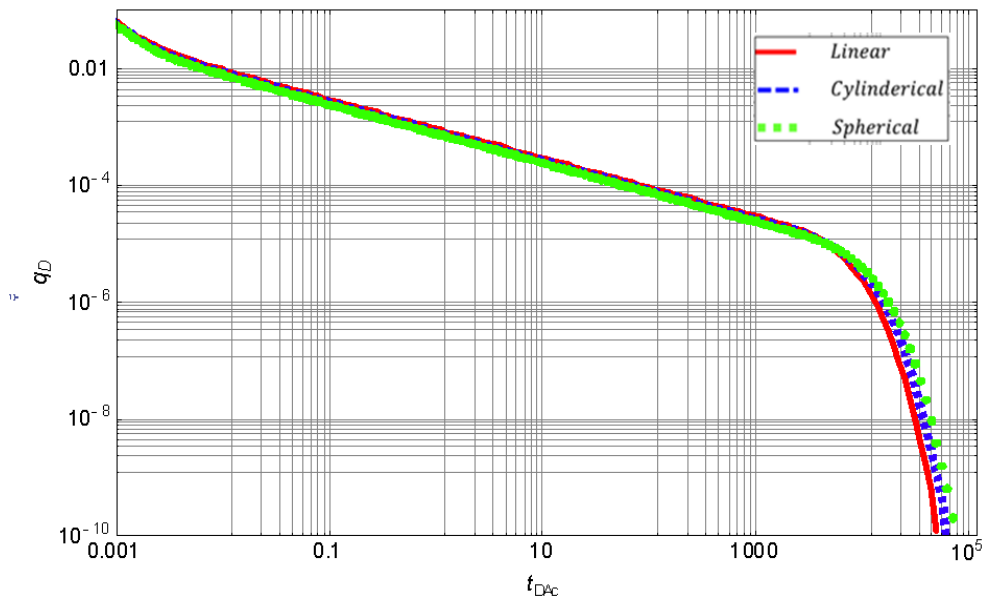


**Figure 43.** Results of Dimensionless Rate with Single Phase Transient Model for  $y_{eD} = 0.559$  and for Different Matrix Geometries as per Bello<sup>9</sup>.

An important point that needs mentioning here is the relation between the two areas  $A$  and  $A_{cw}$ . All through, we are sticking with,  $A_D = 1$  and  $y_{eD} = 1$  in this thesis. This

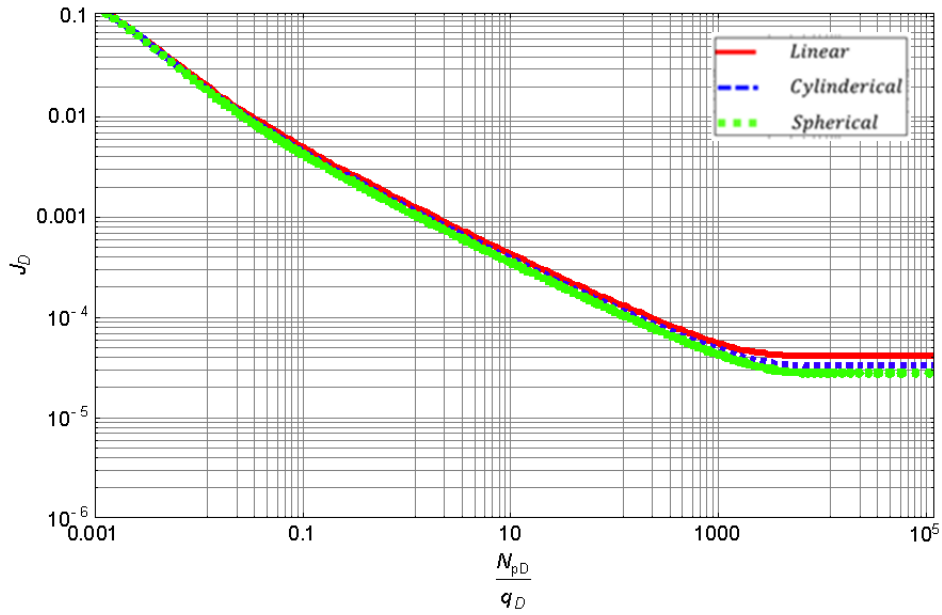


**Figure 44.** Results of Dimensionless Productivity Index with Single Phase Transient Model for  $y_{eD} = 0.559$  and for Case 1.

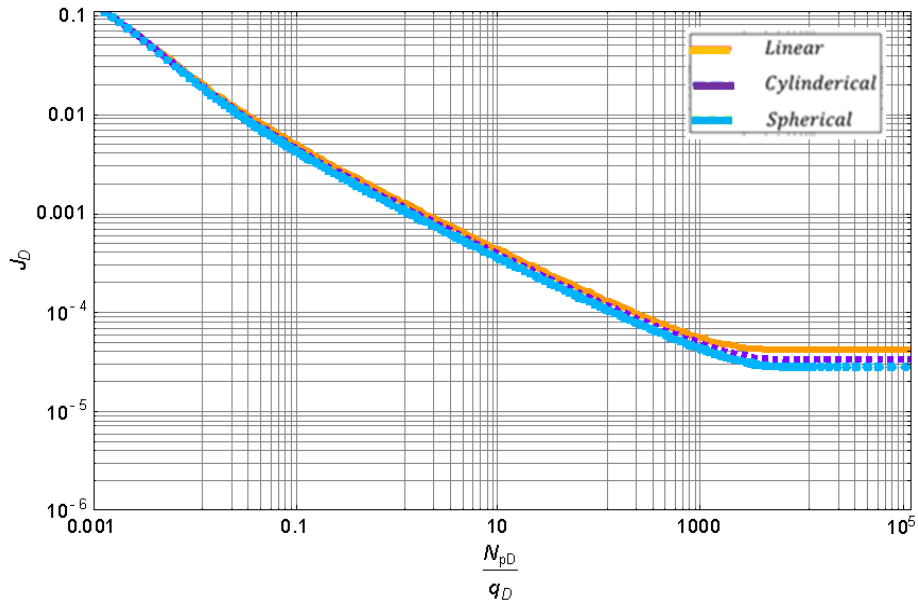


**Figure 45.** Results of Dimensionless Productivity Index with Single Phase Transient Model for  $y_{eD} = 0.559$  and for Case 2.

**Table 11.** Shape Factors Calculation Dataset as per Bello<sup>9</sup>.

	Case 1	Case 2		
		<i>Slab</i>	<i>Cyl.</i>	<i>Sphere</i>
$x_e$	2000 ft	2000 ft	2000 ft	2000 ft
$y_e$	500 ft	500 ft	500 ft	500 ft
$h$	200 ft	200 ft	200 ft	200 ft
$L$ ( <i>Slab</i> )	50 ft	50 ft		
$D$ ( <i>Cyl.</i> )	100 ft		50 ft	
$D$ ( <i>Sphere</i> )	150 ft			50 ft
$k_f$	100 md	100 md	400 md	901.41 md
$k_m$	$10^{-5}$ md	$10^{-5}$ md	$10^{-5}$ md	$10^{-5}$ md
$\omega$	$10^{-3}$	$10^{-3}$	$10^{-3}$	$10^{-3}$
<i>Computed Values</i>				
$y_{eD}$	0.559	0.559	0.559	0.559
$\sigma$	0.0048 ft <sup>2</sup>	0.0048 ft <sup>2</sup>	0.0128 ft <sup>2</sup>	0.024 ft <sup>2</sup>
$\lambda_{Ac}$ ( <i>Slab</i> )	$3.84 \times 10^{-4}$	0.000384		
$\lambda_{Ac}$ ( <i>Cyl.</i> )	$2.56 \times 10^{-4}$		0.000256	
$\lambda_{Ac}$ ( <i>Sphere</i> )	$2.13 \times 10^{-4}$			0.000213
$A_{cw} = 2x_e h$	$8.0 \times 10^5$ ft <sup>2</sup>	$8.0 \times 10^5$ ft <sup>2</sup>	$1.6 \times 10^7$ ft <sup>2</sup>	$4.0 \times 10^8$ ft <sup>3</sup>
$A_{cm} = (2/L \text{ or } 4/L \text{ or } 6/L) V_{cm}$	$1.6 \times 10^7$ ft <sup>2</sup>	$1.6 \times 10^7$ ft <sup>2</sup>	$3.2 \times 10^7$ ft <sup>2</sup>	$4.8 \times 10^7$ ft <sup>2</sup>
$V_{cm} = A_{cw} y_e$	$4.0 \times 10^8$ ft <sup>3</sup>	$4.0 \times 10^8$ ft <sup>3</sup>	$4.0 \times 10^8$ ft <sup>3</sup>	$4.0 \times 10^8$ ft <sup>3</sup>
$A = 2x_e y_e$	$2.0 \times 10^6$ ft <sup>2</sup>	$2.0 \times 10^6$ ft <sup>2</sup>	$2.0 \times 10^6$ ft <sup>2</sup>	$2.0 \times 10^6$ ft <sup>2</sup>
<i>Dual Porosity Proppant Number</i>				
$\lambda/\omega$ ( <i>Slab</i> )	0.384	0.384		
$\lambda/\omega$ ( <i>Cyl.</i> )	0.256		0.256	
$\lambda/\omega$ ( <i>Sphere</i> )	0.213			0.213

implies that  $y_e$  gets translated to drainage area,  $A$ . For  $y_{eD} \neq 1$ , the condition,  $A_D = 1$ , still holds if we incorporates,  $y_e$ , according to following formulation:



$$A_D = \frac{A}{A_{cw}} = 1 = N \left[ \frac{\sqrt{A_{cw} y_{eD=1}}}{\sqrt{A_{cw} y_{eD \neq 1}}} \left( \frac{\sqrt{A_{cw} y_{eD=1}}}{\sqrt{A_{cw} y_{eD \neq 1}}} \right) \right] \dots (5-16a)$$

$$y_{eD} = \frac{y_e}{\sqrt{A_{cw}}} = \frac{1}{\sqrt{N}} \left( \frac{y_e y_{eD \neq 1}}{\sqrt{A_{cw} y_{eD=1}}} \right) \dots (5-16b)$$

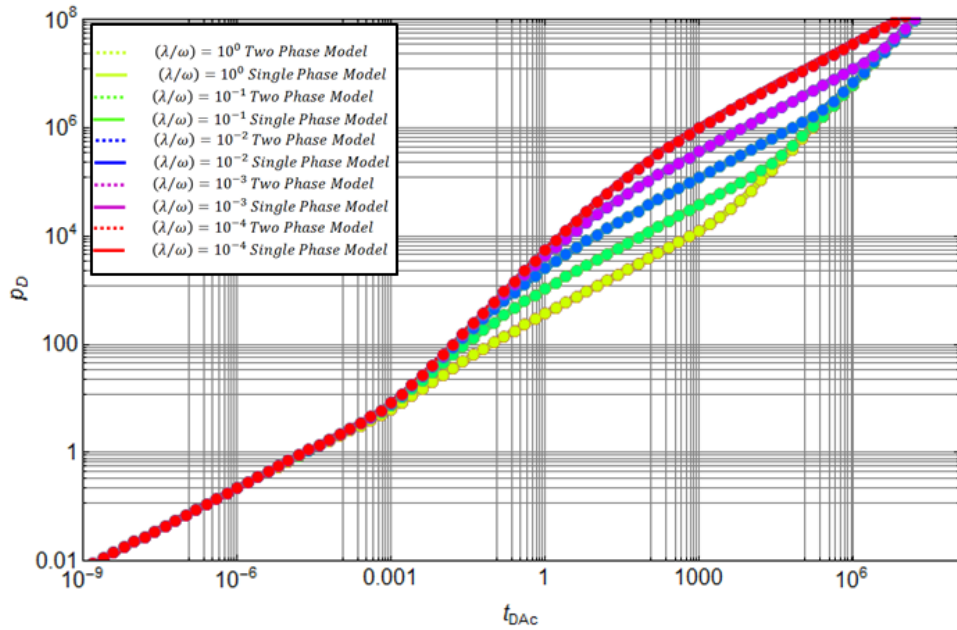
$$[A_{cw}]_{y_{eD \neq 1}} = N [A_{cw}]_{y_{eD=1}} \dots (5-16c)$$

$$A = [A_{cw}]_{y_{eD=1}} \dots (5-16d)$$

where  $N$  is the multiplier on area,  $[A_{cw}]_{y_{eD=1}}$ . For  $y_{eD} = 1$ ,  $N = 1$  this simplifies to eqn.(5-16d). It is imperative we maintain the relation between  $y_e$  and  $A$  and  $A_D = 1$ .

### Validation of the Full Transient Model

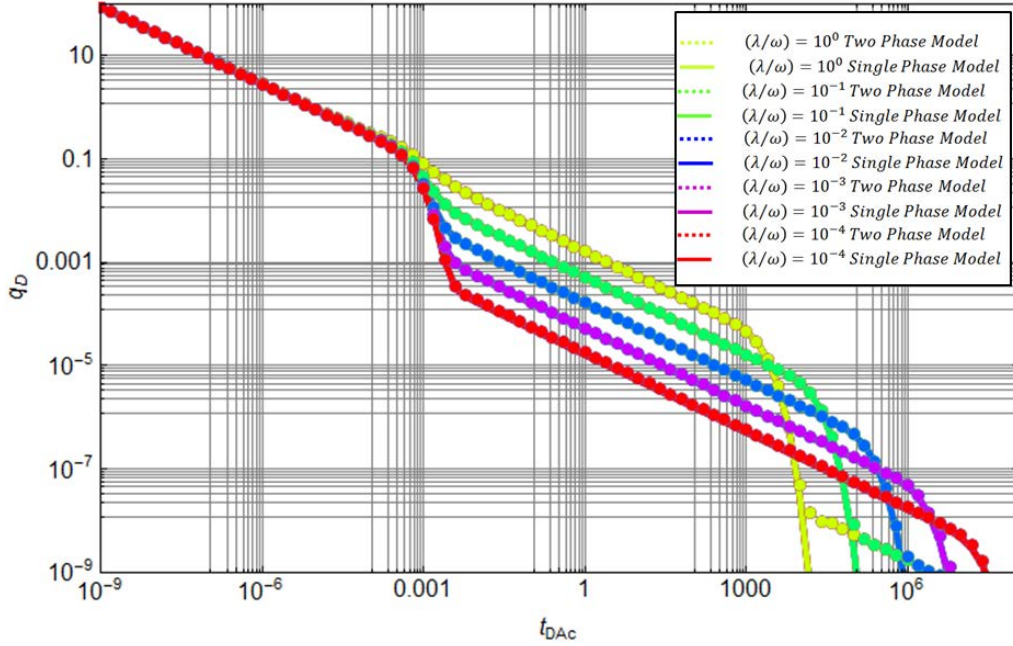
For the purpose of validation we used the solution of single phase model of Bello<sup>9</sup> and compared it with our solution, as in Table 12. The difference is we have assumed that aquifer is equal to size of reservoir, implying  $\kappa_f = 0.99$ , in the fracture function.



**Figure 46.** Validation of Full Transient Model with Bello's Transient Model (Constant Rate Case).

**Table 12.** Full Transient Model

<p>Full Transient Matrix and Aquifer Fractured Dual Permeability Model (Appendix H)</p>	$f(s)$ $= \omega \left[ \left( \frac{\omega_{aq}}{\omega \kappa_f} \right) + \left( \frac{1}{3s} \right) \left( \frac{\lambda}{\omega} \right) \sqrt{3s \left( \frac{1-\omega}{\omega} \right) (\Lambda) \left( \frac{\kappa_{fb}}{\kappa_f} \right) \left( \frac{\omega}{\lambda} \right)} \right]$ $\times \tanh \left( \sqrt{3s \left( \frac{1-\omega}{\omega} \right) (\Lambda) \left( \frac{\kappa_{fb}}{\kappa_f} \right) \left( \frac{\omega}{\lambda} \right)} \right)$ $+ \left( \frac{\lambda_{aq}}{12 s \kappa_f} \right) \sqrt{s \left( \frac{12(1-\omega_{aq})}{\lambda_{aq}(1-\kappa_f)} \right)} \tanh \left( \sqrt{s \left( \frac{12(1-\omega_{aq})}{\lambda_{aq}(1-\kappa_f)} \right)} \right)$
---	--



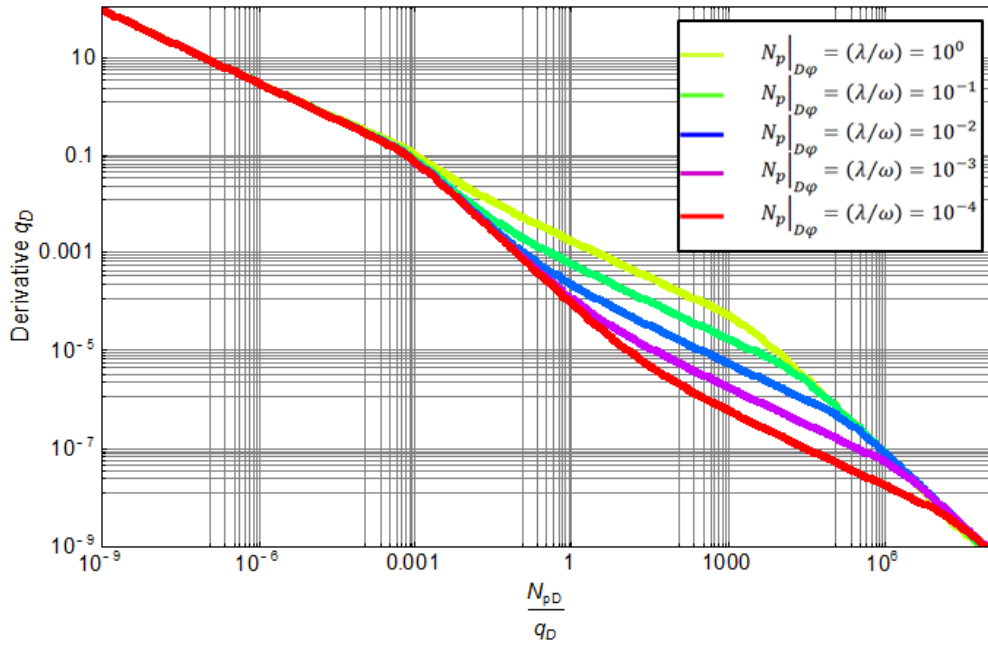
**Figure 47.** Validation of Full Transient Model (dotted) with Bello's Transient Model (Constant Pressure Case).

Figure 46 and figure 47 shows the comparison for each case with Bello's model. The values of various other parameters are:  $\omega_{aq} = \omega = 10^{-3}$ ,  $\lambda_{aq} = 10^{-11}$ ,  $\kappa_{fb} = 1$ ,  $\Lambda = 1$  and  $y_{eD} = 1$ . The solution departs from Bello's model when the interporosity transfer function,  $\lambda$ , is large (see bottom of figure 47) and as seen for dual porosity proppant number,  $N_p|_{D\varphi} = 1$  ( $N_p|_{D\varphi} = 10^0$  in figure 47). This happens because under these conditions the model behaves like a linear composite two layer model. Just like its single porosity two layer radial two layer counterpart, this model also has the initial response of layer1, a transition region and then the total system response of layer1 and

layer2 together. Theoretically, every model will show these three responses but the final solution depends on the values of parameters, the ranges of dimensionless time used.

### **Derivative Analysis Using Single Phase Flow Model**

This analysis is carried out entirely with the help of Bello's model. The aim is to derive the value of  $\lambda_{rmf}$  and  $\omega$ . All analysis is done using constant bottomhole pressure constraint. Figure 48 and figure 49 shows  $\frac{dq_D}{d(\ln t_D)}$  versus  $\frac{N_{pD}}{q_D}$  with changing  $\lambda_{rmf}$  from  $10^{-3}$  to  $10^{-7}$  and keeping  $\omega = 10^{-3}$  constant. This gives the range of dual porosity proppant number,  $N_p|_{D\varphi}$ , from 1 to  $10^{-4}$ . As pointed out earlier, the amount of successful stimulation archived is dependent on correctly predicting this dual porosity proppant number. This boils down to evaluating two unknowns,  $\omega$  and  $\lambda_{rmf}$ , which the stimulation changes as it introduces fracture volume over and above the existing natural fracture volume.



**Figure 48.** Results with Single Phase Transient Model for  $y_{eD} = 1$  as per Bello<sup>9</sup>.

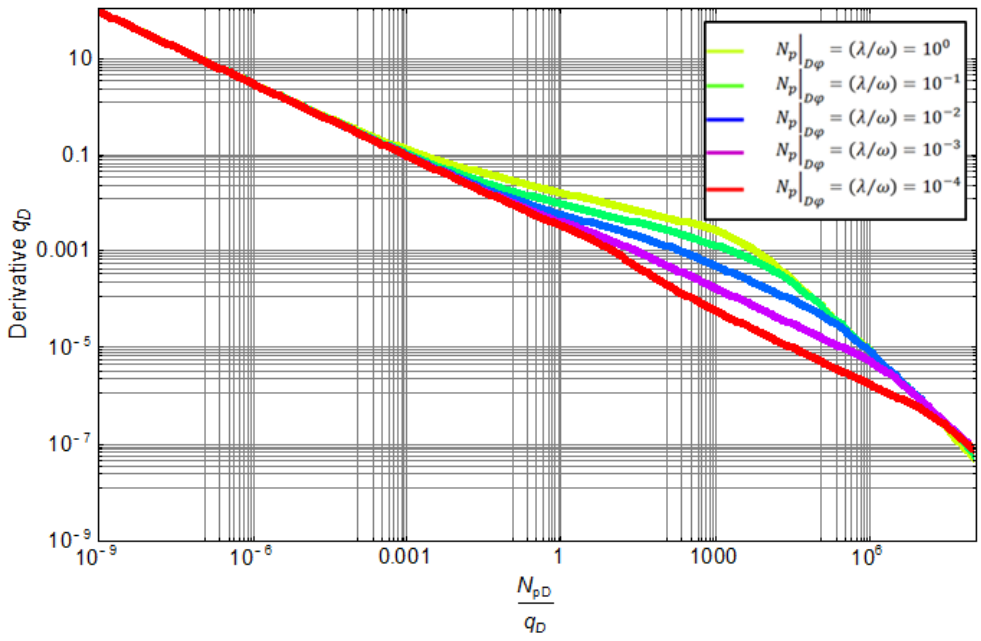


**Figure 49.** Results with Single Phase Model for  $y_{eD} = 100$  as per Bello<sup>9</sup>.

As can be seen in figure 48 and figure 49, the early part represents fracture only flow and hence is half-slope. For the value of  $y_{eD} = 100$  (as seen in figure 49) we see that there is a definite development of bilinear quarter slope after the initial half-slope. It can be concluded that the matrix recharge has kept pace with depletion in the fracture system. However the ability of matrix to recharge fracture (magnitude of  $\lambda$  decides this recharge) is reduced, the bilinear flow period starts to get shorter and shorter till the time it becomes insignificantly small. This is the dual porosity behavior where the pressure depletion at the well (matrix does not directly communicate with the well) is just about being felt by all the matrix blocks through the fracture system (matrix depletes because of pressure difference between inside and outside of the matrix block). For the matrix blocks which are further away from the well the pressure depletion remains in effect for a very short duration of time (seen as a blip of bilinear flow for  $N_p|_{D\phi} = \left(\frac{\lambda}{\omega}\right) = 10^{-4}$  figure 49). The matrix-fracture system continues to deplete (system flow) till the time it goes into boundary dominated flow (unit slope).

If the pore volume of the fracture is not sufficient enough, as is the case with  $y_{eD} = 1$  (and seen in figure 48), the matrix lags so far behind in recharging the fracture, that it results in the fracture boundary dominated flow (unit slope) first followed by matrix linear flow (half-slope flow and no bilinear flow is possible because fracture is already in boundary dominated flow). This is followed by the system flow which goes into boundary dominated flow, and at this stage both the fracture and matrix are in boundary dominated flow (unit slope). Thus it can be concluded if sufficient pore

volume is not present then the fracture will go into boundary dominated flow first before the matrix recharge kicks in and reverts it back to linear flow.

Figure 50 shows  $q_D$  versus  $t_D$  and  $\frac{q_D}{d(\ln t_D)}$  versus  $t_D$  using instantaneous solutions in the same graph. Figure 51 compares the derivatives calculated from constant rate case (using numerical Laplace domain solution) and the derivative calculated from constant pressure case (using real domain solution) and using material balance time. The constant rate derivative is slightly higher than the constant pressure derivative but both are in good agreement.

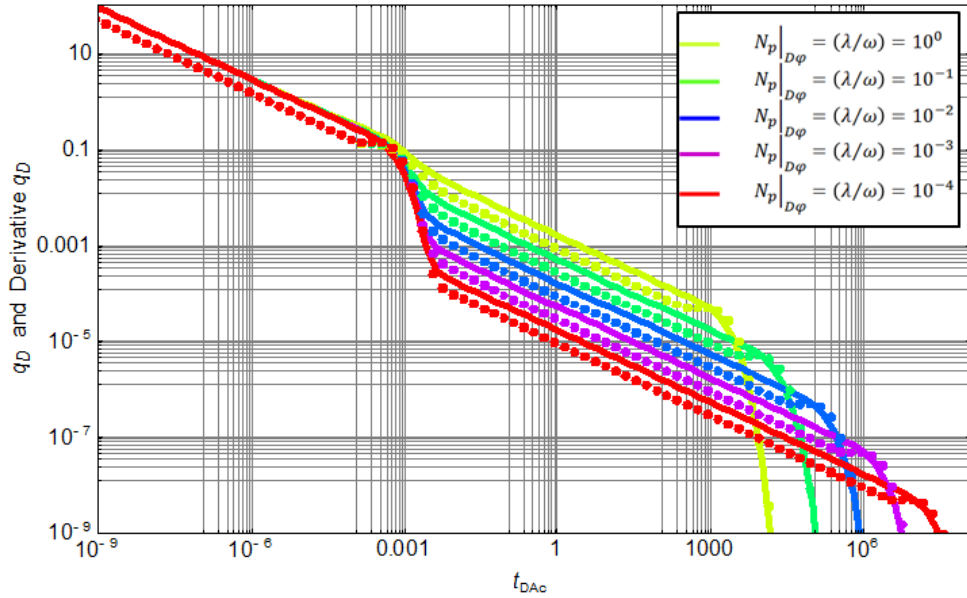


**Figure 50.** Reproduction of Rate (solid line) and the Derivative (dotted line) with Single Phase Transient Model for  $y_{eD} = 1$  Calculated from Laplace Inversion.

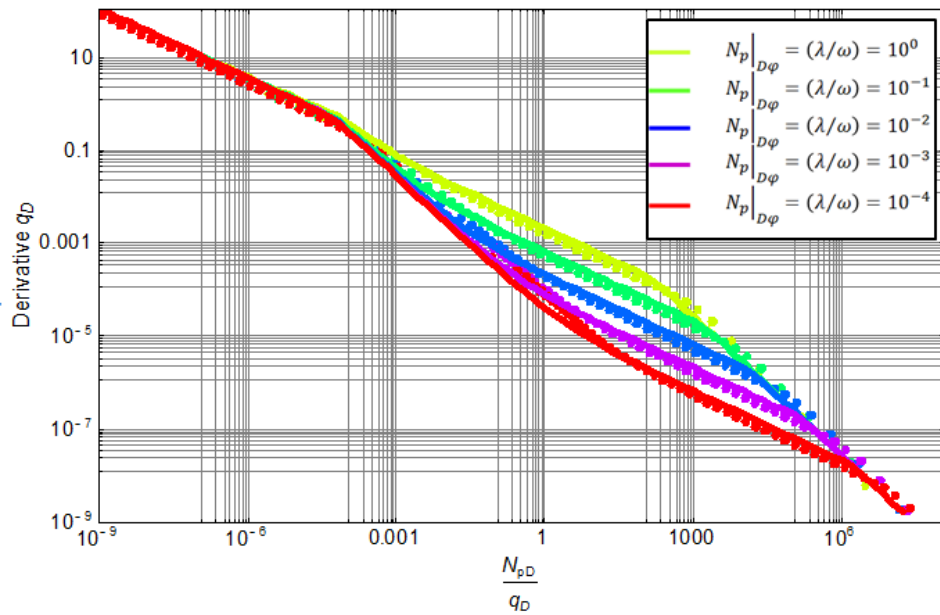


**Figure 51.** Reproduction of Constant Rate Derivative from Laplace Solution (solid line) and Constant Pressure Derivative (dotted line) using Material Balance Time with Single Phase Transient Model for  $y_{eD} = 1$ .



The focus of this chapter is  $y_{eD} = 1$ . Using eqn.(5-9) and eqn.(5-10) we arrive at the following plots shown in figure 52 and figure 53. These are plots which shows  $\frac{dJ_D}{d(\ln t_D)}$  versus  $t_D\lambda$ . With the help of this analysis we convert from area  $A_{cw} = 2x_e h$  to area  $A$  which is horizontal spread (drainage area). The following empirical relation for two layered reservoirs, put forward by Ehlig-Economides and Ayoub<sup>33</sup>, for convergence of solution then applies:

$$t_{DA}\lambda = t_{DAc}\lambda \approx 1 \dots\dots\dots(5-17)$$

This is seen in figure 53 where the convergence of all fracture boundary dominated flow and matrix transient flow occurs into a single curve as the above relation applies. Also, based on area  $A$ , the time to reach pseudosteady state/boundary dominated flow is given by yet another empirical relation which is:

$$t_{DA} \approx 0.1 \dots\dots\dots(5-18)$$

The combined effect of these two empirical relations gives the dimensionless time to boundary dominated flow for dual porosity as seen in figure 54 and figure 55. The slopes of dimensionless productivity index are zero or they are all constant (horizontal) during boundary dominated flow after the value  $t_{DA}\lambda = t_{DAc}\lambda = 1$ .

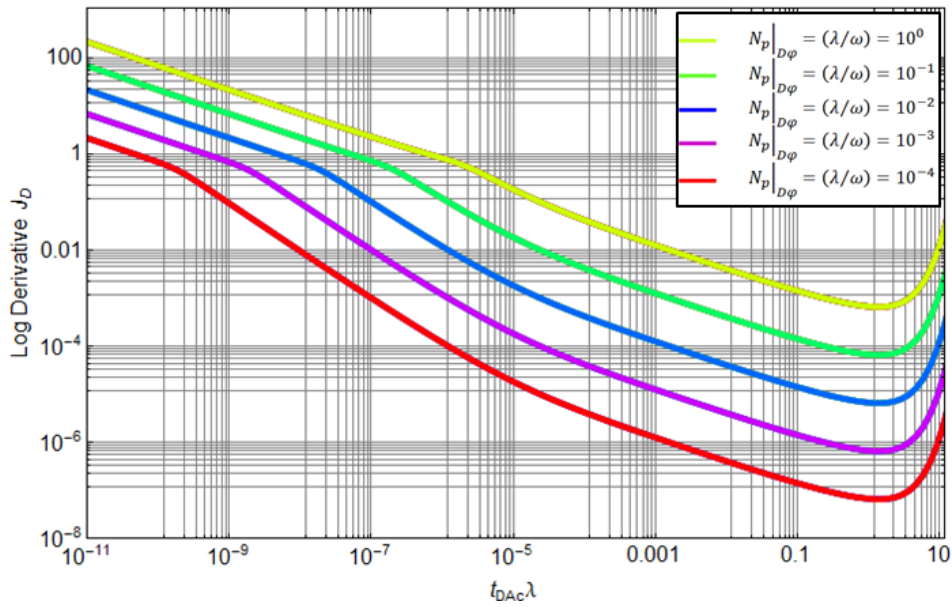


**Figure 52.** Single Phase Derivative Analysis for  $y_{eD} = 1$  and  $A = A_{cw}$ .

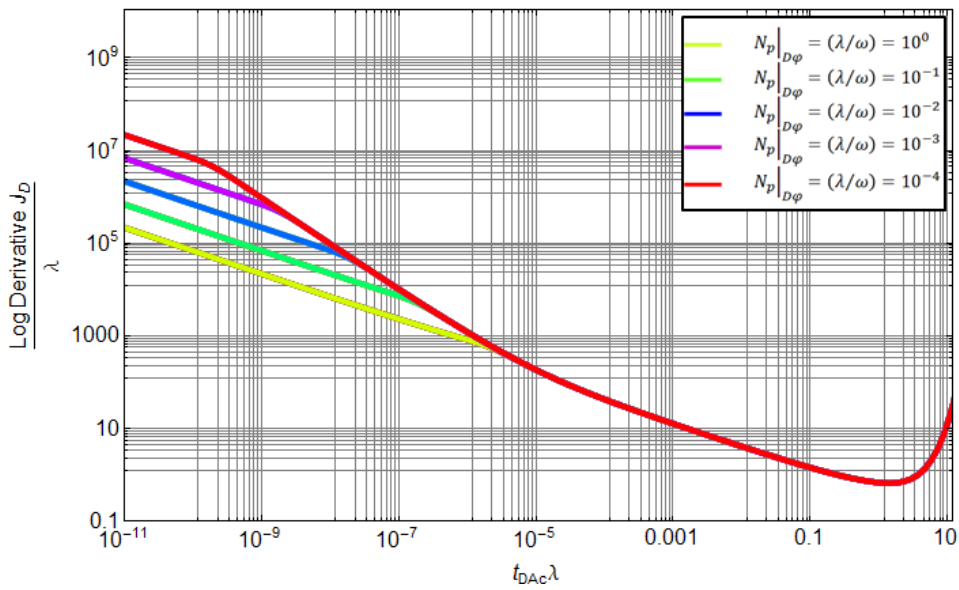


**Figure 53.** Single Phase Derivative Analysis for  $y_{eD} = 1$  and  $A = A_{cw}$ .

For both figure 52 and figure 53 Euler constant correction is applied to dimensionless time (X-Axis). The combined effect of these two empirical relations is also evident from  $J_D$  versus  $t_{DAc}$ , figure 54 and figure 55, which are in pseudosteady state after  $t_{DA}\lambda > 1$ . Also evident from figure 53 and figure 55 is that all matrix transient flows superpose on each other and thus a single (system linear flow) curve can be used to describe the entire performance. The assumption we are making here is that the early fracture flow is of no interest to us. The explanation put forward for eqn.(5-17), from Stewart<sup>34</sup>, is that for this particular value of dimensionless time the matrix and fracture system come to equilibrium, nearly at the same local pressure, and behave as a joint total system. For:

$$t_{DA}\lambda = t_{DAc}\lambda < 1 \dots\dots\dots(5-19)$$

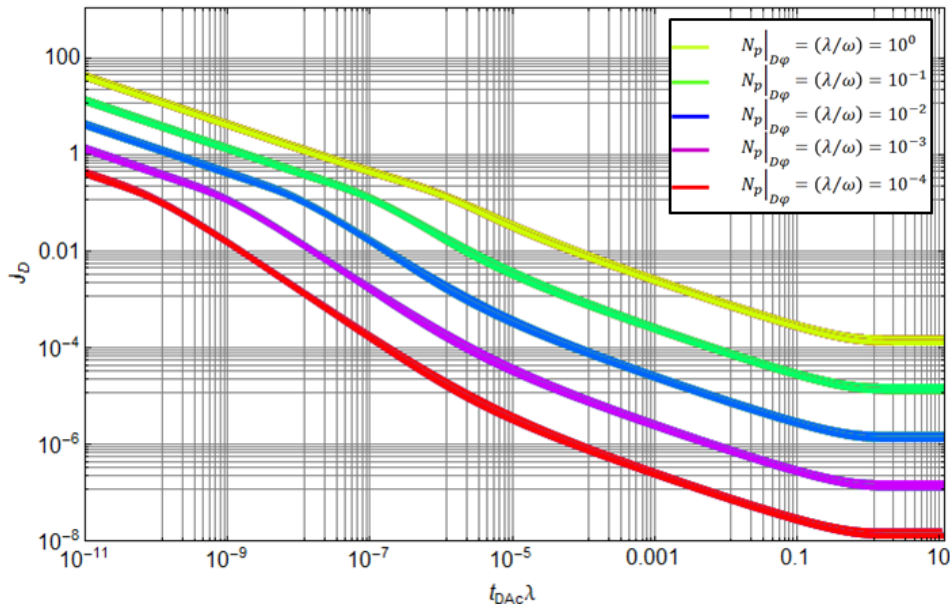


**Figure 54.** Single Phase Transient Model  $J_D$  Results for  $y_{eD} = 1$  and  $A = A_{cw}$  (Both for Constant Rate and Constant Bottomhole Pressure Case are Shown).

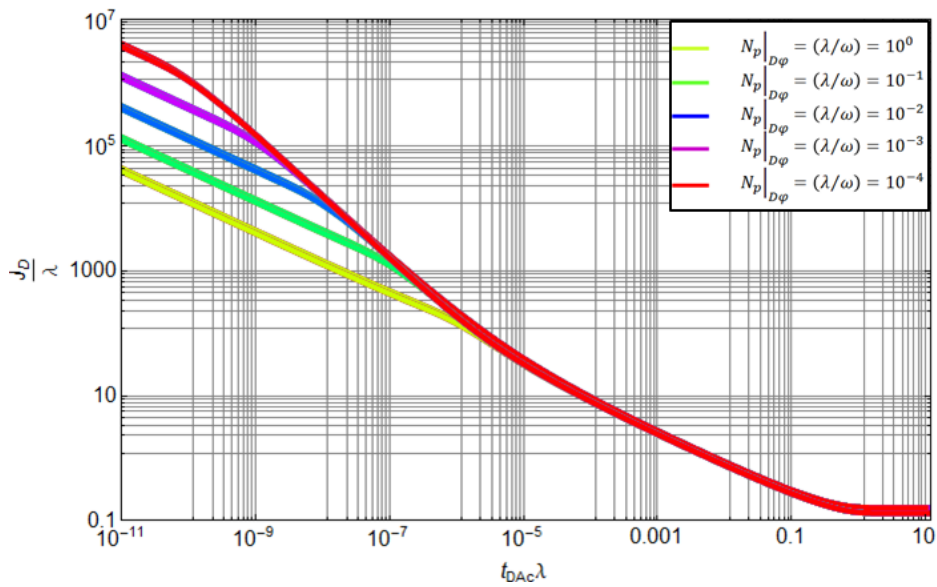


**Figure 55.** Single Phase Transient Model  $\frac{J_D}{\lambda}$  Results for  $y_{eD} = 1$  and  $A = A_{cw}$  (Both for Constant Rate and Constant Bottomhole Pressure Case are Shown).

the matrix pressure lags behind the fracture pressure. Also, figure 53 and figure 55 cannot be applied initially because  $\lambda$  is unknown parameter to begin with. So as a first step for analysis, it is suggested, we use figure 52 and figure 54. Subsequent verification can be done with figure 53 and figure 55.

The analysis, which is iterative, consists of calculating productivity index first. Productivity index is a function of dimensionless productivity index according to:

$$J = \left( \frac{2\pi k h}{\mu B} \right) J_D \dots\dots\dots (3-52)$$

Since time is a known quantity, we can use figure 52 and figure 54 to know, for the linear region, what the value of  $\lambda = \lambda_{rmf}$  is going to be for a given dual porosity proppant number. The dual porosity proppant number points towards the value of  $\omega$ .

### **Derivative Analysis Using Two Phase Flow (Aquifer) Model**

Here the aim of this analysis is to derive five unknown parameters,  $\lambda_{rmf}$ ,  $\lambda_{aq}$ ,  $\omega$ ,  $\omega_{aq}$  and  $\kappa_f$ . As in the previous section, for the purpose of this thesis, we assume  $\omega_{aq} = \omega$  and that  $\kappa_f \leq 1$ . It is imperative that the height of reservoir and the aquifer be known. This leaves three unknowns in all but two,  $\lambda_{rmf}$  and  $\lambda_{aq}$  are unique parameters whereas  $\omega$  is an assumed (dependent on dual porosity proppant number value) parameter. Once again the process is iterative.

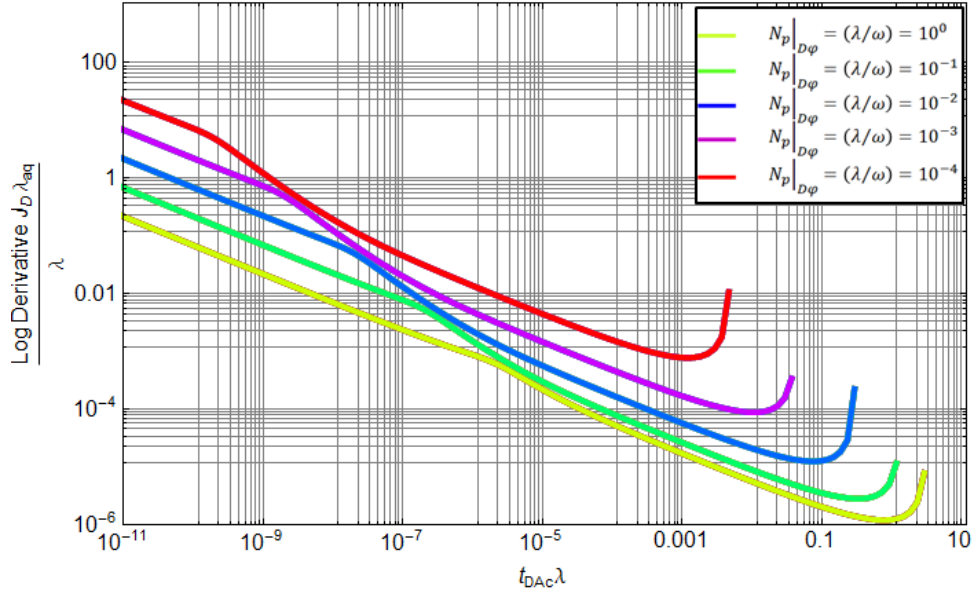


**Figure 56.** Two Phase Derivative Analysis for  $y_{eD} = 1$  and  $A = A_{cw}$  with  $\lambda_{aq}$ .

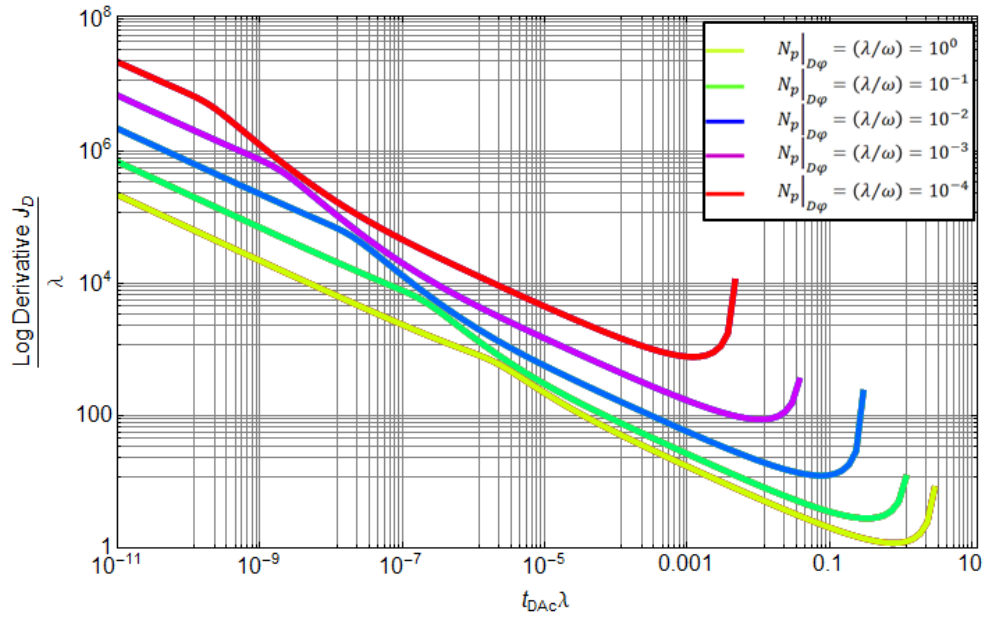


**Figure 57.** Two Phase Derivative Analysis for  $y_{eD} = 1$  and  $A = A_{cw}$  without  $\lambda_{aq}$ .

Step 1. Assume the value of  $\lambda_{aq}$ . Eqn.(3-21) is a good starting point. Go to figure 56 and try to determine the value of  $\lambda_{rmf}$  as per previous section.

Step 2. Repeat the process of step 1 now using figure 57. This makes the solution independent of variations in  $\lambda = \lambda_{rmf}$ .

Step 3. Calculate the ratio of two values on the Y-Axis which then gives  $\lambda_{aq}$ . Compare with the assumed value in step 1. Here the value of  $\lambda_{aq} = 10^{-6}$  is used in the model.

Step 4. If difference cannot be reduced then we take the effect of aquifer into account by changing  $\kappa_f$ , figure 60.  $\lambda = \lambda_{rmf}$  and  $\omega$  are then arrived at after couple of  $\lambda_{aq}$  iterations. It is imperative that  $kh$  values of both the reservoir and the aquifer are known ahead in time so as to reduce the uncertainty in  $\kappa_f$  value.

Similar to the previous section, figure 58 and figure 59 show the results of variation of dimensionless productivity index with time for both cases. A major point to be noted here is that in the previous case all matrix linear flow collapsed into one curve with half-slope, here those half-slope lines are parallel. Once again, if aquifer is absent, then these all parallel half-slope lines will collapse into one which is shown in figure 53. Figure 56 and figure 57 are generated with the value of  $\kappa_f = 0.99$ . The aquifer has nearly the same flow capacity as the reservoir. It's the value of  $\kappa_f$ , the aquifer effect, which sets them apart and appears as family of curves (figure 58 and figure 59 shows  $J_D$  versus  $t_D\lambda$  for constant rate and constant pressure cases). The entire variation for different value of  $\kappa_f$  for  $\frac{dJ_D}{d(\ln t_D)}$  versus  $t_D\lambda$  is shown in figure 60.

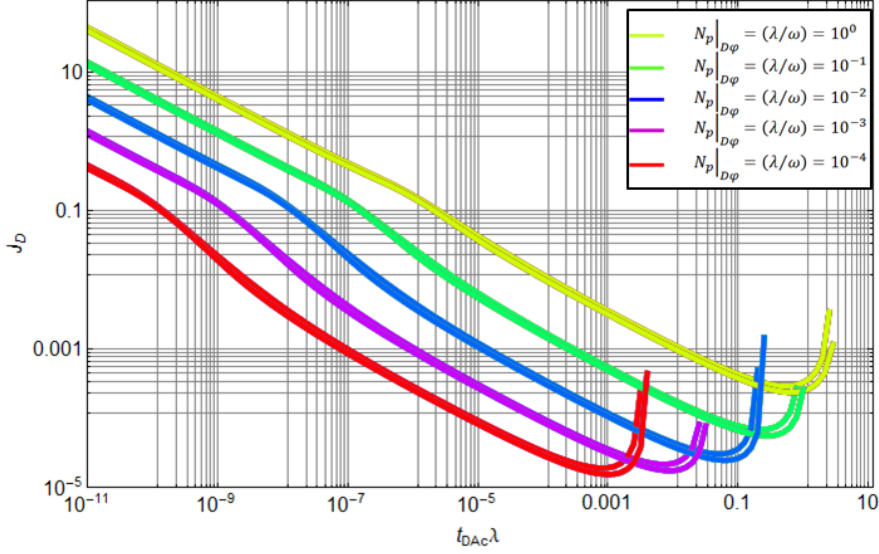


**Figure 58.** Two Phase Transient Model  $J_D$  Results for  $y_{eD} = 1$  and  $A = A_{cw}$  (Both for Constant Rate and Constant Bottomhole Pressure Case are Shown).

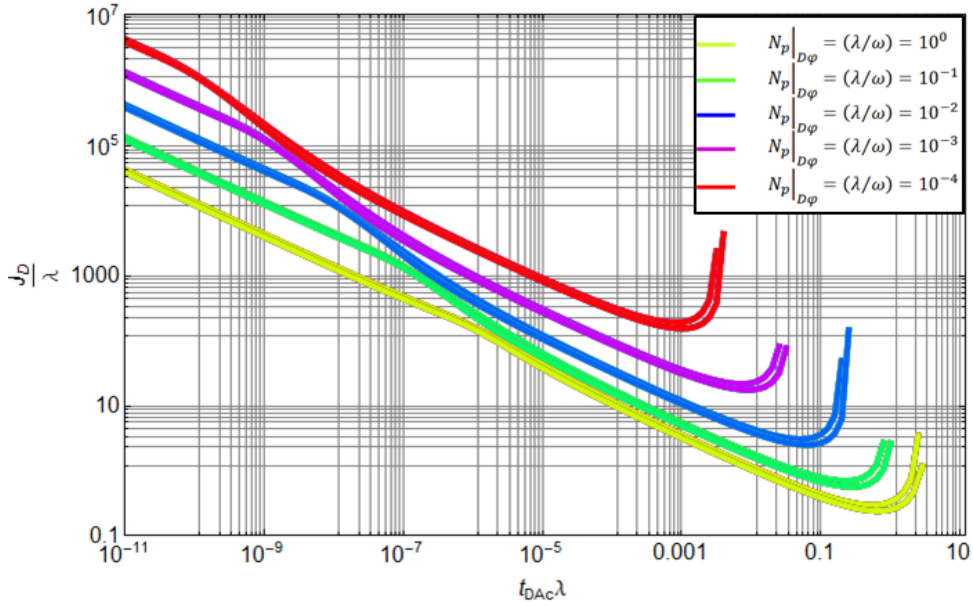


**Figure 59.** Two Phase Transient Model  $\frac{J_D}{\lambda}$  Results for  $y_{eD} = 1$  and  $A = A_{cw}$  (Both for Constant Rate and Constant Bottomhole Pressure Case are Shown).



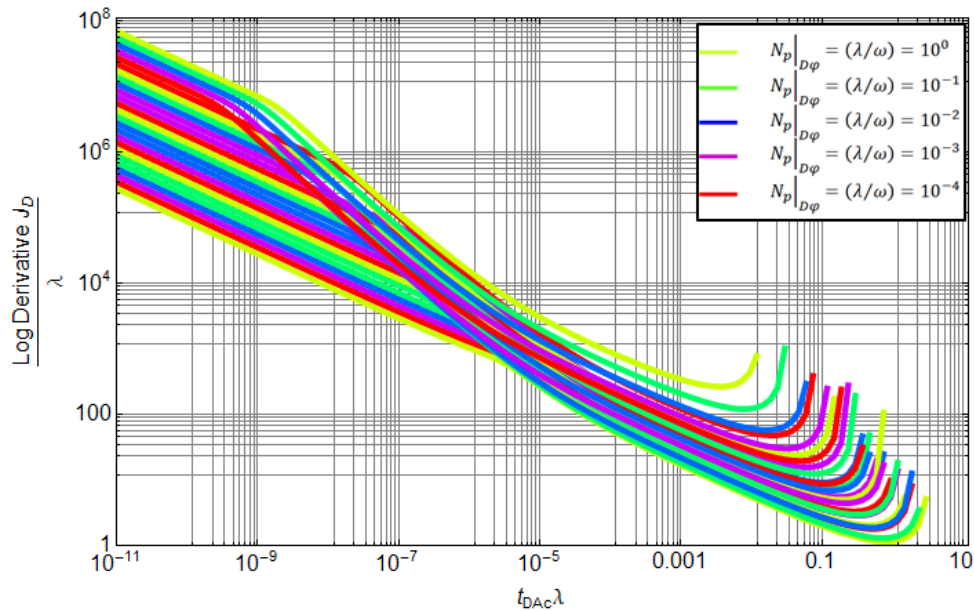


**Figure 60.** Derivative Analysis for  $\kappa_f = 0.1, 0.16, 0.25, 0.4$  and  $0.63$ , and  $y_{eD} = 1$  and  $A = A_{cw}$ .

### Application to Sample Synthetic Field Model

In order to further demonstrate the theory of dimensionless productivity index derivative analysis, a field scale synthetic model was used. For this purpose the Brugge<sup>52</sup> simulation model was run on INTERSECT<sup>53</sup>. Two major changes were made to the dataset. The PVT was changed to live oil having a very low GOR (250 scf/STB) so that no gas gets liberated in the model (INTERSECT needs 3-phase data as input) and the permeability and porosity fields were modified using multipliers so as to make their magnitude suitable for unconventional (microdarcy) range. The other major change incorporated was that the whole model was converted into dual porosity model with no peripheral injectors. Figure 61 and figure 62 gives the input data used in simulation.

REPORT Optional properties (not required, but used if supplied):

Property	Minimum	Maximum	Average
PERM_I	0 mD	0.0519 mD	0.00278804 mD
PERM_J	0 mD	0.0519 mD	0.00278804 mD
PERM_K	0 mD	0.0052 mD	0.000277525 mD
SATURATION_FUNCTION_DRAINAGE_TABLE_NO	0	1	0.5
NET_TO_GROSS_RATIO	0.0548	1	0.981029
POROSITY	0.04 ft3/ft3	0.1347 ft3/ft3	0.0920515 ft3/ft3
MATRIX_FRACTURE_COUPLING	0.0016 1/ft2	0.0016 1/ft2	0.0016 1/ft2

**Figure 61.** INTERSECT Output of Major Parameters Used in Simulation Model.

Description	Value
Number of properties:	
In this folder:	46
Includes sub folders:	70
Grid cells (nI x nJ x nGridLayers)	139 x 48 x 9
Total number of grid cells:	60048
Total number of cells in filtered area:	58555
Unit:	mD

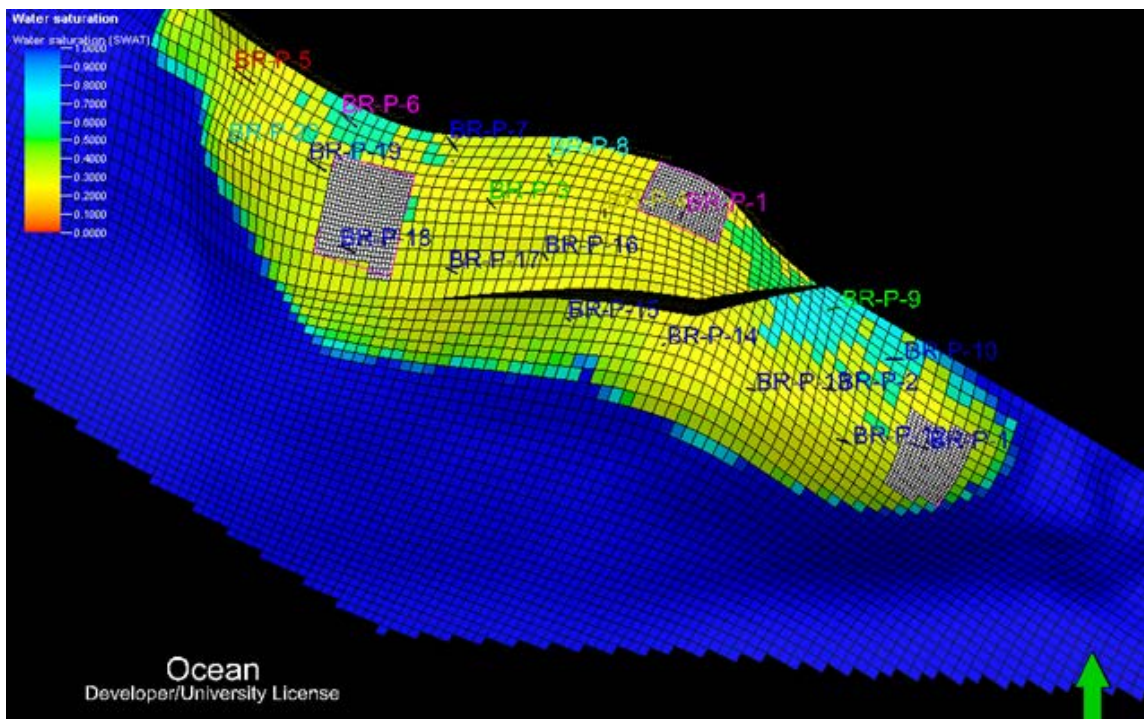
  

Name	Type	Min	Max	Delta
$k_x$ PERMX[0]	Cont.	0.0000	0.0519	0.0519
$k_y$ PERMY[0]	Cont.	0.0000	0.0519	0.0519
$k_z$ PERMZ[0]	Cont.	0.0000	0.0052	0.0052
PERM_T...	Cont.	0.00	0.05	0.05
TRANX[0]	Cont.	0.00	0.00	0.00
TRANY[0]	Cont.	0.00	0.00	0.00
TRANZ[0]	Cont.	0.00	0.03	0.03
TRANSM...	Cont.	0.00	0.03	0.03
$V_p$ PORV[0]	Cont.	0	184297	184297
DX[0]	Cont.	173.55	529.33	355.78
DY[0]	Cont.	119.78	723.04	603.26
DZ[0]	Cont.	12.19	34.37	22.18
$T_H$ MULTX[0]	Cont.	1.00	1.00	0.00
$T_H$ MULTY[0]	Cont.	1.00	1.00	0.00
$T_H$ MULTZ[0]	Cont.	1.00	1.00	0.00
$\Phi$ PORO[0]	Cont.	0.0400	0.1347	0.0947

**Figure 62.** PETREL Input of Major Parameters Used in Simulation Model.

Three wells, BR-P-1, BR-P-11 and BR-P-18 were converted into horizontal wells and were surrounded by LGR. This was essential in order to capture linear flow and the

convergence skin of the horizontal well. The LGR forces the flow to become predominantly linear around the well even though the matrix shape is for a cube. The value of shape function (matrix fracture coupling in figure 61) was derived assuming hydraulic fracture spacing is around 200 ft. Figure 63 shows the overall simulation model with oil and water saturations. The wells flowed at a constant BHP of 1000 psi.



**Figure 63.** Unconventional Synthetic Simulation Model in PETREL Showing LGR.

For the three horizontal wells the average hydraulic fracture half-length came to be the following magnitude; 1040 ft (BR-P-1), 1040 ft (BR-P-11) and 1455 ft (BR-P-18) and the corresponding horizontal well lengths are: 1,714 ft, 1,744 ft and 3,470 ft.

### *Analysis of the Results*

Two scenarios were run using this model:

1. Infinite-acting LGR Boundary (INTERSECT Flux Boundary Condition) run for 10,957 days (~30 years).
  - a. Average fracture permeability same as the matrix permeability.
  - b. Average fracture permeability 10X that of the matrix permeability.
2. Pseudosteady State LGR Boundary (INTERSECT No Flow Boundary Condition) run for 2,585,970 days (~7085 years).
  - a. Average fracture permeability same as the matrix permeability.

Analysis for Scenario 1:

**Well# BR-P-18**

For this well, as shown in the figure 64, by changing the fracture permeability to

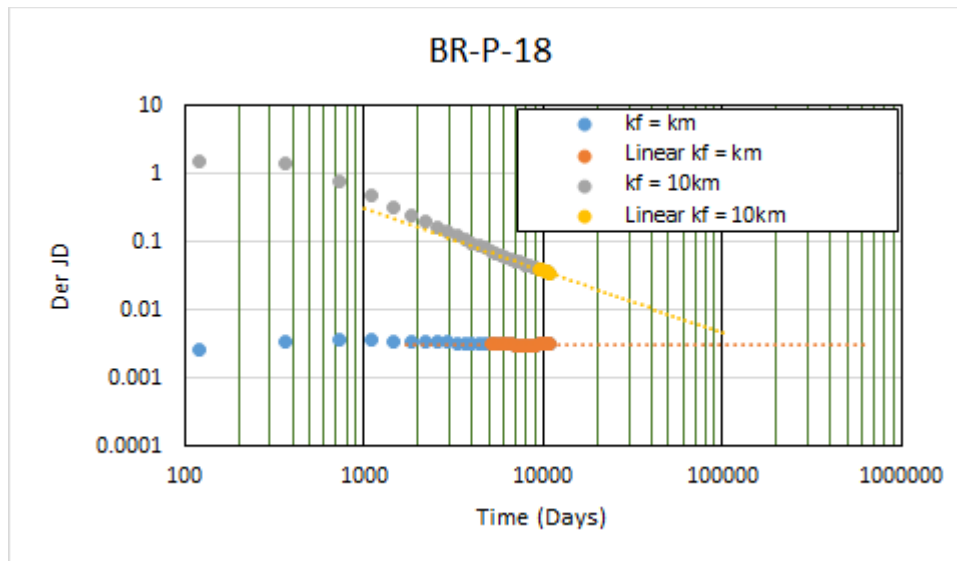


**Figure 64.** Derivative Response in an Infinite Acting Reservoir Showing Radial and Pseudosteady State Flow in the Same Well by Changing Fracture Permeabilities Ten Times.

ten times to that of matrix permeability, converts the predominantly flat derivative curve (radial flow) to a pseudosteady state one (derivative slope is 1). This is dictated by the permeability field around the well. The take away from this figure is that depending on the fracture permeability and time for production, the matrix may not get to drain out at all and the fracture may go into pseudosteady state. Conversely, both the fractures and the matrix could also be in pseudosteady state, a scenario difficult to attain in an infinite-

acting reservoir. It confirms what we see in figure 50 through figure 55 where, under transient conditions, a unit slope precedes the linear slope.

**Well# BR-P-11**

For this well, from figure 65, the flow converts from bilinear flow to linear flow in the same well by changing fracture permeabilities ten times.

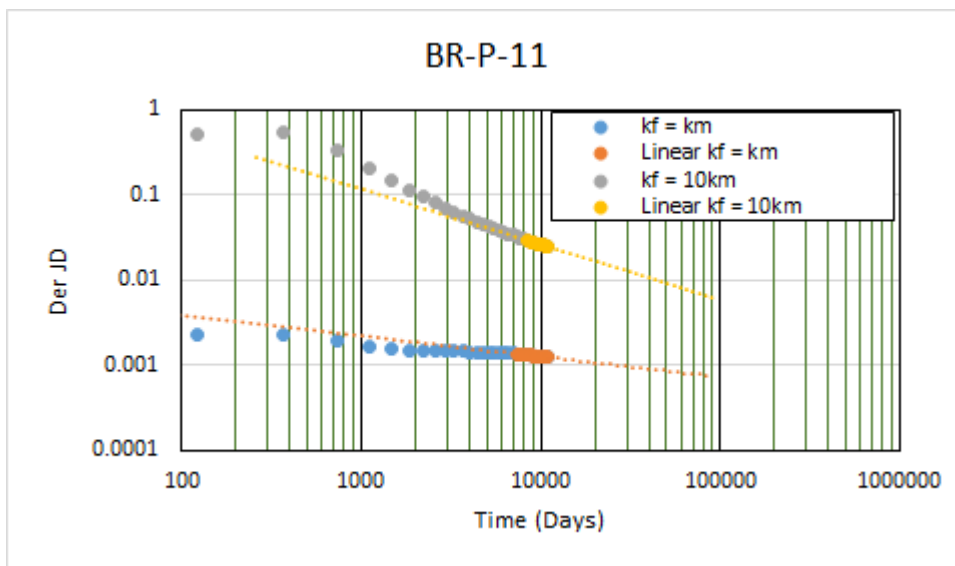


**Figure 65.** Derivative Response in an Infinite Acting Reservoir Showing Bilinear Converts to Linear Flow in the Same Well by Changing Fracture Permeabilities Ten Times.

This figure clearly shows that the production is predominantly coming from the fractures (bilinear flow period is only possible if the fractures are predominantly draining with the matrix). Since the reservoir is infinite-acting, matrix support is totally masked by the fractures. We need to confirm this by making no flow boundary and allowing excessive time for production. This is the motivation for Scenario 2.

**Well# BR-P-1**

As can be seen from figure 66, in both the examples, the flow is linear.

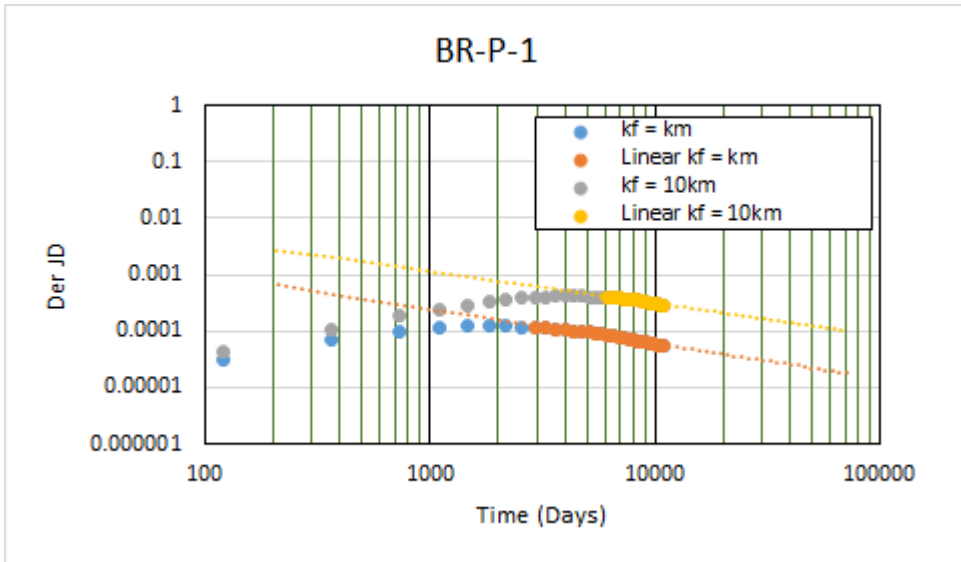


**Figure 66.** Derivative Response in an Infinite Acting Reservoir Showing No Effect on Linear Flow in the Same Well by Changing Fracture Permeabilities Ten Times.

It is not clear from the above figure if in both examples the flow is linear in fracture only or it is system (fracture and matrix) linear flow. In Scenario 2 this difference will be more clear.

Analysis for Scenario 2:

Since a lot of unconventional (horizontal/multilateral) wells are located in tight spacing, it is more than likely that the SRV is bound by no flow boundary. The underlying assumption of this statement is that the production has proceeded for sufficiently long time and the pressure boundaries make their presence felt. Also, to show the system (matrix + fracture) effect, we have run the simulation for considerable amount of time. In all the simulation runs there was no water production.

**Well# BR-P-18**

For this well, as seen in figure 67, for the entire period of time there is linear flow.

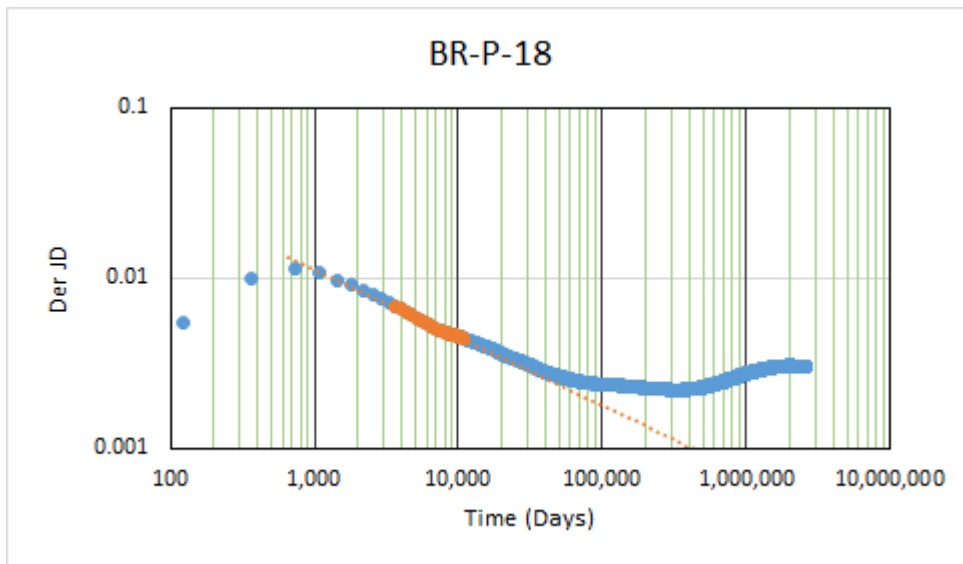


**Figure 67.** Derivative Response of a Well With No Flow Boundary Showing Predominantly Linear Flow.



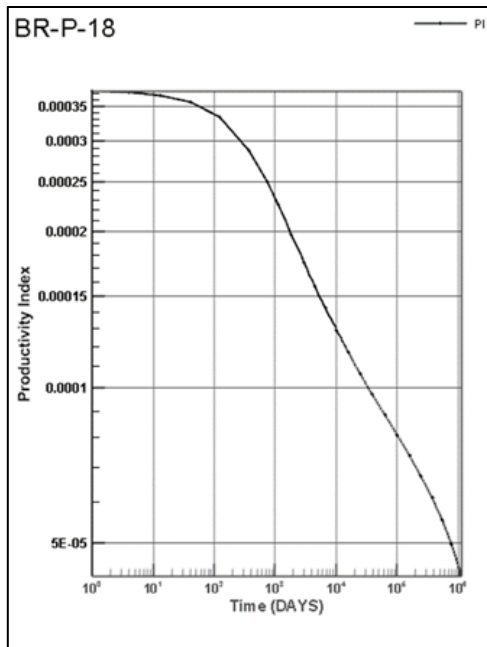


**Figure 68.** Productivity Index of above Well from INTERSECT.

The corresponding productivity index, from the simulator, is shown in figure 68. As compared to the Case 1 runs and for fracture permeability equal to matrix permeability, figure 67 clearly shows that, under bounded reservoir conditions, both matrix and fracture drain together and the system response is linear (there is no radial flow). Also seen in the figure are boundary effects (twice the derivative becomes constant).

**Well# BR-P-11**

From the figure 69, for bounded conditions, the well response is linear.

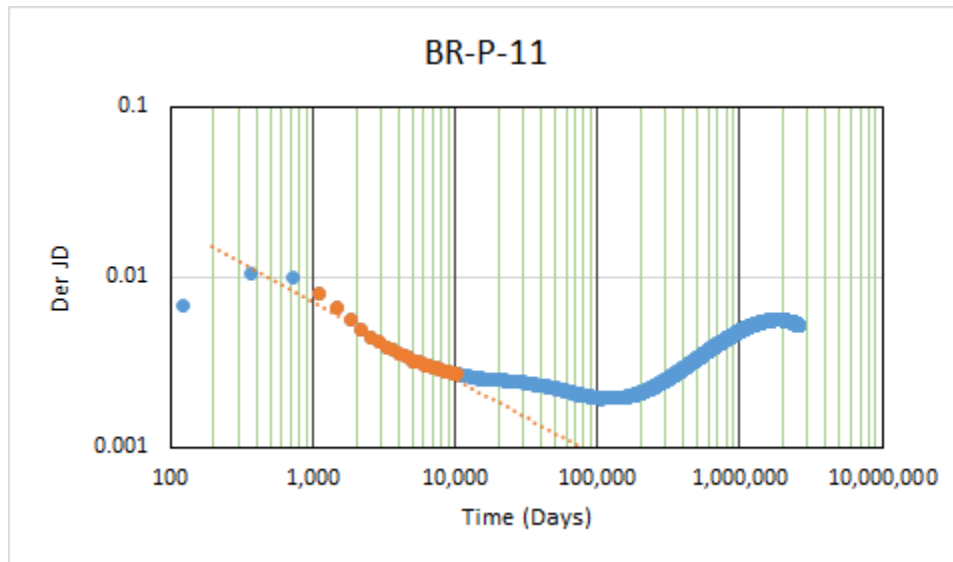


**Figure 69.** Derivative Response of a Well with No Flow Boundary Showing Predominantly Linear Flow and Boundary Effects.

As compared to the previous well, this well shows stronger aquifer. The derivative of dimensionless productivity index is pointing downward and can be seen to behave similar to steady state pressure derivative, which suggests steady state aquifer support. Referring back to the productivity equation, eqn.(3-52), for a steady state reservoir the denominator remains constant but eventually the numerator tends to zero. Everything remaining constant, we can conclude from eqn.(3-52) that for steady state condition, the

tendency of dimensionless productivity index (and hence its derivative) would be to fall to zero in a similar fashion as the derivative of dimensionless pressure.

**Well# BR-P-1**

From figure 70, we can see that fracture dominates the performance. After linear

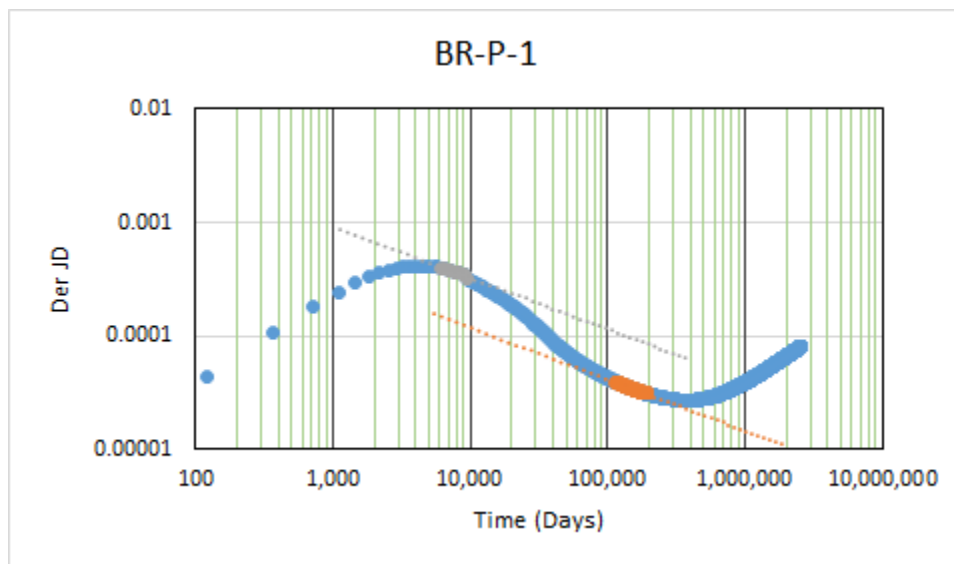


**Figure 70.** Derivative Response of a Well With No Flow Boundary Showing Fracture Linear Flow Followed by Matrix Linear Flow.

flow, the fracture goes into pseudosteady state which is then followed by a linear matrix response. Another important point to be noted is that the curve is very smooth suggesting that the boundary effects do not have a significant role to play. This could be because this well is near to the crest and is most detached from the aquifer as the previous two wells are. They are nearer to the oil water contact, refer figure 63.

## Conclusions

The following conclusions can be derived from this work:

1. An unconventional reservoir, as represented by Stimulated Rock Volume, is subjected to multiple boundary conditions other than simple depletion corresponding to all boundaries at pseudosteady state condition. These variable and multiple boundary conditions constitute the various drive mechanisms that affect long term deliverability of these reservoirs and a method is demonstrated to quantify them. Only transient linear flow reservoirs were considered.
2. If linear flow is the predominant regime of production for these reservoirs, it is a known fact that the pressure derivative will have only one value, called the half-slope. Strictly speaking this is only possible for constant rate case. If we make use of the derivative of dimensionless productivity index, then this drawdown area generation parameter helps in quantifying the time to reach boundary dominated flow, for dual porosity reservoirs and constant pressure case, based on the empirical relation  $t_{DA}\lambda \approx 1$  and  $t_{DA} \approx 0.1$ . Thus the entire production performance of linear flow unconventional reservoir is subjected to two limiting factors; half-slope and time to reach boundary dominated flow. This eliminates multiple production scenarios that are possible with conventional rate transient analysis. These all derivative curves collapse into a single curve for a given Dual Porosity Proppant Number,  $\left(\frac{\lambda}{\omega}\right)$ , if  $\frac{dJ_D}{d(\ln t_D)}$  versus  $t_D\lambda$  is plotted and if no aquifer is present. It is for this reason this plot also helps to quantify the aquifer effect.

3. The concept of constant volume fracture is introduced. For a given Dual Porosity Proppant Number, under transient linear flow conditions, if either the area/volume ratios is kept constant, using 1D, 2D or 3D matrix geometry (characteristic length) or the area/volume ratios are variable but the ratio of matrix to fracture permeabilities vary in such a way that its product with shape factor (constant characteristic lengths) are in the ratio 1:2:3, then the transient linear response is same for all these fracture configurations (provided no boundary effects are reached). As the derivative of dimensionless productivity index has a fixed value for this transient linear response, long term production performance of a horizontal fractured well in a dual porosity reservoir, can theoretically be derived without regard to fracture configuration (matrix geometry).

## NOMENCLATURE

### CHAPTER II

GOR = Gas oil ratio, SCF/STB.

$k_v/k_h$  = Vertical to horizontal permeability ratio.

MBAL = Material balance.

OWC = Oil-Water contact.

OOWC = Original oil-water contact.

OGOC = Original gas-oil contact.

OOIP = Original Oil-in-Place, STB.

PV = Pore volume, ft<sup>3</sup>.

$R_{si}$  = Initial gas oil ratio, SCF/STB.

$R_L$  = Condensate yield, STB/MMSCF.

WF = Waterflood.

### CHAPTER III / CHAPTER V

$k_f$  = Fracture permeability (single porosity), md.

$k_{fb}$  = Fracture block bulk permeability, md.

$k_{mb}$  = Matrix block bulk permeability, md.

$k_{aq}$  = Aquifer block bulk permeability, md.

$k_a$  = Aquifer block permeability, md.

$k_b$  = Lumped parameter barrier permeability, md.

$p_i$  = Initial pressure, psi.

$p_f$  = Fracture pressure, psi.

$p_m$  = Matrix pressure, psi.

$p_a$  = Aquifer pressure, psi.

$p_{fb}$  = Fracture block pressure, psi.

$p_{mb}$  = Matrix block pressure, psi.

$p_{aq}$  = Aquifer block pressure, psi.

$p_{ch}$  = Characteristic pressure, psi.

$\bar{p}$  = Average reservoir pressure, psi.

$p_{wf}$  = Wellbore flowing pressure, psi.

$\varphi$  = Reservoir bulk porosity, fraction.

$\varphi_{fb}$  = Fracture block bulk porosity, fraction.

$\varphi_{mb}$  = Matrix block bulk porosity, fraction.

$\varphi_{aq}$  = Aquifer block bulk porosity, fraction.

$\varphi_a$  = Aquifer block porosity, fraction.

$c_t$  = Total reservoir compressibility,  $\text{psi}^{-1}$ .

$c_f$  = Fracture block compressibility / Formation compressibility,  $\text{psi}^{-1}$ .

$c_m$  = Matrix block compressibility,  $\text{psi}^{-1}$ .

$c_a$  = Aquifer block compressibility,  $\text{psi}^{-1}$ .

$c_o$  = Oil compressibility,  $\text{psi}^{-1}$ .

$c_g$  = Gas compressibility,  $\text{psi}^{-1}$ .

$c_w$  = Water compressibility,  $\text{psi}^{-1}$ .

$S_o$  = Saturation of oil, fraction.

$S_g$  = Saturation of gas, fraction.

$S_{cw}$  = Connate water saturation, fraction.

$R_{so}$  = Gas oil ratio, SCF/STB.

$R_p$  = Producing gas oil ratio, SCF/STB.

$R_v$  = Volatilized oil gas ratio, STB/SCF.

$\sigma_{mf}$  = Matrix Fracture bulk source term,  $\text{ft}^3/\text{D}/\text{ft}^3$ .

$\sigma_m$  = Matrix Fracture source term,  $\text{ft}^3/\text{D}/\text{ft}^3$ .

$\alpha$  = Matrix shape function for matrix-fracture,  $\text{ft}^{-2}$ .

$\underline{\alpha}$  = Matrix shape function for aquifer-fracture,  $\text{ft}^{-2}$ .

$\alpha_1 = 141.2 (2\pi)$  conversion constant, field units.

$\beta$  = Lumping parameter, dimensionless.

$V$  = Reservoir volume,  $\text{ft}^3$ .

$V_f$  = Fracture block volume (dual porosity) / Fracture volume (single porosity),  $\text{ft}^3$ .

$V_m$  = Matrix block volume,  $\text{ft}^3$ .

$V_{aq}$  = Aquifer block volume,  $\text{ft}^3$ .

$x$  = Linear dimension, ft.

$y$  = Linear dimension (perpendicular to  $x$ ), ft.

$z$  = Linear vertical dimension, ft.

$A_{cw} = x_e h$ , Area of cross-section of reservoir,  $\text{ft}^2$ .

$A = x_e y_e$ , Horizontal (Lateral) Area of reservoir,  $\text{ft}^2$ .



$B$  = Formation volume factor, RB/STB.

$B_o$  = Oil formation volume factor, RB/STB.

$B_g$  = Gas formation volume factor, RB/SCF.

$x_e$  = Length of horizontal well (dual porosity) / Lateral dimension (single porosity), ft.

$x_f$  = Fracture half-length (single porosity), ft.

$y_e$  = Lateral extent, fracture half-length (dual porosity), ft.

$r_w$  = Wellbore radius, ft.

$r_e$  = External radius of reservoir, ft.

$w$  = Width of fracture (single porosity), ft.

$h$  = Height of reservoir, ft.

$h_m$  = Linear dimension of matrix, ft.

$h_f$  = Linear dimension of fracture, ft.

$h_a$  = Linear dimension of aquifer, ft.

$h_b$  = Linear dimension of lumped parameter barrier, ft.

$h_{rm}$  = Linear dimension of matrix block (fracture spacing), ft.

$h_{rf}$  = Linear dimension of fracture block, ft.

$h_{mb}$  = Linear dimension of matrix block, ft.

$h_{fb}$  = Linear dimension of fracture block, ft.

$h_{aq}$  = Linear dimension of aquifer block, ft.

$\mu$  = Viscosity of matrix fluid, cp.

$\mu_a$  = Viscosity of aquifer fluid, cp.

$\mu_{aq}$  = Viscosity of aquifer block fluid, cp.  
 $\mu_{fb}$  = Viscosity of fracture block fluid, cp.  
 $\mu_{rf}$  = Viscosity of fracture block fluid, cp.  
 $\mu_{mb}$  = Viscosity of matrix block fluid, cp.  
 $\mu_o$  = Viscosity of oil, cp.  
 $\mu_g$  = Viscosity of gas, cp.  
 $\mu_w$  = Viscosity of water, cp.  
 $\lambda_t$  = Total mobility, md/cp.  
 $\lambda_o$  = Mobility of oil, md/cp.  
 $\lambda_g$  = Mobility of gas, md/cp.  
 $\lambda_w$  = Mobility of water, md/cp.  
 $\eta$  = Reservoir diffusivity, ft<sup>2</sup>/hr.  
 $\eta_f$  = Fracture diffusivity, ft<sup>2</sup>/hr.  
 $T_b$  = Lumped parameter transmissibility, md-ft.  
 $(T_b)_{eff}$  = Effective lumped parameter transmissibility, md-ft.  
 $J$  = Productivity index, STB/D/psi.  
 $s$  = Skin, dimensionless / Laplace space operator.  
 $s_h$  = Convergence skin, dimensionless.  
 $s_{hcw}$  = Linear convergence skin, dimensionless.  
 $u$  = Laplace space operator.  
 $q$  = Flow rate, STB/D.

$N_p$  = Cumulative production, STB.

$d_z$  = Distance to nearest horizontal boundary, ft.

$L_w$  = Length of horizontal well, ft.

$\omega$  = Dimensionless storativity matrix-fracture, dimensionless.

$\omega_{aq}$  = Dimensionless storativity aquifer-fracture, dimensionless.

$\lambda$  = Dimensionless interporosity flow parameter matrix-fracture, dimensionless.

$\lambda_{aq}$  = Dimensionless interporosity flow parameter aquifer-fracture, dimensionless.

$\eta_{fD}$  = Dimensionless diffusivity ratio, dimensionless.

$\sigma_{mfD}$  = Matrix Fracture bulk source term, dimensionless.

$A_D$  = Dimensionless area, dimensionless.

$C_{fD}$  = Dimensionless fracture conductivity, dimensionless.

$I_x$  = Penetration ratio, dimensionless.

$p_D$  = Dimensionless pressure, dimensionless.

$p_{jD}$  = Dimensionless pressure, dimensionless.

$p_{fD}$  = Dimensionless fracture pressure aquifer-fracture, dimensionless.

$p_{fbD}$  = Dimensionless fracture pressure matrix-fracture, dimensionless.

$p_{mD}$  = Dimensionless matrix pressure, dimensionless.

$p_{mbD}$  = Dimensionless matrix block pressure matrix-fracture, dimensionless.

$p_{aqD}$  = Dimensionless aquifer block pressure aquifer-fracture, dimensionless.

$p_{wFD}$  = Dimensionless well (fracture) pressure, dimensionless.

$\overline{p_{AvD}}$  = Dimensionless average reservoir pressure, dimensionless.

$q_D$  = Dimensionless rate, dimensionless.  
 $q_{wfD}$  = Dimensionless well (fracture) flow rate, dimensionless.  
 $\overline{q_{AvD}}$  = Dimensionless rate based on average reservoir pressure, dimensionless.  
 $N_{pD}$  = Dimensionless cumulative production, dimensionless.  
 $N_p|_{S\varphi}$  = Single porosity proppant number, dimensionless.  
 $N_p|_{D\varphi}$  = Dual porosity proppant number, dimensionless.  
 $x_D$  = Dimensionless linear dimension, dimensionless.  
 $y_D$  = Dimensionless linear dimension (perpendicular to  $x_D$ ), dimensionless.  
 $z_D$  = Dimensionless vertical linear dimension, dimensionless.  
 $x_{De}$  = Dimensionless outer boundary linear dimension, dimensionless.  
 $y_{De} = x_{De}$  Dimensionless outer boundary linear dimension, dimensionless.  
 $t_D = t_{DAc}$  Dimensionless time based on area,  $A_{cw}$ , dimensionless.  
 $t_{DA}$  = Dimensionless time based on area,  $A$ , dimensionless.  
 $\kappa_f$  = Dimensionless transmissibility-mobility aquifer-fracture, dimensionless.  
 $\kappa_{fb}$  = Dimensionless transmissibility-mobility matrix-fracture, dimensionless.  
 $\kappa_{mb}$  = Dimensionless transmissibility-mobility matrix-fracture, dimensionless.  
 $\kappa_{aq}$  = Dimensionless transmissibility-mobility aquifer-fracture, dimensionless.  
 $J_D$  = Dimensionless productivity index, dimensionless.  
 $\varepsilon$  = Ratio of linear matrix dimension to linear aquifer dimension, dimensionless.  
 $\Lambda$  = Ratio of dimensionless storativity (matrix-fracture) to dimensionless storativity  
 (aquifer-fracture), dimensionless.

## CHAPTER IV

$\overline{p_D}$  = Laplace domain dimensionless pressure, dimensionless.

$\overline{p_{D\_pp}}$  = Laplace domain dimensionless pressure partial penetration case, dimensionless.

$\overline{q_D}$  = Laplace domain dimensionless rate, dimensionless.

$\overline{N_{pD}}$  = Laplace domain dimensionless cumulative production, dimensionless.

$K_0$  = Bessel function of the second kind, order zero.

$K_1$  = Bessel function of the second kind, order one.

$r_D$  = Dimensionless radius, dimensionless.

$r_{D1}$  = Dimensionless radius for single well scenario, dimensionless.

$r_{D2}$  = Dimensionless radius for single well scenario, dimensionless.

$r_{D3}$  = Dimensionless radius for single well scenario, dimensionless.

$r_{D4}$  = Dimensionless radius for single well scenario, dimensionless.

$\beta$  = Relative well location for single well scenario, fraction.

$\delta$  = Relative well location for single well scenario, fraction.

$a$  = Drainage area width, ft.

$b$  = Drainage area length, ft.

$m$  = Summation counter.

$n$  = Summation counter.

$r_{D3i}$  = Dimensionless radius for multi well scenario forming fracture, dimensionless.

$r_{D3j}$  = Dimensionless radius for multi well scenario forming fracture, dimensionless.

$r_{D4i}$  = Dimensionless radius for multi well scenario forming fracture, dimensionless.

$r_{D4j}$  = Dimensionless radius for multi well scenario forming fracture, dimensionless.

$\beta_i$  = Relative well location for multi well scenario forming fracture, fraction.

$\beta_j$  = Relative well location for multi well scenario forming fracture, fraction.

$\delta_i$  = Relative well location for multi well scenario forming fracture, fraction.

$\delta_j$  = Relative well location for multi well scenario forming fracture, fraction.

$n_w$  = Well number counter for multi well scenario forming fracture.

$x_o$  = Location of observation well for boundary element method.

$x_w$  = Location of source well for boundary element method.

$p_f$  = Pressure drop between two observation wells in fracture for constant rate case.

$p_R$  = Pressure drop between two observation wells in reservoir for constant rate case.

$r_{Dq}$  = Distance between two observation wells for boundary element method.

$q_D$  = Dimensionless rate generated between two observation wells for constant rate case.

$p_{f\_CPress}$  = Pressure drop between two observation wells in fracture for constant pressure case.

$p_{R\_CPress}$  = Pressure drop between two observation wells in reservoir for constant pressure case.

$q_{D\_CPress}$  = Dimensionless rate generated between two observation wells for constant pressure case.

$\tilde{q}$  = Point source flow rate, STB/D.

$L = h$  Total length of the point source / height of reservoir, ft.

$$\nabla = \frac{\partial}{\partial x} i + \frac{\partial}{\partial y} j \quad \text{Vector.}$$

$$\nabla^2 = \frac{\partial^2}{\partial x^2} + \frac{\partial^2}{\partial y^2} \quad \text{Laplace operator.}$$

$\nabla \bullet u =$  Divergence of vector field  $u$  over the domain  $\Omega$ .

$u \bullet n =$  Flux of vector field  $u$  at a point on the boundary  $\Gamma$ .

$u = u i + v j$  Vector field, dimensioned.

$n =$  Normal vector, dimensioned.

$\Omega =$  Domain of a function, dimensioned.

$\Gamma =$  Boundary of domain, dimensioned.

$\delta =$  Dirac delta function.

$P(x, y) =$  Point source placed at a point inside the domain  $\Omega$ .

$Q(\xi, \eta) =$  Point on a circular boundary at a distance  $r$ .

$p =$  Point at the boundary  $\Gamma$ .

$q =$  Point at the boundary  $\Gamma$ .

$r = |Q - P| = \sqrt{(\xi - x)^2 + (\eta - y)^2}$  Distance of point source at the center of circular domain to any point away from the center.

$d\Omega_Q =$  Subscript of differential inside the domain  $\Omega$ .

$ds_q =$  Subscript of differential at the boundary  $\Gamma$ .

$[H] =$  Square matrix of influence coefficients.

$[G] =$  Square matrix of influence coefficients.

$\{u\}_1 =$  Matrix (Vector) of principal variable of the domain  $\Omega$  having boundary  $\Gamma_1$ .

$\{u_n\}_1 =$  Matrix (Vector) of the flux of principal variable at the boundary  $\Gamma_1$ .

$\{u\}_2 =$  Matrix (Vector) of principal variable of the domain  $\Omega$  having boundary  $\Gamma_2$ .

$\{u_n\}_2 =$  Matrix (Vector) of the flux of principal variable at the boundary  $\Gamma_2$ .



## REFERENCES

1. Maugeri, L.: “The Shale Oil Boom: A U.S. Phenomenon,” Discussion Paper 2013-05, [Belfer Center for Science and International Affairs, Harvard Kennedy School](#), June 2013.
2. Fan, L., Martin, R. B., Thompson, J. W., Atwood, K., Robinson, J. R., & Lindsay, G. J.: “An Integrated Approach for Understanding Oil and Gas Reserves Potential in Eagle Ford Shale Formation,” paper SPE 148751 presented at the 2011 Canadian Unconventional Resources Conference, Calgary, Alberta, Nov. 15-17.
3. Gay, M. O., Fletcher, S., Meyer, N., and Gross, S.: “Water Management in Shale Gas Plays,” *IHS Water White Paper* (Aug. 2012), <http://connectoilandgas.ihs.com/StaticDocuments/LandingPage/WaterManagement.pdf>.
4. Zhu, H., and Tomson, R.: “Exploring Water Treatment, Reuse and Alternative Sources in Shale Production,” *Shale Play Water Management – Digital Edition*, (Nov. 2013), <http://www.shaleplaywatermanagement.com/2013/11/exploring-water-treatment-reuse-and-alternative-sources-in-shale-production/>.
5. Lewis, M.: “Transforming a Train Wreck...the Bakken Express,” presentation delivered to the EMGI Investment House (July 2007), <http://discoverygeo.com/Papers/Bakken%20Slides%20for%20SIPES.pdf>.
6. Schepel, K. J.: “Advanced Reservoir Characterization and Proof-of-Concept Drilling in Eagle Ford and Eaglebine Shales,” presentation delivered at the DUG Eagleford, San Antonio, Texas, (Sept. 2013), [http://media.corporate-ir.net/media\\_files/IROL/68/68298/DUG%20Eagleford%202013%20Presentation%20\(Schepel%20Print%20Version\).pdf](http://media.corporate-ir.net/media_files/IROL/68/68298/DUG%20Eagleford%202013%20Presentation%20(Schepel%20Print%20Version).pdf).
7. Craft, J. R.: “Building Momentum: Multi-Bench and Pad Development in the Southern Midland Basin,” presentation delivered at the DUG Permian Basin, Fort Worth, Texas, (May 2014), [http://ir.approachresources.com/files/doc\\_presentations/2014/DUG%20Permian%20Basin%202014.pdf](http://ir.approachresources.com/files/doc_presentations/2014/DUG%20Permian%20Basin%202014.pdf).
8. Dittrick, P.: “Accenture: US Shale Gas Operations Offer Lessons for Other Countries,” *Oil and Gas J.* (14 January 2013).
9. Bello, R. O.: “Rate Transient Analysis in Shale Gas Reservoirs with Transient Linear Behavior,” PhD Dissertation, Texas A&M University, May 2009.

10. Barrufet, M. A.: "PETE 616 – Engineering Critical Reservoirs Class Notes, Fall 2007.
11. McCain, W. D.: *The Properties of Petroleum Fluids*, 2<sup>nd</sup> ed., PennWell Publishing Company, Tulsa (1990).
12. Papa, M.: *Annual Stockholder Presentation* (September 2013), [http://www.peakoildynamic.com/2013\\_09\\_01\\_archive.html](http://www.peakoildynamic.com/2013_09_01_archive.html).
13. Dake, L. P.: *The Fundamentals of Reservoir Engineering*, 72-98, Elsevier Publishing Company, Amsterdam (1994).
14. Kabir, C. S., Al-Khayat, N. I., and Choudhary, M. K.: "Lessons Learned From Energy Models: Iraq's South Rumaila Case Study", paper SPE 105131 presented at the 2007 Annual Middle East Petroleum and Gas Conference, Dubai, Apr. 14-19.
15. Pletcher, J. L.: "Improvements to Reservoir Material Balance Methods", paper SPE 75354 presented at the 2000 SPE Annual Technical Conference and Exhibition, Dallas, Texas, Oct. 1-4.
16. Esor, E., Dresda, S., and Monico, C.: "Use of Material Balance to Enhance 3D Reservoir Simulation: A Case Study", paper SPE 90362 presented at the 2004 SPE Annual Technical Conference and Exhibition, Houston, Texas, Sep. 26-29.
17. Williams, M. A., Keating, J. F., and Barghouty, M. F.: "The Stratigraphic Method: A Structured Approach to History-Matching Complex Simulation Models", paper SPE 38014 presented at the 1997 SPE Reservoir Simulation Symposium, Dallas, Texas, June 8-11.
18. Ambastha, A. K., Al-Matar, D., Ma, E., and Kasischke, B.: "Full-Field Parallel Simulation model: A Unique Tool for Reservoir Management of the Greater Burgan Oil Field", paper SPE 102281 presented at the 2006 SPE Annual technical Conference and Exhibition, San Antonio, Texas, Sep. 24-27.
19. Hoffman, B. T., Caers, J. K., Wen, Xian-Huan, and Strebelle, S.: "A Practical Data-Integration Approach to History Matching: Application to a Deepwater Reservoir", paper SPE 95557 presented at the 2005 SPE Annual Technical Conference and Exhibition, Dallas, Texas, Oct. 9-12.
20. Emanuel, A. S., and Milliken, W. J.: "History Matching Finite Difference Models with 3D Streamlines", paper SPE 49000 presented at the 1998 SPE Annual Technical Conference and Exhibition, New Orleans, Louisiana, Sep. 27-30.
21. King, G. R., Jones, M., Tankersley, T., Flodin, E., Jenkins, S., Zhumagulova, A., Eaton, W., Bateman, P., Laidlaw, C., Fitzmorris, R., Ma, X., and Dagistanova, K.:

- “Use of Brown-Field Experimental Design Methods for Post-Processing Conventional History Match Results”, paper SPE 159341 presented at the 2012 SPE Annual Technical Conference and Exhibition, San Antonio, Texas, Oct. 8-10.
22. Bartlett, R. M., Singh, P. K., Howie, J. M., Humphrey, K., Kurtz, J. A., and Croft, M. K.: “Unlocking Atlantis: An Integrated Approach to Reservoir Management of a Giant Subsalt Field”, paper OTC 20397 presented at the 2010 Offshore Technology Conference, Houston, Texas, May 3-6.
  23. Ambastha, A. K., and Aziz, K.: “Material Balance Calculations for Solution-Gas drive Reservoirs with Gravity Segregation”, paper SPE 16959 presented at the 1987 SPE Annual Technical Conference and Exhibition, Dallas, Texas, Sep 27-30.
  24. Ypma, J. G. J.: “Compositional Effects in Gravity-Dominated Nitrogen Displacements” SPERE (August 1988), 867.
  25. *MBAL™*, Integrated Petroleum Modeling (IPM) Toolkit, Petroleum Experts Limited, Edinburgh, Scotland.
  26. Campbell, R. A. and Campbell, J. M., Sr.: *Mineral Property Economics, Vol. 3: Petroleum Property Evaluation*, Campbell Petroleum Series, Norman, OK (1978) 26.
  27. Havlena, D. and Odeh, A. S.: “The Material Balance as an Equation of a Straight Line”, *JPT* (August 1963) 896.
  28. Chevron Phase Calculation Program (CPCP), Chevron propriety Phase-behavior software.
  29. Warren, J. E. and Root, P. J.: “The Behavior of Naturally Fractured Reservoirs,” paper SPE 426 presented at the 1962 SPE Annual Technical Conference and Exhibition,, Los Angeles, California, Oct 7-10.
  30. Pruess, K.: *Brief Guide to the MINC - Method for Modeling Flow and Transport in Fractured Media*. Earth Sciences Division, Lawrence Berkeley National Laboratory, Berkeley. (May 1992).
  31. De Swaan, A.: “Analytical Solutions for Determining Naturally Fractured Reservoir Properties by Well Testing,” paper SPE 5346 presented at the 1975 SPE-AMIE 45<sup>th</sup> California Regional Meeting, Ventura, California, Apr. 2-4.
  32. Kazemi, H.: “Pressure Transient Analysis of Naturally Fractured Reservoirs with Uniform Fracture Distribution,” paper SPE 2156A presented at the 1968 SPE Annual Technical Conference and Exhibition,, Houston, Texas, 29 Sept.- 2 Oct.

33. Ehlig-Economides, C. and Ayoub, J. A.: "Vertical Interference Testing across a Low-Permeability Zone," *SPE Formation Evaluation*, (Oct 1986) 497-510.
34. Stewart, G.: *Well Test Analysis and Design*, PennWell Corporation, Tulsa (2011).
35. Economides, M. J., Oligney, R., Valko, P. P.: *Unified Fracture Design: Bridging the Gap Between Theory and Practice*, Orsa Press, Tulsa (2002).
36. Valko, P. P. and Amini, S.: "The Method of Distributed Volumetric Sources for Calculating the Transient and Pseudosteady-State Productivity of Complex Well-Fracture Configurations," paper SPE 106279 presented at the 2007 SPE Hydraulic Fracturing Technology Conference, College Station, Texas, Jan. 29-31.
37. Amini, S.: "Development and Application of the Method of Distributed Volumetric Sources to the Problem of Unsteady-State Fluid Flow in Reservoirs," PhD Dissertation, Texas A&M University, May 2007.
38. Romero, D. J., Valko, P. P., and Economides, M. J.: "Optimization of Productivity Index and the Fracture Geometry of a Stimulated Well with Fracture Face and Choke Skins," paper SPE 81908 presented at the 2002 SPE International Symposium and Exhibition on Formation Damage Control, Lafayette, Louisiana, Feb. 20 – 21.
39. Raghavan, R.: *Well Test Analysis*, Prentice Hall, Upper Saddle River, New Jersey (1993).
40. Valko, P. P. and Abate, J.: "Numerical Laplace Inversion using GWR Function," *Wolfram Library Archive*, (February 2002)  
<http://library.wolfram.com/infocenter/MathSource/4738/>.
41. El-Bambi, A. H.: "Analysis of Tight Gas Wells," PhD Dissertation, Texas A&M University, May 1998.
42. Lichtenberger, G. J.: "Data Acquisition and Interpretation of Horizontal Well Pressure-Transient Tests," paper SPE 25922 presented at the 1993 Rocky Mountain Regional/Low Permeability Reservoirs Symposium, Denver, Colorado, Apr. 12-14.
43. Muskat, M.: "The Production Histories of Oil Producing Gas-Drive Reservoirs," *Journal of Applied Physics* (1945).
44. Walsh, M.P. and Lake, L.W.: *A Generalized Approach to Primary Hydrocarbon Recovery*. Elsevier Publishing Company, Amsterdam (2003).
45. Martin, J.C.: "Simplified Equations of Flow in Gas Drive Reservoirs and the

- Theoretical Foundation of Multiphase Pressure Buildup Analyses,” SPE-1235-G. *Trans.*, AIME, 216: 321–323.
46. Matthews, C.S., Brons, F., and Hazebroek, P. 1954. A Method for Determination of Average Pressure in a Bounded Reservoir. *Trans.*, AIME **201**, 182–191.
  47. Helmy, M. W. and Wattenbarger, R. A.: “New Shape Factors for Well Produced at Constant Pressure,” paper SPE 39970 presented at the 1998 SPE Gas Technology Symposium, Calgary, Alberta, Mar 15-18.
  48. van Everdingen, A.F. and Hurst, W. 1949. The Application of the Laplace Transformation to Flow Problems in Reservoirs. *Trans.*, AIME **186**, 305.
  49. Ozkan, E.: “Performance of Horizontal Wells,” PhD Dissertation, University of Tulsa, 1988.
  50. Katsikadelis, J. T.: *Boundary Elements: Theory and Applications*, Elsevier Publishing Company, Amsterdam (2002).
  51. Brown, M. L.: “Analytical Trilinear Pressure Transient Model for Multiply Fractured Horizontal Wells in Tight Shale Reservoir,” MS Dissertation, Colorado School of Mines, May 2009.
  52. Peters, L., Arts, R., Brouwer, G., Geel, C.: “Results of the Brugge Benchmark Study for Flooding Optimization and History Matching,” paper SPE 119094 presented at the 2009 Reservoir Simulation Symposium, Woodlands, Feb. 2 – 4.
  53. *INTERSECT™*, NextGen Reservoir Simulator, built by collaboration of Schlumberger, Chevron and Total, marketed by Schlumberger SIS, Abingdon Technology Center, Oxfordshire, UK.

APPENDIX A: PSEUDOSTEADY STATE DUAL POROSITY MODEL –  
 FORMULATION AND LAPLACE DOMAIN SOLUTION (WARREN & ROOT  
 MODEL)

The governing differential equation for linear fluid flow in matrix and fracture is given by:

Fracture: 
$$\frac{k_{fb}}{\mu} \nabla^2 p_f = \varphi_{fb} c_f \frac{\partial p_f}{\partial t} - \alpha \frac{k_{mb}}{\mu} (p_m - p_f) \dots\dots\dots (A-1a)$$

Matrix: 
$$0 = \varphi_{mb} c_m \frac{\partial p_m}{\partial t} + \alpha \frac{k_{mb}}{\mu} (p_m - p_f) \dots\dots\dots (A-1b)$$

The second term in eqn.(A-1a) is referred to as the source term,  $\sigma_m$ . During pseudosteady state the pressure (average pressure) change inside the matrix is constant.

Also, all properties need to be put as bulk properties:

$$k_{mb} = k_m \left( \frac{V_m}{V_{f+m}} \right) \dots\dots\dots (A-2a)$$

$$k_{fb} = k_f \left( \frac{V_f}{V_{f+m}} \right) \dots\dots\dots (A-2b)$$

Similarly, the matrix fracture bulk source term,  $\sigma_{mf}$ , is expressed as:

$$\sigma_{mf} = \sigma_m \left( \frac{V_m}{V_{f+m}} \right) = \alpha \frac{k_m}{\mu} \left( \frac{V_m}{V_{f+m}} \right) (p_m - p_f) \dots\dots\dots (A-3)$$

where  $\alpha$ , is the shape function:

$$\alpha = \frac{4n(n+2)}{h_m^2} \dots\dots\dots (A-4)$$

If we define dimensionless variables as:

$$x_D = \frac{x}{\sqrt{A_{cw}}} \dots\dots\dots (A-5a)$$

$$p_{jD} = \frac{p_i - p}{p_{ch}} = \frac{2\pi kh}{\alpha_1 q B \mu} p_i - p_j \Big|_{j=fb \text{ or } mb \text{ or } aq} \dots\dots\dots (A-5b)$$

The derivatives of the above entities will be:

$$\partial(x_D \sqrt{A_{cw}}) = \partial x \quad \partial(x_D \sqrt{A_{cw}}) \{ \partial(x_D \sqrt{A_{cw}}) \} = \partial^2 x \dots\dots\dots (A-6a)$$

$$\partial(p_D p_{ch} - p_i) = p_{ch} \partial p_D = - \partial p \quad p_{ch} \partial^2 p_D = \partial^2 p \dots\dots\dots (A-6b)$$

Substituting  $x_D$  in eqn.(A-1a) and eqn.(A-1b), we have:

Fracture: 
$$\frac{k_{fb}}{\mu} \frac{\partial^2 p_f}{\partial x_D^2} = \varphi_{fb} c_f A_{cw} \frac{\partial p_f}{\partial t} - \alpha A_{cw} \frac{k_{mb}}{\mu} (p_m - p_f)$$

Matrix: 
$$0 = \varphi_{mb} c_m A_{cw} \frac{\partial p_m}{\partial t} + \alpha A_{cw} \frac{k_{mb}}{\mu} (p_m - p_f)$$

Substituting  $p_D$  in eqn.(A-1a) and eqn.(A-1b), we have:

$$\text{Fracture: } \frac{k_{fb}}{\mu} p_{ch} \frac{\partial^2 p_{fD}}{\partial x_D^2} = \varphi_{fb} c_f A_{cw} \frac{\partial(p_{fD} p_{ch} - p_i)}{\partial t} - \alpha A_{cw} \frac{k_{mb}}{\mu} \{(p_{mD} p_{ch} - p_i) - (p_{fD} p_{ch} - p_i)\}$$

$$\text{Matrix: } 0 = \varphi_{mb} c_m A_{cw} \frac{\partial(p_{mD} p_{ch} - p_i)}{\partial t} + \alpha A_{cw} \frac{k_{mb}}{\mu} \{(p_{mD} p_{ch} - p_i) - (p_{fD} p_{ch} - p_i)\}$$

On cancellation of common terms, results in:

$$\text{Fracture: } \frac{\partial^2 p_{fD}}{\partial x_D^2} = \frac{\varphi_{fb} \mu c_f A_{cw}}{k_{fb}} \frac{\partial p_{fD}}{\partial t} - \alpha A_{cw} \frac{k_{mb}}{k_{fb}} \{p_{mD} - p_{fD}\} \quad \dots (A-7a)$$

$$\text{Matrix: } 0 = \frac{\varphi_{mb} \mu c_m A_{cw}}{k_{fb}} \frac{\partial p_{mD}}{\partial t} + \alpha A_{cw} \frac{k_{mb}}{k_{fb}} \{p_{mD} - p_{fD}\} \quad \dots (A-7b)$$

We also have the following:

$$\omega = \frac{\varphi_{fb} c_f}{(\varphi c_t)_{mb+fb}} \dots \dots \dots (A-8)$$



Substituting  $\omega$  in eqn.(A-7a) and eqn.(A-7b) and assuming compressibility is constant, we have:

$$\text{Fracture: } \frac{\partial^2 p_{fD}}{\partial x_D^2} = \omega \frac{(\varphi c_t)_{m+f} \mu A_{cw}}{k_{fb}} \frac{\partial p_{fD}}{\partial t} - \alpha A_{cw} \frac{k_{mb}}{k_{fb}} \{p_{mD} - p_{fD}\} \quad \dots\dots\dots (\text{A-9a})$$

$$\text{Matrix: } 0 = (1 - \omega) \frac{(\varphi c_t)_{m+f} \mu A_{cw}}{k_{fb}} \frac{\partial p_{mD}}{\partial t} + \alpha A_{cw} \frac{k_{mb}}{k_{fb}} \{p_{mD} - p_{fD}\} \quad \dots (\text{A-9b})$$

Here expression for dimensionless time and dimensionless interporosity flow parameter are as:

$$t_D = \frac{k_{fb} t}{(\varphi c_t)_{m+f} \mu A_{cw}} \dots\dots\dots (\text{A-10})$$

$$\lambda = \alpha A_{cw} \frac{k_{mb}}{k_{fb}} \dots\dots\dots (\text{A-11})$$

Then the final form of the dimensionless form of the governing equations are:

$$\text{Fracture: } \nabla^2 p_{fD} = \omega \frac{\partial p_{fD}}{\partial t_D} - \lambda \{p_{mD} - p_{fD}\} \quad \dots\dots\dots (\text{A-12a})$$

$$\text{Matrix: } 0 = (1 - \omega) \frac{\partial p_{mD}}{\partial t_D} + \lambda \{p_{mD} - p_{fD}\} \quad \dots\dots\dots (\text{A-12b})$$

The Laplace transform of the above equations is:

Fracture: 
$$\frac{\partial^2 \overline{p_{fD}}}{\partial x_D^2} = \omega s \overline{p_{fD}} - \lambda \{ \overline{p_{mD}} - \overline{p_{fD}} \} \dots\dots\dots (A-13a)$$

Matrix: 
$$0 = (1 - \omega) s \overline{p_{mD}} + \lambda \{ \overline{p_{mD}} - \overline{p_{fD}} \} \dots\dots\dots (A-13b)$$

Solving eqn.(A-13b) for  $\overline{p_{mD}}$ :

$$\overline{p_{mD}} = \frac{\lambda}{(1-\omega)s+\lambda} \overline{p_{fD}} \dots\dots\dots (A-14)$$

Substituting this in eqn.(A-13a) we have:

$$\begin{aligned} \frac{\partial^2 \overline{p_{fD}}}{\partial x_D^2} &= \omega s \overline{p_{fD}} - \lambda \overline{p_{fD}} \left\{ \frac{\lambda - (1-\omega)s - \lambda}{(1-\omega)s + \lambda} \right\} \\ &= \left[ \omega + \left\{ \frac{\lambda(1-\omega)}{(1-\omega)s + \lambda} \right\} \right] s \overline{p_{fD}} \\ &= \left[ \frac{\omega(1-\omega)s + \lambda}{(1-\omega)s + \lambda} \right] s \overline{p_{fD}} \\ \frac{\partial^2 \overline{p_{fD}}}{\partial x_D^2} - sf(s) \overline{p_{fD}} &= 0 \dots\dots\dots (A-15) \end{aligned}$$

Where,

$$f(s) = \frac{\omega(1-\omega)s+\lambda}{(1-\omega)s+\lambda} \dots\dots\dots (A-16a)$$

$$f(s) = \frac{1+s\left(\frac{\omega}{\lambda}\right) - s\omega\left(\frac{\omega}{\lambda}\right)}{1+\frac{s}{\omega}\left(\frac{\omega}{\lambda}\right) - s\left(\frac{\omega}{\lambda}\right)} \dots\dots\dots (A-16b)$$

Eqn.(A-15) is a homogeneous partial differential equation with the following general solution:

$$\overline{p_{fD}} = A \cosh(x_D \sqrt{sf(s)}) + B \sinh(x_D \sqrt{sf(s)}) \dots\dots\dots (A-17)$$

For a closed linear reservoir, the initial and boundary conditions are:

Initial Condition:  $\overline{p_{fD}}(x_D, s) = 0 \dots\dots\dots (A-18a)$

Inner Boundary Condition:  $\left. \frac{\partial \overline{p_{fD}}}{\partial x_D} \right|_{x_D=0} = -\frac{2\pi}{s} \dots\dots\dots (A-18b)$

Outer Boundary Condition:  $\left. \frac{\partial \overline{p_{fD}}}{\partial x_D} \right|_{x_D=x_{De}} = 0 \dots\dots\dots (A-18c)$

Differentiating with respect to  $x_D$  and using the inner boundary condition, we have:

$$\left. \frac{d\overline{p}_{fD}}{dx_D} \right|_{x_D=0} = -\frac{2\pi}{s} = \sqrt{sf(s)} A \sinh(x_D \sqrt{sf(s)}) + \sqrt{sf(s)} B \cosh(x_D \sqrt{sf(s)})$$

Since  $\sinh x_D|_{x_D=0} = 0$ , implies:

$$B = -\frac{2\pi}{s\sqrt{sf(s)}} \dots\dots\dots (A-19)$$

Using outer boundary condition and substituting eqn.(A-18c) in eqn.(A-17) we have:

$$\left. \frac{d\overline{p}_{fD}}{dx_D} \right|_{x_D=x_{De}} = 0 = \sqrt{sf(s)} A \sinh(x_{De} \sqrt{sf(s)}) - \frac{2\pi}{s} \cosh(x_{De} \sqrt{sf(s)})$$

$$A = \frac{2\pi}{s\sqrt{sf(s)}} \frac{\cosh(x_{De} \sqrt{sf(s)})}{\sinh(x_{De} \sqrt{sf(s)})} \dots\dots\dots (A-20)$$

Hence the particular solution for constant rate of eqn.(A-17) in Laplace domain is:

$$\overline{p}_{fD} = \frac{2\pi}{s\sqrt{sf(s)}} \frac{\cosh(x_{De} \sqrt{sf(s)})}{\sinh(x_{De} \sqrt{sf(s)})} \cosh(x_D \sqrt{sf(s)}) - \frac{2\pi}{s\sqrt{sf(s)}} \sinh(x_D \sqrt{sf(s)}) \dots (A-21)$$

The particular solution at the well for constant rate is given by:

$$\overline{p}_{wfD} = \frac{2\pi}{s\sqrt{sf(s)}} \frac{\cosh(x_{De}\sqrt{sf(s)})}{\sinh(x_{De}\sqrt{sf(s)})} \dots\dots\dots (A-22a)$$

$$\overline{p}_{wfD} = \frac{2\pi}{s\sqrt{sf(s)}} \frac{1+\exp(-2x_{De}\sqrt{sf(s)})}{1-\exp(-2x_{De}\sqrt{sf(s)})} \dots\dots\dots (A-22b)$$

The particular solution at the well for constant pressure is given by:

$$\overline{q}_{wfD} = \frac{\sqrt{sf(s)}}{2\pi s} \frac{\sinh(x_{De}\sqrt{sf(s)})}{\cosh(x_{De}\sqrt{sf(s)})} \dots\dots\dots (A-22c)$$

$$\overline{q}_{wfD} = \frac{\sqrt{sf(s)}}{2\pi s} \frac{1-\exp(-2x_{De}\sqrt{sf(s)})}{1+\exp(-2x_{De}\sqrt{sf(s)})} \dots\dots\dots (A-22d)$$

Where  $f(s)$  is given by eqn.(A-16) and  $s$  is the Laplace space variable.

APPENDIX B: TRANSIENT DUAL POROSITY MODEL – FORMULATION AND  
LAPLACE DOMAIN SOLUTION (BELLO MODEL)

The governing differential equation for linear fluid flow in matrix and fracture is given by:

Fracture: 
$$\frac{k_{fb}}{\mu} \nabla^2 p_f = \varphi_{fb} c_f \frac{\partial p_f}{\partial t} - \frac{k_{mb}}{\mu h_m/2} \frac{\partial p_m}{\partial z} \Big|_{z=h_m/2} \dots\dots\dots (B-1a)$$

Matrix: 
$$\frac{k_{mb}}{\mu} \nabla^2 p_m = \varphi_{mb} c_m \frac{\partial p_m}{\partial t} \dots\dots\dots (B-1b)$$

The second term in eqn.(B-1a) is referred to as the source term,  $\sigma_m$ . Here the following symbols for matrix/fracture permeability stands for bulk property:

$$k_{mb} = k_m \left( \frac{V_m}{V_{f+m}} \right) \dots\dots\dots (B-2a)$$

$$k_{fb} = k_f \left( \frac{V_f}{V_{f+m}} \right) \dots\dots\dots (B-2b)$$

For a matrix block, the initial and boundary conditions are:

Initial Condition:  $p_{mb}(z, t = 0) = p_i$  ..... (B-3a)

Inner Boundary Condition:  $\frac{\partial p_{mb}}{\partial z} \Big|_{z=0} = 0$  for all t ..... (B-3b)

Outer Boundary Condition:  $p_{mb} \Big|_{z=\frac{h_m}{2}} = p_f$  for all t ..... (B-3c)

For a fracture block, the initial and boundary conditions are:

Initial Condition:  $p_{fb}(x, t = 0) = p_i$  ..... (B-4a)

Inner Boundary Condition:  $q = -\left(\frac{k_f A_{cw}}{\mu}\right) \frac{\partial p_{fb}}{\partial x} \Big|_{x=0}$  for all t and const. rate .. (B-4b)

Outer Boundary Condition  $\frac{\partial p_{fb}}{\partial x} \Big|_{x=x_e} = 0$  for all t ..... (B-4c)

If we define dimensionless variables as:

$$x_D = \frac{x}{\sqrt{A_{cw}}} \quad \text{for all fracture} \quad \dots\dots\dots (B-5a)$$

$$z_D = \frac{z}{h_{rm}/2} \quad \text{for all matrix} \quad \dots\dots\dots (B-5b)$$

$$p_D = \frac{p_i - p}{p_{ch}} = \frac{2\pi kh}{\alpha_1 q B \mu} (p_i - p) \quad \dots\dots\dots (B-5c)$$

The derivatives of the above entities will be:

$$\partial(x_D \sqrt{A_{cw}}) = \partial x \quad \partial(x_D \sqrt{A_{cw}}) \{ \partial(x_D \sqrt{A_{cw}}) \} = \partial^2 x \quad \dots \text{(B-6a)}$$

$$\partial(z_D h_{rm}/2) = \partial z \quad \partial(z_D h_{rm}/2) \{ \partial(z_D h_{rm}/2) \} = \partial^2 z \quad \dots \text{(B-6b)}$$

$$\partial(p_D p_{ch} - p_i) = p_{ch} \partial p_D = - \partial p \quad p_{ch} \partial^2 p_D = \partial^2 p \quad \dots \text{(B-6c)}$$

Substituting  $x_D$  in eqn.(B-1a) and eqn.(B-1b), we have:

$$\text{Fracture:} \quad \frac{k_{fb}}{\mu} \frac{\partial^2 p_f}{\partial x_D^2} = \varphi_{fb} c_f A_{cw} \frac{\partial p_f}{\partial t} - \frac{k_{mb} A_{cw}}{\mu h_m/2} \frac{\partial p_m}{\partial x} \Big|_{x=h_m/2}$$

$$\text{Matrix:} \quad \frac{k_{mb}}{\mu} \frac{\partial^2 p_m}{\partial z_D^2} = \varphi_{mb} c_m \frac{h_m^2}{4} \frac{\partial p_m}{\partial t}$$

Substituting  $p_D$  in eqn.(B-1a) and eqn.(B-1b), we have:

$$\text{Fracture:} \quad \frac{k_{fb}}{\mu} p_{ch} \frac{\partial^2 p_{fD}}{\partial x_D^2} = \varphi_{fb} c_f A_{cw} \frac{\partial(p_{fD} p_{ch} - p_i)}{\partial t} - \frac{k_{mb} A_{cw}}{\mu h_m/2} \frac{\partial(p_{mD} p_{ch} - p_i)}{\partial z} \Big|_{z=h_m/2}$$

$$\text{Matrix:} \quad \frac{k_{mb}}{\mu} p_{ch} \frac{\partial^2 p_{mD}}{\partial z_D^2} = \varphi_{mb} c_m \frac{h_m^2}{4} \frac{\partial(p_{mD} p_{ch} - p_i)}{\partial t}$$



On cancellation of common terms and putting in additional terms, results in:

$$\text{Fracture:} \quad \frac{\partial^2 p_{fD}}{\partial x_D^2} = \frac{\varphi_{fb} \mu c_f A_{cw}}{k_{fb}} \frac{\partial p_{fD}}{\partial t} - \frac{k_{mb} A_{cw}}{k_{fb} h_m/2} \frac{\partial p_{mD}}{\partial z} \Big|_{z=h_m/2} \dots\dots (B-7a)$$

$$\text{Matrix:} \quad \frac{\partial^2 p_{mD}}{\partial z_D^2} = \frac{\varphi_{mb} \mu c_m}{k_{mb}} \frac{k_{fb} A_{cw}}{k_{fb} A_{cw}} \frac{h_m^2}{4} \frac{\partial p_{mD}}{\partial t} \dots\dots\dots (B-7b)$$

We also have the following:

$$\omega = \frac{\varphi_{fb} c_f}{(\varphi c_t)_{mb+fb}} \dots\dots\dots (B-8)$$

Substituting  $\omega$  in eqn.(B-7a) and eqn.(B-7b) and assuming compressibility is constant, we have:

$$\text{Fracture:} \quad \frac{\partial^2 p_{fD}}{\partial x_D^2} = \omega \frac{(\varphi c_t)_{m+f} \mu A_{cw}}{k_{fb}} \frac{\partial p_{fD}}{\partial t} - \frac{k_{mb} A_{cw}}{k_{fb} h_m^2/4} \frac{\partial p_{mD}}{\partial z_D} \Big|_{z_D=1} \dots\dots\dots (B-9a)$$

$$\text{Matrix:} \quad \frac{\partial^2 p_{mD}}{\partial z_D^2} = (1 - \omega) \frac{(\varphi c_t)_{m+f} \mu}{k_{mb}} \frac{k_{fb} A_{cw}}{k_{fb} A_{cw}} \frac{h_m^2}{4} \frac{\partial p_{mD}}{\partial t} \dots\dots\dots (B-9b)$$

Here expression for dimensionless time and dimensionless interporosity flow parameter are as:

$$t_D = \frac{k_{fb} t}{(\varphi c_t)_{m+f} \mu A_{cw}} \dots\dots\dots (B-10)$$

$$\lambda = \frac{12}{h_m^2} A_{cw} \frac{k_{mb}}{k_{fb}} \dots\dots\dots (B-11)$$

Then the final form of the dimensionless form of the governing equations are:

Fracture:  $\nabla^2 p_{fD} = \omega \frac{\partial p_{fD}}{\partial t_D} - \frac{\lambda}{3} \frac{\partial p_{mD}}{\partial z_D} \Big|_{z_D=1} \dots\dots\dots (B-12a)$

Matrix:  $\nabla^2 p_{mD} = \frac{3(1-\omega)}{\lambda} \frac{\partial p_{mD}}{\partial t_D} \dots\dots\dots (B-12b)$

Taking Laplace transform of the above equations:

Fracture:  $\frac{\partial^2 \overline{p_{fD}}}{\partial x_D^2} = \omega \{s \overline{p_{fD}} - \overline{p_{fD}}(x_D, 0)\} - \frac{\lambda}{3} \frac{\partial \overline{p_{mD}}}{\partial z_D} \Big|_{z_D=1} \dots\dots (B-13a)$

Matrix:  $\frac{\partial^2 \overline{p_{mD}}}{\partial z_D^2} = \frac{3(1-\omega)}{\lambda} \{s \overline{p_{mD}} - \overline{p_{mD}}(z_D, 0)\} \dots\dots\dots (B-13b)$

Matrix Equation

Let us find the solution of eqn.(B-13b) for  $\overline{p_{mD}}$  first. For a matrix block and in Laplace domain, the initial and boundary conditions are:

Initial Condition:  $\overline{p_{mD}}(x_D = 1, s \rightarrow \infty) = 0$  ..... (B-14a)

Inner Boundary Condition:  $\left. \frac{\partial \overline{p_{mD}}}{\partial z_D} \right|_{z_D=0} = 0$  ..... (B-14b)

Outer Boundary Condition:  $\overline{p_{mD}}|_{z_D=1} = \overline{p_{fD}}$  ..... (B-14c)

Applying initial condition, we have:

$$\frac{\partial^2 \overline{p_{mD}}}{\partial z_D^2} - \frac{3(1-\omega)}{\lambda} s \overline{p_{mD}} = 0$$
 ..... (B-15)

The above is a homogeneous partial differential equation with the following general solution:

$$\overline{p_{mD}} = A \cosh\left(z_D \sqrt{s \frac{3(1-\omega)}{\lambda}}\right) + B \sinh\left(z_D \sqrt{s \frac{3(1-\omega)}{\lambda}}\right)$$
 ..... (B-16)

Differentiating with respect to  $z_D$  and using the inner boundary condition, we have:

$$\left. \frac{d\bar{p}_{mD}}{dz_D} \right|_{z_D=0} = 0 = \sqrt{s \frac{3(1-\omega)}{\lambda}} A \sinh \left( z_D \sqrt{s \frac{3(1-\omega)}{\lambda}} \right) + \sqrt{s \frac{3(1-\omega)}{\lambda}} B \cosh \left( z_D \sqrt{s \frac{3(1-\omega)}{\lambda}} \right)$$

Since  $\sinh z_D|_{z_D=0} = 0$ , implies:

$$B = 0 \dots\dots\dots (B-17)$$

Using outer boundary condition and substituting eqn.(B-14c) in eqn.(B-16) we have:

$$\bar{p}_{fD} = A \cosh \left( z_D \sqrt{s \frac{3(1-\omega)}{\lambda}} \right)_{z_D=1}$$

$$A = \frac{\bar{p}_{fD}}{\cosh \left( \sqrt{s \frac{3(1-\omega)}{\lambda}} \right)} \dots\dots\dots (B-18)$$

Hence the particular solution for constant rate of eqn.(B-15) in Laplace domain is:

$$\bar{p}_{mD} = \frac{\bar{p}_{fD}}{\cosh \left( \sqrt{s \frac{3(1-\omega)}{\lambda}} \right)} \cosh \left( z_D \sqrt{s \frac{3(1-\omega)}{\lambda}} \right) \dots\dots\dots (B-19)$$

Fracture Equation

To find the solution of fracture eqn.(B-13a) for  $\overline{p_{fD}}$ , we need to convert the initial and boundary conditions in eqn.(B-4) to dimensionless form in Laplace domain as:

Initial Condition:  $\overline{p_{fD}}(x_D = 1, s \rightarrow \infty) = 0$  ..... (B-20a)

Inner Boundary Condition:  $\left. \frac{\partial \overline{p_{fD}}}{\partial x_D} \right|_{x_D=0} = -\frac{2\pi}{s}$  ..... (B-20b)

Outer Boundary Condition  $\left. \frac{\partial \overline{p_{fD}}}{\partial x_D} \right|_{x_D=x_{eD}} = 0$  ..... (B-20c)

Applying initial condition, we have:

$$\frac{\partial^2 \overline{p_{fD}}}{\partial x_D^2} = \omega s \overline{p_{fD}} - \frac{\lambda}{3} \left. \frac{\partial \overline{p_{mD}}}{\partial x_D} \right|_{x_D=1} \text{ ..... (B-21)}$$

But from eqn.(B-19) we have

$$\left. \frac{\partial \overline{p_{mD}}}{\partial z_D} \right|_{z_D=1} = \frac{\sqrt{s \frac{3(1-\omega)}{\lambda}}}{\cosh\left(\sqrt{s \frac{3(1-\omega)}{\lambda}}\right)} \sinh\left(\sqrt{s \frac{3(1-\omega)}{\lambda}}\right) \overline{p_{fD}} \text{ ..... (B-22)}$$

This derivative will change sign when expressed in terms of  $\overline{p_{fD}}$ , which inserted into eqn.(B-21) gives:

$$\begin{aligned} \frac{\partial^2 \overline{p_{fD}}}{\partial z_D^2} &= \omega s \overline{p_{fD}} + \frac{\lambda}{3} \left\{ \frac{\sqrt{s \frac{3(1-\omega)}{\lambda}}}{\cosh\left(\sqrt{s \frac{3(1-\omega)}{\lambda}}\right)} \sinh\left(\sqrt{s \frac{3(1-\omega)}{\lambda}}\right) \overline{p_{fD}} \right\} \\ &= s \overline{p_{fD}} \left\{ \omega + \frac{\lambda}{3s} \sqrt{\frac{3(1-\omega)s}{\lambda}} \tanh\left(\sqrt{s \frac{3(1-\omega)}{\lambda}}\right) \right\} \dots\dots\dots (B-23) \end{aligned}$$

This is of the form:

$$\frac{\partial^2 \overline{p_{fD}}}{\partial x_D^2} - sf(s)\overline{p_{fD}} = 0 \dots\dots\dots (B-24)$$

Where,

$$f(s) = \omega + \frac{\lambda}{3s} \sqrt{\frac{3(1-\omega)s}{\lambda}} \tanh\left(\sqrt{s \frac{3(1-\omega)}{\lambda}}\right) \dots\dots\dots (B-25a)$$

$$f(s) = \omega \left[ 1 + \left(\frac{1}{3s}\right) \left(\frac{\lambda}{\omega}\right) \sqrt{3s \left(\frac{1-\omega}{\omega}\right) \left(\frac{\omega}{\lambda}\right)} \tanh\left(\sqrt{3s \left(\frac{1-\omega}{\omega}\right) \left(\frac{\omega}{\lambda}\right)}\right) \right] \dots\dots\dots (B-25b)$$

Again, eqn.(B-24) is a homogeneous partial differential equation which is the same as eqn.(A-17). Refer to Appendix A for the rest of the derivation.

APPENDIX C: PSEUDOSTEADY STATE AQUIFER DUAL POROSITY MODEL –  
 FORMULATION AND LAPLACE DOMAIN SOLUTION (LINEAR EQUIVALENT  
 EHLIG-ECONOMIDES AND AYOUB MODEL)

The governing differential equation for linear fluid flow in matrix and fracture is given by:

$$\text{Fracture:} \quad \left(\frac{kh}{\mu}\right)_f \nabla^2 p_f = \varphi_f c_f h_f \frac{\partial p_f}{\partial t} - \alpha \frac{k_a}{\mu_a} (p_a - p_f) \quad \dots\dots\dots (\text{C-1a})$$

$$\text{Matrix (Aquifer):} \quad 0 = \varphi_a c_a h_a \frac{\partial p_a}{\partial t} + \alpha \frac{k_a}{\mu_a} (p_a - p_f) \quad \dots\dots\dots (\text{C-1b})$$

The second term in eqn.(C-1a) is referred to as the source term,  $\sigma_a$ . During pseudosteady state the pressure (average pressure) change inside the matrix is constant. Also, all properties need to be put as bulk properties:

$$\left(\frac{kh}{\mu}\right)_{aq} = \frac{k_a h_a}{\mu_a} \left(\frac{V_{aq}}{V_{f+aq}}\right) = \left(\frac{\frac{k_{aq} h_{aq}}{\mu_{aq}}}{\frac{k_{fb} h_{fb}}{\mu_{fb}} + \frac{k_{aq} h_{aq}}{\mu_{aq}}}\right) \quad \dots\dots\dots (\text{C-2a})$$

$$\left(\frac{kh}{\mu}\right)_{fb} = \frac{k_f h_f}{\mu_f} \left(\frac{V_f}{V_{f+aq}}\right) = \left(\frac{\frac{k_{fb} h_{fb}}{\mu_{fb}}}{\frac{k_{fb} h_{fb}}{\mu_{fb}} + \frac{k_{aq} h_{aq}}{\mu_{aq}}}\right) \quad \dots\dots\dots (\text{C-2b})$$

$$(\varphi h)_{aq} = \left(\frac{V_{aq}}{V_{f+aq}}\right) = \left(\frac{\varphi_{aq} h_{aq}}{\varphi_{fb} h_{fb} + \varphi_{aq} h_{aq}}\right) \quad \dots\dots\dots (\text{C-2c})$$

$$(\varphi h)_{fb} = \left( \frac{V_f}{V_{f+a}} \right) = \left( \frac{\varphi_{rf} h_{rf}}{\varphi_{fb} h_{fb} + \varphi_{aq} h_{aq}} \right) \dots\dots\dots (C-2d)$$

Similarly, the matrix fracture bulk source term,  $\sigma_{aq}$ , is expressed as:

$$\sigma_{aq} = \sigma_a \left( \frac{V_a}{V_{f+a}} \right) = \underline{\alpha} \frac{k_a}{\mu_a} \left( \frac{V_a}{V_{f+a}} \right) (p_{aq} - p_{fb}) = \underline{\alpha} \left( \frac{k_{fb} h_{fb}}{\mu_{fb}} + \frac{k_{aq} h_{aq}}{\mu_{aq}} \right) \left( \frac{k}{\mu} \right)_{aq} (p_{aq} - p_{fb}) \dots\dots\dots (C-3)$$

where  $\underline{\alpha}$ , is the shape function:

$$\underline{\alpha} = \frac{(T_b)_{eff}}{k_{aq}} \dots\dots\dots (C-4a)$$

And,

$$\lambda_{aqf} = \underline{\alpha} \left( \frac{k_{aq}}{k_{rf}} \right) A_{cw} = \left( \frac{(T_b)_{eff}}{k_{rf}} \right) A_{cw} \dots\dots\dots (C-4b)$$

In terms of bulk properties the governing equations can be recast into:

Fracture:  $\left( \frac{k_{fb} h_{fb}}{\mu_{fb}} + \frac{k_{aq} h_{aq}}{\mu_{aq}} \right) \left( \frac{kh}{\mu} \right)_{fb} \nabla^2 p_{fb} = (\varphi_{fb} h_{fb} + \varphi_{aq} h_{aq}) (\varphi h)_{fb} c_f \frac{\partial p_{fb}}{\partial t} -$

$$\underline{\alpha} \left( \frac{k_{fb} h_{fb}}{\mu_{fb}} + \frac{k_{aq} h_{aq}}{\mu_{aq}} \right) \left( \frac{k}{\mu} \right)_{aq} (p_{aq} - p_{fb}) \dots\dots\dots (C-5a)$$

Matrix (Aquifer):  $0 = (\varphi_{fb} h_{fb} + \varphi_{aq} h_{aq}) (\varphi h)_{aq} c_a \frac{\partial p_{aq}}{\partial t} + \underline{\alpha} \left( \frac{k_{fb} h_{fb}}{\mu_{fb}} + \right.$

$$\left. \frac{k_{aq} h_{aq}}{\mu_{aq}} \right) \left( \frac{k}{\mu} \right)_{aq} (p_{aq} - p_{fb}) \dots\dots\dots (C-5b)$$



If we assume  $x$  is the linear dimension and define dimensionless variables as:

$$x_D = \frac{x}{\sqrt{A_{cw}}} \dots\dots\dots (C-6a)$$

$$p_{jD} = \frac{p_i - p}{p_{ch}} = \frac{2\pi}{\alpha_1 q B} \left( \frac{k_{fb} h_{fb}}{\mu_{fb}} + \frac{k_{aq} h_{aq}}{\mu_{aq}} \right) (p_i - p_j) \Big|_{j=fb \text{ or } aq} \dots\dots (C-6b)$$

The derivatives of the above entities will be:

$$\partial(x_D \sqrt{A_{cw}}) = \partial x \quad \partial(x_D \sqrt{A_{cw}}) \{ \partial(x_D \sqrt{A_{cw}}) \} = \partial^2 x \dots\dots\dots (C-7a)$$

$$\partial(p_D p_{ch} - p_i) = p_{ch} \partial p_D = -\partial p \quad p_{ch} \partial^2 p_D = \partial^2 p \dots\dots\dots (C-7b)$$

Substituting  $x_D$  in eqn.(C-1a) and eqn.(C-1b), we have:

$$\begin{aligned} \text{Fracture: } \left( \frac{k_{fb} h_{fb}}{\mu_{fb}} + \frac{k_{aq} h_{aq}}{\mu_{aq}} \right) \left( \frac{kh}{\mu} \right)_{fb} \frac{\partial^2 p_f}{\partial x_D^2} &= (\varphi_{fb} h_{fb} + \varphi_{aq} h_{aq}) (\varphi h)_{fb} c_f A_{cw} \frac{\partial p_f}{\partial t} - \\ &\underline{\alpha} A_{cw} \left( \frac{k_{fb} h_{fb}}{\mu_{fb}} + \frac{k_{aq} h_{aq}}{\mu_{aq}} \right) \left( \frac{k}{\mu} \right)_{aq} (p_{aq} - p_{fb}) \end{aligned}$$

Matrix (Aquifer):

$$0 =$$

$$\begin{aligned} (\varphi_{fb} h_{fb} + \varphi_{aq} h_{aq}) (\varphi h)_{aq} c_{aq} A_{cw} \frac{\partial p_{aq}}{\partial t} + \\ \underline{\alpha} A_{cw} \left( \frac{k_{fb} h_{fb}}{\mu_{fb}} + \frac{k_{aq} h_{aq}}{\mu_{aq}} \right) \left( \frac{k}{\mu} \right)_{aq} (p_{aq} - p_f) \end{aligned}$$

Substituting  $p_D$  in eqn.(C-1a) and eqn.(C-1b), we have:

$$\begin{aligned} \text{Fracture: } & \left( \frac{k_{fb} h_{fb}}{\mu_{fb}} + \frac{k_{aq} h_{aq}}{\mu_{aq}} \right) \left( \frac{kh}{\mu} \right)_{fb} p_{ch} \frac{\partial^2 p_{fD}}{\partial x_D^2} = (\varphi_{fb} h_{fb} + \varphi_{aq} h_{aq}) \times \\ & (\varphi h)_{fb} c_f A_{cw} \frac{\partial(p_{fD} p_{ch} - p_i)}{\partial t} - \underline{\alpha} A_{cw} \left( \frac{k_{fb} h_{fb}}{\mu_{fb}} + \frac{k_{aq} h_{aq}}{\mu_{aq}} \right) \left( \frac{k}{\mu} \right)_{aq} \{(\partial p_{aqD} p_{ch} - p_i) - \\ & (p_{fD} p_{ch} - p_i)\} \end{aligned}$$

$$\begin{aligned} \text{Matrix (Aquifer): } & 0 = (\varphi_{fb} h_{fb} + \varphi_{aq} h_{aq}) (\varphi h)_{aq} c_{aq} A_{cw} \frac{\partial(p_{aqD} p_{ch} - p_i)}{\partial t} + \\ & \underline{\alpha} A_{cw} \left( \frac{k_{fb} h_{fb}}{\mu_{fb}} + \frac{k_{aq} h_{aq}}{\mu_{aq}} \right) \left( \frac{k}{\mu} \right)_{aq} \times \{(\partial p_{aqD} p_{ch} - p_i) - (p_{fD} p_{ch} - p_i)\} \end{aligned}$$

On cancellation of common terms, results in:

$$\text{Fracture: } \left( \frac{kh}{\mu} \right)_{fb} \frac{\partial^2 p_{fD}}{\partial x_D^2} = (\varphi h)_{fb} \frac{(\varphi_{fb} h_{fb} + \varphi_{aq} h_{aq}) c_f A_{cw}}{\left( \frac{k_{fb} h_{fb}}{\mu_{fb}} + \frac{k_{aq} h_{aq}}{\mu_{aq}} \right)} \frac{\partial p_{fD}}{\partial t} - \underline{\alpha} A_{cw} \left( \frac{k}{\mu} \right)_{aq} \{p_{aqD} - p_{fD}\} \dots \dots \text{(C-8a)}$$

$$\text{Matrix (Aquifer): } 0 = (\varphi h)_{aq} \frac{(\varphi_{fb} h_{fb} + \varphi_{aq} h_{aq}) c_{aq} A_{cw}}{\left( \frac{k_{fb} h_{fb}}{\mu_{fb}} + \frac{k_{aq} h_{aq}}{\mu_{aq}} \right)} \frac{\partial p_{aqD}}{\partial t} + \underline{\alpha} A_{cw} \left( \frac{k}{\mu} \right)_{aq} \{p_{aqD} - p_{fD}\} \text{(C-8b)}$$

Reapplying eqn.(C-2) to the above we get:

$$\text{Fracture: } \left( \frac{\frac{k_{fb} h_{fb}}{\mu_{fb}}}{\frac{k_{fb} h_{fb}}{\mu_{fb}} + \frac{k_{aq} h_{aq}}{\mu_{aq}}} \right) \frac{\partial^2 p_{fD}}{\partial x_D^2} = (\varphi h)_{fb} \frac{(\varphi_{fb} h_{fb} + \varphi_{aq} h_{aq}) c_f A_{cw}}{\left( \frac{k_{fb} h_{fb}}{\mu_{fb}} + \frac{k_{aq} h_{aq}}{\mu_{aq}} \right)} \frac{\partial p_{fD}}{\partial t} -$$

$$\underline{\alpha} A_{cw} \left( \frac{\frac{k_{aq}}{\mu_{aq}}}{\frac{k_{fb} h_{fb}}{\mu_{fb}} + \frac{k_{aq} h_{aq}}{\mu_{aq}}} \right) \{p_{aqD} - p_{fD}\} \dots\dots\dots \text{(C-9a)}$$

Matrix (Aquifer):

$$0 =$$

$$(\varphi h)_{aq} \frac{(\varphi_{fb} h_{fb} + \varphi_{aq} h_{aq}) c_{aq} A_{cw}}{\left( \frac{k_{fb} h_{fb}}{\mu_{fb}} + \frac{k_{aq} h_{aq}}{\mu_{aq}} \right)} \frac{\partial p_{aqD}}{\partial t} +$$

$$\underline{\alpha} A_{cw} \left( \frac{\frac{k_{aq}}{\mu_{aq}}}{\frac{k_{fb} h_{fb}}{\mu_{fb}} + \frac{k_{aq} h_{aq}}{\mu_{aq}}} \right) \{p_{aqD} - p_{fD}\} \dots\dots\dots \text{(C-9b)}$$

We also have the following:

$$\omega_{aq} = \frac{\varphi_{fb} c_f}{(\varphi c_t)_{aq+fb}} \dots\dots\dots \text{(C-10)}$$

Substituting  $\omega$  in eqn.(C-9a) and eqn.(C-9b) and assuming compressibility is constant, we have:

$$\text{Fracture: } \kappa_{fb} \frac{\partial^2 p_{fD}}{\partial x_D^2} = \omega_{aq} \frac{\partial p_{fD}}{\partial t_D} - \lambda_{aq} \{p_{aqD} - p_{fD}\} \dots\dots\dots \text{(C-11a)}$$

$$\text{Matrix (Aquifer): } 0 = (1 - \omega_{aq}) \frac{\partial p_{aqD}}{\partial t_D} + \lambda_{aq} \{p_{aqD} - p_{fD}\} \dots \text{(C-11b)}$$

Here expression for dimensionless time and dimensionless interporosity flow parameter, are as:

$$t_D = \frac{\left(\frac{k_{fb} h_{fb}}{\mu_{fb}} + \frac{k_{aq} h_{aq}}{\mu_{aq}}\right) t}{(\varphi_{fb} h_{fb} + \varphi_{aq} h_{aq}) c_f A_{cw}} \dots\dots\dots (C-12a)$$

$$\lambda_{aq} = \underline{\alpha} A_{cw} \left( \frac{\frac{k_{aq}}{\mu_{aq}}}{\frac{k_{fb} h_{fb}}{\mu_{fb}} + \frac{k_{aq} h_{aq}}{\mu_{aq}}} \right) \dots\dots\dots (C-12b)$$

$$\kappa_{fb} = \left( \frac{\frac{k_{fb} h_{fb}}{\mu_{fb}}}{\frac{k_{fb} h_{fb}}{\mu_{fb}} + \frac{k_{aq} h_{aq}}{\mu_{aq}}} \right) \dots\dots\dots (C-12c)$$

Where:  $\underline{\alpha} = \frac{(T_b)_{eff}}{k_{aq}} \dots\dots\dots (C-12d)$

Where:  $(T_b)_{eff} = \left( \frac{1}{\frac{1}{T_b} + \frac{h_{aq}}{3k_{aq}}} \right) \dots\dots\dots (C-12e)$

and:  $T_b = \left( \frac{k_b}{h_b} \right) \dots\dots\dots (C-12f)$

$$p_{aqD} = 2\pi \left( \frac{k_{fb} h_{fb}}{\mu_{fb}} + \frac{k_{aq} h_{aq}}{\mu_{aq}} \right) \frac{p_i - p_{aq}}{qB} \dots\dots\dots (C-12g)$$

$$p_{fD} = 2\pi \left( \frac{k_{fb} h_{fb}}{\mu_{fb}} + \frac{k_{aq} h_{aq}}{\mu_{aq}} \right) \frac{p_i - p_f}{qB} \dots\dots\dots (C-12h)$$

Then the final form of the dimensionless governing equations is:

$$\text{Fracture:} \quad \kappa_{fb} \nabla^2 p_{fD} = \omega_{aq} \frac{\partial p_{fD}}{\partial t_D} - \lambda_{aq} \{p_{aqD} - p_{fD}\} \quad \dots\dots\dots (\text{C-13a})$$

$$\text{Matrix (Aquifer):} \quad 0 = (1 - \omega_{aq}) \frac{\partial p_{aqD}}{\partial t_D} + \lambda_{aq} \{p_{aqD} - p_{fD}\} \quad \dots\dots\dots (\text{C-13b})$$

Applying the initial condition of aquifer to the Laplace transform equations results in:

$$\text{Fracture:} \quad \kappa_{fb} \frac{\partial^2 \overline{p_{fD}}}{\partial x_D^2} = \omega_{aq} s \overline{p_{fD}} - \lambda_{aq} \{ \overline{p_{aqD}} - \overline{p_{fD}} \} \quad \dots\dots (\text{C-14a})$$

$$\text{Matrix (Aquifer):} \quad 0 = (1 - \omega_{aq}) s \overline{p_{aqD}} + \lambda_{aq} \{ \overline{p_{aqD}} - \overline{p_{fD}} \} \quad \dots\dots (\text{C-14b})$$

Solving eqn.(C-14b) for  $\overline{p_{aqD}}$ :

$$\overline{p_{aqD}} = \frac{\lambda_{aq}}{(1 - \omega_{aq})s + \lambda_{aq}} \overline{p_{fD}} \quad \dots\dots\dots (\text{C-15})$$

Substituting this in eqn.(C-14a) we have:

$$\begin{aligned} \frac{\partial^2 \overline{p_{fD}}}{\partial x_D^2} &= \left(\frac{\omega_{aq}}{\kappa_{fb}}\right) s \overline{p_{fD}} - \left(\frac{\lambda_{aq}}{\kappa_{fb}}\right) \overline{p_{fD}} \left\{ \frac{\lambda_{aq} - (1 - \omega_{aq})s - \lambda_{aq}}{(1 - \omega_{aq})s + \lambda_{aq}} \right\} \\ &= \left(\frac{1}{\kappa_{fb}}\right) \left[ \omega_{aq} + \left\{ \frac{\lambda_{aq}(1 - \omega_{aq})s}{(1 - \omega_{aq})s + \lambda_{aq}} \right\} \right] s \overline{p_{fD}} \\ &= \left(\frac{1}{\kappa_{fb}}\right) \left[ \frac{\omega_{aq}(1 - \omega_{aq})s + \lambda_{aq}}{(1 - \omega_{aq})s + \lambda_{aq}} \right] s \overline{p_{fD}} \\ \frac{\partial^2 \overline{p_{fD}}}{\partial x_D^2} - sf(s) \overline{p_{fD}} &= 0 \dots\dots\dots (C-16) \end{aligned}$$

Where,

$$f(s) = \frac{\omega_{aq}(1 - \omega_{aq})s + \lambda_{aq}}{\kappa_{fb}[(1 - \omega_{aq})s + \lambda_{aq}]} \dots\dots\dots (C-17)$$

If both the matrix (aquifer) and the fracture (reservoir) have the same fluid then  $\kappa_{fb} = 1$ . Eqn.(C-16) is a homogeneous partial differential equation which is the same as eqn.(A-17). Refer to Appendix A for the rest of the derivation.

APPENDIX D: TRANSIENT AQUIFER DUAL POROSITY MODEL –  
 FORMULATION AND LAPLACE DOMAIN SOLUTION (LINEAR EQUIVALENT  
 BOURDET MODEL)

The governing differential equation for linear fluid flow in matrix and fracture is given by:

Fracture: 
$$\left(\frac{kh}{\mu}\right)_f \nabla^2 p_f = \varphi_{fb} c_f h_f \frac{\partial p_f}{\partial t} - \left(\frac{k_a}{\mu_a h_a}\right) \frac{\partial p_a}{\partial z} \Big|_{z=h_a} \dots\dots\dots (D-1a)$$

Matrix (Aquifer): 
$$\left(\frac{kh}{\mu}\right)_a \nabla^2 p_a = \varphi_a c_a \frac{\partial p_a}{\partial t} \dots\dots\dots (D-1b)$$

The second term in eqn.(D-1a) is referred to as the source term,  $\sigma_a$ . Here all properties need to be put as bulk properties:

$$\left(\frac{kh}{\mu}\right)_{aq} = \frac{k_a h_a}{\mu_a} \left(\frac{V_a}{V_{f+a}}\right) = \left(\frac{\frac{k_{aq} h_{aq}}{\mu_{aq}}}{\frac{k_{fb} h_{fb}}{\mu_{fb}} + \frac{k_{aq} h_{aq}}{\mu_{aq}}}\right) \dots\dots\dots (D-2a)$$

$$\left(\frac{kh}{\mu}\right)_{fb} = \frac{k_f h_f}{\mu_f} \left(\frac{V_f}{V_{f+a}}\right) = \left(\frac{\frac{k_{fb} h_{fb}}{\mu_{fb}}}{\frac{k_{fb} h_{fb}}{\mu_{fb}} + \frac{k_{aq} h_{aq}}{\mu_{aq}}}\right) \dots\dots\dots (D-2b)$$

$$(\varphi h)_{aq} = \left(\frac{V_{aq}}{V_{f+aq}}\right) = \left(\frac{\varphi_{aq} h_{aq}}{\varphi_{fb} h_{fb} + \varphi_{aq} h_{aq}}\right) \dots\dots\dots (D-2c)$$

$$(\varphi h)_{fb} = \left(\frac{V_f}{V_{f+aq}}\right) = \left(\frac{\varphi_{rf} h_{rf}}{\varphi_{fb} h_{fb} + \varphi_{aq} h_{aq}}\right) \dots\dots\dots (D-2d)$$

In terms of bulk properties the governing equations can be recast into:

$$\begin{aligned} \text{Fracture: } \left( \frac{k_{fb} h_{fb}}{\mu_{fb}} + \frac{k_{aq} h_{aq}}{\mu_{aq}} \right) \left( \frac{kh}{\mu} \right)_{fb} \nabla^2 p_{fb} &= (\varphi_{fb} h_{fb} + \varphi_{aq} h_{aq}) (\varphi h)_{fb} c_f \frac{\partial p_{fb}}{\partial t} - \\ &\left( \frac{k_{fb} h_{fb}}{\mu_{fb}} + \frac{k_{aq} h_{aq}}{\mu_{aq}} \right) \left( \frac{kh}{\mu} \right)_{aq} \left( \frac{1}{h_a^2} \right) \frac{\partial p_a}{\partial z} \Big|_{z=h_a} \dots\dots (D-3a) \end{aligned}$$

$$\begin{aligned} \text{Matrix (Aquifer): } \left( \frac{k_{fb} h_{fb}}{\mu_{fb}} + \frac{k_{aq} h_{aq}}{\mu_{aq}} \right) \left( \frac{kh}{\mu} \right)_{aq} \nabla^2 p_a &= (\varphi_{fb} h_{fb} + \varphi_{aq} h_{aq}) \times \\ &(\varphi h)_{aq} c_a \frac{\partial p_{aq}}{\partial t} \dots\dots\dots (D-3b) \end{aligned}$$

For an aquifer block, the initial and boundary conditions are:

$$\text{Initial Condition: } p_{aq}(z, t = 0) = p_i \dots\dots\dots (D-4a)$$

$$\text{Inner Boundary Condition: } \frac{\partial p_{aq}}{\partial z} \Big|_{z=0} = 0 \quad \text{for all } t \quad \dots\dots\dots (D-4b)$$

$$\text{Outer Boundary Condition: } p_{aq} \Big|_{z=h_{aq}} = p_f \quad \text{for all } t \quad \dots\dots\dots (D-4c)$$

For a fracture block, the initial and boundary conditions are:

$$\text{Initial Condition: } p_f(x, t = 0) = p_i \dots\dots\dots (D-5a)$$

$$\text{Inner Boundary Condition: } q = - \left( \frac{k_f A_{cw}}{\mu} \right) \frac{\partial p_f}{\partial x} \Big|_{x=0} \quad \text{for all } t \text{ and const. rate ..} (D-5b)$$

$$\text{Outer Boundary Condition } \frac{\partial p_f}{\partial x} \Big|_{x=x_e} = 0 \quad \text{for all } t \quad \dots\dots\dots (D-5c)$$



If we assume  $x$  is the linear dimension and define dimensionless variables as:

$$x_D = \frac{x}{\sqrt{A_{cw}}} \quad \text{for all fracture} \quad \dots\dots\dots (D-6a)$$

$$z_D = \frac{z}{h_{aq}} \quad \text{for all aquifer} \quad \dots\dots\dots (D-6b)$$

$$p_{jD} = \frac{p_i - p}{p_{ch}} = \frac{2\pi}{\alpha_{1qB}} \left( \frac{k_{fb} h_{fb}}{\mu_{fb}} + \frac{k_{aq} h_{aq}}{\mu_{aq}} \right) (p_i - p_j) \Big|_{j=fb \text{ or } aq} \dots\dots\dots (D-6c)$$

The derivatives of the above entities will be:

$$\partial(x_D \sqrt{A_{cw}}) = \partial x \quad \partial(x_D \sqrt{A_{cw}}) \{ \partial(x_D \sqrt{A_{cw}}) \} = \partial^2 x \quad \dots\dots\dots (D-7a)$$

$$\partial(z_D h_{aq}) = \partial z \quad \partial(z_D h_{aq}) \{ \partial(z_D h_{aq}) \} = \partial^2 z \quad \dots\dots\dots (D-7b)$$

$$\partial(p_D p_{ch} - p_i) = p_{ch} \partial p_D = -\partial p \quad p_{ch} \partial^2 p_D = \partial^2 p \quad \dots\dots\dots (D-7c)$$

Substituting  $x_D$  in eqn.(D-1a) and eqn.(D-1b), we have:

$$\begin{aligned} \text{Fracture: } \left( \frac{k_{fb} h_{fb}}{\mu_{fb}} + \frac{k_{aq} h_{aq}}{\mu_{aq}} \right) \left( \frac{kh}{\mu} \right)_{fb} \frac{\partial^2 p_f}{\partial x_D^2} &= (\varphi_{fb} h_{fb} + \varphi_{aq} h_{aq}) (\varphi h)_{fb} c_f A_{cw} \frac{\partial p_f}{\partial t} - \\ &\quad \left( \frac{k_{fb} h_{fb}}{\mu_{fb}} + \frac{k_{aq} h_{aq}}{\mu_{aq}} \right) \left( \frac{kh}{\mu} \right)_{aq} \left( \frac{1}{h_a^2} \right) \left( \frac{A_{cw}}{h_a} \right) \frac{\partial p_a}{\partial z} \Big|_{z=h_a} \end{aligned}$$

$$\begin{aligned} \text{Matrix (Aquifer): } \left( \frac{k_{fb} h_{fb}}{\mu_{fb}} + \frac{k_{aq} h_{aq}}{\mu_{aq}} \right) \left( \frac{kh}{\mu} \right)_{aq} \frac{\partial^2 p_{aq}}{\partial z_D^2} &= (\varphi_{fb} h_{fb} + \varphi_{aq} h_{aq}) \times \\ &\quad (\varphi h)_{aq} c_{aq} (h_a^2) \frac{\partial p_{aq}}{\partial t} \end{aligned}$$

Substituting  $p_D$  in eqn.(D-1a) and eqn.(D-1b), we have:

$$\text{Fracture: } \left( \frac{k_{fb} h_{fb}}{\mu_{fb}} + \frac{k_{aq} h_{aq}}{\mu_{aq}} \right) \left( \frac{kh}{\mu} \right)_{fb} p_{ch} \frac{\partial^2 p_{fD}}{\partial x_D^2} = (\varphi_{fb} h_{fb} + \varphi_{aq} h_{aq}) (\varphi h)_{fb} \times$$

$$c_f A_{cw} \frac{\partial(p_{fD} p_{ch} - p_i)}{\partial t} - \left( \frac{k_{fb} h_{fb}}{\mu_{fb}} + \frac{k_{aq} h_{aq}}{\mu_{aq}} \right) \left( \frac{kh}{\mu} \right)_{aq} \left( \frac{1}{h_a^2} \right) \left( \frac{A_{cw}}{h_a} \right) \frac{\partial(p_{aqD} p_{ch} - p_i)}{\partial z} \Big|_{z=h_a}$$

$$\text{Matrix (Aquifer): } \left( \frac{k_{fb} h_{fb}}{\mu_{fb}} + \frac{k_{aq} h_{aq}}{\mu_{aq}} \right) \left( \frac{kh}{\mu} \right)_{aq} \frac{\partial^2 p_{aqD}}{\partial z_D^2} = (\varphi_{fb} h_{fb} + \varphi_{aq} h_{aq}) \times$$

$$(\varphi h)_{aq} c_{aq} (h_a^2) \frac{\partial(p_{aqD} p_{ch} - p_i)}{\partial t}$$

On cancellation of common terms results in:

$$\text{Fracture: } \left( \frac{kh}{\mu} \right)_{fb} \frac{\partial^2 p_{fD}}{\partial x_D^2} =$$

$$(\varphi h)_{fb} \frac{(\varphi_{fb} h_{fb} + \varphi_{aq} h_{aq}) c_f A_{cw}}{\left( \frac{k_{fb} h_{fb}}{\mu_{fb}} + \frac{k_{aq} h_{aq}}{\mu_{aq}} \right)} \times \frac{\partial p_{fD}}{\partial t} - \left( \frac{kh}{\mu} \right)_{aq} \left( \frac{A_{cw}}{h_a^3} \right) \frac{\partial p_{aqD}}{\partial z_D} \Big|_{z_D=1} \dots \dots \dots (\text{C-8a})$$

$$\text{Matrix (Aquifer): } \left( \frac{kh}{\mu} \right)_{fb} \frac{\partial^2 p_{fD}}{\partial z_D^2} = (\varphi h)_{aq} \frac{(\varphi_{fb} h_{fb} + \varphi_{aq} h_{aq}) c_{aq} (h_a^2)}{\left( \frac{k_{fb} h_{fb}}{\mu_{fb}} + \frac{k_{aq} h_{aq}}{\mu_{aq}} \right)} \frac{\partial p_{aqD}}{\partial t} \dots \dots \dots (\text{C-8b})$$

Reapplying eqn.(D-2) and putting in additional terms to the above we get:

$$\text{Fracture: } \left( \frac{\frac{k_{fb} h_{fb}}{\mu_{fb}}}{\frac{k_{fb} h_{fb}}{\mu_{fb}} + \frac{k_{aq} h_{aq}}{\mu_{aq}}} \right) \frac{\partial^2 p_{fD}}{\partial x_D^2} = (\varphi h)_{fb} \frac{(\varphi_{fb} h_{fb} + \varphi_{aq} h_{aq}) c_f A_{cw}}{\left( \frac{k_{fb} h_{fb}}{\mu_{fb}} + \frac{k_{aq} h_{aq}}{\mu_{aq}} \right)} \frac{\partial p_{fD}}{\partial t} -$$

$$\left( \frac{\frac{k_{aq} h_{aq}}{\mu_{aq}}}{\frac{k_{fb} h_{fb}}{\mu_{fb}} + \frac{k_{aq} h_{aq}}{\mu_{aq}}} \right) \left( \frac{A_{cw}}{h_a^3} \right) \frac{\partial p_{aqD}}{\partial z_D} \Big|_{z_D=1}$$

$$\text{Matrix (Aquifer): } \left( \frac{\frac{k_{aq} h_{aq}}{\mu_{aq}}}{\frac{k_{fb} h_{fb}}{\mu_{fb}} + \frac{k_{aq} h_{aq}}{\mu_{aq}}} \right) \frac{\partial^2 p_{aqD}}{\partial z_D^2} = (\varphi h)_{aq} \frac{(\varphi_{fb} h_{fb} + \varphi_{aq} h_{aq}) c_{aq} (h_a^2)}{\left( \frac{k_{fb} h_{fb}}{\mu_{fb}} + \frac{k_{aq} h_{aq}}{\mu_{aq}} \right)} \frac{\partial p_{aqD}}{\partial t}$$

The above equations simplify to:

Fracture:

$$\left( \frac{\frac{k_{fb} h_{fb}}{\mu_{fb}}}{\frac{k_{fb} h_{fb}}{\mu_{fb}} + \frac{k_{aq} h_{aq}}{\mu_{aq}}} \right) \frac{\partial^2 p_{fD}}{\partial x_D^2} =$$

$$(\varphi h)_{fb} \frac{(\varphi_{fb} h_{fb} + \varphi_{aq} h_{aq}) c_f A_{cw}}{\left( \frac{k_{fb} h_{fb}}{\mu_{fb}} + \frac{k_{aq} h_{aq}}{\mu_{aq}} \right)} \frac{\partial p_{fD}}{\partial t} -$$

$$\left( \frac{\frac{k_{aq} h_{aq}}{\mu_{aq}}}{\frac{k_{fb} h_{fb}}{\mu_{fb}} + \frac{k_{aq} h_{aq}}{\mu_{aq}}} \right) \left( \frac{A_{cw}}{h_a^3} \right) \left( \frac{\frac{k_{fb} h_{fb}}{\mu_{fb}}}{\frac{k_{fb} h_{fb}}{\mu_{fb}} + \frac{k_{aq} h_{aq}}{\mu_{aq}}} \right) \frac{\partial p_{aqD}}{\partial z_D} \Big|_{z_D=1} \dots \dots \dots (D-9a)$$

Matrix (Aquifer):

$$\left( \frac{\frac{k_{aq} h_{aq}}{\mu_{aq}}}{\frac{k_{fb} h_{fb}}{\mu_{fb}} + \frac{k_{aq} h_{aq}}{\mu_{aq}}} \right) \frac{\partial^2 p_{aqD}}{\partial z_D^2} =$$

$$(\varphi h)_{aq} \frac{(\varphi_{fb} h_{fb} + \varphi_{aq} h_{aq}) c_{aq} (h_a^2)}{\left( \frac{k_{fb} h_{fb}}{\mu_{fb}} + \frac{k_{aq} h_{aq}}{\mu_{aq}} \right)} \left( \frac{A_{cw}}{A_{cw}} \right) \left( \frac{\frac{k_{fb}}{\mu_{fb}}}{\frac{k_{fb} h_{fb}}{\mu_{fb}} + \frac{k_{aq} h_{aq}}{\mu_{aq}}} \right) \left( \frac{\frac{k_{aq}}{\mu_{fb}}}{\frac{k_{fb} h_{fb}}{\mu_{fb}} + \frac{k_{aq} h_{aq}}{\mu_{aq}}} \right) \frac{\partial p_{aqD}}{\partial t} \dots\dots (D-9b)$$

We also have the following:

$$\omega_{aq} = \frac{\varphi_{fb} c_f}{(\varphi c_t)_{aq+fb}} \dots\dots\dots (D-10)$$

Substituting  $\omega$  in eqn.(C-9a) and eqn.(C-9b) and assuming compressibility is constant, we have:

Fracture: 
$$\kappa_{fb} \frac{\partial^2 p_{fD}}{\partial x_D^2} = \omega_{aq} \frac{\partial p_{fD}}{\partial t_D} - \left( \frac{\lambda_{aq}}{12} \right) \frac{\partial p_{aqD}}{\partial z_D} \Big|_{z_D=1}$$

Matrix (Aquifer): 
$$(1 - \kappa_{fb}) \frac{\partial^2 p_{aqD}}{\partial z_D^2} = \frac{12(1-\omega_{aq})}{\lambda_{aq}} \frac{\partial p_{aqD}}{\partial t_D}$$

Here expression for dimensionless time and dimensionless interporosity flow parameter are as:

$$t_D = \frac{\left(\frac{k_{fb} h_{fb}}{\mu_{fb}} + \frac{k_{aq} h_{aq}}{\mu_{aq}}\right) t}{(\varphi_{fb} h_{fb} + \varphi_{aq} h_{aq}) c_f A_{cw}} \dots\dots\dots (D-11)$$

$$\lambda_{aq} = \frac{12}{h_m^2} A_{cw} \frac{\left(\frac{\frac{k_{aq}}{\mu_{aq}}}{\frac{k_{fb} h_{fb}}{\mu_{fb}} + \frac{k_{aq} h_{aq}}{\mu_{aq}}}\right)}{\left(\frac{\frac{k_{fb}}{\mu_{fb}}}{\frac{k_{fb} h_{fb}}{\mu_{fb}} + \frac{k_{aq} h_{aq}}{\mu_{aq}}}\right)} \dots\dots\dots (D-12)$$

Then the final form of the dimensionless governing equations is:

Fracture:  $\kappa_{fb} \nabla^2 p_{fD} = \omega_{aq} \frac{\partial p_{fD}}{\partial t_D} - \left(\frac{\lambda_{aq}}{12}\right) \frac{\partial p_{aqD}}{\partial z_D} \Big|_{z_D=1} \dots (D-13a)$

Matrix (Aquifer):  $(1 - \kappa_{fb}) \nabla^2 p_{aqD} = \frac{12(1-\omega)}{\lambda_{aq}} \frac{\partial p_{aqD}}{\partial t_D} \dots\dots\dots (D-13b)$

Taking Laplace transform of the above equations:

Fracture:  $\kappa_{fb} \frac{\partial^2 \overline{p_{fD}}}{\partial x_D^2} = \omega_{aq} \{s \overline{p_{fD}} - \overline{p_{fD}}(x_D, 0)\} - \left(\frac{\lambda_{aq}}{12}\right) \frac{\partial \overline{p_{aqD}}}{\partial z_D} \Big|_{z_D=1}$

Matrix (Aquifer):  $(1 - \kappa_{fb}) \frac{\partial^2 \overline{p_{aqD}}}{\partial x_D^2} = \frac{12(1-\omega_{aq})}{\lambda_{aq}} \{s \overline{p_{aqD}} - \overline{p_{aqD}}(x_D, 0)\}$

Matrix (Aquifer) Equation

Let us find the solution of eqn.(D-13b) for  $\overline{p_{mD}}$  first. For a matrix block and in Laplace domain, the initial and boundary conditions are:

Initial Condition:  $\overline{p_{aqD}}(z_D = 1, s \rightarrow \infty) = 0$ ..... (D-14a)

Inner Boundary Condition:  $\left. \frac{\partial \overline{p_{aqD}}}{\partial z_D} \right|_{z_D=0} = 0$  ..... (D-14b)

Outer Boundary Condition:  $\overline{p_{aqD}}|_{z_D=1} = \overline{p_{fD}}$  ..... (D-14c)

Applying initial condition, we have:

$$\frac{\partial^2 \overline{p_{aqD}}}{\partial z_D^2} - \frac{12(1-\omega_{aq})}{\lambda_{aq}} s \overline{p_{aqD}} = 0 \text{ ..... (D-15)}$$

The above is a homogeneous partial differential equation with the following general solution:

$$\overline{p_{aqD}} = A \cosh\left(z_D \sqrt{s \frac{12(1-\omega_{aq})}{\lambda_{aq}}}\right) + B \sinh\left(z_D \sqrt{s \frac{12(1-\omega_{aq})}{\lambda_{aq}}}\right) \text{ ..... (D-16)}$$

Differentiating with respect to  $z_D$  and using the inner boundary condition, we have:

$$\left. \frac{d\bar{p}_{aqD}}{dz_D} \right|_{z_D=0} = 0 = \sqrt{s \frac{12(1-\omega_{aq})}{\lambda_{aq}}} A \sinh \left( z_D \sqrt{s \frac{12(1-\omega_{aq})}{\lambda_{aq}}} \right) + \sqrt{s \frac{12(1-\omega_{aq})}{\lambda_{aq}}} B \cosh \left( z_D \sqrt{s \frac{12(1-\omega_{aq})}{\lambda_{aq}}} \right)$$

Since  $\sinh z_D|_{z_D=0} = 0$ , implies:

$$B = 0 \dots\dots\dots (D-17)$$

Using outer boundary condition and substituting eqn.(D-14c) in eqn.(D-16) we have:

$$\bar{p}_{fD} = A \cosh \left( z_D \sqrt{s \frac{12(1-\omega_{aq})}{\lambda_{aq}}} \right) \Big|_{z_D=1}$$

$$A = \frac{\bar{p}_{fD}}{\cosh \left( \sqrt{s \frac{12(1-\omega_{aq})}{\lambda_{aq}}} \right)} \dots\dots\dots (D-18)$$

Hence the particular solution for constant rate of eqn.(D-15) in Laplace domain is:

$$\bar{p}_{aqD} = \frac{\bar{p}_{fD}}{\cosh \left( \sqrt{s \frac{12(1-\omega_{aq})}{\lambda_{aq}}} \right)} \cosh \left( z_D \sqrt{s \frac{12(1-\omega_{aq})}{\lambda_{aq}}} \right) \dots\dots (D-19)$$

Fracture Equation

To find the solution of fracture eqn.(D-13a) for  $\overline{p_{fD}}$ , we need to convert the initial and boundary conditions in eqn.(D-4) to dimensionless form in Laplace domain as:

Initial Condition:  $\overline{p_{fD}}(x_D = 1, s \rightarrow \infty) = 0$  ..... (D-20a)

Inner Boundary Condition:  $\frac{\partial \overline{p_{fD}}}{\partial x_D} \Big|_{x_D=0} = -\frac{2\pi}{s}$  ..... (D-20b)

Outer Boundary Condition  $\frac{\partial \overline{p_{fD}}}{\partial x_D} \Big|_{x_D=x_{eD}} = 0$  ..... (D-20c)

Applying initial condition, we have:

$$\frac{\partial^2 \overline{p_{fD}}}{\partial x_D^2} = \omega_{aq} s \overline{p_{fD}} - \left(\frac{\lambda_{aq}}{12}\right) \frac{\partial \overline{p_{aqD}}}{\partial z_D} \Big|_{z_D=1} \dots\dots (D-21)$$

But from eqn.(D-19) we have

$$\frac{\partial \overline{p_{mD}}}{\partial z_D} \Big|_{z_D=1} = \frac{\sqrt{s \frac{12(1-\omega_{aq})}{\lambda_{aq}}}}{\cosh\left(\sqrt{s \frac{12(1-\omega_{aq})}{\lambda_{aq}}}\right)} \sinh\left(\sqrt{s \frac{12(1-\omega_{aq})}{\lambda_{aq}}}\right) \overline{p_{fD}} \dots (D-22)$$



This derivative will change sign when expressed in terms of  $\overline{p_{fD}}$ , which inserted into eqn.(D-21) gives:

$$\begin{aligned} \frac{\partial^2 \overline{p_{fD}}}{\partial x_D^2} &= \omega_{aq} s \overline{p_{fD}} + \frac{\lambda_{aq}}{12} \left\{ \frac{\sqrt{s \frac{12(1-\omega_{aq})}{\lambda_{aq}}}}{\cosh\left(\sqrt{s \frac{12(1-\omega_{aq})}{\lambda_{aq}}}\right)} \sinh\left(\sqrt{s \frac{12(1-\omega_{aq})}{\lambda_{aq}}}\right) \overline{p_{fD}} \right\} \\ &= s \overline{p_{fD}} \left\{ \omega_{aq} + \frac{\lambda_{aq}}{12 s} \sqrt{s \frac{12(1-\omega_{aq})}{\lambda_{aq}}} \tanh\left(\sqrt{s \frac{12(1-\omega_{aq})}{\lambda_{aq}}}\right) \right\} \dots\dots\dots (D-23) \end{aligned}$$

This is of the form:

$$\frac{\partial^2 \overline{p_{fD}}}{\partial x_D^2} - sf(s)\overline{p_{fD}} = 0 \dots\dots\dots (D-24)$$

Where,

$$f(s) = \omega_{aq} + \frac{\lambda_{aq}}{12 s} \sqrt{s \frac{12(1-\omega_{aq})}{\lambda_{aq}}} \tanh\left(\sqrt{s \frac{12(1-\omega_{aq})}{\lambda_{aq}}}\right) .. (D-25)$$

Again, eqn.(D-24) is a homogeneous partial differential equation which is the same as eqn.(A-17). Refer to Appendix A for the rest of the derivation.

APPENDIX E: FULL PSEUDOSTEADY STATE MATRIX AND AQUIFER  
 FRACTURED DUAL PERMEABILITY DUAL MOBILITY MODEL –  
 FORMULATION AND LAPLACE DOMAIN SOLUTION

The governing differential equation for linear fluid flow in limited aquifer (matrix block) and the fractured reservoir (reservoir fracture block and reservoir matrix block) is given by:

$$\text{Fracture:} \quad \left(\frac{kh}{\mu}\right)_f \nabla^2 p_f = \varphi_f c_f h_f \frac{\partial p_f}{\partial t} - \underline{\alpha} \frac{k_a}{\mu_a} (p_a - p_f) - \alpha \left(\frac{k}{\mu}\right)_m (p_m - p_f) \dots (E-1a)$$

$$\text{Matrix (Aquifer):} \quad \left(\frac{kh}{\mu}\right)_{aq} \nabla^2 p_{aq} = \varphi_a c_a h_a \frac{\partial p_a}{\partial t} + \underline{\alpha} \left(\frac{k}{\mu}\right)_a (p_a - p_f) \dots (E-1b)$$

$$\text{Matrix (Reservoir):} \quad \left(\frac{kh}{\mu}\right)_m \nabla^2 p_m = \varphi_m c_m h_m \frac{\partial p_m}{\partial t} + \alpha \left(\frac{k}{\mu}\right)_m (p_m - p_f) \dots (E-1c)$$

Since the aquifer is limited, the aquifer height is related to the linear dimension of reservoir ( $y$  is lateral dimension of fractured reservoir and  $y_{aq}$  is vertical dimension of aquifer) by:

$$y_{aq} = h_{aq} = \varepsilon y \dots (E-1d)$$

The second and third terms in eqn.(E-1a) is referred to as the source terms,  $\sigma_a$  and  $\sigma_m$ . During pseudosteady state the pressure (average pressure) change inside the matrix is

constant. This means that LHS of eqn.(E-1b) and eqn.(E-1c) are both zero (to be done later). Also, all properties need to be put as bulk properties:

Aquifer:

$$\left(\frac{kh}{\mu}\right)_{aq} = \frac{k_a h_a}{\mu_a} \left(\frac{V_a}{V_{f+a}}\right) = \left(\frac{\frac{k_{aq} h_{aq}}{\mu_{aq}}}{\frac{k_{fb} h_{fb}}{\mu_{fb}} + \frac{k_{aq} h_{aq}}{\mu_{aq}}}\right) \dots\dots\dots(E-2a)$$

$$\left(\frac{kh}{\mu}\right)_f = \frac{k_f h_f}{\mu_f} \left(\frac{V_f}{V_{f+a}}\right) = \left(\frac{\frac{k_{fb} h_{fb}}{\mu_{fb}}}{\frac{k_{fb} h_{fb}}{\mu_{fb}} + \frac{k_{aq} h_{aq}}{\mu_{aq}}}\right) \dots\dots\dots(E-2b)$$

$$(\varphi h)_{aq} = \left(\frac{V_{aq}}{V_{f+aq}}\right) = \left(\frac{\varphi_{aq} h_{aq}}{\varphi_{fb} h_{fb} + \varphi_{aq} h_{aq}}\right) \dots\dots\dots(E-2c)$$

$$(\varphi h)_f = \left(\frac{V_f}{V_{f+aq}}\right) = \left(\frac{\varphi_{fb} h_{fb}}{\varphi_{fb} h_{fb} + \varphi_{aq} h_{aq}}\right) \dots\dots\dots(E-2d)$$

Reservoir:

$$\left(\frac{kh}{\mu}\right)_{mb} = \frac{k_m}{\mu_m} \left(\frac{V_m}{V_{f+m}}\right) = \left(\frac{\frac{k_{mb} h_{mb}}{\mu_{mb}}}{\frac{k_{fb} h_{fb}}{\mu_{fb}} + \frac{k_{mb} h_{mb}}{\mu_{mb}}}\right) \dots\dots\dots(E-2e)$$

$$\left(\frac{kh}{\mu}\right)_{fb} = \frac{k_f}{\mu_f} \left(\frac{V_f}{V_{f+m}}\right) = \left(\frac{\frac{k_{fb} h_{fb}}{\mu_{fb}}}{\frac{k_{fb} h_{fb}}{\mu_{fb}} + \frac{k_{mb} h_{mb}}{\mu_{mb}}}\right) \dots\dots\dots(E-2f)$$

$$(\varphi h)_{mb} = \left(\frac{V_m}{V_{f+m}}\right) = \left(\frac{\varphi_{mb} h_{mb}}{\varphi_{fb} h_{fb} + \varphi_{mb} h_{mb}}\right) \dots\dots\dots(E-2g)$$

$$(\varphi h)_{fb} = \left( \frac{V_f}{V_{f+m}} \right) = \left( \frac{\varphi_{fb} h_{fb}}{\varphi_{fb} h_{fb} + \varphi_{mb} h_{mb}} \right) \dots\dots\dots (E-2h)$$

Similarly, the aquifer and matrix fracture bulk source terms are,  $\sigma_{aq}$ , and  $\sigma_{mf}$ , is expressed as:

$$\begin{aligned} \sigma_{aq} &= \sigma_a \left( \frac{V_a}{V_{f+a}} \right) = \underline{\alpha} \frac{k_a}{\mu_a} \left( \frac{V_a}{V_{f+a}} \right) (p_{aq} - p_{fb}) = \\ &\underline{\alpha} \left( \frac{k_{fb} h_{fb}}{\mu_{fb}} + \frac{k_{aq} h_{aq}}{\mu_{aq}} \right) \times \left( \frac{kh}{\mu} \right)_{aq} \left( \frac{1}{h} \right)_{aq} (p_{aq} - p_{fb}) \dots\dots\dots (E-3a) \end{aligned}$$

$$\begin{aligned} \sigma_{mf} &= \sigma_m \left( \frac{V_m}{V_{f+m}} \right) = \alpha \frac{k_m}{\mu} \left( \frac{V_m}{V_{f+m}} \right) (p_{mb} - p_{fb}) = \alpha \left( \frac{k_{fb} h_{fb}}{\mu_{fb}} + \frac{k_{mb} h_{mb}}{\mu_{mb}} \right) \times \\ &\left( \frac{kh}{\mu} \right)_{mb} \left( \frac{1}{h} \right)_{mb} (p_{mb} - p_{fb}) \dots\dots (E-3b) \end{aligned}$$

where  $\underline{\alpha}$ , is the shape function:

$$\underline{\alpha} = \frac{(T_b)_{eff}}{k_{aq}} \dots\dots\dots (E-4a)$$

And,

$$\lambda_{aqf} = \underline{\alpha} \left( \frac{k_{aq}}{k_{rf}} \right) A_{cw} = \left( \frac{(T_b)_{eff}}{k_{rf}} \right) A_{cw} \dots\dots\dots (E-4b)$$

$$(T_b)_{eff} = \frac{1}{\frac{1}{T_b} + \frac{h_{aq}}{3k_{aq}}} \dots\dots\dots (E-4c)$$

$$T_b = \frac{k_b}{h_b} \dots\dots\dots (E-4d)$$

And where  $\alpha$ , is the shape function:

$$\alpha = \frac{4n(n+2)}{h_m^2} \dots\dots\dots (E-4e)$$

In terms of bulk properties the governing equations can be recast into:

Fracture:

$$\left(\frac{k_{fb} h_{fb}}{\mu_{fb}} + \frac{k_{aq} h_{aq}}{\mu_{aq}}\right) \left(\frac{kh}{\mu}\right)_{fb} \frac{\partial^2 p_{fb}}{\partial y^2} =$$

$$(\varphi_{fb} h_{fb} + \varphi_{aq} h_{aq})(\varphi h)_{fb} c_f \frac{\partial p_{fb}}{\partial t} - \underline{\alpha} \left(\frac{k_{fb} h_{fb}}{\mu_{fb}} + \frac{k_{aq} h_{aq}}{\mu_{aq}}\right) \left(\frac{kh}{\mu}\right)_{aq} \times$$

$$\left(\frac{1}{h}\right)_{aq} (p_{aq} - p_{fb}) - \alpha \left(\frac{k_{fb} h_{fb}}{\mu_{fb}} + \frac{k_{mb} h_{mb}}{\mu_{mb}}\right) \left(\frac{kh}{\mu}\right)_{mb} \left(\frac{1}{h}\right)_{mb} (p_{mb} - p_{fb}) \dots \dots \dots (E-5a)$$

Matrix (Aquifer):

$$\left(\frac{1}{\varepsilon^2}\right) \left(\frac{k_{fb} h_{fb}}{\mu_{fb}} + \frac{k_{aq} h_{aq}}{\mu_{aq}}\right) \left(\frac{kh}{\mu}\right)_{aq} \frac{\partial^2 p_{aq}}{\partial y^2} = (\varphi_{fb} h_{fb} + \varphi_{aq} h_{aq})(\varphi h)_{aq} c_a \frac{\partial p_{aq}}{\partial t} +$$

$$\underline{\alpha} \left(\frac{k_{fb} h_{fb}}{\mu_{fb}} + \frac{k_{aq} h_{aq}}{\mu_{aq}}\right) \left(\frac{kh}{\mu}\right)_{aq} \left(\frac{1}{h}\right)_{aq} (p_{aq} - p_{fb}) \dots \dots \dots (E-5b)$$

Matrix (Reservoir):

$$\left(\frac{k_{fb} h_{fb}}{\mu_{fb}} + \frac{k_{mb} h_{mb}}{\mu_{mb}}\right) \left(\frac{kh}{\mu}\right)_{mb} \frac{\partial^2 p_{mb}}{\partial z^2} = (\varphi_{fb} h_{fb} + \varphi_{mb} h_{mb})(\varphi h)_{mb} c_m \frac{\partial p_{mb}}{\partial t} +$$

$$\left(\frac{k_{fb} h_{fb}}{\mu_{fb}} + \frac{k_{mb} h_{mb}}{\mu_{mb}}\right) \left(\frac{kh}{\mu}\right)_{mb} \left(\frac{1}{h}\right)_{mb} (p_{mb} - p_{fb}) \dots \dots \dots (E-5c)$$

If we assume  $y$  is the overall linear dimension and define dimensionless variables as:

$$y_D = \frac{y}{\sqrt{A_{cw}}} \quad \text{for all fracture} \quad \dots\dots\dots(\text{E-6a})$$

$$\varepsilon y_D = \frac{\varepsilon y}{\sqrt{A_{cw}}} \quad \text{for all aquifer} \quad \dots\dots\dots (\text{E-6b})$$

$$z_D = \frac{z}{\sqrt{A_{cw}}} \quad \text{for all matrix} \quad \dots\dots\dots(\text{E-6c})$$

$$p_{jD} = \frac{p_i - p}{p_{ch}} = \frac{2\pi}{\alpha_1 q B} \left( \frac{k_{fb} h_{fb}}{\mu_{fb}} + \frac{k_{aq} h_{aq}}{\mu_{aq}} \right) (p_i - p_j) \Big|_{j=f \text{ or } aq} \quad \dots (\text{E-6d})$$

$$p_{jD} = \frac{p_i - p}{p_{ch}} = \frac{2\pi}{\alpha_1 q B} \left( \frac{k_{fb} h_{fb}}{\mu_{fb}} + \frac{k_{mb} h_{mb}}{\mu_{mb}} \right) (p_i - p_j) \Big|_{j=fb \text{ or } mb} \quad \dots (\text{E-6e})$$

The derivatives of the above entities will be:

$$\partial(y_D \sqrt{A_{cw}}) = \partial y \quad \partial(y_D \sqrt{A_{cw}}) \{ \partial(y_D \sqrt{A_{cw}}) \} = \partial^2 y \quad \dots\dots\dots(\text{E-7a})$$

$$\partial(z_D \sqrt{A_{cw}}) = \partial z \quad \partial(z_D \sqrt{A_{cw}}) \{ \partial(z_D \sqrt{A_{cw}}) \} = \partial^2 z \quad \dots\dots\dots (\text{E-7b})$$

$$\varepsilon \partial(y_D \sqrt{A_{cw}}) = \partial y \quad \varepsilon^2 \partial(y_D \sqrt{A_{cw}}) \{ \partial(y_D \sqrt{A_{cw}}) \} = \partial^2 y \quad \dots\dots(\text{E-7c})$$

$$\partial(p_D p_{ch} - p_i) = p_{ch} \partial p_D = -\partial p \quad p_{ch} \partial^2 p_D = \partial^2 p \quad \dots\dots\dots (\text{E-7d})$$

Solution of Matrix (Aquifer)

Substituting  $y_D$  in eqn.(E-5b), we have:

$$\left(\frac{1}{\varepsilon^2}\right) \left(\frac{k_{fb} h_{fb}}{\mu_{fb}} + \frac{k_{aq} h_{aq}}{\mu_{aq}}\right) \left(\frac{kh}{\mu}\right)_{aq} \frac{\partial^2 p_{aq}}{\partial y_D^2} = (\varphi_{fb} h_{fb} + \varphi_{aq} h_{aq})(\varphi h)_{aq} c_a A_{cw} \frac{\partial p_{aq}}{\partial t} +$$

$$\underline{\alpha} A_{cw} \left(\frac{k_{fb} h_{fb}}{\mu_{fb}} + \frac{k_{aq} h_{aq}}{\mu_{aq}}\right) \left(\frac{kh}{\mu}\right)_{aq} \left(\frac{1}{h}\right)_{aq} (p_{aq} - p_{fb})$$

Substituting  $p_D$  in above, we have:

$$\left(\frac{1}{\varepsilon^2}\right) \left(\frac{k_{fb} h_{fb}}{\mu_{fb}} + \frac{k_{aq} h_{aq}}{\mu_{aq}}\right) \left(\frac{kh}{\mu}\right)_{aq} p_{ch} \frac{\partial^2 (p_{aqD} p_{ch} - p_i)}{\partial y_D^2} =$$

$$(\varphi_{fb} h_{fb} + \varphi_{aq} h_{aq}) (\varphi h)_{aq} c_a A_{cw} \frac{\partial (p_{aqD} p_{ch} - p_i)}{\partial t} +$$

$$\underline{\alpha} A_{cw} \left(\frac{k_{fb} h_{fb}}{\mu_{fb}} + \frac{k_{aq} h_{aq}}{\mu_{aq}}\right) \left(\frac{kh}{\mu}\right)_{aq} \left(\frac{1}{h}\right)_{aq} \{(\partial p_{aqD} p_{ch} - p_i) - (p_{fD} p_{ch} - p_i)\}$$

On cancellation of common terms, results in:

$$\left(\frac{1}{\varepsilon^2}\right) \left(\frac{kh}{\mu}\right)_{aq} \frac{\partial^2 p_{aqD}}{\partial y_D^2} =$$

$$\frac{(\varphi_{fb} h_{fb} + \varphi_{aq} h_{aq})}{\left(\frac{k_{fb} h_{fb}}{\mu_{fb}} + \frac{k_{aq} h_{aq}}{\mu_{aq}}\right)} (\varphi h)_{aq} c_a A_{cw} \frac{\partial p_{aqD}}{\partial t} + \underline{\alpha} A_{cw} \left(\frac{kh}{\mu}\right)_{aq} \left(\frac{1}{h}\right)_{aq} (p_{aqD} - p_{fD}) \dots\dots (E-8)$$

Reapplying eqn.(E-2) to the above we get:

$$\begin{aligned} & \left(\frac{1}{\varepsilon^2}\right) \left( \frac{\frac{k_{aq} h_{aq}}{\mu_{aq}}}{\frac{k_{fb} h_{fb}}{\mu_{fb}} + \frac{k_{aq} h_{aq}}{\mu_{aq}}} \right) \frac{\partial^2 p_{aqD}}{\partial y_D^2} = \\ & (\varphi h)_{aq} \frac{(\varphi_{fb} h_{fb} + \varphi_{aq} h_{aq})}{\left(\frac{k_{fb} h_{fb}}{\mu_{fb}} + \frac{k_{aq} h_{aq}}{\mu_{aq}}\right)} c_a A_{cw} \frac{\partial p_{aqD}}{\partial t} + \\ & \underline{\alpha} A_{cw} \left( \frac{\frac{k_{aq} h_{aq}}{\mu_{aq}}}{\frac{k_{fb} h_{fb}}{\mu_{fb}} + \frac{k_{aq} h_{aq}}{\mu_{aq}}} \right) \left(\frac{1}{h}\right)_{aq} (p_{aqD} - p_{fD}) \dots\dots\dots (E-9) \end{aligned}$$

We also have the following:

$$\omega_{aq} = \frac{\varphi_{fb} c_f}{(\varphi c_t)_{aq+fb}} \dots\dots\dots (E-10)$$

Substituting  $\omega_{aq}$  in eqn.(E-9) and assuming compressibility is constant, we have:

$$\left(\frac{1}{\varepsilon^2}\right) (1 - \kappa_f) \frac{\partial^2 p_{aqD}}{\partial y_D^2} = (1 - \omega_{aq}) \frac{\partial p_{aqD}}{\partial t_D} + \lambda_{aq} (p_{aqD} - p_{fD}) \dots (E-11)$$

Dimensionless time and dimensionless interporosity flow parameter, are given by:

$$t_D = \frac{\left(\frac{k_{fb} h_{fb}}{\mu_{fb}} + \frac{k_{aq} h_{aq}}{\mu_{aq}}\right) t}{(\varphi_{fb} h_{fb} + \varphi_{aq} h_{aq}) c_f A_{cw}} \dots\dots\dots (E-12a)$$

$$\lambda_{aq} = \underline{\alpha} A_{cw} \left( \frac{\frac{k_{aq}}{\mu_{aq}}}{\frac{k_{fb} h_{fb}}{\mu_{fb}} + \frac{k_{aq} h_{aq}}{\mu_{aq}}} \right) \dots\dots\dots (E-12b)$$

$$\kappa_f = \left( \frac{\frac{k_{fb} h_{fb}}{\mu_{fb}}}{\frac{k_{fb} h_{fb}}{\mu_{fb}} + \frac{k_{aq} h_{aq}}{\mu_{aq}}} \right) \dots\dots\dots (E-12c)$$



Where: 
$$\underline{\alpha} = \frac{(T_b)_{eff}}{k_{aq}} \dots\dots\dots (E-12d)$$

Where: 
$$(T_b)_{eff} = \left( \frac{1}{\frac{1}{T_b} + \frac{h_{aq}}{3k_{aq}}} \right) \dots\dots\dots (E-12e)$$

and: 
$$T_b = \left( \frac{k_b}{h_b} \right) \dots\dots\dots (E-12f)$$

$$p_{aqD} = 2\pi \left( \frac{k_{fb} h_{fb}}{\mu_{fb}} + \frac{k_{aq} h_{aq}}{\mu_{aq}} \right) \frac{p_i - p_{aq}}{qB} \dots\dots (E-12g)$$

$$p_{fD} = 2\pi \left( \frac{k_{fb} h_{fb}}{\mu_{fb}} + \frac{k_{aq} h_{aq}}{\mu_{aq}} \right) \frac{p_i - p_f}{qB} \dots\dots (E-12h)$$

The final form of the above equation, since the LHS is zero, is:

$$0 = \varepsilon^2 \left( \frac{1-\omega_{aq}}{1-\kappa_f} \right) \frac{\partial p_{aqD}}{\partial t_D} + \varepsilon^2 \left( \frac{\lambda_{aq}}{1-\kappa_f} \right) (p_{aqD} - p_{fD}) \dots\dots\dots (E-13)$$

Applying the initial condition of aquifer to the Laplace transform equations results in:

$$0 = \varepsilon^2 \left( \frac{1-\omega_{aq}}{1-\kappa_f} \right) s \overline{p_{aqD}} + \varepsilon^2 \left( \frac{\lambda_{aq}}{1-\kappa_f} \right) (\overline{p_{aqD}} - \overline{p_{fD}}) \dots\dots\dots (E-14)$$

Solving eqn.(E-14) for  $\overline{p_{aqD}}$ :

$$\overline{p_{aqD}} = \frac{\lambda_{aq}}{(1-\omega_{aq})s + \lambda_{aq}} \overline{p_{fD}} \dots\dots\dots (E-15)$$

Solution of Matrix (Reservoir)

Substituting  $z_D$  in eqn.(E-5b), we have:

$$\left(\frac{k_{fb} h_{fb}}{\mu_{fb}} + \frac{k_{mb} h_{mb}}{\mu_{mb}}\right) \left(\frac{kh}{\mu}\right)_{mb} \frac{\partial^2 p_{mb}}{\partial z_D^2} = (\varphi_{fb} h_{fb} + \varphi_{mb} h_{mb})(\varphi h)_{mb} c_m A_{cw} \frac{\partial p_{mb}}{\partial t} +$$

$$\alpha A_{cw} \left(\frac{k_{fb} h_{fb}}{\mu_{fb}} + \frac{k_{mb} h_{mb}}{\mu_{mb}}\right) \left(\frac{kh}{\mu}\right)_{mb} \left(\frac{1}{h}\right)_{mb} (p_{mb} - p_{fb})$$

Substituting  $p_D$  in above, we have:

$$\left(\frac{k_{fb} h_{fb}}{\mu_{fb}} + \frac{k_{mb} h_{mb}}{\mu_{mb}}\right) \left(\frac{kh}{\mu}\right)_{mb} p_{ch} \frac{\partial^2 p_{mb}}{\partial z_D^2} =$$

$$(\varphi_{fb} h_{fb} + \varphi_{mb} h_{mb}) \times$$

$$(\varphi h)_{mb} c_m A_{cw} \frac{(p_{mbD} p_{ch} - p_i)}{\partial t} +$$

$$\alpha A_{cw} \left(\frac{k_{fb} h_{fb}}{\mu_{fb}} + \frac{k_{mb} h_{mb}}{\mu_{mb}}\right) \left(\frac{kh}{\mu}\right)_{mb} \left(\frac{1}{h}\right)_{mb} \{(\partial p_{mbD} p_{ch} - p_i) - (p_{fD} p_{ch} - p_i)\}$$

On cancellation of common terms, results in:

$$\left(\frac{kh}{\mu}\right)_{mb} \frac{\partial^2 p_{mbD}}{\partial z_D^2} = (\varphi h)_{mb} \frac{(\varphi_{fb} h_{fb} + \varphi_{mb} h_{mb})}{\left(\frac{k_{fb} h_{fb}}{\mu_{fb}} + \frac{k_{mb} h_{mb}}{\mu_{mb}}\right)} c_m A_{cw} \frac{\partial p_{mbD}}{\partial t} + \alpha A_{cw} \left(\frac{kh}{\mu}\right)_{mb} \left(\frac{1}{h}\right)_{mb} (p_{mbD} - p_{fbD}) \dots \text{ (E-16)}$$

Reapplying eqn.(E-2) and converting this equation into aquifer-fracture domain we get:

$$\left( \frac{\frac{k_{mb} h_{mb}}{\mu_{mb}}}{\frac{k_{fb} h_{fb}}{\mu_{fb}} + \frac{k_{mb} h_{mb}}{\mu_{mb}}} \right) \frac{\partial^2 p_{mbD}}{\partial z_D^2} =$$

$$(\varphi h)_{mb} \frac{(\varphi_{fb} h_{fb} + \varphi_{mb} h_{mb})}{(\varphi_{fb} h_{fb} + \varphi_{aq} h_{aq})} \frac{\left( \frac{k_{fb} h_{fb}}{\mu_{fb}} + \frac{k_{aq} h_{aq}}{\mu_{aq}} \right)}{\left( \frac{k_{fb} h_{fb}}{\mu_{fb}} + \frac{k_{mb} h_{mb}}{\mu_{mb}} \right)} \frac{(\varphi_{fb} h_{fb} + \varphi_{aq} h_{aq})}{\left( \frac{k_{fb} h_{fb}}{\mu_{fb}} + \frac{k_{aq} h_{aq}}{\mu_{aq}} \right)} c_m A_{cw} \frac{\partial p_{mbD}}{\partial t} +$$

$$\alpha A_{cw} \left( \frac{\frac{k_{mb} h_{mb}}{\mu_{mb}}}{\frac{k_{fb} h_{fb}}{\mu_{fb}} + \frac{k_{mb} h_{mb}}{\mu_{mb}}} \right) \left( \frac{1}{h} \right)_{mb} (p_{mbD} - p_{fbD}) \dots\dots\dots (E-17)$$

We also have the following:

$$\omega = \frac{\varphi_{fb} c_f}{(\varphi c_t)_{mb+fb}} \dots\dots\dots (E-18a)$$

$$\Lambda = \frac{\omega_{aq}}{\omega} = \frac{(\varphi_{fb} h_{fb} + \varphi_{mb} h_{mb})}{(\varphi_{fb} h_{fb} + \varphi_{aq} h_{aq})} \dots\dots\dots (E-18b)$$

Substituting  $\omega$  and  $\Lambda$  in eqn.(E-17) and assuming compressibility is constant, we have:

$$(1 - \kappa_{fb}) \frac{\partial^2 p_{mbD}}{\partial z_D^2} = (1 - \omega) (\Lambda) \left( \frac{\kappa_{fb}}{\kappa_f} \right) \frac{\partial p_{mbD}}{\partial t_D} + \lambda (p_{mbD} - p_{fbD}) \dots (E-19)$$

Here dimensionless time and dimensionless interporosity flow parameter and others, are as:

$$t_{bD} = \frac{\left(\frac{k_{fb} h_{fb}}{\mu_{fb}} + \frac{k_{mb} h_{mb}}{\mu_{mb}}\right) t}{(\varphi_{fb} h_{fb} + \varphi_{mb} h_{mb}) c_f A_{cw}} = \left(\frac{\kappa_f}{\kappa_{fb}}\right) \left(\frac{1}{\Lambda}\right) t_D \dots (E-20a)$$

$$\lambda = \alpha A_{cw} \left(\frac{\frac{k_{mb}}{\mu_{mb}}}{\frac{k_{fb} h_{fb}}{\mu_{fb}} + \frac{k_{mb} h_{mb}}{\mu_{mb}}}\right) \dots (E-20b)$$

$$\kappa_{fb} = \left(\frac{\frac{k_{fb} h_{fb}}{\mu_{fb}}}{\frac{k_{fb} h_{fb}}{\mu_{fb}} + \frac{k_{mb} h_{mb}}{\mu_{mb}}}\right) \dots (E-20c)$$

$$p_{mbD} = 2\pi \left(\frac{k_{fb} h_{fb}}{\mu_{fb}} + \frac{k_{mb} h_{mb}}{\mu_{mb}}\right) \frac{p_i - p_{mb}}{q_B} \dots (E-20d)$$

$$p_{fbD} = 2\pi \left(\frac{k_{fb} h_{fb}}{\mu_{fb}} + \frac{k_{mb} h_{mb}}{\mu_{mb}}\right) \frac{p_i - p_{fb}}{q_B} \dots (E-20e)$$

The final form of the above equation, since the LHS is zero for pseudosteady state, is:

$$0 = \left(\frac{1-\omega}{1-\kappa_{fb}}\right) (\Lambda) \left(\frac{\kappa_{fb}}{\kappa_f}\right) \frac{\partial p_{mbD}}{\partial t_D} + \left(\frac{\lambda}{1-\kappa_{fb}}\right) (p_{mbD} - p_{fbD}) \dots (E-21)$$

Applying the initial condition of aquifer to the Laplace transform equations results in:

$$0 = (1 - \omega)(\Lambda) \left(\frac{\kappa_{fb}}{\kappa_f}\right) s \overline{p_{mbD}} + \lambda (\overline{p_{mbD}} - \overline{p_{fbD}}) \dots (E-22)$$

Solving eqn.(E-22) the Laplace domain solution,  $\overline{p_{mbD}}$ , is:

$$\overline{p_{mbD}} = \frac{\lambda}{(1-\omega)(\Lambda) \left(\frac{\kappa_{fb}}{\kappa_f}\right) s + \lambda} \overline{p_{fbD}} \dots (E-23)$$

Solution of Fracture

There are two different dimensionless pressures. The dimensionless pressure which is reservoir matrix-fracture domain based and dimensionless pressure which is aquifer-fracture domain based. We know dimensionless time measurement is based on latter and this is the reason for normalizing everything on that domain. We have the two equations as:

$$\overline{p_{aqD}} = \frac{\lambda_{aq}}{(1-\omega_{aq})^s + \lambda_{aq}} \overline{p_{fD}} \quad \dots\dots\dots (E-15)$$

$$\overline{p_{mbD}} = \frac{\lambda}{(1-\omega)(\Lambda)\left(\frac{\kappa_{fb}}{\kappa_f}\right)^{s+\lambda}} \overline{p_{fbD}} \quad \dots\dots\dots (E-23)$$

We also know fracture domains are the same:

$$\frac{\overline{p_{fbD}}}{\left(\frac{k_{fb} h_{fb}}{\mu_{fb}} + \frac{k_{mb} h_{mb}}{\mu_{mb}}\right)} = \frac{\overline{p_{fD}}}{\left(\frac{k_{fb} h_{fb}}{\mu_{fb}} + \frac{k_{aq} h_{aq}}{\mu_{aq}}\right)}$$

$$\overline{p_{fbD}} = \left(\frac{\kappa_f}{\kappa_{fb}}\right) \overline{p_{fD}} \dots\dots\dots (E-24)$$

Again, for the fracture we have:

$$\left(\frac{k_{fb} h_{fb}}{\mu_{fb}} + \frac{k_{aq} h_{aq}}{\mu_{aq}}\right) \left(\frac{kh}{\mu}\right)_{fb} \frac{\partial^2 p_{fb}}{\partial y^2} =$$

$$(\varphi_{fb} h_{fb} + \varphi_{aq} h_{aq}) (\varphi h)_{fb} c_f \frac{\partial p_{fb}}{\partial t} -$$

$$\underline{\alpha} \left(\frac{k_{fb} h_{fb}}{\mu_{fb}} + \frac{k_{aq} h_{aq}}{\mu_{aq}}\right) \left(\frac{kh}{\mu}\right)_{aq} \left(\frac{1}{h}\right)_{aq} (p_{aq} - p_{fb}) -$$

$$\alpha \left(\frac{k_{fb} h_{fb}}{\mu_{fb}} + \frac{k_{mb} h_{mb}}{\mu_{mb}}\right) \left(\frac{kh}{\mu}\right)_{mb} \left(\frac{1}{h}\right)_{mb} (p_{mb} - p_{fb}) \dots\dots\dots (E-5a)$$

Substituting  $y_D$  in eqn.(E-5a), we have:

$$\begin{aligned} \left( \frac{k_{fb} h_{fb}}{\mu_{fb}} + \frac{k_{aq} h_{aq}}{\mu_{aq}} \right) \left( \frac{kh}{\mu} \right)_{fb} \frac{\partial^2 p_{fb}}{\partial y_D^2} &= (\varphi_{fb} h_{fb} + \varphi_{aq} h_{aq}) (\varphi h)_{fb} c_f A_{cw} \frac{\partial p_{fb}}{\partial t} - \\ &\underline{\alpha} A_{cw} \left( \frac{k_{fb} h_{fb}}{\mu_{fb}} + \frac{k_{aq} h_{aq}}{\mu_{aq}} \right) \left( \frac{kh}{\mu} \right)_{aq} \left( \frac{1}{h} \right)_{aq} (p_{aq} - p_{fb}) - \\ &\alpha A_{cw} \left( \frac{k_{fb} h_{fb}}{\mu_{fb}} + \frac{k_{mb} h_{mb}}{\mu_{mb}} \right) \left( \frac{kh}{\mu} \right)_{mb} \left( \frac{1}{h} \right)_{mb} (p_{mb} - p_{fb}) \end{aligned}$$

Substituting  $p_D$  in eqn.(E-5a), we have:

$$\begin{aligned} \left( \frac{k_{fb} h_{fb}}{\mu_{fb}} + \frac{k_{aq} h_{aq}}{\mu_{aq}} \right) \left( \frac{kh}{\mu} \right)_{fb} p_{ch} \frac{\partial^2 (p_{fD} p_{ch} - p_i)}{\partial y_D^2} &= \\ (\varphi_{fb} h_{fb} + \varphi_{aq} h_{aq}) (\varphi h)_{fb} c_f A_{cw} \frac{\partial (p_{fD} p_{ch} - p_i)}{\partial t} - \\ &\underline{\alpha} A_{cw} \left( \frac{k_{fb} h_{fb}}{\mu_{fb}} + \frac{k_{aq} h_{aq}}{\mu_{aq}} \right) \times \\ &\left( \frac{kh}{\mu} \right)_{aq} \left( \frac{1}{h} \right)_{aq} \{ (p_{aqD} p_{ch} - p_i) - (p_{fD} p_{ch} - p_i) \} - \\ &\alpha A_{cw} \left( \frac{k_{fb} h_{fb}}{\mu_{fb}} + \frac{k_{mb} h_{mb}}{\mu_{mb}} \right) \left( \frac{kh}{\mu} \right)_{mb} \left( \frac{1}{h} \right)_{mb} \{ (p_{mbD} p_{ch} - p_i) - (p_{fD} p_{ch} - p_i) \} \end{aligned}$$

Rearranging and canceling common terms results in:

$$\begin{aligned} & \left(\frac{kh}{\mu}\right)_{fb} \frac{\partial^2 p_{fD}}{\partial y_D^2} = \\ & (\varphi h)_{fb} \frac{(\varphi_{fb} h_{fb} + \varphi_{aq} h_{aq})}{\left(\frac{k_{fb} h_{fb}}{\mu_{fb}} + \frac{k_{aq} h_{aq}}{\mu_{aq}}\right)} c_f A_{cw} \frac{\partial p_{fD}}{\partial t} - \underline{\alpha} A_{cw} \left(\frac{kh}{\mu}\right)_{aq} \times \left(\frac{1}{h}\right)_{aq} (p_{aqD} - p_{fD}) - \\ & \alpha A_{cw} \frac{\left(\frac{k_{fb} h_{fb}}{\mu_{fb}} + \frac{k_{mb} h_{mb}}{\mu_{mb}}\right)}{\left(\frac{k_{fb} h_{fb}}{\mu_{fb}} + \frac{k_{aq} h_{aq}}{\mu_{aq}}\right)} \left(\frac{kh}{\mu}\right)_{mb} \left(\frac{1}{h}\right)_{mb} (p_{mbD} - p_{fD}) \end{aligned}$$

Substituting back eqns. (E-2a) to eqn.(E-2h) into the above eqn. we get:

$$\begin{aligned} & \left(\frac{\frac{k_{fb} h_{fb}}{\mu_{fb}}}{\frac{k_{fb} h_{fb}}{\mu_{fb}} + \frac{k_{aq} h_{aq}}{\mu_{aq}}}\right) \frac{\partial^2 p_{fD}}{\partial y_D^2} = \left(\frac{\varphi_{fb} h_{fb}}{\varphi_{fb} h_{fb} + \varphi_{aq} h_{aq}}\right) \frac{(\varphi_{fb} h_{fb} + \varphi_{aq} h_{aq})}{\left(\frac{k_{fb} h_{fb}}{\mu_{fb}} + \frac{k_{aq} h_{aq}}{\mu_{aq}}\right)} c_f A_{cw} \frac{\partial p_{fD}}{\partial t} - \\ & \underline{\alpha} A_{cw} \left(\frac{\frac{k_{aq} h_{aq}}{\mu_{aq}}}{\frac{k_{fb} h_{fb}}{\mu_{fb}} + \frac{k_{aq} h_{aq}}{\mu_{aq}}}\right) \left(\frac{1}{h}\right)_{aq} (p_{aqD} - p_{fD}) - \\ & \alpha A_{cw} \frac{\left(\frac{k_{fb} h_{fb}}{\mu_{fb}} + \frac{k_{mb} h_{mb}}{\mu_{mb}}\right)}{\left(\frac{k_{fb} h_{fb}}{\mu_{fb}} + \frac{k_{aq} h_{aq}}{\mu_{aq}}\right)} \left(\frac{\frac{k_{mb} h_{mb}}{\mu_{mb}}}{\frac{k_{fb} h_{fb}}{\mu_{fb}} + \frac{k_{mb} h_{mb}}{\mu_{mb}}}\right) \left(\frac{1}{h}\right)_{mb} (p_{mbD} - p_{fD}) \end{aligned}$$

Introducing some additional terms and we know,  $h_{fb} = h_{mb}$  :

$$\begin{aligned} \left( \frac{\frac{k_{fb} h_{fb}}{\mu_{fb}}}{\frac{k_{fb} h_{fb}}{\mu_{fb}} + \frac{k_{aq} h_{aq}}{\mu_{aq}}} \right) \frac{\partial^2 p_{fD}}{\partial y_D^2} &= \left( \frac{\varphi_{fb} h_{fb}}{\varphi_{fb} h_{fb} + \varphi_{aq} h_{aq}} \right) \left( \frac{\varphi_{fb} h_{fb} + \varphi_{aq} h_{aq}}{\frac{k_{fb} h_{fb}}{\mu_{fb}} + \frac{k_{aq} h_{aq}}{\mu_{aq}}} \right) c_f A_{cw} \frac{\partial p_{fD}}{\partial t} - \\ &\underline{\alpha} A_{cw} \left( \frac{\frac{k_{aq} h_{aq}}{\mu_{aq}}}{\frac{k_{fb} h_{fb}}{\mu_{fb}} + \frac{k_{aq} h_{aq}}{\mu_{aq}}} \right) \left( \frac{1}{h} \right)_{aq} (p_{aqD} - p_{fD}) - \\ &\alpha A_{cw} \left( \frac{\frac{k_{fb} h_{fb}}{\mu_{fb}} + \frac{k_{mb} h_{mb}}{\mu_{mb}}}{\frac{k_{fb} h_{fb}}{\mu_{fb}} + \frac{k_{aq} h_{aq}}{\mu_{aq}}} \right) \left( \frac{k_{fb} h_{fb}}{\mu_{fb}} \right) \left( \frac{\frac{k_{mb} h_{mb}}{\mu_{mb}}}{\frac{k_{fb} h_{fb}}{\mu_{fb}} + \frac{k_{mb} h_{mb}}{\mu_{mb}}} \right) \left( \frac{1}{h} \right)_{mb} (p_{mbD} - p_{fbD}) \end{aligned}$$

The resultant form of the governing differential equations are:

$$\kappa_f \frac{\partial^2 p_{fD}}{\partial y_D^2} = \omega_{aq} \frac{\partial p_{fD}}{\partial t} - \lambda_{aq} (p_{aqD} - p_{fD}) - (\lambda \kappa_f) (p_{mbD} - p_{fbD})$$

The final form of the governing differential equations is:

$$\nabla^2 p_{fD} = \left( \frac{\omega_{aq}}{\kappa_f} \right) \frac{\partial p_{fD}}{\partial t} - \left( \frac{\lambda_{aq}}{\kappa_f} \right) (p_{aqD} - p_{fD}) - \lambda (p_{mbD} - p_{fbD}) \dots \text{(E-25)}$$

Taking Laplace transform of the above equation:

$$\frac{d^2 \overline{p_{fD}}}{dy_D^2} = \left( \frac{\omega_{aq}}{\kappa_f} \right) \{s \overline{p_{fD}} - \overline{p_{fD}}(y_D, 0)\} - \left( \frac{\lambda_{aq}}{\kappa_f} \right) \{ \overline{p_{aqD}} - \overline{p_{fD}} \} - \lambda \{ \overline{p_{mbD}} - \overline{p_{fbD}} \} \dots \text{(E-26)}$$



For a closed linear reservoir the initial and boundary conditions, in Laplace domain, for fracture are:

Initial Condition:  $\overline{p}_{fD}(y_D, s) = 0 \dots \dots \dots (E-27a)$

Inner Boundary Condition:  $\left. \frac{d\overline{p}_{fD}}{dy_D} \right|_{y_D=0} = -\frac{2\pi}{s} \dots \dots \dots (E-27b)$

Outer Boundary Condition:  $\left. \frac{d\overline{p}_{fD}}{dy_D} \right|_{y_D=y_{De}} = 0 \dots \dots \dots (E-27c)$

Substituting this, eqn.(E-15) and eqn.(E-23) in eqn.(E-26) we have:

$$\frac{d^2 \overline{p}_{fD}}{dy_D^2} = \left(\frac{\omega_{aq}}{\kappa_f}\right) \{S\overline{p}_{fD}\} - \left(\frac{\lambda_{aq}}{\kappa_f}\right) \left\{ \frac{\lambda_{aq}}{(1-\omega_{aq})s + \lambda_{aq}} \overline{p}_{fD} - \overline{p}_{fD} \right\} - \lambda \left\{ \frac{\lambda}{(1-\omega)(\Lambda) \left(\frac{\kappa_{fb}}{\kappa_f}\right)^{s+\lambda}} \overline{p}_{fbD} - \overline{p}_{fbD} \right\}$$

$$\frac{d^2 \overline{p}_{fD}}{dy_D^2} = \left(\frac{\omega_{aq}}{\kappa_f}\right) \{S\overline{p}_{fD}\} + \left(\frac{\lambda_{aq}}{\kappa_f}\right) \left\{ \frac{(1-\omega_{aq})}{(1-\omega_{aq})s + \lambda_{aq}} \right\} \{S\overline{p}_{fD}\} + \lambda \left\{ \frac{(1-\omega)(\Lambda) \left(\frac{\kappa_{fb}}{\kappa_f}\right)}{(1-\omega)(\Lambda) \left(\frac{\kappa_{fb}}{\kappa_f}\right)^{s+\lambda}} \right\} \{S\overline{p}_{fbD}\}$$

Using eqn.(E-24), converting everything into consistent aquifer-fracture domain, we have:

$$\frac{d^2 \overline{p}_{fD}}{dy_D^2} = \left[ \left(\frac{\omega_{aq}}{\kappa_f}\right) + \lambda \left\{ \frac{(1-\omega)(\Lambda) \left(\frac{\kappa_{fb}}{\kappa_f}\right)}{(1-\omega)(\Lambda) \left(\frac{\kappa_{fb}}{\kappa_f}\right)^{s+\lambda}} \right\} + \left(\frac{\lambda_{aq}}{\kappa_f}\right) \left\{ \frac{(1-\omega_{aq})}{(1-\omega_{aq})s + \lambda_{aq}} \right\} \right] \{S\overline{p}_{fD}\}$$

This is of the form:

$$\frac{d^2 \overline{p_{fD}}}{dy_D^2} - sf(s) \overline{p_{fD}} = 0 \dots\dots\dots (E-28)$$

Where,

$$f(s) = \left[ \left( \frac{\omega_{aq}}{\kappa_f} \right) + \lambda \left( \frac{(1-\omega)(\Lambda) \left( \frac{\kappa_{fb}}{\kappa_f} \right)}{(1-\omega)(\Lambda) \left( \frac{\kappa_{fb}}{\kappa_f} \right) s + \lambda} \right) + \left( \frac{\lambda_{aq}}{\kappa_f} \right) \left( \frac{(1-\omega_{aq})}{(1-\omega_{aq})s + \lambda_{aq}} \right) \right] \dots\dots\dots (E-29)$$

Which, when combining the first two reservoir terms, can also be also written as:

$$f(s) = \left[ \left( \frac{\omega_{aq}}{\kappa_f} \right) + \left( \frac{\left( \frac{\lambda}{\omega} \right) (1-\omega)(\Lambda) \left( \frac{\kappa_{fb}}{\kappa_f} \right)}{\left( \frac{1-\omega}{\omega} \right) (\Lambda) \left( \frac{\kappa_{fb}}{\kappa_f} \right) s + \left( \frac{\lambda}{\omega} \right)} \right) + \left( \frac{\lambda_{aq}}{\kappa_f} \right) \left( \frac{(1-\omega_{aq})}{(1-\omega_{aq})s + \lambda_{aq}} \right) \right] \dots\dots\dots (E-30)$$

Eqn.(E-16) is a homogeneous partial differential equation which is the same as eqn.(A-17). Refer to Appendix A for the rest of the derivation.

APPENDIX F: TRANSIENT MATRIX FRACTURED DUAL PERMEABILITY  
 DUAL MOBILITY MODEL – FORMULATION AND LAPLACE DOMAIN  
 SOLUTION

The governing differential equation for linear fluid flow in limited aquifer (matrix block) and the fractured reservoir (reservoir fracture block and reservoir matrix block) is given by:

$$\text{Fracture:} \quad \left(\frac{kh}{\mu}\right)_f \nabla^2 p_f = \varphi_f c_f h_f \frac{\partial p_f}{\partial t} - \underline{\alpha} \frac{k_a}{\mu_a} (p_a - p_f) - \left(\frac{k}{\mu h/2}\right)_m \frac{\partial p_m}{\partial z} \Big|_{z=h_m/2} \quad (\text{F-1a})$$

$$\text{Matrix (Aquifer):} \quad \left(\frac{kh}{\mu}\right)_a \nabla^2 p_a = \varphi_a c_a h_a \frac{\partial p_a}{\partial t} + \underline{\alpha} \left(\frac{k}{\mu}\right)_a (p_a - p_f) \quad \dots\dots\dots(\text{F-1b})$$

$$\text{Matrix (Reservoir):} \quad \left(\frac{kh}{\mu}\right)_m \nabla^2 p_m = \varphi_m c_m h_m \frac{\partial p_m}{\partial t} \quad \dots\dots\dots(\text{F-1c})$$

Since the aquifer is limited, the aquifer height is related to the linear dimension of reservoir ( $y$  is a lateral dimension in the fractured reservoir and  $y_{aq}$  is vertical dimension in the aquifer) by:

$$y_{aq} = h_{aq} = \varepsilon y \quad \dots\dots\dots(\text{F-1d})$$

The second term in eqn.(F-1a) is referred to as the source terms,  $\sigma_a$  and  $\sigma_m$ . The reservoir matrix is in transient but aquifer is in pseudosteady state. Also, all properties need to be put as bulk properties:

Aquifer:

$$\left(\frac{kh}{\mu}\right)_{aq} = \frac{k_a h_a}{\mu_a} \left(\frac{V_a}{V_{f+a}}\right) = \left(\frac{\frac{k_{aq} h_{aq}}{\mu_{aq}}}{\frac{k_{fb} h_{fb}}{\mu_{fb}} + \frac{k_{aq} h_{aq}}{\mu_{aq}}}\right) \dots\dots\dots(F-2a)$$

$$\left(\frac{kh}{\mu}\right)_f = \frac{k_f h_f}{\mu_f} \left(\frac{V_f}{V_{f+a}}\right) = \left(\frac{\frac{k_{fb} h_{fb}}{\mu_{fb}}}{\frac{k_{fb} h_{fb}}{\mu_{fb}} + \frac{k_{aq} h_{aq}}{\mu_{aq}}}\right) \dots\dots\dots(F-2b)$$

$$(\varphi h)_{aq} = \left(\frac{V_{aq}}{V_{f+aq}}\right) = \left(\frac{\varphi_{aq} h_{aq}}{\varphi_{fb} h_{fb} + \varphi_{aq} h_{aq}}\right) \dots\dots\dots(F-2c)$$

$$(\varphi h)_f = \left(\frac{V_f}{V_{f+aq}}\right) = \left(\frac{\varphi_{fb} h_{fb}}{\varphi_{fb} h_{fb} + \varphi_{aq} h_{aq}}\right) \dots\dots\dots(F-2d)$$

Reservoir:

$$\left(\frac{kh}{\mu}\right)_{mb} = \frac{k_m}{\mu_m} \left(\frac{V_m}{V_{f+m}}\right) = \left(\frac{\frac{k_{mb} h_{mb}}{\mu_{mb}}}{\frac{k_{fb} h_{fb}}{\mu_{fb}} + \frac{k_{mb} h_{mb}}{\mu_{mb}}}\right) \dots\dots\dots(F-2e)$$

$$\left(\frac{kh}{\mu}\right)_{fb} = \frac{k_f}{\mu_f} \left(\frac{V_f}{V_{f+m}}\right) = \left(\frac{\frac{k_{fb} h_{fb}}{\mu_{fb}}}{\frac{k_{fb} h_{fb}}{\mu_{fb}} + \frac{k_{mb} h_{mb}}{\mu_{mb}}}\right) \dots\dots\dots(F-2f)$$

$$(\varphi h)_{mb} = \left(\frac{V_m}{V_{f+m}}\right) = \left(\frac{\varphi_{mb} h_{mb}}{\varphi_{fb} h_{fb} + \varphi_{mb} h_{mb}}\right) \dots\dots\dots(F-2g)$$

$$(\varphi h)_{fb} = \left(\frac{V_f}{V_{f+m}}\right) = \left(\frac{\varphi_{fb} h_{fb}}{\varphi_{fb} h_{fb} + \varphi_{mb} h_{mb}}\right) \dots\dots\dots(F-2h)$$

Similarly, the aquifer and matrix fracture bulk source terms are,  $\sigma_{aq}$ , and  $\sigma_{mf}$ , is expressed as:

$$\sigma_{aq} = \sigma_a \left( \frac{V_a}{V_{f+a}} \right) = \underline{\alpha} \frac{k_a}{\mu_a} \left( \frac{V_a}{V_{f+a}} \right) (p_{aq} - p_{fb}) =$$

$$\underline{\alpha} \left( \frac{k_{fb} h_{fb}}{\mu_{fb}} + \frac{k_{aq} h_{aq}}{\mu_{aq}} \right) \times \left( \frac{kh}{\mu} \right)_{aq} \left( \frac{1}{h} \right)_{aq} (p_{aq} - p_{fb}) \dots \dots \dots (F-3a)$$

$$\sigma_{mf} = \sigma_m \left( \frac{V_m}{V_{f+m}} \right) = \left( \frac{k}{\mu h/2} \right)_{mb} \frac{\partial p_m}{\partial z} \Big|_{z=h_{mb}/2} =$$

$$\left( \frac{k_{fb} h_{fb}}{\mu_{fb}} + \frac{k_{mb} h_{mb}}{\mu_{mb}} \right) \times \left( \frac{kh}{\mu} \right)_{mb} \left( \frac{1}{h^2/2} \right)_{mb} \frac{\partial p_{mb}}{\partial z} \Big|_{z=h_{mb}/2} \dots \dots \dots (F-3b)$$

where  $\underline{\alpha}$ , is the shape function:

$$\underline{\alpha} = \frac{(T_b)_{eff}}{k_{aq}} \dots \dots \dots (F-4a)$$

And,

$$\lambda_{aqf} = \underline{\alpha} \left( \frac{k_{aq}}{k_{rf}} \right) A_{cw} = \left( \frac{(T_b)_{eff}}{k_{rf}} \right) A_{cw} \dots \dots \dots (F-4b)$$

$$(T_b)_{eff} = \frac{1}{\frac{1}{T_b} + \frac{h_{aq}}{3k_{aq}}} \dots \dots \dots (F-4c)$$

$$T_b = \frac{k_b}{h_b} \dots \dots \dots (F-4d)$$

And where  $\alpha$ , is the shape function:

$$\alpha = \frac{4n(n+2)}{h_m^2} \dots \dots \dots (F-4e)$$

In terms of bulk properties the governing equations can be recast into:

Fracture:

$$\begin{aligned} & \left( \frac{k_{fb} h_{fb}}{\mu_{fb}} + \frac{k_{aq} h_{aq}}{\mu_{aq}} \right) \left( \frac{kh}{\mu} \right)_{fb} \frac{\partial^2 p_{fb}}{\partial y^2} = \\ & (\varphi_{fb} h_{fb} + \varphi_{aq} h_{aq}) (\varphi h)_{fb} c_f \frac{\partial p_{fb}}{\partial t} - \alpha \left( \frac{k_{fb} h_{fb}}{\mu_{fb}} + \frac{k_{aq} h_{aq}}{\mu_{aq}} \right) \left( \frac{kh}{\mu} \right)_{aq} \left( \frac{1}{h} \right)_{aq} (p_{aq} - \\ & p_{fb}) - \left( \frac{k_{fb} h_{fb}}{\mu_{fb}} + \frac{k_{mb} h_{mb}}{\mu_{mb}} \right) \left( \frac{kh}{\mu} \right)_{mb} \left( \frac{1}{h^2/2} \right)_{mb} \frac{\partial p_{mb}}{\partial z} \Big|_{z=h_{mb}/2} \dots \dots \dots (F-5a) \end{aligned}$$

Matrix (Aquifer):

$$\begin{aligned} & \left( \frac{1}{\varepsilon^2} \right) \left( \frac{k_{fb} h_{fb}}{\mu_{fb}} + \frac{k_{aq} h_{aq}}{\mu_{aq}} \right) \left( \frac{kh}{\mu} \right)_{aq} \frac{\partial^2 p_{aq}}{\partial y^2} = (\varphi_{fb} h_{fb} + \varphi_{aq} h_{aq}) (\varphi h)_{aq} c_a \frac{\partial p_{aq}}{\partial t} + \\ & \alpha \left( \frac{k_{fb} h_{fb}}{\mu_{fb}} + \frac{k_{aq} h_{aq}}{\mu_{aq}} \right) \left( \frac{kh}{\mu} \right)_{aq} \left( \frac{1}{h} \right)_{aq} (p_{aq} - p_{fb}) \dots \dots \dots (F-5b) \end{aligned}$$

Matrix (Reservoir):

$$\left( \frac{k_{fb} h_{fb}}{\mu_{fb}} + \frac{k_{mb} h_{mb}}{\mu_{mb}} \right) \left( \frac{kh}{\mu} \right)_{mb} \frac{\partial^2 p_{mb}}{\partial z^2} = (\varphi_{fb} h_{fb} + \varphi_{mb} h_{mb}) (\varphi h)_{mb} c_m \frac{\partial p_{mb}}{\partial t} \dots \dots \dots (F-5c)$$

For an matrix block, the initial and boundary conditions are:

Initial Condition:  $p_{aq}(z, t = 0) = p_i \dots \dots \dots (F-6a)$

Inner Boundary Condition:  $\frac{\partial p_{aq}}{\partial z} \Big|_{z=0} = 0$  for all t  $\dots \dots \dots (F-6b)$

Outer Boundary Condition:  $p_{aq} \Big|_{z=h_{aq}} = p_f$  for all t  $\dots \dots \dots (F-6c)$

For a fracture block, the initial and boundary conditions are:

$$\text{Initial Condition: } p_f(x, t = 0) = p_i \dots\dots\dots(\text{F-6d})$$

$$\text{Inner Boundary Condition: } q = - \left( \frac{k_f A_{cw}}{\mu} \right) \frac{\partial p_f}{\partial x} \Big|_{x=0} \text{ for all t and const. rate ...}(\text{F-6e})$$

$$\text{Outer Boundary Condition } \frac{\partial p_f}{\partial x} \Big|_{x=x_e} = 0 \text{ for all t } \dots\dots\dots(\text{F-6f})$$

If we assume  $y$  is the overall linear dimension and define dimensionless variables as:

$$y_D = \frac{y}{\sqrt{A_{cw}}} \text{ for all fracture } \dots\dots\dots(\text{F-7a})$$

$$\varepsilon y_D = \frac{\varepsilon y}{\sqrt{A_{cw}}} \text{ for all aquifer } \dots\dots\dots(\text{F-7b})$$

$$z_D = \frac{z}{h_{rm}/2} \text{ for all matrix } \dots\dots\dots(\text{F-7c})$$

$$p_{jD} = \frac{p_i - p}{p_{ch}} = \frac{2\pi}{\alpha_1 q B} \left( \frac{k_{fb} h_{fb}}{\mu_{fb}} + \frac{k_{aq} h_{aq}}{\mu_{aq}} \right) (p_i - p_j) \Big|_{j=f \text{ or } aq} \dots\dots\dots(\text{F-7d})$$

$$p_{jD} = \frac{p_i - p}{p_{ch}} = \frac{2\pi}{\alpha_1 q B} \left( \frac{k_{fb} h_{fb}}{\mu_{fb}} + \frac{k_{mb} h_{mb}}{\mu_{mb}} \right) (p_i - p_j) \Big|_{j=fb \text{ or } mb} \dots\dots\dots(\text{F-7e})$$

The derivatives of the above entities will be:

$$\partial(y_D \sqrt{A_{cw}}) = \partial y \quad \partial(y_D \sqrt{A_{cw}}) \{ \partial(y_D \sqrt{A_{cw}}) \} = \partial^2 y \dots\dots\dots(\text{F-8a})$$

$$\partial(z_D h_{rm}/2) = \partial z \quad \partial(z_D h_{rm}/2) \{ \partial(z_D h_{rm}/2) \} = \partial^2 z \dots\dots\dots(\text{F-8b})$$

$$\varepsilon \partial(y_D \sqrt{A_{cw}}) = \partial y \quad \varepsilon^2 \partial(y_D \sqrt{A_{cw}}) \{ \partial(y_D \sqrt{A_{cw}}) \} = \partial^2 y \dots\dots\dots(\text{F-8c})$$

$$\partial(p_D p_{ch} - p_i) = p_{ch} \partial p_D = - \partial p \quad p_{ch} \partial^2 p_D = \partial^2 p \dots\dots\dots(\text{F-8d})$$

Solution of Matrix (Aquifer)

Substituting  $y_D$  in eqn.(F-5b), we have:

$$\left(\frac{1}{\varepsilon^2}\right) \left(\frac{k_{fb} h_{fb}}{\mu_{fb}} + \frac{k_{aq} h_{aq}}{\mu_{aq}}\right) \left(\frac{kh}{\mu}\right)_{aq} \frac{\partial^2 p_{aq}}{\partial y_D^2} = (\varphi_{fb} h_{fb} + \varphi_{aq} h_{aq})(\varphi h)_{aq} c_a A_{cw} \frac{\partial p_{aq}}{\partial t} +$$

$$\underline{\alpha} A_{cw} \left(\frac{k_{fb} h_{fb}}{\mu_{fb}} + \frac{k_{aq} h_{aq}}{\mu_{aq}}\right) \left(\frac{kh}{\mu}\right)_{aq} \left(\frac{1}{h}\right)_{aq} (p_{aq} - p_{fb})$$

Substituting  $p_D$  in above, we have:

$$\left(\frac{1}{\varepsilon^2}\right) \left(\frac{k_{fb} h_{fb}}{\mu_{fb}} + \frac{k_{aq} h_{aq}}{\mu_{aq}}\right) \left(\frac{kh}{\mu}\right)_{aq} p_{ch} \frac{\partial^2 (p_{aqD} p_{ch} - p_i)}{\partial y_D^2} = (\varphi_{fb} h_{fb} + \varphi_{aq} h_{aq}) \times$$

$$(\varphi h)_{aq} c_a A_{cw} \frac{\partial (p_{aqD} p_{ch} - p_i)}{\partial t} +$$

$$\underline{\alpha} A_{cw} \left(\frac{k_{fb} h_{fb}}{\mu_{fb}} + \frac{k_{aq} h_{aq}}{\mu_{aq}}\right) \left(\frac{kh}{\mu}\right)_{aq} \left(\frac{1}{h}\right)_{aq} \{(\partial p_{aqD} p_{ch} - p_i) - (p_{fD} p_{ch} - p_i)\}$$

On cancellation of common terms, results in:

$$\left(\frac{1}{\varepsilon^2}\right) \left(\frac{kh}{\mu}\right)_{aq} \frac{\partial^2 p_{aqD}}{\partial y_D^2} =$$

$$\frac{(\varphi_{fb} h_{fb} + \varphi_{aq} h_{aq})}{\left(\frac{k_{fb} h_{fb}}{\mu_{fb}} + \frac{k_{aq} h_{aq}}{\mu_{aq}}\right)} (\varphi h)_{aq} c_a A_{cw} \frac{\partial p_{aqD}}{\partial t} + \underline{\alpha} A_{cw} \left(\frac{kh}{\mu}\right)_{aq} \left(\frac{1}{h}\right)_{aq} (p_{aqD} - p_{fD}) \dots\dots (F-9)$$



Reapplying eqn.(F-2) to the above we get:

$$\left(\frac{1}{\varepsilon^2}\right) \left( \frac{\frac{k_{aq} h_{aq}}{\mu_{aq}}}{\frac{k_{fb} h_{fb}}{\mu_{fb}} + \frac{k_{aq} h_{aq}}{\mu_{aq}}} \right) \frac{\partial^2 p_{aqD}}{\partial y_D^2} =$$

$$(\varphi h)_{aq} \frac{(\varphi_{fb} h_{fb} + \varphi_{aq} h_{aq})}{\left( \frac{k_{fb} h_{fb}}{\mu_{fb}} + \frac{k_{aq} h_{aq}}{\mu_{aq}} \right)} c_a A_{cw} \frac{\partial p_{aqD}}{\partial t} +$$

$$\underline{\alpha} A_{cw} \left( \frac{\frac{k_{aq} h_{aq}}{\mu_{aq}}}{\frac{k_{fb} h_{fb}}{\mu_{fb}} + \frac{k_{aq} h_{aq}}{\mu_{aq}}} \right) \left( \frac{1}{h} \right)_{aq} (p_{aqD} - p_{fD}) \dots\dots\dots (F-10)$$

We also have the following:

$$\omega_{aq} = \frac{\varphi_{fb} c_f}{(\varphi c_t)_{aq+fb}} \dots\dots\dots (F-11)$$

Substituting  $\omega_{aq}$  in eqn.(F-10) and assuming compressibility is constant, we have:

$$\left(\frac{1}{\varepsilon^2}\right) (1 - \kappa_f) \frac{\partial^2 p_{aqD}}{\partial y_D^2} = (1 - \omega_{aq}) \frac{\partial p_{aqD}}{\partial t_D} + \lambda_{aq} (p_{aqD} - p_{fD}) \dots\dots (F-12)$$

Here expression for dimensionless time and dimensionless interporosity flow parameter, are as:

$$t_D = \frac{\left( \frac{k_{fb} h_{fb}}{\mu_{fb}} + \frac{k_{aq} h_{aq}}{\mu_{aq}} \right) t}{(\varphi_{fb} h_{fb} + \varphi_{aq} h_{aq}) c_f A_{cw}} \dots\dots\dots (F-13a)$$

$$\lambda_{aq} = \underline{\alpha} A_{cw} \left( \frac{\frac{k_{aq}}{\mu_{aq}}}{\frac{k_{fb} h_{fb}}{\mu_{fb}} + \frac{k_{aq} h_{aq}}{\mu_{aq}}} \right) \dots\dots\dots (F-13b)$$

$$\kappa_f = \left( \frac{\frac{k_{fb} h_{fb}}{\mu_{fb}}}{\frac{k_{fb} h_{fb}}{\mu_{fb}} + \frac{k_{aq} h_{aq}}{\mu_{aq}}} \right) \dots\dots\dots (F-13c)$$

Where:  $\underline{\alpha} = \frac{(T_b)_{eff}}{k_{aq}} \dots\dots\dots (F-13d)$

Where:  $(T_b)_{eff} = \left( \frac{1}{\frac{1}{T_b} + \frac{h_{aq}}{3k_{aq}}} \right) \dots\dots\dots (F-13e)$

and:  $T_b = \left( \frac{k_b}{h_b} \right) \dots\dots\dots (F-13f)$

$$p_{aqD} = 2\pi \left( \frac{k_{fb} h_{fb}}{\mu_{fb}} + \frac{k_{aq} h_{aq}}{\mu_{aq}} \right) \frac{p_i - p_{aq}}{q_B} \dots\dots\dots (F-13g)$$

$$p_{fD} = 2\pi \left( \frac{k_{fb} h_{fb}}{\mu_{fb}} + \frac{k_{aq} h_{aq}}{\mu_{aq}} \right) \frac{p_i - p_f}{q_B} \dots\dots\dots (F-13h)$$

The final form of the above equation, since the LHS is zero, is:

$$0 = \varepsilon^2 \left( \frac{1 - \omega_{aq}}{1 - \kappa_f} \right) \frac{\partial p_{aqD}}{\partial t_D} + \varepsilon^2 \left( \frac{\lambda_{aq}}{1 - \kappa_f} \right) (p_{aqD} - p_{fD}) \dots\dots\dots (F-14)$$

Applying the initial condition of aquifer to the Laplace transform equations results in:

$$0 = \varepsilon^2 \left( \frac{1-\omega_{aq}}{1-\kappa_f} \right) s \overline{p_{aqD}} + \varepsilon^2 \left( \frac{\lambda_{aq}}{1-\kappa_f} \right) (\overline{p_{aqD}} - \overline{p_{fD}}) \dots\dots\dots (F-15)$$

Solving eqn.(F-15) for  $\overline{p_{aqD}}$ :

$$\overline{p_{aqD}} = \frac{\lambda_{aq}}{(1-\omega_{aq})s + \lambda_{aq}} \overline{p_{fD}} \dots\dots\dots(F-16)$$

Solution of Matrix (Reservoir)

Substituting  $y_D$  in eqn.(F-5b), we have:

$$\left( \frac{k_{fb} h_{fb}}{\mu_{fb}} + \frac{k_{mb} h_{mb}}{\mu_{mb}} \right) \times \left( \frac{kh}{\mu} \right)_{mb} \frac{\partial^2 p_{mb}}{\partial z_D^2} =$$

$$(\varphi_{fb} h_{fb} + \varphi_{mb} h_{mb})(\varphi h)_{mb} c_m \left( \frac{h_{mb}^2}{4} \right) \frac{\partial p_{mb}}{\partial t} \dots\dots\dots(F-17)$$

Substituting  $p_D$  in above, we have:

$$\left( \frac{k_{fb} h_{fb}}{\mu_{fb}} + \frac{k_{mb} h_{mb}}{\mu_{mb}} \right) \left( \frac{kh}{\mu} \right)_{mb} p_{ch} \frac{\partial^2 (p_{mb} p_{ch} - p_i)}{\partial z_D^2} =$$

$$(\varphi_{fb} h_{fb} + \varphi_{mb} h_{mb})(\varphi h)_{mb} c_m \left( \frac{h_{mb}^2}{4} \right) \frac{\partial (p_{mb} p_{ch} - p_i)}{\partial t}$$

On cancellation of common terms, results in:

$$\left( \frac{kh}{\mu} \right)_{mb} \frac{\partial^2 p_{mbD}}{\partial z_D^2} = \frac{(\varphi_{fb} h_{fb} + \varphi_{mb} h_{mb})}{\left( \frac{k_{fb} h_{fb}}{\mu_{fb}} + \frac{k_{mb} h_{mb}}{\mu_{mb}} \right)} (\varphi h)_{mb} c_m \left( \frac{h_{mb}^2}{4} \right) \frac{\partial p_{mbD}}{\partial t} \dots\dots\dots(F-18)$$

Reapplying eqn.(F-2) to the above we get:

$$\left( \frac{\frac{k_{mb} h_{mb}}{\mu_{mb}}}{\frac{k_{fb} h_{fb}}{\mu_{fb}} + \frac{k_{mb} h_{mb}}{\mu_{mb}}} \right) \frac{\partial^2 p_{mbD}}{\partial z_D^2} = (\varphi h)_{mb} \frac{(\varphi_{fb} h_{fb} + \varphi_{mb} h_{mb})}{\left( \frac{k_{fb} h_{fb}}{\mu_{fb}} + \frac{k_{mb} h_{mb}}{\mu_{mb}} \right)} c_m \left( \frac{h_{mb}^2}{4} \right) \frac{\partial p_{mbD}}{\partial t} \dots\dots\dots(F-19)$$

On simplify the above and putting in additional terms we get:

$$\left( \frac{\frac{k_{mb} h_{mb}}{\mu_{mb}}}{\frac{k_{fb} h_{fb}}{\mu_{fb}} + \frac{k_{mb} h_{mb}}{\mu_{mb}}} \right) \frac{\partial^2 p_{mbD}}{\partial z_D^2} = (\varphi h)_{mb} \frac{(\varphi_{fb} h_{fb} + \varphi_{mb} h_{mb})}{\left( \frac{k_{fb} h_{fb}}{\mu_{fb}} + \frac{k_{mb} h_{mb}}{\mu_{mb}} \right)} c_m \left( \frac{h_{mb}^2}{4} \right) \left( \frac{A_{cw}}{A_{cw}} \right) \left( \frac{\frac{\frac{k_{fb}}{\mu_{fb}}}{\frac{k_{fb} h_{fb}}{\mu_{fb}} + \frac{k_{mb} h_{mb}}{\mu_{mb}}}}{\frac{\frac{k_{fb}}{\mu_{fb}}}{\frac{k_{fb} h_{fb}}{\mu_{fb}} + \frac{k_{mb} h_{mb}}{\mu_{mb}}}} \right) \left( \frac{\frac{\frac{k_{mb}}{\mu_{mb}}}{\frac{k_{fb} h_{fb}}{\mu_{fb}} + \frac{k_{mb} h_{mb}}{\mu_{mb}}}}{\frac{\frac{k_{mb}}{\mu_{mb}}}{\frac{k_{fb} h_{fb}}{\mu_{fb}} + \frac{k_{mb} h_{mb}}{\mu_{mb}}}} \right) \frac{\partial p_{mbD}}{\partial t} \dots\dots\dots (F-20)$$

Converting this equation into aquifer-fracture domain we get:

$$\left( \frac{\frac{k_{mb} h_{mb}}{\mu_{mb}}}{\frac{k_{fb} h_{fb}}{\mu_{fb}} + \frac{k_{mb} h_{mb}}{\mu_{mb}}} \right) \frac{\partial^2 p_{mbD}}{\partial z_D^2} = (\varphi h)_{mb} \frac{(\varphi_{fb} h_{fb} + \varphi_{mb} h_{mb})}{(\varphi_{fb} h_{fb} + \varphi_{aq} h_{aq})} \frac{\left( \frac{k_{fb} h_{fb}}{\mu_{fb}} + \frac{k_{aq} h_{aq}}{\mu_{aq}} \right)}{\left( \frac{k_{fb} h_{fb}}{\mu_{fb}} + \frac{k_{mb} h_{mb}}{\mu_{mb}} \right)} \frac{(\varphi_{fb} h_{fb} + \varphi_{aq} h_{aq})}{\left( \frac{k_{fb} h_{fb}}{\mu_{fb}} + \frac{k_{aq} h_{aq}}{\mu_{aq}} \right)} c_m \left( \frac{h_{mb}^2}{4} \right) \left( \frac{A_{cw}}{A_{cw}} \right) \times \left( \frac{\frac{\frac{k_{fb}}{\mu_{fb}}}{\frac{k_{fb} h_{fb}}{\mu_{fb}} + \frac{k_{mb} h_{mb}}{\mu_{mb}}}}{\frac{\frac{k_{fb}}{\mu_{fb}}}{\frac{k_{fb} h_{fb}}{\mu_{fb}} + \frac{k_{mb} h_{mb}}{\mu_{mb}}}} \right) \left( \frac{\frac{\frac{k_{mb}}{\mu_{mb}}}{\frac{k_{fb} h_{fb}}{\mu_{fb}} + \frac{k_{mb} h_{mb}}{\mu_{mb}}}}{\frac{\frac{k_{mb}}{\mu_{mb}}}{\frac{k_{fb} h_{fb}}{\mu_{fb}} + \frac{k_{mb} h_{mb}}{\mu_{mb}}}} \right) \frac{\partial p_{mbD}}{\partial t} \dots\dots\dots(F-21)$$

We also have the following:

$$\omega = \frac{\varphi_{fb} c_f}{(\varphi c_t)_{mb+fb}} \dots\dots\dots (F-22a)$$

$$\Lambda = \left( \frac{\omega_{aq}}{\omega} \right) = \frac{(\varphi_{fb} h_{fb} + \varphi_{mb} h_{mb})}{(\varphi_{fb} h_{fb} + \varphi_{aq} h_{aq})} \dots\dots\dots (F-22b)$$

Substituting  $\omega$  in eqn.(F-9) and assuming compressibility is constant, we have:

$$(1 - \kappa_{fb}) \frac{\partial^2 p_{mbD}}{\partial z_D^2} = \frac{3(1-\omega)}{\lambda} (\Lambda) \left( \frac{\kappa_{fb}}{\kappa_f} \right) \frac{\partial p_{mbD}}{\partial t_D} \dots\dots\dots (F-23)$$

Here dimensionless time and dimensionless interporosity flow parameter and others, are:

$$t_{bD} = \frac{\left( \frac{k_{fb} h_{fb}}{\mu_{fb}} + \frac{k_{aq} h_{aq}}{\mu_{aq}} \right) t}{(\varphi_{fb} h_{fb} + \varphi_{aq} h_{aq}) c_f A_{cw}} = \left( \frac{\kappa_f}{\kappa_{fb}} \right) \left( \frac{1}{\Lambda} \right) t_D \dots\dots\dots (F-24a)$$

$$\lambda = \frac{12}{h_m^2} A_{cw} \frac{\left( \frac{\frac{k_{mb}}{\mu_{mb}}}{\frac{k_{fb} h_{fb}}{\mu_{fb}} + \frac{k_{mb} h_{mb}}{\mu_{mb}}} \right)}{\left( \frac{\frac{k_{fb}}{\mu_{fb}}}{\frac{k_{fb} h_{fb}}{\mu_{fb}} + \frac{k_{mb} h_{mb}}{\mu_{mb}}} \right)} \dots\dots\dots (F-24b)$$

$$\kappa_{fb} = \left( \frac{\frac{k_{fb} h_{fb}}{\mu_{fb}}}{\frac{k_{fb} h_{fb}}{\mu_{fb}} + \frac{k_{aq} h_{aq}}{\mu_{aq}}} \right) \dots\dots\dots (F-24c)$$

$$p_{mbD} = 2\pi \left( \frac{k_{fb} h_{fb}}{\mu_{fb}} + \frac{k_{mb} h_{mb}}{\mu_{mb}} \right) \frac{p_i - p_{mb}}{qB} \dots\dots\dots (F-24d)$$

$$p_{fbD} = 2\pi \left( \frac{k_{fb} h_{fb}}{\mu_{fb}} + \frac{k_{mb} h_{mb}}{\mu_{mb}} \right) \frac{p_i - p_{fb}}{qB} \dots\dots\dots (F-24e)$$

The final form of the above equation, is:

$$\left( \frac{1}{\varepsilon^2} \right) (1 - \kappa_{fb}) \nabla^2 p_{mbD} = \frac{3(1-\omega)}{\lambda} (\Lambda) \left( \frac{\kappa_{fb}}{\kappa_f} \right) \frac{\partial p_{mbD}}{\partial t_D} \dots\dots\dots (F-25)$$

Let us find the solution of eqn.(F-13) for  $\overline{p_{aqD}}$  first. For aquifer block and in Laplace domain, the initial and boundary conditions are:

Initial Condition:  $\overline{p_{mbD}}(z_D = 1, s \rightarrow \infty) = 0$ .....(F-26a)

Inner Boundary Condition:  $\left. \frac{d\overline{p_{mbD}}}{dz_D} \right|_{z_D=0} = 0$  .....(F-26b)

Outer Boundary Condition:  $\overline{p_{mbD}}|_{z_D=1} = \overline{p_{fbD}}$  .....(F-26c)

Applying the initial condition of aquifer to the Laplace transform equations results in:

$$\left(\frac{1}{\varepsilon^2}\right) (1 - \kappa_f) \frac{\partial^2 \overline{p_{mbD}}}{\partial z_D^2} = \frac{3(1-\omega)}{\lambda} (\Lambda) \left(\frac{\kappa_{fb}}{\kappa_f}\right) \{s\overline{p_{mbD}} - \overline{p_{mbD}}(z_D, 0)\}$$

$$\frac{\partial^2 \overline{p_{mbD}}}{\partial z_D^2} - \varepsilon^2 \left(\frac{3(1-\omega)}{\lambda} (\Lambda) \left(\frac{\kappa_{fb}}{\kappa_f}\right)\right) s\overline{p_{mbD}} = 0$$
 .....(F-27)

The above is a homogeneous partial differential equation with the following general solution:

$$\overline{p_{mbD}} = A \cosh\left(z_D \sqrt{s \left(\frac{3(1-\omega)}{\lambda} (\Lambda) \left(\frac{\kappa_{fb}}{\kappa_f}\right)\right)}\right) + B \sinh\left(z_D \sqrt{s \left(\frac{3(1-\omega)}{\lambda} (\Lambda) \left(\frac{\kappa_{fb}}{\kappa_f}\right)\right)}\right)$$
 .....(F-28)

Differentiating with respect to  $z_D$  and using the inner boundary condition, we have:

$$\left. \frac{d\overline{p_{mbD}}}{dz_D} \right|_{z_D=0} = 0 = \sqrt{s \left( \frac{3(1-\omega)}{\lambda} (\Lambda) \left( \frac{\kappa_{fb}}{\kappa_f} \right) \right)} A \sinh \left( z_D \sqrt{s \left( \frac{3(1-\omega)}{\lambda} (\Lambda) \left( \frac{\kappa_{fb}}{\kappa_f} \right) \right)} \right) + \sqrt{s \left( \frac{3(1-\omega)}{\lambda} (\Lambda) \left( \frac{\kappa_{fb}}{\kappa_f} \right) \right)} B \cosh \left( z_D \sqrt{s \left( \frac{3(1-\omega)}{\lambda} (\Lambda) \left( \frac{\kappa_{fb}}{\kappa_f} \right) \right)} \right)$$

Since  $\sinh z_D|_{z_D=0} = 0$ , implies:

$$B = 0 \dots\dots\dots(F-29)$$

Using outer boundary condition and substituting eqn.(F-26c) in eqn.(F-28) we have:

$$\overline{p_{fbD}} = A \cosh \left( z_D \sqrt{s \left( \frac{3(1-\omega)}{\lambda} (\Lambda) \left( \frac{\kappa_{fb}}{\kappa_f} \right) \right)} \right) \Big|_{z_D=1}$$

$$A = \frac{\overline{p_{fbD}}}{\cosh \left( \sqrt{s \left( \frac{3(1-\omega)}{\lambda} (\Lambda) \left( \frac{\kappa_{fb}}{\kappa_f} \right) \right)} \right)} \dots\dots\dots(F-30)$$

Hence the particular solution for constant rate of eqn.(F-27) in Laplace domain is:

$$\overline{p_{mbD}} = \frac{\overline{p_{fbD}}}{\cosh \left( \sqrt{s \left( \frac{3(1-\omega)}{\lambda} (\Lambda) \left( \frac{\kappa_{fb}}{\kappa_f} \right) \right)} \right)} \cosh \left( z_D \sqrt{s \left( \frac{3(1-\omega)}{\lambda} (\Lambda) \left( \frac{\kappa_{fb}}{\kappa_f} \right) \right)} \right) \dots\dots(F-31)$$

Solution of Fracture

There are two different dimensionless pressures. The dimensionless pressure which is reservoir matrix-fracture domain based and dimensionless pressure which is aquifer-fracture domain based. We know dimensionless time measurement is based on latter and this is the reason for normalizing everything on that domain. We have the two equations as:

$$\overline{p_{aqD}} = \frac{\lambda_{aq}}{(1-\omega_{aq})s + \lambda_{aq}} \overline{p_{fD}} \dots\dots\dots(F-16)$$

$$\overline{p_{mbD}} = \frac{\overline{p_{fbdD}}}{\cosh\left(\sqrt{s\left(\frac{3(1-\omega)}{\lambda}(\Lambda)\left(\frac{\kappa_{fb}}{\kappa_f}\right)\right)}\right)} \cosh\left(z_D \sqrt{s\left(\frac{3(1-\omega)}{\lambda}(\Lambda)\left(\frac{\kappa_{fb}}{\kappa_f}\right)\right)}\right) \dots\dots(F-31)$$

We also know fracture domains are the same:

$$\frac{\overline{p_{fbdD}}}{\left(\frac{k_{fb} h_{fb}}{\mu_{fb}} + \frac{k_{mb} h_{mb}}{\mu_{mb}}\right)} = \frac{\overline{p_{fD}}}{\left(\frac{k_{fb} h_{fb}}{\mu_{fb}} + \frac{k_{aq} h_{aq}}{\mu_{aq}}\right)}$$

$$\overline{p_{fbdD}} = \left(\frac{\kappa_{fb}}{\kappa_f}\right) \overline{p_{fD}} \dots\dots\dots(F-32)$$



Again, for the fracture we have:

$$\begin{aligned} & \left( \frac{k_{fb} h_{fb}}{\mu_{fb}} + \frac{k_{aq} h_{aq}}{\mu_{aq}} \right) \left( \frac{kh}{\mu} \right)_{fb} \frac{\partial^2 p_{fb}}{\partial y^2} = \\ & (\varphi_{fb} h_{fb} + \varphi_{aq} h_{aq}) (\varphi h)_{fb} c_f \frac{\partial p_{fb}}{\partial t} - \underline{\alpha} \left( \frac{k_{fb} h_{fb}}{\mu_{fb}} + \frac{k_{aq} h_{aq}}{\mu_{aq}} \right) \left( \frac{kh}{\mu} \right)_{aq} \left( \frac{1}{h} \right)_{aq} (p_{aq} - \\ & p_{fb}) - \left( \frac{k_{fb} h_{fb}}{\mu_{fb}} + \frac{k_{mb} h_{mb}}{\mu_{mb}} \right) \left( \frac{kh}{\mu} \right)_{mb} \left( \frac{1}{h^2/2} \right)_{mb} \frac{\partial p_{mb}}{\partial z} \Big|_{z=h_{mb}/2} \dots \dots \dots (F-5a) \end{aligned}$$

Substituting  $y_D$  in eqn.(F-5a), we have:

$$\begin{aligned} & \left( \frac{k_{fb} h_{fb}}{\mu_{fb}} + \frac{k_{aq} h_{aq}}{\mu_{aq}} \right) \left( \frac{kh}{\mu} \right)_{fb} \frac{\partial^2 p_{fb}}{\partial y_D^2} = (\varphi_{fb} h_{fb} + \varphi_{aq} h_{aq}) (\varphi h)_{fb} c_f A_{cw} \frac{\partial p_{fb}}{\partial t} - \\ & \underline{\alpha} A_{cw} \left( \frac{k_{fb} h_{fb}}{\mu_{fb}} + \frac{k_{aq} h_{aq}}{\mu_{aq}} \right) \left( \frac{kh}{\mu} \right)_{aq} \left( \frac{1}{h} \right)_{aq} (p_{aq} - p_{fb}) - \\ & \left( \frac{k_{fb} h_{fb}}{\mu_{fb}} + \frac{k_{mb} h_{mb}}{\mu_{mb}} \right) \left( \frac{kh}{\mu} \right)_{mb} \left( \frac{A_{cw}}{h^2/2} \right)_{mb} \frac{\partial p_{mb}}{\partial z} \Big|_{z=h_{mb}/2} \end{aligned}$$

Substituting  $p_D$  in eqn.(F-5a), we have:

$$\begin{aligned} & \left( \frac{k_{fb} h_{fb}}{\mu_{fb}} + \frac{k_{aq} h_{aq}}{\mu_{aq}} \right) \left( \frac{kh}{\mu} \right)_{fb} \frac{\partial^2 (p_{fD} p_{ch} - p_i)}{\partial y_D^2} = \\ & (\varphi_{fb} h_{fb} + \varphi_{aq} h_{aq}) \times (\varphi h)_{fb} c_f A_{cw} \frac{\partial (p_{fD} p_{ch} - p_i)}{\partial t} - \\ & \underline{\alpha} A_{cw} \left( \frac{k_{fb} h_{fb}}{\mu_{fb}} + \frac{k_{aq} h_{aq}}{\mu_{aq}} \right) \left( \frac{kh}{\mu} \right)_{aq} \left( \frac{1}{h} \right)_{aq} \{ (p_{aqD} p_{ch} - p_i) - (p_{fD} p_{ch} - p_i) \} - \\ & \left( \frac{k_{fb} h_{fb}}{\mu_{fb}} + \frac{k_{mb} h_{mb}}{\mu_{mb}} \right) \left( \frac{kh}{\mu} \right)_{mb} \times \left( \frac{A_{cw}}{h^2/2} \right)_{mb} \frac{\partial (p_{mb} p_{ch} - p_i)}{\partial z} \Big|_{z=h_{mb}/2} \end{aligned}$$

Rearranging and canceling common terms results in:

$$\left(\frac{kh}{\mu}\right)_{fb} \frac{\partial^2 p_{fD}}{\partial y_D^2} =$$

$$(\varphi h)_{fb} \frac{(\varphi_{fb} h_{fb} + \varphi_{aq} h_{aq})}{\left(\frac{k_{fb} h_{fb}}{\mu_{fb}} + \frac{k_{aq} h_{aq}}{\mu_{aq}}\right)} c_f A_{cw} \frac{\partial p_{fD}}{\partial t} - \underline{\alpha} A_{cw} \left(\frac{kh}{\mu}\right)_{aq} \left(\frac{1}{h}\right)_{aq} (p_{aqD} - p_{fD}) -$$

$$\frac{\left(\frac{k_{fb} h_{fb}}{\mu_{fb}} + \frac{k_{mb} h_{mb}}{\mu_{mb}}\right)}{\left(\frac{k_{fb} h_{fb}}{\mu_{fb}} + \frac{k_{aq} h_{aq}}{\mu_{aq}}\right)} \left(\frac{kh}{\mu}\right)_{mb} \left(\frac{A_{cw}}{h^2/2}\right)_{mb} \frac{\partial p_{mbD}}{\partial z} \Big|_{z=h_{mb}/2}$$

Substituting back eqns. (F-2a) to eqn.(F-2h) into the above eqn. we get:

$$\left(\frac{\frac{k_{fb} h_{fb}}{\mu_{fb}}}{\frac{k_{fb} h_{fb}}{\mu_{fb}} + \frac{k_{aq} h_{aq}}{\mu_{aq}}}\right) \frac{\partial^2 p_{fD}}{\partial y_D^2} = \left(\frac{\varphi_{fb} h_{fb}}{\varphi_{fb} h_{fb} + \varphi_{aq} h_{aq}}\right) \frac{(\varphi_{fb} h_{fb} + \varphi_{aq} h_{aq})}{\left(\frac{k_{fb} h_{fb}}{\mu_{fb}} + \frac{k_{aq} h_{aq}}{\mu_{aq}}\right)} c_f A_{cw} \frac{\partial p_{fD}}{\partial t} -$$

$$\underline{\alpha} A_{cw} \left(\frac{\frac{k_{aq} h_{aq}}{\mu_{aq}}}{\frac{k_{fb} h_{fb}}{\mu_{fb}} + \frac{k_{aq} h_{aq}}{\mu_{aq}}}\right) \left(\frac{1}{h}\right)_{aq} (p_{aqD} - p_{fD}) -$$

$$\frac{\left(\frac{k_{fb} h_{fb}}{\mu_{fb}} + \frac{k_{mb} h_{mb}}{\mu_{mb}}\right)}{\left(\frac{k_{fb} h_{fb}}{\mu_{fb}} + \frac{k_{aq} h_{aq}}{\mu_{aq}}\right)} \left(\frac{\frac{k_{mb} h_{mb}}{\mu_{mb}}}{\frac{k_{fb} h_{fb}}{\mu_{fb}} + \frac{k_{mb} h_{mb}}{\mu_{mb}}}\right) \left(\frac{A_{cw}}{h^2/2}\right)_{mb} \frac{\partial p_{mbD}}{\partial z} \Big|_{z=h_{mb}/2}$$

Introducing some additional terms, normalizing other terms and  $h_{fb} = h_{mb}$  we have:

$$\left( \frac{\frac{k_{fb} h_{fb}}{\mu_{fb}}}{\frac{k_{fb} h_{fb}}{\mu_{fb}} + \frac{k_{aq} h_{aq}}{\mu_{aq}}} \right) \frac{\partial^2 p_{fD}}{\partial y_D^2} = \left( \frac{\varphi_{fb} h_{fb}}{\varphi_{fb} h_{fb} + \varphi_{aq} h_{aq}} \right) \left( \frac{\varphi_{fb} h_{fb} + \varphi_{aq} h_{aq}}{\frac{k_{fb} h_{fb}}{\mu_{fb}} + \frac{k_{aq} h_{aq}}{\mu_{aq}}} \right) c_f A_{cw} \frac{\partial p_{fD}}{\partial t} -$$

$$\underline{\alpha} A_{cw} \left( \frac{\frac{k_{aq} h_{aq}}{\mu_{aq}}}{\frac{k_{fb} h_{fb}}{\mu_{fb}} + \frac{k_{aq} h_{aq}}{\mu_{aq}}} \right) \left( \frac{1}{h} \right)_{aq} (p_{aqD} - p_{fD}) -$$

$$\left( \frac{\frac{k_{fb} h_{fb}}{\mu_{fb}} + \frac{k_{mb} h_{mb}}{\mu_{mb}}}{\frac{k_{fb} h_{fb}}{\mu_{fb}} + \frac{k_{aq} h_{aq}}{\mu_{aq}}} \right) \left( \frac{\frac{k_{fb} h_{fb}}{\mu_{fb}}}{\frac{k_{fb} h_{fb}}{\mu_{fb}}} \right) \left( \frac{\frac{k_{mb} h_{mb}}{\mu_{mb}}}{\frac{k_{fb} h_{fb}}{\mu_{fb}} + \frac{k_{mb} h_{mb}}{\mu_{mb}}} \right) \left( \frac{A_{cw}}{h^3/4} \right)_{mb} \frac{\partial p_{mbD}}{\partial z_D} \Big|_{z_D=1}$$

The resultant form of the governing differential equations is:

$$\kappa_f \frac{\partial^2 p_{fD}}{\partial y_D^2} = \omega_{aq} \frac{\partial p_{fD}}{\partial t} - \lambda_{aq} (p_{aqD} - p_{fD}) - \left( \frac{\lambda}{3} \right) (\kappa_f) \frac{\partial p_{mbD}}{\partial z_D} \Big|_{z_D=1}$$

The final form of the governing differential equations is:

$$\nabla^2 p_{fD} = \left( \frac{\omega_{aq}}{\kappa_f} \right) \frac{\partial p_{fD}}{\partial t} - \left( \frac{\lambda_{aq}}{\kappa_f} \right) (p_{aqD} - p_{fD}) - \left( \frac{\lambda}{3} \right) \frac{\partial p_{mbD}}{\partial z_D} \Big|_{z_D=1} \dots\dots(F-33)$$

Taking Laplace transform of the above equation:

$$\frac{d^2 \overline{p_{fD}}}{dy_D^2} = \left( \frac{\omega_{aq}}{\kappa_f} \right) \{ s \overline{p_{fD}} - \overline{p_{fD}}(y_D, 0) \} - \left( \frac{\lambda_{aq}}{\kappa_f} \right) \{ \overline{p_{aqD}} - \overline{p_{fD}} \} - \left( \frac{\lambda}{3} \right) \frac{\partial \overline{p_{mbD}}}{\partial z_D} \Big|_{z_D=1} \dots\dots(F-34)$$

For a closed reservoir the initial and boundary conditions, for fracture are:

$$\text{Initial Condition: } \overline{p_{fD}}(y_D, s) = 0 \dots\dots\dots (\text{F-35a})$$

$$\text{Inner Boundary Condition: } \left. \frac{d\overline{p_{fD}}}{dy_D} \right|_{y_D=0} = -\frac{2\pi}{s} \dots\dots\dots (\text{F-35b})$$

$$\text{Outer Boundary Condition: } \left. \frac{d\overline{p_{fD}}}{dy_D} \right|_{y_D=y_{De}} = 0 \dots\dots\dots (\text{F-35c})$$

Applying initial condition, we have:

$$\frac{d^2\overline{p_{fD}}}{dy_D^2} = \left(\frac{\omega_{aq}}{\kappa_f}\right) \{s\overline{p_{fD}}\} - \left(\frac{\lambda_{aq}}{\kappa_f}\right) \{\overline{p_{aqD}} - \overline{p_{fD}}\} - \left(\frac{\lambda}{3}\right) \left. \frac{\partial \overline{p_{mbD}}}{\partial z_D} \right|_{z_D=1} \dots\dots\dots (\text{F-36})$$

But from eqn.(F-31) we have

$$\left. \frac{\partial \overline{p_{mbD}}}{\partial z_D} \right|_{z_D=1} = \frac{\sqrt{s \left( \frac{3(1-\omega)}{\lambda} (\Lambda) \left( \frac{\kappa_{fb}}{\kappa_f} \right) \right)}}{\cosh \left( \sqrt{s \left( \frac{3(1-\omega)}{\lambda} (\Lambda) \left( \frac{\kappa_{fb}}{\kappa_f} \right) \right)} \right)} \sinh \left( \sqrt{s \left( \frac{3(1-\omega)}{\lambda} (\Lambda) \left( \frac{\kappa_{fb}}{\kappa_f} \right) \right)} \right) \overline{p_{fbD}}$$

This derivative will change sign when expressed in terms of  $\overline{p_{fD}}$ , and using eqn.(F-34)

we have:

$$\begin{aligned} \frac{d^2\overline{p_{fD}}}{dy_D^2} = & \left(\frac{\omega_{aq}}{\kappa_f}\right) \{s\overline{p_{fD}}\} + \left(\frac{\lambda_{aq}}{\kappa_f}\right) \left\{ \frac{\lambda_{aq}}{(1-\omega_{aq})s + \lambda_{aq}} \overline{p_{fD}} - \overline{p_{fD}} \right\} + \\ & \left(\frac{\lambda}{3}\right) \sqrt{s \left( \frac{3(1-\omega)}{\lambda} (\Lambda) \left( \frac{\kappa_{fb}}{\kappa_f} \right) \right)} \tanh \left( \sqrt{s \left( \frac{3(1-\omega)}{\lambda} (\Lambda) \left( \frac{\kappa_{fb}}{\kappa_f} \right) \right)} \right) \overline{p_{fbD}} \end{aligned}$$

Using eqn.(F-32), converting everything into consistent aquifer-fracture domain, we have:

$$\frac{d^2 \overline{p}_{fD}}{dy_D^2} = \left[ \left( \frac{\omega_{aq}}{\kappa_f} \right) + \left( \frac{\lambda}{3s} \right) \sqrt{s \left( \frac{3(1-\omega)}{\lambda} (\Lambda) \left( \frac{\kappa_{fb}}{\kappa_f} \right) \right)} \tanh \left( \sqrt{s \left( \frac{3(1-\omega)}{\lambda} (\Lambda) \left( \frac{\kappa_{fb}}{\kappa_f} \right) \right)} \right) + \right. \\ \left. \left( \frac{\lambda_{aq}}{\kappa_f} \right) \left\{ \frac{(1-\omega_{aq})}{(1-\omega_{aq})s + \lambda_{aq}} \right\} \right] \{s \overline{p}_{fD}\} \dots\dots\dots(F-37)$$

This is of the form:

$$\frac{d^2 \overline{p}_{fD}}{dy_D^2} - sf(s) \overline{p}_{fD} = 0 \dots\dots\dots(F-38)$$

Where,

$$f(s) = \left[ \left( \frac{\omega_{aq}}{\kappa_f} \right) + \left( \frac{\lambda}{3s} \right) \sqrt{s \left( \frac{3(1-\omega)}{\lambda} (\Lambda) \left( \frac{\kappa_{fb}}{\kappa_f} \right) \right)} \tanh \left( \sqrt{s \left( \frac{3(1-\omega)}{\lambda} (\Lambda) \left( \frac{\kappa_{fb}}{\kappa_f} \right) \right)} \right) + \left( \frac{\lambda_{aq}}{\kappa_f} \right) \left\{ \frac{(1-\omega_{aq})}{(1-\omega_{aq})s + \lambda_{aq}} \right\} \right] \dots(F-39a)$$

$$f(s) = \omega \left[ \left( \frac{\omega_{aq}}{\kappa_f} \right) + \left( \frac{1}{3s} \right) \left( \frac{\lambda}{\omega} \right) \sqrt{3s \left( \frac{1-\omega}{\omega} \right) (\Lambda) \left( \frac{\kappa_{fb}}{\kappa_f} \right) \left( \frac{\omega}{\lambda} \right)} \tanh \left( \sqrt{3s \left( \frac{1-\omega}{\omega} \right) (\Lambda) \left( \frac{\kappa_{fb}}{\kappa_f} \right) \left( \frac{\omega}{\lambda} \right)} \right) \right] + \\ \left( \frac{\lambda_{aq}}{\kappa_f} \right) \left\{ \frac{(1-\omega_{aq})}{(1-\omega_{aq})s + \lambda_{aq}} \right\} \dots\dots\dots(F-39b)$$

Eqn.(F-38) is a homogeneous partial differential equation which is the same as eqn.(A-17). Refer to Appendix A for the rest of the derivation.

APPENDIX G: TRANSIENT AQUIFER FRACTURED DUAL PERMEABILITY

DUAL MOBILITY MODEL – FORMULATION AND LAPLACE DOMAIN

SOLUTION

The governing differential equation for linear fluid flow in limited aquifer (matrix block) and the fractured reservoir (reservoir fracture block and reservoir matrix block) is given by:

$$\text{Fracture: } \left(\frac{kh}{\mu}\right)_f \nabla^2 p_f = \varphi_f c_f h_f \frac{\partial p_f}{\partial t} - \left(\frac{k}{\mu h}\right)_a \frac{\partial p_a}{\partial y_a} \Big|_{y_{aq}=h_{aq}} - \alpha \left(\frac{k}{\mu}\right)_m (p_m - p_f) \dots \text{(G-1a)}$$

$$\text{Matrix (Aquifer): } \left(\frac{kh}{\mu}\right)_a \nabla^2 p_a = \varphi_a c_a h_a \frac{\partial p_a}{\partial t} \dots \text{(G-1b)}$$

$$\text{Matrix (Reservoir): } \left(\frac{kh}{\mu}\right)_m \nabla^2 p_m = \varphi_m c_m h_m \frac{\partial p_m}{\partial t} + \alpha \left(\frac{k}{\mu}\right)_m (p_m - p_f) \dots \text{(G-1c)}$$

Since the aquifer is limited, the aquifer height is related to the linear dimension of reservoir ( $y$  is a lateral dimension in the fractured reservoir and  $y_{aq}$  is vertical dimension in the aquifer) by:

$$y_{aq} = h_{aq} = \varepsilon y \dots \text{(G-1d)}$$

The second term in eqn.(G-1a) is referred to as the source terms,  $\sigma_a$  and  $\sigma_m$ . The reservoir matrix is in pseudosteady state but aquifer is in transient. Also, all properties need to be put as bulk properties:

Aquifer:

$$\left(\frac{kh}{\mu}\right)_{aq} = \frac{k_a h_a}{\mu_a} \left(\frac{V_a}{V_{f+a}}\right) = \left(\frac{\frac{k_{aq} h_{aq}}{\mu_{aq}}}{\frac{k_{fb} h_{fb}}{\mu_{fb}} + \frac{k_{aq} h_{aq}}{\mu_{aq}}}\right) \dots\dots\dots (G-2a)$$

$$\left(\frac{kh}{\mu}\right)_f = \frac{k_f h_f}{\mu_f} \left(\frac{V_f}{V_{f+a}}\right) = \left(\frac{\frac{k_{fb} h_{fb}}{\mu_{fb}}}{\frac{k_{fb} h_{fb}}{\mu_{fb}} + \frac{k_{aq} h_{aq}}{\mu_{aq}}}\right) \dots\dots\dots (G-2b)$$

$$(\varphi h)_{aq} = \left(\frac{V_{aq}}{V_{f+aq}}\right) = \left(\frac{\varphi_{aq} h_{aq}}{\varphi_{fb} h_{fb} + \varphi_{aq} h_{aq}}\right) \dots\dots\dots (G-2c)$$

$$(\varphi h)_f = \left(\frac{V_f}{V_{f+aq}}\right) = \left(\frac{\varphi_{fb} h_{fb}}{\varphi_{fb} h_{fb} + \varphi_{aq} h_{aq}}\right) \dots\dots\dots (G-2d)$$

Reservoir:

$$\left(\frac{kh}{\mu}\right)_{mb} = \frac{k_m}{\mu_m} \left(\frac{V_m}{V_{f+m}}\right) = \left(\frac{\frac{k_{mb} h_{mb}}{\mu_{mb}}}{\frac{k_{fb} h_{fb}}{\mu_{fb}} + \frac{k_{mb} h_{mb}}{\mu_{mb}}}\right) \dots\dots\dots (G-2e)$$

$$\left(\frac{kh}{\mu}\right)_{fb} = \frac{k_f}{\mu_f} \left(\frac{V_f}{V_{f+m}}\right) = \left(\frac{\frac{k_{fb} h_{fb}}{\mu_{fb}}}{\frac{k_{fb} h_{fb}}{\mu_{fb}} + \frac{k_{mb} h_{mb}}{\mu_{mb}}}\right) \dots\dots\dots (G-2f)$$

$$(\varphi h)_{mb} = \left(\frac{V_m}{V_{f+m}}\right) = \left(\frac{\varphi_{mb} h_{mb}}{\varphi_{fb} h_{fb} + \varphi_{mb} h_{mb}}\right) \dots\dots\dots (G-2g)$$

$$(\varphi h)_{fb} = \left(\frac{V_f}{V_{f+m}}\right) = \left(\frac{\varphi_{fb} h_{fb}}{\varphi_{fb} h_{fb} + \varphi_{mb} h_{mb}}\right) \dots\dots\dots (G-2h)$$

Similarly, the aquifer and matrix fracture bulk source terms are,  $\sigma_{aq}$ , and  $\sigma_{mf}$ , is expressed as:

$$\sigma_{aq} = \sigma_a \left( \frac{V_a}{V_{f+a}} \right) = \left( \frac{k}{\mu h/2} \right)_a \frac{\partial p_a}{\partial y_a} \Big|_{y_a=h_a} = \left( \frac{k_{fb} h_{fb}}{\mu_{fb}} + \frac{k_{aq} h_{aq}}{\mu_{aq}} \right) \left( \frac{kh}{\mu} \right)_{aq} \left( \frac{1}{h^2/2} \right)_{aq} \frac{\partial p_{aq}}{\partial y_{aq}} \Big|_{y_{aq}=h_{aq}} \dots\dots (G-3a)$$

$$\sigma_{mf} = \sigma_m \left( \frac{V_m}{V_{f+m}} \right) = \alpha \frac{k_m}{\mu} \left( \frac{V_m}{V_{f+m}} \right) (p_{mb} - p_{fb}) = \alpha \left( \frac{k_{fb} h_{fb}}{\mu_{fb}} + \frac{k_{mb} h_{mb}}{\mu_{mb}} \right) \left( \frac{kh}{\mu} \right)_{mb} \left( \frac{1}{h} \right)_{mb} (p_{mb} - p_{fb}) \dots\dots (G-3b)$$

Here, the assumption is, the aquifer transient effect is restricted to the permeable barrier and:

$$k_{aq} = \frac{(h_a + h_b)}{\left( \frac{h_b}{k_b} + \frac{h_a}{k_a} \right)} \quad (h_a \gg h_b, k_b \gg k_a) \dots\dots\dots (G-4)$$



In terms of bulk properties the governing equations can be recast into:

Fracture:

$$\left(\frac{k_{fb} h_{fb}}{\mu_{fb}} + \frac{k_{aq} h_{aq}}{\mu_{aq}}\right) \left(\frac{kh}{\mu}\right)_{fb} \frac{\partial^2 p_{fb}}{\partial y^2} =$$

$$(\varphi_{fb} h_{fb} + \varphi_{aq} h_{aq})(\varphi h)_{fb} c_f \frac{\partial p_{fb}}{\partial t} -$$

$$\left(\frac{1}{\varepsilon}\right) \left(\frac{k_{fb} h_{fb}}{\mu_{fb}} + \frac{k_{aq} h_{aq}}{\mu_{aq}}\right) \left(\frac{kh}{\mu}\right)_{aq} \left(\frac{1}{h^2/2}\right)_{aq} \frac{\partial p_{aq}}{\partial y} \Big|_{y_{aq}=h_{aq}} -$$

$$\alpha \left(\frac{k_{fb} h_{fb}}{\mu_{fb}} + \frac{k_{mb} h_{mb}}{\mu_{mb}}\right) \left(\frac{kh}{\mu}\right)_{mb} \left(\frac{1}{h}\right)_{mb} (p_{mb} - p_{fb}) \dots \dots \dots (G-5a)$$

Matrix (Aquifer):

$$\left(\frac{1}{\varepsilon^2}\right) \left(\frac{k_{fb} h_{fb}}{\mu_{fb}} + \frac{k_{aq} h_{aq}}{\mu_{aq}}\right) \left(\frac{kh}{\mu}\right)_{aq} \frac{\partial^2 p_{aq}}{\partial y^2} = (\varphi_{fb} h_{fb} + \varphi_{aq} h_{aq})(\varphi h)_{aq} c_a \frac{\partial p_{aq}}{\partial t} \dots \dots (G-5b)$$

Matrix (Reservoir):

$$\left(\frac{k_{fb} h_{fb}}{\mu_{fb}} + \frac{k_{mb} h_{mb}}{\mu_{mb}}\right) \left(\frac{kh}{\mu}\right)_{mb} \frac{\partial^2 p_{mb}}{\partial z^2} = (\varphi_{fb} h_{fb} + \varphi_{mb} h_{mb})(\varphi h)_{mb} c_m \frac{\partial p_{mb}}{\partial t} +$$

$$\left(\frac{k_{fb} h_{fb}}{\mu_{fb}} + \frac{k_{mb} h_{mb}}{\mu_{mb}}\right) \left(\frac{kh}{\mu}\right)_{mb} \left(\frac{1}{h}\right)_{mb} (p_{mb} - p_{fb}) \dots \dots \dots (G-5c)$$

For an aquifer block, the initial and boundary conditions are:

Initial Condition:  $p_{aq}(y_{aq}, t = 0) = p_i \dots \dots \dots (G-6a)$

Inner Boundary Condition:  $\frac{\partial p_{aq}}{\partial y_{aq}} \Big|_{y_{aq}=0} = 0$  for all t  $\dots \dots \dots (G-6b)$

Outer Boundary Condition:  $p_{aq} \Big|_{y_{aq}=h_{aq}} = p_f$  for all t  $\dots \dots \dots (G-6c)$

For a fracture block, the initial and boundary conditions are:

Initial Condition:  $p_f(x, t = 0) = p_i$  ..... (G-6d)

Inner Boundary Condition:  $q = -\left(\frac{k_f A_{cw}}{\mu}\right) \frac{\partial p_f}{\partial x} \Big|_{x=0}$  for all t and const. rate .. (G-6e)

Outer Boundary Condition  $\frac{\partial p_f}{\partial x} \Big|_{x=x_e} = 0$  for all t ..... (G-6f)

If we assume  $y$  is the overall linear dimension and define dimensionless variables as:

$$y_D = \frac{y}{\sqrt{A_{cw}}} \text{ for all fracture ..... (G-7a)}$$

$$\varepsilon y_D = \frac{\varepsilon y}{h_{aq}} \text{ for all aquifer ..... (G-7b)}$$

$$z_D = \frac{z}{\sqrt{A_{cw}}} \text{ for all matrix ..... (G-7c)}$$

$$p_{jD} = \frac{p_i - p}{p_{ch}} = \frac{2\pi}{\alpha_1 q B} \left( \frac{k_{fb} h_{fb}}{\mu_{fb}} + \frac{k_{aq} h_{aq}}{\mu_{aq}} \right) (p_i - p_j) \Big|_{j=f \text{ or } aq} \text{ ..... (G-7d)}$$

$$p_{jD} = \frac{p_i - p}{p_{ch}} = \frac{2\pi}{\alpha_1 q B} \left( \frac{k_{fb} h_{fb}}{\mu_{fb}} + \frac{k_{mb} h_{mb}}{\mu_{mb}} \right) (p_i - p_j) \Big|_{j=fb \text{ or } mb} \text{ ..... (G-7e)}$$

The derivatives of the above entities will be:

$$\partial(y_D \sqrt{A_{cw}}) = \partial y \quad \partial(y_D \sqrt{A_{cw}}) \{ \partial(y_D \sqrt{A_{cw}}) \} = \partial^2 y \text{ ..... (G-8a)}$$

$$\partial(z_D \sqrt{A_{cw}}) = \partial z \quad \partial(z_D \sqrt{A_{cw}}) \{ \partial(z_D \sqrt{A_{cw}}) \} = \partial^2 z \text{ ..... (G-8b)}$$

$$\varepsilon \partial(y_D h_{aq}) = \partial y \quad \varepsilon^2 \partial(y_D h_{aq}) \{ \partial(y_D h_{aq}) \} = \partial^2 y \text{ ..... (G-8c)}$$

$$\partial(p_D p_{ch} - p_i) = p_{ch} \partial p_D = -\partial p \quad p_{ch} \partial^2 p_D = \partial^2 p \text{ ..... (G-8d)}$$

### Solution of Matrix (Aquifer)

Substituting  $y_D$  in eqn.(G-5b), we have:

$$\left(\frac{1}{\varepsilon^2}\right) \left(\frac{k_{fb} h_{fb}}{\mu_{fb}} + \frac{k_{aq} h_{aq}}{\mu_{aq}}\right) \left(\frac{kh}{\mu}\right)_{aq} \frac{\partial^2 p_{aq}}{\partial y_D^2} = (\varphi_{fb} h_{fb} + \varphi_{aq} h_{aq}) (\varphi h)_{aq} c_a (h_{aq}^2) \frac{\partial p_{aq}}{\partial t}$$

Substituting  $p_D$  in above, we have:

$$\left(\frac{1}{\varepsilon^2}\right) \left(\frac{k_{fb} h_{fb}}{\mu_{fb}} + \frac{k_{aq} h_{aq}}{\mu_{aq}}\right) \left(\frac{kh}{\mu}\right)_{aq} p_{ch} \frac{\partial^2 (p_{aqD} p_{ch} - p_i)}{\partial y_D^2} = (\varphi_{fb} h_{fb} + \varphi_{aq} h_{aq}) \times$$

$$(\varphi h)_{aq} c_a (h_{aq}^2) \frac{\partial (p_{aqD} p_{ch} - p_i)}{\partial t}$$

On cancellation of common terms, results in:

$$\left(\frac{1}{\varepsilon^2}\right) \left(\frac{kh}{\mu}\right)_{aq} \frac{\partial^2 p_{aqD}}{\partial y_D^2} = \frac{(\varphi_{fb} h_{fb} + \varphi_{aq} h_{aq})}{\left(\frac{k_{fb} h_{fb}}{\mu_{fb}} + \frac{k_{aq} h_{aq}}{\mu_{aq}}\right)} (\varphi h)_{aq} c_a (h_{aq}^2) \frac{\partial p_{aqD}}{\partial t}$$

Reapplying eqn.(G-2) to the above we get:

$$\left(\frac{1}{\varepsilon^2}\right) \left(\frac{\frac{k_{aq} h_{aq}}{\mu_{aq}}}{\frac{k_{fb} h_{fb}}{\mu_{fb}} + \frac{k_{aq} h_{aq}}{\mu_{aq}}}\right) \frac{\partial^2 p_{aqD}}{\partial y_D^2} = (\varphi h)_{aq} \frac{(\varphi_{fb} h_{fb} + \varphi_{aq} h_{aq})}{\left(\frac{k_{fb} h_{fb}}{\mu_{fb}} + \frac{k_{aq} h_{aq}}{\mu_{aq}}\right)} c_a (h_{aq}^2) \frac{\partial p_{aqD}}{\partial t}$$

On simplify the above and putting in additional terms we get:

$$\left(\frac{1}{\varepsilon^2}\right) \left(\frac{\frac{k_{aq} h_{aq}}{\mu_{aq}}}{\frac{k_{fb} h_{fb}}{\mu_{fb}} + \frac{k_{aq} h_{aq}}{\mu_{aq}}}\right) \frac{\partial^2 p_{aqD}}{\partial y_D^2} =$$

$$(\varphi h)_{aq} \frac{(\varphi_{fb} h_{fb} + \varphi_{aq} h_{aq})}{\left(\frac{k_{fb} h_{fb}}{\mu_{fb}} + \frac{k_{aq} h_{aq}}{\mu_{aq}}\right)} C_a \left(\frac{A_{cw}}{A_{cw}}\right) \left(\frac{\frac{k_{fb}}{\mu_{fb}}}{\frac{k_{fb} h_{fb}}{\mu_{fb}} + \frac{k_{aq} h_{aq}}{\mu_{aq}}}\right) \left(\frac{\frac{k_{aq}}{\mu_{fb}}}{\frac{k_{fb} h_{fb}}{\mu_{fb}} + \frac{k_{aq} h_{aq}}{\mu_{aq}}}\right) (h_{aq}^2) \frac{\partial p_{aqD}}{\partial t} \dots\dots\dots (G-9)$$

We also have the following:

$$\omega_{aq} = \frac{\varphi_{fb} c_f}{(\varphi c_t)_{aq+fb}} \dots\dots\dots (G-10)$$

Substituting  $\omega_{aq}$  in eqn.(G-9) and assuming compressibility is constant, we have:

$$\left(\frac{1}{\varepsilon^2}\right) (1 - \kappa_f) \frac{\partial^2 p_{aqD}}{\partial y_D^2} = \frac{12(1-\omega_{aq})}{\lambda_{aq}} \frac{\partial p_{aqD}}{\partial t_D} \dots\dots\dots (G-11)$$

Dimensionless time and dimensionless interporosity flow parameter, are given by:

$$t_D = \frac{\left(\frac{k_{fb} h_{fb}}{\mu_{fb}} + \frac{k_{aq} h_{aq}}{\mu_{aq}}\right) t}{(\varphi_{fb} h_{fb} + \varphi_{aq} h_{aq}) c_f A_{cw}} \dots\dots\dots (G-12a)$$

$$\lambda_{aq} = \frac{12}{h_{aq}^2} A_{cw} \frac{\left(\frac{\frac{k_{aq}}{\mu_{aq}}}{\frac{k_{fb} h_{fb}}{\mu_{fb}} + \frac{k_{aq} h_{aq}}{\mu_{aq}}}\right)}{\left(\frac{\frac{k_{fb}}{\mu_{fb}}}{\frac{k_{fb} h_{fb}}{\mu_{fb}} + \frac{k_{aq} h_{aq}}{\mu_{aq}}}\right)} \dots\dots\dots (G-12b)$$

$$\kappa_f = \left(\frac{\frac{k_{fb} h_{fb}}{\mu_{fb}}}{\frac{k_{fb} h_{fb}}{\mu_{fb}} + \frac{k_{aq} h_{aq}}{\mu_{aq}}}\right) \dots\dots\dots (G-12c)$$

Where:  $\underline{\alpha} = \frac{12}{h_{aq}^2}$  (for a slab draining from single face) .... (G-12d)

$$p_{aqD} = 2\pi \left(\frac{k_{fb} h_{fb}}{\mu_{fb}} + \frac{k_{aq} h_{aq}}{\mu_{aq}}\right) \frac{p_i - p_{aq}}{qB} \dots\dots\dots (G-12e)$$

$$p_{fD} = 2\pi \left(\frac{k_{fb} h_{fb}}{\mu_{fb}} + \frac{k_{aq} h_{aq}}{\mu_{aq}}\right) \frac{p_i - p_f}{qB} \dots\dots\dots (G-12g)$$

The final form of the above equation, is:

$$\left(\frac{1}{\varepsilon^2}\right) (1 - \kappa_f) \nabla^2 p_{aqD} = \frac{12(1 - \omega_{aq})}{\lambda_{aq}} \frac{\partial p_{aqD}}{\partial t_D} \dots\dots\dots (G-13)$$

We will find the solution of eqn.(G-13) for  $\overline{p_{aqD}}$  first.

For aquifer block and in Laplace domain, the initial and boundary conditions are:

Initial Condition:  $\overline{p_{aqD}}(\varepsilon y_D = 1, s \rightarrow \infty) = 0 \dots\dots\dots (G-14a)$

Inner Boundary Condition:  $\left. \frac{d\overline{p_{aqD}}}{\varepsilon dy_D} \right|_{\varepsilon y_D=0} = 0 \dots\dots\dots (G-14b)$

Outer Boundary Condition:  $\overline{p_{aqD}} \Big|_{\varepsilon y_D=1} = \overline{p_{fD}} \dots\dots\dots (G-14c)$

From the initial condition of aquifer to the Laplace transform equations we have:

$$\left(\frac{1}{\varepsilon^2}\right) (1 - \kappa_f) \frac{\partial^2 \overline{p_{aqD}}}{\partial y_D^2} = \frac{12(1-\omega_{aq})}{\lambda_{aq}} \{s\overline{p_{aqD}} - \overline{p_{aqD}}(y_D, 0)\}$$

$$\frac{\partial^2 \overline{p_{aqD}}}{\partial y_D^2} - \varepsilon^2 \left(\frac{12(1-\omega_{aq})}{\lambda_{aq}(1-\kappa_f)}\right) s\overline{p_{aqD}} = 0 \dots\dots\dots (G-15)$$

The above is a homogeneous partial differential equation with the following general solution:

$$\overline{p_{aqD}} = A \cosh\left(\varepsilon y_D \sqrt{s \left(\frac{12(1-\omega_{aq})}{\lambda_{aq}(1-\kappa_f)}\right)}\right) + B \sinh\left(\varepsilon y_D \sqrt{s \left(\frac{12(1-\omega_{aq})}{\lambda_{aq}(1-\kappa_f)}\right)}\right) \dots\dots (G-16)$$

Differentiating with respect to  $y_D$  and using the inner boundary condition, we have:

$$\frac{d\overline{p_{aqD}}}{dy_D} \Big|_{\varepsilon y_D=0} = 0 =$$

$$\varepsilon \sqrt{s \left( \frac{12(1-\omega_{aq})}{\lambda_{aq}(1-\kappa_f)} \right)} A \sinh \left( \varepsilon y_D \sqrt{s \left( \frac{12(1-\omega_{aq})}{\lambda_{aq}(1-\kappa_f)} \right)} \right) +$$

$$\varepsilon \sqrt{s \left( \frac{12(1-\omega_{aq})}{\lambda_{aq}(1-\kappa_f)} \right)} B \cosh \left( \varepsilon y_D \sqrt{s \left( \frac{12(1-\omega_{aq})}{\lambda_{aq}(1-\kappa_f)} \right)} \right)$$

Since  $\sinh y_D|_{y_D=0} = 0$ , implies:

$$B = 0 \dots\dots\dots (G-17)$$

Using outer boundary condition and substituting eqn.(G-14c) in eqn.(G-16) we have:

$$\overline{p_{fD}} = A \cosh \left( \varepsilon y_D \sqrt{s \left( \frac{12(1-\omega_{aq})}{\lambda_{aq}(1-\kappa_f)} \right)} \right) \Big|_{\varepsilon y_D=1}$$

$$A = \frac{\overline{p_{fD}}}{\cosh \left( \sqrt{s \left( \frac{12(1-\omega_{aq})}{\lambda_{aq}(1-\kappa_f)} \right)} \right)} \dots\dots\dots (G-18)$$

Hence the particular solution for constant rate of eqn.(G-15) in Laplace domain is:

$$\overline{p_{aqD}} = \frac{\overline{p_{fD}}}{\cosh \left( \sqrt{s \left( \frac{12(1-\omega_{aq})}{\lambda_{aq}(1-\kappa_f)} \right)} \right)} \cosh \left( \varepsilon y_D \sqrt{s \left( \frac{12(1-\omega_{aq})}{\lambda_{aq}(1-\kappa_f)} \right)} \right) \dots\dots\dots (G-19)$$

Solution of Matrix (Reservoir)

Substituting  $z_D$  in eqn.(G-5b), we have:

$$\left(\frac{k_{fb} h_{fb}}{\mu_{fb}} + \frac{k_{mb} h_{mb}}{\mu_{mb}}\right) \left(\frac{kh}{\mu}\right)_{mb} \frac{\partial^2 p_{mb}}{\partial z_D^2} = (\varphi_{fb} h_{fb} + \varphi_{mb} h_{mb})(\varphi h)_{mb} c_m A_{cw} \frac{\partial p_{mb}}{\partial t} + \alpha A_{cw} \left(\frac{k_{fb} h_{fb}}{\mu_{fb}} + \frac{k_{mb} h_{mb}}{\mu_{mb}}\right) \left(\frac{kh}{\mu}\right)_{mb} \left(\frac{1}{h}\right)_{mb} (p_{mb} - p_{fb})$$

Substituting  $p_D$  in above, we have:

$$\left(\frac{k_{fb} h_{fb}}{\mu_{fb}} + \frac{k_{mb} h_{mb}}{\mu_{mb}}\right) \left(\frac{kh}{\mu}\right)_{mb} p_{ch} \frac{\partial^2 p_{mb}}{\partial z_D^2} = (\varphi_{fb} h_{fb} + \varphi_{mb} h_{mb}) \times (\varphi h)_{mb} c_m A_{cw} \frac{(p_{mbD} p_{ch} - p_i)}{\partial t} + \alpha A_{cw} \left(\frac{k_{fb} h_{fb}}{\mu_{fb}} + \frac{k_{mb} h_{mb}}{\mu_{mb}}\right) \times \left(\frac{kh}{\mu}\right)_{mb} \left(\frac{1}{h}\right)_{mb} \{(\partial p_{mbD} p_{ch} - p_i) - (p_{fD} p_{ch} - p_i)\}$$

On cancellation of common terms, results in:

$$\left(\frac{kh}{\mu}\right)_{mb} \frac{\partial^2 p_{mbD}}{\partial z_D^2} = (\varphi h)_{mb} \frac{(\varphi_{fb} h_{fb} + \varphi_{mb} h_{mb})}{\left(\frac{k_{fb} h_{fb}}{\mu_{fb}} + \frac{k_{mb} h_{mb}}{\mu_{mb}}\right)} c_m A_{cw} \frac{\partial p_{mbD}}{\partial t} + \alpha A_{cw} \left(\frac{kh}{\mu}\right)_{mb} \left(\frac{1}{h}\right)_{mb} (p_{mbD} - p_{fbD}) \dots \dots \dots (G-20)$$



Reapplying eqn.(G-2) and converting this equation into aquifer-fracture domain we get:

$$\left( \frac{\frac{k_{mb} h_{mb}}{\mu_{mb}}}{\frac{k_{fb} h_{fb}}{\mu_{fb}} + \frac{k_{mb} h_{mb}}{\mu_{mb}}} \right) \frac{\partial^2 p_{mbD}}{\partial z_D^2} =$$

$$(\varphi h)_{mb} \frac{(\varphi_{fb} h_{fb} + \varphi_{mb} h_{mb})}{(\varphi_{fb} h_{fb} + \varphi_{aq} h_{aq})} \frac{\left( \frac{k_{fb} h_{fb}}{\mu_{fb}} + \frac{k_{aq} h_{aq}}{\mu_{aq}} \right)}{\left( \frac{k_{fb} h_{fb}}{\mu_{fb}} + \frac{k_{mb} h_{mb}}{\mu_{mb}} \right)} \frac{(\varphi_{fb} h_{fb} + \varphi_{aq} h_{aq})}{\left( \frac{k_{fb} h_{fb}}{\mu_{fb}} + \frac{k_{aq} h_{aq}}{\mu_{aq}} \right)} c_m A_{cw} \frac{\partial p_{mbD}}{\partial t} +$$

$$\alpha A_{cw} \left( \frac{\frac{k_{mb} h_{mb}}{\mu_{mb}}}{\frac{k_{fb} h_{fb}}{\mu_{fb}} + \frac{k_{mb} h_{mb}}{\mu_{mb}}} \right) \left( \frac{1}{h} \right)_{mb} (p_{mbD} - p_{fbD}) \dots\dots\dots (G-21)$$

We also have the following:

$$\omega = \frac{\varphi_{fb} c_f}{(\varphi c_t)_{mb+fb}} \dots\dots\dots (G-22a)$$

$$\Lambda = \frac{\omega_{aq}}{\omega} = \frac{(\varphi_{fb} h_{fb} + \varphi_{mb} h_{mb})}{(\varphi_{fb} h_{fb} + \varphi_{aq} h_{aq})} \dots\dots\dots (G-22b)$$

Substituting  $\omega$  and  $\Lambda$  in eqn.(G-21) and assuming compressibility is constant, we have:

$$(1 - \kappa_{fb}) \frac{\partial^2 p_{mbD}}{\partial z_D^2} = (1 - \omega) (\Lambda) \left( \frac{\kappa_{fb}}{\kappa_f} \right) \frac{\partial p_{mbD}}{\partial t_D} + \lambda (p_{mbD} - p_{fbD}) \dots\dots\dots (G-23)$$

Here dimensionless time and dimensionless interporosity flow parameter and others, are as:

$$t_{bD} = \frac{\left(\frac{k_{fb} h_{fb}}{\mu_{fb}} + \frac{k_{mb} h_{mb}}{\mu_{mb}}\right) t}{(\varphi_{fb} h_{fb} + \varphi_{mb} h_{mb}) c_f A_{cw}} = \left(\frac{\kappa_f}{\kappa_{fb}}\right) \left(\frac{1}{\Lambda}\right) t_D \dots\dots (G-24a)$$

$$\lambda = \alpha A_{cw} \left(\frac{\frac{k_{mb}}{\mu_{mb}}}{\frac{k_{fb} h_{fb}}{\mu_{fb}} + \frac{k_{mb} h_{mb}}{\mu_{mb}}}\right) \dots\dots\dots (G-24b)$$

$$\kappa_{fb} = \left(\frac{\frac{k_{fb} h_{fb}}{\mu_{fb}}}{\frac{k_{fb} h_{fb}}{\mu_{fb}} + \frac{k_{mb} h_{mb}}{\mu_{mb}}}\right) \dots\dots\dots (G-24c)$$

$$p_{mbD} = 2\pi \left(\frac{k_{fb} h_{fb}}{\mu_{fb}} + \frac{k_{mb} h_{mb}}{\mu_{mb}}\right) \frac{p_i - p_{mb}}{q_B} \dots\dots\dots (G-24d)$$

$$p_{fbD} = 2\pi \left(\frac{k_{fb} h_{fb}}{\mu_{fb}} + \frac{k_{mb} h_{mb}}{\mu_{mb}}\right) \frac{p_i - p_{fb}}{q_B} \dots\dots\dots (G-24e)$$

The final form of the above equation, since the LHS is zero for pseudosteady state, is:

$$0 = \left(\frac{1-\omega}{1-\kappa_{fb}}\right) (\Lambda) \left(\frac{\kappa_{fb}}{\kappa_f}\right) \frac{\partial p_{mbD}}{\partial t_D} + \left(\frac{\lambda}{1-\kappa_{fb}}\right) (p_{mbD} - p_{fbD}) \dots\dots\dots (G-25)$$

Applying the initial condition of aquifer to the Laplace transform equations results in:

$$0 = (1 - \omega)(\Lambda) \left(\frac{\kappa_{fb}}{\kappa_f}\right) s \overline{p_{mbD}} + \lambda (\overline{p_{mbD}} - \overline{p_{fbD}}) \dots\dots\dots (G-26)$$

Solving eqn.(G-26) the Laplace domain solution,  $\overline{p_{mbD}}$ , is:

$$\overline{p_{mbD}} = \frac{\lambda}{(1-\omega)(\Lambda) \left(\frac{\kappa_{fb}}{\kappa_f}\right) s + \lambda} \overline{p_{fbD}} \dots\dots\dots (G-27)$$

Solution of Fracture

There are two different dimensionless pressures. The dimensionless pressure which is reservoir matrix-fracture domain based and dimensionless pressure which is aquifer-fracture domain based. We know dimensionless time measurement is based on latter and this is the reason for normalizing everything on that domain. We have the two equations as:

$$\overline{p_{aqD}} = \frac{\overline{p_{fD}}}{\cosh\left(\sqrt{s\left(\frac{12(1-\omega_{aq})}{\lambda_{aq}(1-\kappa_f)}\right)}\right)} \cosh\left(\varepsilon y_D \sqrt{s\left(\frac{12(1-\omega_{aq})}{\lambda_{aq}(1-\kappa_f)}\right)}\right) \dots\dots\dots (G-19)$$

$$\overline{p_{mbD}} = \frac{\lambda}{(1-\omega)(\Lambda)\left(\frac{\kappa_{fb}}{\kappa_f}\right)^{s+\lambda}} \overline{p_{fbD}} \dots\dots\dots (G-27)$$

We also know fracture domains are the same:

$$\frac{\overline{p_{fbD}}}{\left(\frac{k_{fb} h_{fb}}{\mu_{fb}} + \frac{k_{mb} h_{mb}}{\mu_{mb}}\right)} = \frac{\overline{p_{fD}}}{\left(\frac{k_{fb} h_{fb}}{\mu_{fb}} + \frac{k_{aq} h_{aq}}{\mu_{aq}}\right)}$$

$$\overline{p_{fbD}} = \left(\frac{\kappa_{fb}}{\kappa_f}\right) \overline{p_{fD}} \dots\dots\dots (G-28)$$

Again, for the fracture we have:

$$\begin{aligned}
 & \left( \frac{k_{fb} h_{fb}}{\mu_{fb}} + \frac{k_{aq} h_{aq}}{\mu_{aq}} \right) \left( \frac{kh}{\mu} \right)_{fb} \frac{\partial^2 p_{fb}}{\partial y^2} = \\
 & (\varphi_{fb} h_{fb} + \varphi_{aq} h_{aq}) (\varphi h)_{fb} c_f \frac{\partial p_{fb}}{\partial t} - \\
 & \left( \frac{1}{\varepsilon} \right) \left( \frac{k_{fb} h_{fb}}{\mu_{fb}} + \frac{k_{aq} h_{aq}}{\mu_{aq}} \right) \left( \frac{kh}{\mu} \right)_{aq} \left( \frac{1}{h^2/2} \right)_{aq} \frac{\partial p_{aq}}{\partial y} \Big|_{y_{aq}=h_{aq}} - \\
 & \alpha \left( \frac{k_{fb} h_{fb}}{\mu_{fb}} + \frac{k_{mb} h_{mb}}{\mu_{mb}} \right) \left( \frac{kh}{\mu} \right)_{mb} \left( \frac{1}{h} \right)_{mb} (p_{mb} - p_{fb}) \dots \dots \dots (G-5a)
 \end{aligned}$$

Substituting  $y_D$  in eqn.(G-5a), we have:

$$\begin{aligned}
 & \left( \frac{k_{fb} h_{fb}}{\mu_{fb}} + \frac{k_{aq} h_{aq}}{\mu_{aq}} \right) \left( \frac{kh}{\mu} \right)_{fb} \frac{\partial^2 p_{fb}}{\partial y_D^2} = (\varphi_{fb} h_{fb} + \varphi_{aq} h_{aq}) (\varphi h)_{fb} c_f A_{cw} \frac{\partial p_{fb}}{\partial t} - \\
 & \left( \frac{1}{\varepsilon} \right) \left( \frac{k_{fb} h_{fb}}{\mu_{fb}} + \frac{k_{aq} h_{aq}}{\mu_{aq}} \right) \left( \frac{kh}{\mu} \right)_{aq} \left( \frac{A_{cw}}{h^2} \right)_{aq} \frac{\partial p_{aq}}{\partial y} \Big|_{y_{aq}=h_{aq}} \alpha A_{cw} \left( \frac{k_{fb} h_{fb}}{\mu_{fb}} + \right. \\
 & \left. \frac{k_{mb} h_{mb}}{\mu_{mb}} \right) \left( \frac{kh}{\mu} \right)_{mb} \left( \frac{1}{h} \right)_{mb} (p_{mb} - p_{fb})
 \end{aligned}$$

Substituting  $p_D$  in eqn.(G-5a), we have:

$$\begin{aligned}
 & \left( \frac{k_{fb} h_{fb}}{\mu_{fb}} + \frac{k_{aq} h_{aq}}{\mu_{aq}} \right) \left( \frac{kh}{\mu} \right)_{fb} \frac{\partial^2 (p_{fD} p_{ch} - p_i)}{\partial y_D^2} = \\
 & (\varphi_{fb} h_{fb} + \varphi_{aq} h_{aq}) (\varphi h)_{fb} c_f A_{cw} \frac{\partial (p_{fD} p_{ch} - p_i)}{\partial t} - \left( \frac{1}{\varepsilon} \right) \left( \frac{k_{fb} h_{fb}}{\mu_{fb}} + \frac{k_{aq} h_{aq}}{\mu_{aq}} \right) \times \\
 & \left( \frac{kh}{\mu} \right)_{aq} \left( \frac{A_{cw}}{h^2} \right)_{aq} \frac{\partial (p_{aq} p_{ch} - p_i)}{\partial y} \Big|_{y_{aq}=h_{aq}} - \alpha A_{cw} \left( \frac{k_{fb} h_{fb}}{\mu_{fb}} + \frac{k_{mb} h_{mb}}{\mu_{mb}} \right) \times \\
 & \left( \frac{kh}{\mu} \right)_{mb} \left( \frac{1}{h} \right)_{mb} \{ (p_{mbD} p_{ch} - p_i) - (p_{fD} p_{ch} - p_i) \}
 \end{aligned}$$

Rearranging and canceling common terms results in:

$$\begin{aligned} \left(\frac{kh}{\mu}\right)_{fb} \frac{\partial^2 p_{fD}}{\partial y_D^2} = \\ (\varphi h)_{fb} \frac{(\varphi_{fb} h_{fb} + \varphi_{aq} h_{aq})}{\left(\frac{k_{fb} h_{fb}}{\mu_{fb}} + \frac{k_{aq} h_{aq}}{\mu_{aq}}\right)} c_f A_{cw} \frac{\partial p_{fD}}{\partial t} - \\ \left(\frac{1}{\varepsilon}\right) \left(\frac{kh}{\mu}\right)_{aq} \left(\frac{A_{cw}}{h^2}\right)_{aq} \frac{\partial p_{aqD}}{\partial y} \Big|_{y_{aq}=h_{aq}} - \\ \alpha A_{cw} \frac{\left(\frac{k_{fb} h_{fb}}{\mu_{fb}} + \frac{k_{mb} h_{mb}}{\mu_{mb}}\right)}{\left(\frac{k_{fb} h_{fb}}{\mu_{fb}} + \frac{k_{aq} h_{aq}}{\mu_{aq}}\right)} \left(\frac{kh}{\mu}\right)_{mb} \left(\frac{1}{h}\right)_{mb} (p_{mbD} - p_{fD}) \end{aligned}$$

Substituting back eqns. (G-2a) to eqn.(G-2h) into the above eqn. we get:

$$\begin{aligned} \left(\frac{\frac{k_{fb} h_{fb}}{\mu_{fb}}}{\frac{k_{fb} h_{fb}}{\mu_{fb}} + \frac{k_{aq} h_{aq}}{\mu_{aq}}}\right) \frac{\partial^2 p_{fD}}{\partial y_D^2} = \left(\frac{\varphi_{fb} h_{fb}}{\varphi_{fb} h_{fb} + \varphi_{aq} h_{aq}}\right) \frac{(\varphi_{fb} h_{fb} + \varphi_{aq} h_{aq})}{\left(\frac{k_{fb} h_{fb}}{\mu_{fb}} + \frac{k_{aq} h_{aq}}{\mu_{aq}}\right)} c_f A_{cw} \frac{\partial p_{fD}}{\partial t} - \\ \left(\frac{1}{\varepsilon}\right) \left(\frac{\frac{k_{aq} h_{aq}}{\mu_{aq}}}{\frac{k_{fb} h_{fb}}{\mu_{fb}} + \frac{k_{aq} h_{aq}}{\mu_{aq}}}\right) \left(\frac{A_{cw}}{h^2}\right)_{aq} \frac{\partial p_{aqD}}{\partial y} \Big|_{y_{aq}=h_{aq}} - \\ \alpha A_{cw} \frac{\left(\frac{k_{fb} h_{fb}}{\mu_{fb}} + \frac{k_{mb} h_{mb}}{\mu_{mb}}\right)}{\left(\frac{k_{fb} h_{fb}}{\mu_{fb}} + \frac{k_{aq} h_{aq}}{\mu_{aq}}\right)} \left(\frac{\frac{k_{mb} h_{mb}}{\mu_{mb}}}{\frac{k_{fb} h_{fb}}{\mu_{fb}} + \frac{k_{mb} h_{mb}}{\mu_{mb}}}\right) \left(\frac{1}{h}\right)_{mb} (p_{mbD} - p_{fD}) \end{aligned}$$

Introducing some additional terms, normalizing other terms and  $h_{fb} = h_{mb}$  we have:

$$\left( \frac{\frac{k_{fb} h_{fb}}{\mu_{fb}}}{\frac{k_{fb} h_{fb}}{\mu_{fb}} + \frac{k_{aq} h_{aq}}{\mu_{aq}}} \right) \frac{\partial^2 p_{fD}}{\partial y_D^2} = \left( \frac{\varphi_{fb} h_{fb}}{\varphi_{fb} h_{fb} + \varphi_{aq} h_{aq}} \right) \left( \frac{\varphi_{fb} h_{fb} + \varphi_{aq} h_{aq}}{\frac{k_{fb} h_{fb}}{\mu_{fb}} + \frac{k_{aq} h_{aq}}{\mu_{aq}}} \right) c_f A_{cw} \frac{\partial p_{fD}}{\partial t} -$$

$$\left( \frac{1}{\varepsilon} \right) \left( \frac{\frac{k_{aq} h_{aq}}{\mu_{aq}}}{\frac{k_{fb} h_{fb}}{\mu_{fb}} + \frac{k_{aq} h_{aq}}{\mu_{aq}}} \right) \left( \frac{A_{cw}}{h^3} \right)_{aq} \frac{\partial p_{aqD}}{\partial y_D} \Big|_{\varepsilon y_D=1} -$$

$$\alpha A_{cw} \left( \frac{\frac{k_{fb} h_{fb}}{\mu_{fb}} + \frac{k_{mb} h_{mb}}{\mu_{mb}}}{\frac{k_{fb} h_{fb}}{\mu_{fb}} + \frac{k_{aq} h_{aq}}{\mu_{aq}}} \right) \left( \frac{k_{fb} h_{fb}}{\mu_{fb}} \right) \left( \frac{\frac{k_{mb} h_{mb}}{\mu_{mb}}}{\frac{k_{fb} h_{fb}}{\mu_{fb}} + \frac{k_{mb} h_{mb}}{\mu_{mb}}} \right) \left( \frac{1}{h} \right)_{mb} (p_{mbD} - p_{fbD})$$

The resultant form of the governing differential equations are:

$$\kappa_f \frac{\partial^2 p_{fD}}{\partial y_D^2} = \omega_{aq} \frac{\partial p_{fD}}{\partial t} - \left( \frac{1}{\varepsilon} \right) \left( \frac{\lambda_{aq}}{12 \kappa_f} \right) \frac{\partial p_{aqD}}{\partial y_D} \Big|_{\varepsilon y_D=1} (\lambda \kappa_f) (p_{mbD} - p_{fbD})$$

The final form of the governing differential equations is:

$$\nabla^2 p_{fD} = \left( \frac{\omega_{aq}}{\kappa_f} \right) \frac{\partial p_{fD}}{\partial t} - \left( \frac{1}{\varepsilon} \right) \left( \frac{\lambda_{aq}}{12 \kappa_f} \right) \frac{\partial p_{aqD}}{\partial y_D} \Big|_{\varepsilon y_D=1} - \lambda (p_{mbD} - p_{fbD}) \dots\dots\dots (G-29)$$

Taking Laplace transform of the above equation:

$$\frac{d^2 \overline{p_{fD}}}{dy_D^2} = \left( \frac{\omega_{aq}}{\kappa_f} \right) \{s \overline{p_{fD}} - \overline{p_{fD}}(y_D, 0)\} - \left( \frac{1}{\varepsilon} \right) \left( \frac{\lambda_{aq}}{12 \kappa_f} \right) \frac{\partial \overline{p_{aqD}}}{\partial y_D} \Big|_{\varepsilon y_D=1} - \lambda \{ \overline{p_{mbD}} - \overline{p_{fbD}} \} \dots\dots\dots (G-30)$$

For a closed reservoir the initial and boundary conditions, in Laplace domain, for fracture are:

Initial Condition:  $\overline{p_{fD}}(y_D, s) = 0 \dots\dots\dots (G-31a)$

Inner Boundary Condition:  $\left. \frac{d\overline{p_{fD}}}{dy_D} \right|_{y_D=0} = -\frac{2\pi}{s} \dots\dots\dots (G-31b)$

Outer Boundary Condition:  $\left. \frac{d\overline{p_{fD}}}{dy_D} \right|_{y_D=y_{De}} = 0 \dots\dots\dots (G-31c)$

Applying initial condition, we have:

$$\frac{d^2\overline{p_{fD}}}{dy_D^2} = \left(\frac{\omega_{aq}}{\kappa_f}\right)\{s\overline{p_{fD}}\} - \left(\frac{1}{\varepsilon}\right)\left(\frac{\lambda_{aq}}{12\kappa_f}\right)\left.\frac{\partial\overline{p_{aqD}}}{\partial y_D}\right|_{\varepsilon y_D=1} - \lambda\{\overline{p_{mbD}} - \overline{p_{fbD}}\} \dots\dots\dots (G-32)$$

But from eqn.(G-19) we have

$$\left.\frac{\partial\overline{p_{aqD}}}{\partial y_D}\right|_{\varepsilon y_D=1} = \frac{\varepsilon \sqrt{s\left(\frac{12(1-\omega_{aq})}{\lambda_{aq}(1-\kappa_f)}\right)}}{\cosh\left(\sqrt{s\left(\frac{12(1-\omega_{aq})}{\lambda_{aq}(1-\kappa_f)}\right)}\right)} \sinh\left(\sqrt{s\left(\frac{12(1-\omega_{aq})}{\lambda_{aq}(1-\kappa_f)}\right)}\right) \overline{p_{fD}}$$

This derivative will change sign when expressed in terms of  $\overline{p_{fD}}$ , and using eqn.(G-30)

we have:

$$\frac{d^2\overline{p_{fD}}}{dy_D^2} = \left(\frac{\omega_{aq}}{\kappa_f}\right)\{s\overline{p_{fD}}\} + \left(\frac{\lambda_{aq}}{12\kappa_f}\right)\sqrt{s\left(\frac{12(1-\omega_{aq})}{\lambda_{aq}(1-\kappa_f)}\right)} \tanh\left(\sqrt{s\left(\frac{12(1-\omega_{aq})}{\lambda_{aq}(1-\kappa_f)}\right)}\right) \overline{p_{fD}} + \lambda\left\{\frac{(1-\omega)(\Lambda)\left(\frac{\kappa_{fb}}{\kappa_f}\right)}{(1-\omega)(\Lambda)\left(\frac{\kappa_{fb}}{\kappa_f}\right)_{s+\lambda}}\right\} \overline{p_{fbD}}$$

Using eqn.(G-28), converting everything into consistent aquifer-fracture domain, we have:

$$\frac{d^2 \overline{p_{fD}}}{dy_D^2} = \left[ \left( \frac{\omega_{aq}}{\kappa_f} \right) + \lambda \left\{ \frac{(1-\omega)(\Lambda) \left( \frac{\kappa_{fb}}{\kappa_f} \right)}{(1-\omega)(\Lambda) \left( \frac{\kappa_{fb}}{\kappa_f} \right)_{s+\lambda}} \right\} + \left( \frac{\lambda_{aq}}{12 s \kappa_f} \right) \sqrt{s \left( \frac{12(1-\omega_{aq})}{\lambda_{aq}(1-\kappa_f)} \right)} \tanh \left( \sqrt{s \left( \frac{12(1-\omega_{aq})}{\lambda_{aq}(1-\kappa_f)} \right)} \right) \right] \{s \overline{p_{fD}}\} \dots (G-33)$$

This is of the form:

$$\frac{d^2 \overline{p_{fD}}}{dy_D^2} - sf(s) \overline{p_{fD}} = 0 \dots\dots\dots (G-34)$$

Where,

$$f(s) = \left[ \left( \frac{\omega_{aq}}{\kappa_f} \right) + \lambda \left( \frac{(1-\omega)(\Lambda) \left( \frac{\kappa_{fb}}{\kappa_f} \right)}{(1-\omega)(\Lambda) \left( \frac{\kappa_{fb}}{\kappa_f} \right)_{s+\lambda}} \right) + \left( \frac{\lambda_{aq}}{12 s \kappa_f} \right) \sqrt{s \left( \frac{12(1-\omega_{aq})}{\lambda_{aq}(1-\kappa_f)} \right)} \tanh \left( \sqrt{s \left( \frac{12(1-\omega_{aq})}{\lambda_{aq}(1-\kappa_f)} \right)} \right) \right] \dots (G-35a)$$

$$f(s) = \left[ \left( \frac{\omega_{aq}}{\kappa_f} \right) + \left( \frac{\left( \frac{\lambda}{\omega} \right) (1-\omega)(\Lambda) \left( \frac{\kappa_{fb}}{\kappa_f} \right)}{\left( \frac{1-\omega}{\omega} \right) (\Lambda) \left( \frac{\kappa_{fb}}{\kappa_f} \right)_{s+\left( \frac{\lambda}{\omega} \right)}} \right) + \left( \frac{\lambda_{aq}}{12 s \kappa_f} \right) \sqrt{s \left( \frac{12(1-\omega_{aq})}{\lambda_{aq}(1-\kappa_f)} \right)} \tanh \left( \sqrt{s \left( \frac{12(1-\omega_{aq})}{\lambda_{aq}(1-\kappa_f)} \right)} \right) \right] \dots (G-35b)$$

Eqn.(G-34) is a homogeneous partial differential equation which is the same as eqn.(A-17). Refer to Appendix A for the rest of the derivation.



APPENDIX H: FULL TRANSIENT MATRIX AND AQUIFER FRACTURED DUAL  
 PERMEABILITY DUAL MOBILITY MODEL – FORMULATION AND LAPLACE  
 DOMAIN SOLUTION

The governing differential equation for linear fluid flow in limited aquifer (matrix block) and the fractured reservoir (reservoir fracture block and reservoir matrix block) is given by:

$$\text{Fracture: } \left(\frac{kh}{\mu}\right)_f \nabla^2 p_f = \varphi_f c_f h_f \frac{\partial p_f}{\partial t} - \left(\frac{k}{\mu h}\right)_a \frac{\partial p_a}{\partial y_a} \Big|_{y_{aq}=h_{aq}} - \left(\frac{k}{\mu h/2}\right)_m \frac{\partial p_m}{\partial z} \Big|_{z=h_m/2} \quad (\text{H-1a})$$

$$\text{Matrix (Aquifer): } \left(\frac{kh}{\mu}\right)_a \nabla^2 p_a = \varphi_a c_a h_a \frac{\partial p_a}{\partial t} \quad \dots\dots\dots (\text{H-1b})$$

$$\text{Matrix (Reservoir): } \left(\frac{kh}{\mu}\right)_m \nabla^2 p_m = \varphi_m c_m h_m \frac{\partial p_m}{\partial t} \quad \dots\dots\dots (\text{H-1c})$$

Since the aquifer is limited, the aquifer height is related to the linear dimension of reservoir ( $y$  is a lateral dimension in the fractured reservoir and  $y_{aq}$  is vertical dimension in the aquifer) by:

$$y_{aq} = h_{aq} = \varepsilon y \quad \dots\dots\dots (\text{H-1d})$$

The second term in eqn.(H-1a) is referred to as the source terms,  $\sigma_a$  and  $\sigma_m$ . The reservoir matrix and the aquifer both are in transient state. Also, all properties need to be put as bulk properties:

Aquifer:

$$\left(\frac{kh}{\mu}\right)_{aq} = \frac{k_a}{\mu_a} \left(\frac{V_a}{V_{f+a}}\right) = \left(\frac{\frac{k_{aq} h_{aq}}{\mu_{aq}}}{\frac{k_{fb} h_{fb}}{\mu_{fb}} + \frac{k_{aq} h_{aq}}{\mu_{aq}}}\right) \dots\dots\dots (H-2a)$$

$$\left(\frac{kh}{\mu}\right)_f = \frac{k_f}{\mu_f} \left(\frac{V_f}{V_{f+a}}\right) = \left(\frac{\frac{k_{fb} h_{fb}}{\mu_{fb}}}{\frac{k_{fb} h_{fb}}{\mu_{fb}} + \frac{k_{aq} h_{aq}}{\mu_{aq}}}\right) \dots\dots\dots (H-2b)$$

$$(\varphi h)_{aq} = \left(\frac{V_{aq}}{V_{f+aq}}\right) = \left(\frac{\varphi_{aq} h_{aq}}{\varphi_{fb} h_{fb} + \varphi_{aq} h_{aq}}\right) \dots\dots\dots (H-2c)$$

$$(\varphi h)_f = \left(\frac{V_f}{V_{f+aq}}\right) = \left(\frac{\varphi_{fb} h_{fb}}{\varphi_{fb} h_{fb} + \varphi_{aq} h_{aq}}\right) \dots\dots\dots (H-2d)$$

Reservoir:

$$\left(\frac{kh}{\mu}\right)_{mb} = \frac{k_m}{\mu_m} \left(\frac{V_m}{V_{f+m}}\right) = \left(\frac{\frac{k_{mb} h_{mb}}{\mu_{mb}}}{\frac{k_{fb} h_{fb}}{\mu_{fb}} + \frac{k_{mb} h_{mb}}{\mu_{mb}}}\right) \dots\dots\dots (H-2e)$$

$$\left(\frac{kh}{\mu}\right)_{fb} = \frac{k_f}{\mu_f} \left(\frac{V_f}{V_{f+m}}\right) = \left(\frac{\frac{k_{fb} h_{fb}}{\mu_{fb}}}{\frac{k_{fb} h_{fb}}{\mu_{fb}} + \frac{k_{mb} h_{mb}}{\mu_{mb}}}\right) \dots\dots\dots (H-2f)$$

$$(\varphi h)_{mb} = \left(\frac{V_m}{V_{f+m}}\right) = \left(\frac{\varphi_{mb} h_{mb}}{\varphi_{fb} h_{fb} + \varphi_{mb} h_{mb}}\right) \dots\dots\dots (H-2g)$$

$$(\varphi h)_{fb} = \left(\frac{V_f}{V_{f+m}}\right) = \left(\frac{\varphi_{fb} h_{fb}}{\varphi_{fb} h_{fb} + \varphi_{mb} h_{mb}}\right) \dots\dots\dots (H-2h)$$

Similarly, the aquifer and matrix fracture bulk source terms are,  $\sigma_{aq}$ , and  $\sigma_{mf}$ , is expressed as:

$$\sigma_{aq} = \sigma_a \left( \frac{V_a}{V_{f+a}} \right) = \left( \frac{k}{\mu h/2} \right)_a \frac{\partial p_a}{\partial y_a} \Big|_{y_a=h_a} = \left( \frac{k_{fb} h_{fb}}{\mu_{fb}} + \frac{k_{aq} h_{aq}}{\mu_{aq}} \right) \left( \frac{kh}{\mu} \right)_{aq} \left( \frac{1}{h^2/2} \right)_{aq} \frac{\partial p_{aq}}{\partial y_{aq}} \Big|_{y_{aq}=h_{aq}} \dots\dots (H-3a)$$

$$\sigma_{mf} = \sigma_m \left( \frac{V_m}{V_{f+m}} \right) = \left( \frac{k}{\mu h/2} \right)_{mb} \frac{\partial p_m}{\partial z} \Big|_{z=h_{mb}/2} = \left( \frac{k_{fb} h_{fb}}{\mu_{fb}} + \frac{k_{mb} h_{mb}}{\mu_{mb}} \right) \left( \frac{kh}{\mu} \right)_{mb} \left( \frac{1}{h^2/2} \right)_{mb} \frac{\partial p_{mb}}{\partial z} \Big|_{z=h_{mb}/2} \dots\dots (H-3b)$$

Here, the assumption is, the aquifer transient effect is restricted to the permeable barrier and:

$$k_{aq} = \frac{(h_a + h_b)}{\left( \frac{h_b}{k_b} + \frac{h_a}{k_a} \right)} \quad (h_a \gg h_b, k_b \gg k_a) \dots\dots\dots (H-4)$$

In terms of bulk properties the governing equations can be recast into:

Fracture:

$$\begin{aligned} & \left( \frac{k_{fb} h_{fb}}{\mu_{fb}} + \frac{k_{aq} h_{aq}}{\mu_{aq}} \right) \left( \frac{kh}{\mu} \right)_{fb} \frac{\partial^2 p_{fb}}{\partial y^2} = \\ & (\varphi_{fb} h_{fb} + \varphi_{aq} h_{aq}) (\varphi h)_{fb} c_f \frac{\partial p_{fb}}{\partial t} - \\ & \left( \frac{1}{\varepsilon} \right) \left( \frac{k_{fb} h_{fb}}{\mu_{fb}} + \frac{k_{aq} h_{aq}}{\mu_{aq}} \right) \left( \frac{kh}{\mu} \right)_{aq} \left( \frac{1}{h^2/2} \right)_{aq} \frac{\partial p_{aq}}{\partial y} \Big|_{y_{aq}=h_{aq}} - \\ & \left( \frac{k_{fb} h_{fb}}{\mu_{fb}} + \frac{k_{mb} h_{mb}}{\mu_{mb}} \right) \left( \frac{kh}{\mu} \right)_{mb} \left( \frac{1}{h^2/2} \right)_{mb} \frac{\partial p_{mb}}{\partial z} \Big|_{z=h_{mb}/2} \dots\dots\dots (H-5a) \end{aligned}$$

Matrix (Aquifer):

$$\left( \frac{1}{\varepsilon^2} \right) \left( \frac{k_{fb} h_{fb}}{\mu_{fb}} + \frac{k_{aq} h_{aq}}{\mu_{aq}} \right) \left( \frac{kh}{\mu} \right)_{aq} \frac{\partial^2 p_{aq}}{\partial y^2} = (\varphi_{fb} h_{fb} + \varphi_{aq} h_{aq}) (\varphi h)_{aq} c_a \frac{\partial p_{aq}}{\partial t} \dots\dots (H-5b)$$

Matrix (Reservoir):

$$\left( \frac{k_{fb} h_{fb}}{\mu_{fb}} + \frac{k_{mb} h_{mb}}{\mu_{mb}} \right) \left( \frac{kh}{\mu} \right)_{mb} \frac{\partial^2 p_{mb}}{\partial z^2} = (\varphi_{fb} h_{fb} + \varphi_{mb} h_{mb}) (\varphi h)_{mb} c_m \frac{\partial p_{mb}}{\partial t} \dots\dots (H-5c)$$

For an aquifer block, the initial and boundary conditions are:

Initial Condition:  $p_{aq}(y_{aq}, t = 0) = p_i \dots\dots\dots (H-6a)$

Inner Boundary Condition:  $\frac{\partial p_{aq}}{\partial y_{aq}} \Big|_{y_{aq}=0} = 0$  for all t  $\dots\dots\dots (H-6b)$

Outer Boundary Condition:  $p_{aq} \Big|_{y_{aq}=h_{aq}} = p_f$  for all t  $\dots\dots\dots (H-6c)$

For a matrix block, the initial and boundary conditions are:

Initial Condition:  $p_{aq}(z, t = 0) = p_i$  ..... (H-6d)

Inner Boundary Condition:  $\frac{\partial p_{aq}}{\partial z} \Big|_{z=0} = 0$  for all t ..... (H-6e)

Outer Boundary Condition:  $p_{aq} \Big|_{z=h_{aq}} = p_f$  for all t ..... (H-6f)

For a fracture block, the initial and boundary conditions are:

Initial Condition:  $p_f(x, t = 0) = p_i$  ..... (H-6g)

Inner Boundary Condition:  $q = -\left(\frac{k_f A_{cw}}{\mu}\right) \frac{\partial p_f}{\partial x} \Big|_{x=0}$  for all t and const. rate .. (H-6h)

Outer Boundary Condition  $\frac{\partial p_f}{\partial x} \Big|_{x=x_e} = 0$  for all t ..... (H-6i)

If we assume  $y$  is the overall linear dimension and define dimensionless variables as:

$$y_D = \frac{y}{\sqrt{A_{cw}}} \text{ for all fracture ..... (H-7a)}$$

$$\varepsilon y_D = \frac{\varepsilon y}{h_{aq}} \text{ for all aquifer ..... (H-7b)}$$

$$z_D = \frac{z}{h_{rm}/2} \text{ for all matrix ..... (H-7c)}$$

$$p_{jD} = \frac{p_i - p}{p_{ch}} = \frac{2\pi}{\alpha_1 q B} \left( \frac{k_{fb} h_{fb}}{\mu_{fb}} + \frac{k_{aq} h_{aq}}{\mu_{aq}} \right) (p_i - p_j) \Big|_{j=f \text{ or } aq} \text{ ..... (H-7d)}$$

$$p_{jD} = \frac{p_i - p}{p_{ch}} = \frac{2\pi}{\alpha_1 q B} \left( \frac{k_{fb} h_{fb}}{\mu_{fb}} + \frac{k_{mb} h_{mb}}{\mu_{mb}} \right) (p_i - p_j) \Big|_{j=fb \text{ or } mb} \text{ ..... (H-7e)}$$

The derivatives of the above entities will be:

$$\partial(y_D \sqrt{A_{cw}}) = \partial y \quad \partial(y_D \sqrt{A_{cw}})\{\partial(y_D \sqrt{A_{cw}})\} = \partial^2 y \quad \dots\dots\dots (H-8a)$$

$$\partial(z_D h_{rm}/2) = \partial z \quad \partial(z_D h_{rm}/2)\{\partial(z_D h_{rm}/2)\} = \partial^2 z \quad \dots\dots\dots (H-8b)$$

$$\varepsilon \partial(y_D h_{aq}) = \partial y \quad \varepsilon^2 \partial(y_D h_{aq})\{\partial(y_D h_{aq})\} = \partial^2 y \quad \dots\dots\dots (H-8c)$$

$$\partial(p_D p_{ch} - p_i) = p_{ch} \partial p_D = - \partial p \quad p_{ch} \partial^2 p_D = \partial^2 p \quad \dots\dots\dots (H-8d)$$

Solution of Matrix (Aquifer)

Substituting  $y_D$  in eqn.(H-5b), we have:

$$\left(\frac{1}{\varepsilon^2}\right) \left(\frac{k_{fb} h_{fb}}{\mu_{fb}} + \frac{k_{aq} h_{aq}}{\mu_{aq}}\right) \left(\frac{kh}{\mu}\right)_{aq} \frac{\partial^2 p_{aq}}{\partial y_D^2} = (\varphi_{fb} h_{fb} + \varphi_{aq} h_{aq}) (\varphi h)_{aq} c_a (h_{aq}^2) \frac{\partial p_{aq}}{\partial t}$$

Substituting  $p_D$  in above, we have:

$$\left(\frac{1}{\varepsilon^2}\right) \left(\frac{k_{fb} h_{fb}}{\mu_{fb}} + \frac{k_{aq} h_{aq}}{\mu_{aq}}\right) \left(\frac{kh}{\mu}\right)_{aq} p_{ch} \frac{\partial^2 (p_{aqD} p_{ch} - p_i)}{\partial y_D^2} = (\varphi_{fb} h_{fb} + \varphi_{aq} h_{aq}) \times$$

$$(\varphi h)_{aq} c_a (h_{aq}^2) \frac{\partial (p_{aqD} p_{ch} - p_i)}{\partial t}$$

On cancellation of common terms, results in:

$$\left(\frac{1}{\varepsilon^2}\right) \left(\frac{kh}{\mu}\right)_{aq} \frac{\partial^2 p_{aqD}}{\partial y_D^2} = \frac{(\varphi_{fb} h_{fb} + \varphi_{aq} h_{aq})}{\left(\frac{k_{fb} h_{fb}}{\mu_{fb}} + \frac{k_{aq} h_{aq}}{\mu_{aq}}\right)} (\varphi h)_{aq} c_a (h_{aq}^2) \frac{\partial p_{aqD}}{\partial t}$$

Reapplying eqn.(H-2) to the above we get:

$$\left(\frac{1}{\varepsilon^2}\right) \left(\frac{\frac{k_{aq} h_{aq}}{\mu_{aq}}}{\frac{k_{fb} h_{fb}}{\mu_{fb}} + \frac{k_{aq} h_{aq}}{\mu_{aq}}}\right) \frac{\partial^2 p_{aqD}}{\partial y_D^2} = (\varphi h)_{aq} \frac{(\varphi_{fb} h_{fb} + \varphi_{aq} h_{aq})}{\left(\frac{k_{fb} h_{fb}}{\mu_{fb}} + \frac{k_{aq} h_{aq}}{\mu_{aq}}\right)} c_a (h_{aq}^2) \frac{\partial p_{aqD}}{\partial t}$$

On simplify the above and putting in additional terms we get:

$$\left(\frac{1}{\varepsilon^2}\right) \left(\frac{\frac{k_{aq} h_{aq}}{\mu_{aq}}}{\frac{k_{fb} h_{fb}}{\mu_{fb}} + \frac{k_{aq} h_{aq}}{\mu_{aq}}}\right) \frac{\partial^2 p_{aqD}}{\partial y_D^2} =$$

$$(\varphi h)_{aq} \frac{(\varphi_{fb} h_{fb} + \varphi_{aq} h_{aq})}{\left(\frac{k_{fb} h_{fb}}{\mu_{fb}} + \frac{k_{aq} h_{aq}}{\mu_{aq}}\right)} c_a \left(\frac{A_{cw}}{A_{cw}}\right) \left(\frac{\frac{k_{fb}}{\mu_{fb}}}{\frac{k_{fb} h_{fb}}{\mu_{fb}} + \frac{k_{aq} h_{aq}}{\mu_{aq}}}\right) \left(\frac{\frac{k_{aq}}{\mu_{fb}}}{\frac{k_{fb} h_{fb}}{\mu_{fb}} + \frac{k_{aq} h_{aq}}{\mu_{aq}}}\right) (h_{aq}^2) \frac{\partial p_{aqD}}{\partial t} \dots \dots (H-9)$$

We also have the following:

$$\omega_{aq} = \frac{\varphi_{fb} c_f}{(\varphi c_t)_{aq+fb}} \dots \dots \dots (H-10)$$

Substituting  $\omega_{aq}$  in eqn.(H-9) and assuming compressibility is constant, we have:

$$\left(\frac{1}{\varepsilon^2}\right) (1 - \kappa_f) \frac{\partial^2 p_{aqD}}{\partial y_D^2} = \frac{12(1-\omega_{aq})}{\lambda_{aq}} \frac{\partial p_{aqD}}{\partial t_D} \dots \dots \dots (H-11)$$

Here expression for dimensionless time and dimensionless interporosity flow parameter, are as:

$$t_D = \frac{\left(\frac{k_{fb} h_{fb}}{\mu_{fb}} + \frac{k_{aq} h_{aq}}{\mu_{aq}}\right) t}{(\varphi_{fb} h_{fb} + \varphi_{aq} h_{aq}) c_f A_{cw}} \dots\dots\dots (H-12a)$$

$$\lambda_{aq} = \frac{12}{h_{aq}^2} A_{cw} \frac{\left(\frac{\frac{k_{aq}}{\mu_{aq}}}{\frac{k_{fb} h_{fb}}{\mu_{fb}} + \frac{k_{aq} h_{aq}}{\mu_{aq}}}\right)}{\left(\frac{\frac{k_{fb}}{\mu_{fb}}}{\frac{k_{fb} h_{fb}}{\mu_{fb}} + \frac{k_{aq} h_{aq}}{\mu_{aq}}}\right)} \dots\dots\dots (H-12b)$$

$$\kappa_f = \left(\frac{\frac{k_{fb} h_{fb}}{\mu_{fb}}}{\frac{k_{fb} h_{fb}}{\mu_{fb}} + \frac{k_{aq} h_{aq}}{\mu_{aq}}}\right) \dots\dots\dots (H-12c)$$

Where:  $\underline{\alpha} = \frac{12}{h_{aq}^2}$  (for a slab draining from single face) .... (H-12d)

$$p_{aqD} = 2\pi \left(\frac{k_{fb} h_{fb}}{\mu_{fb}} + \frac{k_{aq} h_{aq}}{\mu_{aq}}\right) \frac{p_i - p_{aq}}{qB} \dots\dots\dots (H-12e)$$

$$p_{fD} = 2\pi \left(\frac{k_{fb} h_{fb}}{\mu_{fb}} + \frac{k_{aq} h_{aq}}{\mu_{aq}}\right) \frac{p_i - p_f}{qB} \dots\dots\dots (H-12g)$$



The final form of the above equation, is:

$$\left(\frac{1}{\varepsilon^2}\right) (1 - \kappa_f) \nabla^2 p_{aqD} = \frac{12(1-\omega_{aq})}{\lambda_{aq}} \frac{\partial p_{aqD}}{\partial t_D} \dots\dots\dots (H-13)$$

Let us find the solution of eqn.(H-13) for  $\overline{p_{aqD}}$  first. For aquifer block and in Laplace domain, the initial and boundary conditions are:

Initial Condition:  $\overline{p_{aqD}}(\varepsilon y_D = 1, s \rightarrow \infty) = 0 \dots\dots\dots (H-14a)$

Inner Boundary Condition:  $\left. \frac{d\overline{p_{aqD}}}{\varepsilon dy_D} \right|_{\varepsilon y_D=0} = 0 \dots\dots\dots (H-14b)$

Outer Boundary Condition:  $\overline{p_{aqD}} \Big|_{\varepsilon y_D=1} = \overline{p_{fD}} \dots\dots\dots (H-14c)$

From the initial condition of aquifer to the Laplace transform equations we have:

$$\left(\frac{1}{\varepsilon^2}\right) (1 - \kappa_f) \frac{\partial^2 \overline{p_{aqD}}}{\partial y_D^2} = \frac{12(1-\omega_{aq})}{\lambda_{aq}} \{s\overline{p_{aqD}} - \overline{p_{aqD}}(y_D, 0)\}$$

$$\frac{\partial^2 \overline{p_{aqD}}}{\partial y_D^2} - \varepsilon^2 \left(\frac{12(1-\omega_{aq})}{\lambda_{aq}(1-\kappa_f)}\right) s\overline{p_{aqD}} = 0 \dots\dots\dots (H-15)$$

The above is a homogeneous partial differential equation with the following general solution:

$$\overline{p_{aqD}} = A \cosh\left(\varepsilon y_D \sqrt{s \left(\frac{12(1-\omega_{aq})}{\lambda_{aq}(1-\kappa_f)}\right)}\right) + B \sinh\left(\varepsilon y_D \sqrt{s \left(\frac{12(1-\omega_{aq})}{\lambda_{aq}(1-\kappa_f)}\right)}\right) \dots \text{(H-16)}$$

Differentiating with respect to  $y_D$  and using the inner boundary condition, we have:

$$\begin{aligned} \left. \frac{d\overline{p_{aqD}}}{dy_D} \right|_{\varepsilon y_D=0} = 0 = \\ \varepsilon \sqrt{s \left(\frac{12(1-\omega_{aq})}{\lambda_{aq}(1-\kappa_f)}\right)} A \sinh\left(\varepsilon y_D \sqrt{s \left(\frac{12(1-\omega_{aq})}{\lambda_{aq}(1-\kappa_f)}\right)}\right) + \\ \varepsilon \sqrt{s \left(\frac{12(1-\omega_{aq})}{\lambda_{aq}(1-\kappa_f)}\right)} B \cosh\left(\varepsilon y_D \sqrt{s \left(\frac{12(1-\omega_{aq})}{\lambda_{aq}(1-\kappa_f)}\right)}\right) \end{aligned}$$

Since  $\sinh y_D|_{y_D=0} = 0$ , implies:

$$B = 0 \dots \dots \dots \text{(H-17)}$$

Using outer boundary condition and substituting eqn.(H-14c) in eqn.(H-16) we have:

$$\begin{aligned} \overline{p_{fD}} = A \cosh\left(\varepsilon y_D \sqrt{s \left(\frac{12(1-\omega_{aq})}{\lambda_{aq}(1-\kappa_f)}\right)}\right) \Big|_{\varepsilon y_D=1} \\ A = \frac{\overline{p_{fD}}}{\cosh\left(\sqrt{s \left(\frac{12(1-\omega_{aq})}{\lambda_{aq}(1-\kappa_f)}\right)}\right)} \dots \dots \dots \text{(H-18)} \end{aligned}$$

Hence the particular solution for constant rate of eqn.(H-15) in Laplace domain is:

$$\overline{p_{aqD}} = \frac{\overline{p_{fD}}}{\cosh\left(\sqrt{s\left(\frac{12(1-\omega_{aq})}{\lambda_{aq}(1-\kappa_f)}\right)}\right)} \cosh\left(\varepsilon y_D \sqrt{s\left(\frac{12(1-\omega_{aq})}{\lambda_{aq}(1-\kappa_f)}\right)}\right) \dots\dots\dots (H-19)$$

Solution of Matrix (Reservoir)

Substituting  $y_D$  in eqn.(H-5b), we have:

$$\left(\frac{k_{fb} h_{fb}}{\mu_{fb}} + \frac{k_{mb} h_{mb}}{\mu_{mb}}\right) \left(\frac{kh}{\mu}\right)_{mb} \frac{\partial^2 p_{mb}}{\partial z_D^2} = (\varphi_{fb} h_{fb} + \varphi_{mb} h_{mb})(\varphi h)_{mb} c_m \left(\frac{h_{mb}^2}{4}\right) \frac{\partial p_{mb}}{\partial t}$$

Substituting  $p_D$  in above, we have:

$$\left(\frac{k_{fb} h_{fb}}{\mu_{fb}} + \frac{k_{mb} h_{mb}}{\mu_{mb}}\right) \left(\frac{kh}{\mu}\right)_{mb} p_{ch} \frac{\partial^2 (p_{mb} p_{ch} - p_i)}{\partial z_D^2} =$$

$$(\varphi_{fb} h_{fb} + \varphi_{mb} h_{mb}) \times (\varphi h)_{mb} c_m \left(\frac{h_{mb}^2}{4}\right) \frac{\partial (p_{mb} p_{ch} - p_i)}{\partial t}$$

On cancellation of common terms, results in:

$$\left(\frac{kh}{\mu}\right)_{mb} \frac{\partial^2 p_{mbD}}{\partial z_D^2} = \frac{(\varphi_{fb} h_{fb} + \varphi_{mb} h_{mb})}{\left(\frac{k_{fb} h_{fb}}{\mu_{fb}} + \frac{k_{mb} h_{mb}}{\mu_{mb}}\right)} (\varphi h)_{mb} c_m \left(\frac{h_{mb}^2}{4}\right) \frac{\partial p_{mbD}}{\partial t}$$

Reapplying eqn.(H-2) to the above we get:

$$\left( \frac{\frac{k_{mb} h_{mb}}{\mu_{mb}}}{\frac{k_{fb} h_{fb}}{\mu_{fb}} + \frac{k_{mb} h_{mb}}{\mu_{mb}}} \right) \frac{\partial^2 p_{mbD}}{\partial z_D^2} = (\varphi h)_{mb} \frac{(\varphi_{fb} h_{fb} + \varphi_{mb} h_{mb})}{\left( \frac{k_{fb} h_{fb}}{\mu_{fb}} + \frac{k_{mb} h_{mb}}{\mu_{mb}} \right)} c_m \left( \frac{h_{mb}^2}{4} \right) \frac{\partial p_{mbD}}{\partial t}$$

On simplify the above and putting in additional terms we get:

$$\left( \frac{\frac{k_{mb} h_{mb}}{\mu_{mb}}}{\frac{k_{fb} h_{fb}}{\mu_{fb}} + \frac{k_{mb} h_{mb}}{\mu_{mb}}} \right) \frac{\partial^2 p_{mbD}}{\partial z_D^2} = (\varphi h)_{mb} \frac{(\varphi_{fb} h_{fb} + \varphi_{mb} h_{mb})}{\left( \frac{k_{fb} h_{fb}}{\mu_{fb}} + \frac{k_{mb} h_{mb}}{\mu_{mb}} \right)} c_m \left( \frac{h_{mb}^2}{4} \right) \left( \frac{A_{cw}}{A_{cw}} \right) \left( \frac{\frac{\frac{k_{fb}}{\mu_{fb}}}{\frac{k_{fb} h_{fb}}{\mu_{fb}} + \frac{k_{mb} h_{mb}}{\mu_{mb}}}}{\frac{k_{fb}}{\mu_{fb}}} \right) \left( \frac{\frac{\frac{k_{mb}}{\mu_{mb}}}{\frac{k_{fb} h_{fb}}{\mu_{fb}} + \frac{k_{mb} h_{mb}}{\mu_{mb}}}}{\frac{k_{mb}}{\mu_{mb}}} \right) \frac{\partial p_{mbD}}{\partial t} \dots \dots (H-20)$$

Converting this equation into aquifer-fracture domain we get:

$$\left( \frac{\frac{k_{mb} h_{mb}}{\mu_{mb}}}{\frac{k_{fb} h_{fb}}{\mu_{fb}} + \frac{k_{mb} h_{mb}}{\mu_{mb}}} \right) \frac{\partial^2 p_{mbD}}{\partial z_D^2} = (\varphi h)_{mb} \frac{(\varphi_{fb} h_{fb} + \varphi_{mb} h_{mb})}{(\varphi_{fb} h_{fb} + \varphi_{aq} h_{aq})} \frac{\left( \frac{k_{fb} h_{fb}}{\mu_{fb}} + \frac{k_{aq} h_{aq}}{\mu_{aq}} \right)}{\left( \frac{k_{fb} h_{fb}}{\mu_{fb}} + \frac{k_{mb} h_{mb}}{\mu_{mb}} \right)} \frac{(\varphi_{fb} h_{fb} + \varphi_{aq} h_{aq})}{\left( \frac{k_{fb} h_{fb}}{\mu_{fb}} + \frac{k_{aq} h_{aq}}{\mu_{aq}} \right)} c_m \left( \frac{h_{mb}^2}{4} \right) \left( \frac{A_{cw}}{A_{cw}} \right) \times$$

$$\left( \frac{\frac{\frac{k_{fb}}{\mu_{fb}}}{\frac{k_{fb} h_{fb}}{\mu_{fb}} + \frac{k_{mb} h_{mb}}{\mu_{mb}}}}{\frac{k_{fb}}{\mu_{fb}}} \right) \left( \frac{\frac{\frac{k_{mb}}{\mu_{mb}}}{\frac{k_{fb} h_{fb}}{\mu_{fb}} + \frac{k_{mb} h_{mb}}{\mu_{mb}}}}{\frac{k_{mb}}{\mu_{mb}}} \right) \frac{\partial p_{mbD}}{\partial t} \dots \dots \dots (H-21)$$

We also have the following:

$$\omega = \frac{\varphi_{fb} c_f}{(\varphi c_t)_{mb+fb}} \dots\dots\dots (H-22a)$$

$$\Lambda = \left( \frac{\omega_{aq}}{\omega} \right) = \frac{(\varphi_{fb} h_{fb} + \varphi_{mb} h_{mb})}{(\varphi_{fb} h_{fb} + \varphi_{aq} h_{aq})} \dots\dots\dots (H-22b)$$

Substituting  $\omega$  in eqn.(H-9) and assuming compressibility is constant, we have:

$$(1 - \kappa_{fb}) \frac{\partial^2 p_{mbD}}{\partial z_D^2} = \frac{3(1-\omega)}{\lambda} (\Lambda) \left( \frac{\kappa_{fb}}{\kappa_f} \right) \frac{\partial p_{mbD}}{\partial t_D} \dots\dots\dots (H-23)$$

Here dimensionless time and dimensionless interporosity flow parameter and others, are:

$$t_D = \frac{\left( \frac{k_{fb} h_{fb}}{\mu_{fb}} + \frac{k_{aq} h_{aq}}{\mu_{aq}} \right) t}{(\varphi_{fb} h_{fb} + \varphi_{aq} h_{aq}) c_f A_{cw}} = \left( \frac{\kappa_f}{\kappa_{fb}} \right) \left( \frac{1}{\Lambda} \right) t_D \dots\dots\dots (H-24a)$$

$$\lambda = \frac{12}{h_m^2} A_{cw} \frac{\left( \frac{\frac{k_{mb}}{\mu_{mb}}}{\frac{k_{fb} h_{fb}}{\mu_{fb}} + \frac{k_{mb} h_{mb}}{\mu_{mb}}} \right)}{\left( \frac{\frac{k_{fb}}{\mu_{fb}}}{\frac{k_{fb} h_{fb}}{\mu_{fb}} + \frac{k_{mb} h_{mb}}{\mu_{mb}}} \right)} \dots\dots\dots (H-24b)$$

$$\kappa_{fb} = \left( \frac{\frac{k_{fb} h_{fb}}{\mu_{fb}}}{\frac{k_{fb} h_{fb}}{\mu_{fb}} + \frac{k_{aq} h_{aq}}{\mu_{aq}}} \right) \dots\dots\dots (H-24c)$$

$$p_{mbD} = 2\pi \left( \frac{k_{fb} h_{fb}}{\mu_{fb}} + \frac{k_{mb} h_{mb}}{\mu_{mb}} \right) \frac{p_i - p_{mb}}{qB} \dots\dots\dots (H-24d)$$

$$p_{fbD} = 2\pi \left( \frac{k_{fb} h_{fb}}{\mu_{fb}} + \frac{k_{mb} h_{mb}}{\mu_{mb}} \right) \frac{p_i - p_{fb}}{qB} \dots\dots\dots (H-24e)$$

The final form of the above equation, is:

$$\left(\frac{1}{\varepsilon^2}\right) (1 - \kappa_{fb}) \nabla^2 p_{mbD} = \frac{3(1-\omega)}{\lambda} (\Lambda) \left(\frac{\kappa_{fb}}{\kappa_f}\right) \frac{\partial p_{mbD}}{\partial t_D} \dots\dots\dots (H-25)$$

We will find the solution of eqn.(H-13) for  $\overline{p_{aqD}}$  first. For aquifer block and in Laplace domain, the initial and boundary conditions are:

Initial Condition:  $\overline{p_{mbD}}(z_D = 1, s \rightarrow \infty) = 0 \dots\dots\dots (H-26a)$

Inner Boundary Condition:  $\left. \frac{d\overline{p_{mbD}}}{dz_D} \right|_{z_D=0} = 0 \dots\dots\dots (H-26b)$

Outer Boundary Condition:  $\overline{p_{mbD}}|_{z_D=1} = \overline{p_{fbD}} \dots\dots\dots (H-26c)$

Applying the initial condition of aquifer to the Laplace transform equations results in:

$$\left(\frac{1}{\varepsilon^2}\right) (1 - \kappa_f) \frac{\partial^2 \overline{p_{mbD}}}{\partial z_D^2} = \frac{3(1-\omega)}{\lambda} (\Lambda) \left(\frac{\kappa_{fb}}{\kappa_f}\right) \{s\overline{p_{mbD}} - \overline{p_{mbD}}(z_D, 0)\}$$

$$\frac{\partial^2 \overline{p_{mbD}}}{\partial z_D^2} - \varepsilon^2 \left( \frac{3(1-\omega)}{\lambda} (\Lambda) \left(\frac{\kappa_{fb}}{\kappa_f}\right) \right) s\overline{p_{mbD}} = 0 \dots\dots\dots (H-27)$$

The above is a homogeneous partial differential equation with the following general solution:

$$\overline{p}_{mbD} = A \cosh \left( z_D \sqrt{s \left( \frac{3(1-\omega)}{\lambda} (\Lambda) \left( \frac{\kappa_{fb}}{\kappa_f} \right) \right)} \right) + B \sinh \left( z_D \sqrt{s \left( \frac{3(1-\omega)}{\lambda} (\Lambda) \left( \frac{\kappa_{fb}}{\kappa_f} \right) \right)} \right) \dots (H-28)$$

Differentiating with respect to  $z_D$  and using the inner boundary condition, we have:

$$\left. \frac{d\overline{p}_{mbD}}{dz_D} \right|_{z_D=0} = 0 = \sqrt{s \left( \frac{3(1-\omega)}{\lambda} (\Lambda) \left( \frac{\kappa_{fb}}{\kappa_f} \right) \right)} A \sinh \left( z_D \sqrt{s \left( \frac{3(1-\omega)}{\lambda} (\Lambda) \left( \frac{\kappa_{fb}}{\kappa_f} \right) \right)} \right) + \sqrt{s \left( \frac{3(1-\omega)}{\lambda} (\Lambda) \left( \frac{\kappa_{fb}}{\kappa_f} \right) \right)} B \cosh \left( z_D \sqrt{s \left( \frac{3(1-\omega)}{\lambda} (\Lambda) \left( \frac{\kappa_{fb}}{\kappa_f} \right) \right)} \right)$$

Since  $\sinh z_D|_{z_D=0} = 0$ , implies:

$$B = 0 \dots \dots \dots (H-29)$$

Using outer boundary condition and substituting eqn.(H-26c) in eqn.(H-28) we have:

$$\overline{p}_{fbD} = A \cosh \left( z_D \sqrt{s \left( \frac{3(1-\omega)}{\lambda} (\Lambda) \left( \frac{\kappa_{fb}}{\kappa_f} \right) \right)} \right) \Big|_{z_D=1}$$

$$A = \frac{\overline{p}_{fbD}}{\cosh \left( \sqrt{s \left( \frac{3(1-\omega)}{\lambda} (\Lambda) \left( \frac{\kappa_{fb}}{\kappa_f} \right) \right)} \right)} \dots \dots \dots (H-30)$$

Hence the particular solution for constant rate of eqn.(H-27) in Laplace domain is:

$$\overline{p}_{mbD} = \frac{\overline{p}_{fbD}}{\cosh \left( \sqrt{s \left( \frac{3(1-\omega)}{\lambda} (\Lambda) \left( \frac{\kappa_{fb}}{\kappa_f} \right) \right)} \right)} \cosh \left( z_D \sqrt{s \left( \frac{3(1-\omega)}{\lambda} (\Lambda) \left( \frac{\kappa_{fb}}{\kappa_f} \right) \right)} \right) \dots (H-31)$$

Solution of Fracture

There are two different dimensionless pressures. The dimensionless pressure which is reservoir matrix-fracture domain based and dimensionless pressure which is aquifer-fracture domain based. We know dimensionless time measurement is based on latter and this is the reason for normalizing everything on that domain. We have the two equations as:

$$\overline{p_{aqD}} = \frac{\overline{p_{fD}}}{\cosh\left(\sqrt{s\left(\frac{12(1-\omega_{aq})}{\lambda_{aq}(1-\kappa_f)}\right)}\right)} \cosh\left(\varepsilon y_D \sqrt{s\left(\frac{12(1-\omega_{aq})}{\lambda_{aq}(1-\kappa_f)}\right)}\right) \dots\dots\dots (H-19)$$

$$\overline{p_{mbD}} = \frac{\overline{p_{fbD}}}{\cosh\left(\sqrt{s\left(\frac{3(1-\omega)}{\lambda}(\Lambda)\left(\frac{\kappa_{fb}}{\kappa_f}\right)\right)}\right)} \cosh\left(z_D \sqrt{s\left(\frac{3(1-\omega)}{\lambda}(\Lambda)\left(\frac{\kappa_{fb}}{\kappa_f}\right)\right)}\right) \dots (H-31)$$

We also know fracture domains are the same:

$$\frac{\overline{p_{fbD}}}{\left(\frac{k_{fb} h_{fb}}{\mu_{fb}} + \frac{k_{mb} h_{mb}}{\mu_{mb}}\right)} = \frac{\overline{p_{fD}}}{\left(\frac{k_{fb} h_{fb}}{\mu_{fb}} + \frac{k_{aq} h_{aq}}{\mu_{aq}}\right)}$$

$$\overline{p_{fbD}} = \left(\frac{\kappa_{fb}}{\kappa_f}\right) \overline{p_{fD}} \dots\dots\dots (H-32)$$



Again, for the fracture we have:

$$\begin{aligned} & \left( \frac{k_{fb} h_{fb}}{\mu_{fb}} + \frac{k_{aq} h_{aq}}{\mu_{aq}} \right) \left( \frac{kh}{\mu} \right)_{fb} \frac{\partial^2 p_{fb}}{\partial y^2} = \\ & (\varphi_{fb} h_{fb} + \varphi_{aq} h_{aq}) (\varphi h)_{fb} c_f \frac{\partial p_{fb}}{\partial t} - \\ & \left( \frac{1}{\varepsilon} \right) \left( \frac{k_{fb} h_{fb}}{\mu_{fb}} + \frac{k_{aq} h_{aq}}{\mu_{aq}} \right) \left( \frac{kh}{\mu} \right)_{aq} \left( \frac{1}{h^2/2} \right)_{aq} \frac{\partial p_{aq}}{\partial y} \Big|_{y_{aq}=h_{aq}} - \\ & \left( \frac{k_{fb} h_{fb}}{\mu_{fb}} + \frac{k_{mb} h_{mb}}{\mu_{mb}} \right) \left( \frac{kh}{\mu} \right)_{mb} \left( \frac{1}{h^2/2} \right)_{mb} \frac{\partial p_{mb}}{\partial z} \Big|_{z=h_{mb}/2} \dots\dots\dots (H-5a) \end{aligned}$$

Substituting  $y_D$  in eqn.(H-5a), we have:

$$\begin{aligned} & \left( \frac{k_{fb} h_{fb}}{\mu_{fb}} + \frac{k_{aq} h_{aq}}{\mu_{aq}} \right) \left( \frac{kh}{\mu} \right)_{fb} \frac{\partial^2 p_{fb}}{\partial y_D^2} = (\varphi_{fb} h_{fb} + \varphi_{aq} h_{aq}) (\varphi h)_{fb} c_f A_{cw} \frac{\partial p_{fb}}{\partial t} - \\ & \left( \frac{1}{\varepsilon} \right) \left( \frac{k_{fb} h_{fb}}{\mu_{fb}} + \frac{k_{aq} h_{aq}}{\mu_{aq}} \right) \left( \frac{kh}{\mu} \right)_{aq} \left( \frac{A_{cw}}{h^2} \right)_{aq} \frac{\partial p_{aq}}{\partial y} \Big|_{y_{aq}=h_{aq}} - \\ & \left( \frac{k_{fb} h_{fb}}{\mu_{fb}} + \frac{k_{mb} h_{mb}}{\mu_{mb}} \right) \left( \frac{kh}{\mu} \right)_{mb} \left( \frac{A_{cw}}{h^2/2} \right)_{mb} \frac{\partial p_{mb}}{\partial z} \Big|_{z=h_{mb}/2} \end{aligned}$$

Substituting  $p_D$  in eqn.(H-5a), we have:

$$\begin{aligned} & \left( \frac{k_{fb} h_{fb}}{\mu_{fb}} + \frac{k_{aq} h_{aq}}{\mu_{aq}} \right) \left( \frac{kh}{\mu} \right)_{fb} \frac{\partial^2 (p_{fD} p_{ch} - p_i)}{\partial y_D^2} = \\ & (\varphi_{fb} h_{fb} + \varphi_{aq} h_{aq}) \times (\varphi h)_{fb} c_f A_{cw} \frac{\partial (p_{fD} p_{ch} - p_i)}{\partial t} - \left( \frac{1}{\varepsilon} \right) \left( \frac{k_{fb} h_{fb}}{\mu_{fb}} + \frac{k_{aq} h_{aq}}{\mu_{aq}} \right) \times \\ & \left( \frac{kh}{\mu} \right)_{aq} \left( \frac{A_{cw}}{h^2} \right)_{aq} \frac{\partial (p_{aq} p_{ch} - p_i)}{\partial y} \Big|_{y_{aq}=h_{aq}} - \left( \frac{k_{fb} h_{fb}}{\mu_{fb}} + \frac{k_{mb} h_{mb}}{\mu_{mb}} \right) \times \\ & \left( \frac{kh}{\mu} \right)_{mb} \left( \frac{A_{cw}}{h^2/2} \right)_{mb} \frac{\partial (p_{mb} p_{ch} - p_i)}{\partial z} \Big|_{z=h_{mb}/2} \end{aligned}$$

Rearranging and canceling common terms results in:

$$\begin{aligned} \left(\frac{kh}{\mu}\right)_{fb} \frac{\partial^2 p_{fD}}{\partial y_D^2} = \\ (\varphi h)_{fb} \frac{(\varphi_{fb} h_{fb} + \varphi_{aq} h_{aq})}{\left(\frac{k_{fb} h_{fb}}{\mu_{fb}} + \frac{k_{aq} h_{aq}}{\mu_{aq}}\right)} c_f A_{cw} \frac{\partial p_{fD}}{\partial t} - \\ \left(\frac{1}{\varepsilon}\right) \left(\frac{kh}{\mu}\right)_{aq} \left(\frac{A_{cw}}{h^2}\right)_{aq} \frac{\partial p_{aqD}}{\partial y} \Big|_{y_{aq}=h_{aq}} - \\ \frac{\left(\frac{k_{fb} h_{fb}}{\mu_{fb}} + \frac{k_{mb} h_{mb}}{\mu_{mb}}\right)}{\left(\frac{k_{fb} h_{fb}}{\mu_{fb}} + \frac{k_{aq} h_{aq}}{\mu_{aq}}\right)} \left(\frac{kh}{\mu}\right)_{mb} \left(\frac{A_{cw}}{h^2/2}\right)_{mb} \frac{\partial p_{mbD}}{\partial z} \Big|_{z=h_{mb}/2} \end{aligned}$$

Substituting back eqns. (H-2a) to eqn.(H-2h) into the above eqn. we get:

$$\begin{aligned} \left(\frac{\frac{k_{fb} h_{fb}}{\mu_{fb}}}{\frac{k_{fb} h_{fb}}{\mu_{fb}} + \frac{k_{aq} h_{aq}}{\mu_{aq}}}\right) \frac{\partial^2 p_{fD}}{\partial y_D^2} = \left(\frac{\varphi_{fb} h_{fb}}{\varphi_{fb} h_{fb} + \varphi_{aq} h_{aq}}\right) \frac{(\varphi_{fb} h_{fb} + \varphi_{aq} h_{aq})}{\left(\frac{k_{fb} h_{fb}}{\mu_{fb}} + \frac{k_{aq} h_{aq}}{\mu_{aq}}\right)} c_f A_{cw} \frac{\partial p_{fD}}{\partial t} - \\ \left(\frac{1}{\varepsilon}\right) \left(\frac{\frac{k_{aq} h_{aq}}{\mu_{aq}}}{\frac{k_{fb} h_{fb}}{\mu_{fb}} + \frac{k_{aq} h_{aq}}{\mu_{aq}}}\right) \left(\frac{A_{cw}}{h^2}\right)_{aq} \frac{\partial p_{aqD}}{\partial y} \Big|_{y_{aq}=h_{aq}} - \\ \frac{\left(\frac{k_{fb} h_{fb}}{\mu_{fb}} + \frac{k_{mb} h_{mb}}{\mu_{mb}}\right)}{\left(\frac{k_{fb} h_{fb}}{\mu_{fb}} + \frac{k_{aq} h_{aq}}{\mu_{aq}}\right)} \left(\frac{\frac{k_{mb} h_{mb}}{\mu_{mb}}}{\frac{k_{fb} h_{fb}}{\mu_{fb}} + \frac{k_{mb} h_{mb}}{\mu_{mb}}}\right) \left(\frac{A_{cw}}{h^2/2}\right)_{mb} \frac{\partial p_{mbD}}{\partial z} \Big|_{z=h_{mb}/2} \end{aligned}$$

Introducing some additional terms, normalizing other terms and  $h_{fb} = h_{mb}$  we have:

$$\left( \frac{\frac{k_{fb} h_{fb}}{\mu_{fb}}}{\frac{k_{fb} h_{fb}}{\mu_{fb}} + \frac{k_{aq} h_{aq}}{\mu_{aq}}} \right) \frac{\partial^2 p_{fD}}{\partial y_D^2} = \left( \frac{\varphi_{fb} h_{fb}}{\varphi_{fb} h_{fb} + \varphi_{aq} h_{aq}} \right) \left( \frac{\varphi_{fb} h_{fb} + \varphi_{aq} h_{aq}}{\frac{k_{fb} h_{fb}}{\mu_{fb}} + \frac{k_{aq} h_{aq}}{\mu_{aq}}} \right) c_f A_{cw} \frac{\partial p_{fD}}{\partial t} -$$

$$\left( \frac{1}{\varepsilon} \right) \left( \frac{\frac{k_{aq} h_{aq}}{\mu_{aq}}}{\frac{k_{fb} h_{fb}}{\mu_{fb}} + \frac{k_{aq} h_{aq}}{\mu_{aq}}} \right) \left( \frac{A_{cw}}{h^3} \right)_{aq} \frac{\partial p_{aqD}}{\partial y_D} \Big|_{\varepsilon y_D=1} -$$

$$\left( \frac{\frac{k_{fb} h_{fb}}{\mu_{fb}} + \frac{k_{mb} h_{mb}}{\mu_{mb}}}{\frac{k_{fb} h_{fb}}{\mu_{fb}} + \frac{k_{aq} h_{aq}}{\mu_{aq}}} \right) \left( \frac{\frac{k_{fb} h_{fb}}{\mu_{fb}}}{\frac{k_{fb} h_{fb}}{\mu_{fb}}} \right) \left( \frac{\frac{k_{mb} h_{mb}}{\mu_{mb}}}{\frac{k_{fb} h_{fb}}{\mu_{fb}} + \frac{k_{mb} h_{mb}}{\mu_{mb}}} \right) \left( \frac{A_{cw}}{h^3/4} \right)_{mb} \frac{\partial p_{mbD}}{\partial z_D} \Big|_{z_D=1}$$

The resultant form of the governing differential equations are:

$$\kappa_f \frac{\partial^2 p_{fD}}{\partial y_D^2} = \omega_{aq} \frac{\partial p_{fD}}{\partial t} - \left( \frac{1}{\varepsilon} \right) \left( \frac{\lambda_{aq}}{12} \right) \frac{\partial p_{aqD}}{\partial y_D} \Big|_{\varepsilon y_D=1} - \left( \frac{\lambda}{3} \right) (\kappa_f) \frac{\partial p_{mbD}}{\partial z_D} \Big|_{z_D=1}$$

The final form of the governing differential equations is:

$$\nabla^2 p_{fD} = \left( \frac{\omega_{aq}}{\kappa_f} \right) \frac{\partial p_{fD}}{\partial t} - \left( \frac{1}{\varepsilon} \right) \left( \frac{\lambda_{aq}}{12 \kappa_f} \right) \frac{\partial p_{aqD}}{\partial y_D} \Big|_{\varepsilon y_D=1} - \left( \frac{\lambda}{3} \right) \frac{\partial p_{mbD}}{\partial z_D} \Big|_{z_D=1} \dots \text{(H-33)}$$

Taking Laplace transform of the above equation:

$$\frac{d^2 \overline{p_{fD}}}{dy_D^2} = \left( \frac{\omega_{aq}}{\kappa_f} \right) \{s \overline{p_{fD}} - \overline{p_{fD}}(y_D, 0)\} - \left( \frac{1}{\varepsilon} \right) \left( \frac{\lambda_{aq}}{12 \kappa_f} \right) \frac{\partial \overline{p_{aqD}}}{\partial y_D} \Big|_{\varepsilon y_D=1} - \left( \frac{\lambda}{3} \right) \frac{\partial \overline{p_{mbD}}}{\partial z_D} \Big|_{z_D=1} \text{(H-34)}$$

For a closed reservoir the initial and boundary conditions, in Laplace domain, for fracture are:

Initial Condition:  $\overline{p}_{fD}(y_D, s) = 0$ ..... (H-35a)

Inner Boundary Condition:  $\left. \frac{d\overline{p}_{fD}}{dy_D} \right|_{y_D=0} = -\frac{2\pi}{s}$ ..... (H-35b)

Outer Boundary Condition:  $\left. \frac{d\overline{p}_{fD}}{dy_D} \right|_{y_D=y_{De}} = 0$ ..... (H-35c)

Applying initial condition, we have:

$$\frac{d^2\overline{p}_{fD}}{dy_D^2} = \left(\frac{\omega_{aq}}{\kappa_f}\right) \{s\overline{p}_{fD}\} - \left(\frac{1}{\varepsilon}\right) \left(\frac{\lambda_{aq}}{12\kappa_f}\right) \left. \frac{\partial\overline{p}_{aqD}}{\partial y_D} \right|_{\varepsilon y_D=1} - \left(\frac{\lambda}{3}\right) \left. \frac{\partial\overline{p}_{mbD}}{\partial z_D} \right|_{z_D=1} \dots\dots\dots (H-36)$$

But from eqn.(H-31) we have:

$$\left. \frac{\partial\overline{p}_{mbD}}{\partial z_D} \right|_{z_D=1} = \frac{\sqrt{s\left(\frac{3(1-\omega)}{\lambda}(\Lambda)\left(\frac{\kappa_{fb}}{\kappa_f}\right)\right)}}{\cosh\left(\sqrt{s\left(\frac{3(1-\omega)}{\lambda}(\Lambda)\left(\frac{\kappa_{fb}}{\kappa_f}\right)\right)}\right)} \sinh\left(\sqrt{s\left(\frac{3(1-\omega)}{\lambda}(\Lambda)\left(\frac{\kappa_{fb}}{\kappa_f}\right)\right)}\right) \overline{p}_{fbD}$$

And from eqn.(H-19) we have

$$\left. \frac{\partial \overline{p_{aqD}}}{\partial y_D} \right|_{\varepsilon y_D=1} = \frac{\varepsilon \sqrt{s \left( \frac{12(1-\omega_{aq})}{\lambda_{aq}(1-\kappa_f)} \right)}}{\cosh \left( \sqrt{s \left( \frac{12(1-\omega_{aq})}{\lambda_{aq}(1-\kappa_f)} \right)} \right)} \sinh \left( \sqrt{s \left( \frac{12(1-\omega_{aq})}{\lambda_{aq}(1-\kappa_f)} \right)} \right) \overline{p_{fD}}$$

This derivative will change sign when expressed in terms of  $\overline{p_{fD}}$ , and using eqn.(H-34)

we have:

$$\begin{aligned} \frac{d^2 \overline{p_{fD}}}{dy_D^2} &= \left( \frac{\omega_{aq}}{\kappa_f} \right) \{s \overline{p_{fD}}\} + \left( \frac{\lambda_{aq}}{12 \kappa_f} \right) \sqrt{s \left( \frac{12(1-\omega_{aq})}{\lambda_{aq}(1-\kappa_f)} \right)} \tanh \left( \sqrt{s \left( \frac{12(1-\omega_{aq})}{\lambda_{aq}(1-\kappa_f)} \right)} \right) \overline{p_{fD}} + \\ &\left( \frac{\lambda}{3} \right) \sqrt{s \left( \frac{3(1-\omega)}{\lambda} (\Lambda) \left( \frac{\kappa_{fb}}{\kappa_f} \right) \right)} \tanh \left( \sqrt{s \left( \frac{3(1-\omega)}{\lambda} (\Lambda) \left( \frac{\kappa_{fb}}{\kappa_f} \right) \right)} \right) \overline{p_{fbD}} \end{aligned}$$

Using eqn.(H-32), converting everything into consistent aquifer-fracture domain, we

have:

$$\begin{aligned} \frac{d^2 \overline{p_{fD}}}{dy_D^2} &= \\ &\left[ \left( \frac{\omega_{aq}}{\kappa_f} \right) + \left( \frac{\lambda_{aq}}{12 s \kappa_f} \right) \sqrt{s \left( \frac{12(1-\omega_{aq})}{\lambda_{aq}(1-\kappa_f)} \right)} \tanh \left( \sqrt{s \left( \frac{12(1-\omega_{aq})}{\lambda_{aq}(1-\kappa_f)} \right)} \right) + \right. \\ &\left. \left( \frac{\lambda}{3 s} \right) \sqrt{s \left( \frac{3(1-\omega)}{\lambda} (\Lambda) \left( \frac{\kappa_{fb}}{\kappa_f} \right) \right)} \tanh \left( \sqrt{s \left( \frac{3(1-\omega)}{\lambda} (\Lambda) \left( \frac{\kappa_{fb}}{\kappa_f} \right) \right)} \right) \right] \{s \overline{p_{fD}}\} \dots \dots \text{(H-37)} \end{aligned}$$

This is of the form:

$$\frac{d^2 \overline{p_{fD}}}{dy_D^2} - sf(s) \overline{p_{fD}} = 0 \dots\dots\dots (H-38)$$

Where,

$$f(s) = \left[ \left( \frac{\omega_{aq}}{\kappa_f} \right) + \left( \frac{\lambda}{3s} \right) \sqrt{s \left( \frac{3(1-\omega)}{\lambda} (\Lambda) \left( \frac{\kappa_{fb}}{\kappa_f} \right) \right)} \tanh \left( \sqrt{s \left( \frac{3(1-\omega)}{\lambda} (\Lambda) \left( \frac{\kappa_{fb}}{\kappa_f} \right) \right)} \right) + \left( \frac{\lambda_{aq}}{12 s \kappa_f} \right) \sqrt{s \left( \frac{12(1-\omega_{aq})}{\lambda_{aq}(1-\kappa_f)} \right)} \tanh \left( \sqrt{s \left( \frac{12(1-\omega_{aq})}{\lambda_{aq}(1-\kappa_f)} \right)} \right) \right] \dots\dots\dots (H-39a)$$

\

$$f(s) = \omega \left[ \left( \frac{\omega_{aq}}{\omega \kappa_f} \right) + \left( \frac{1}{3s} \right) \left( \frac{\lambda}{\omega} \right) \sqrt{3s \left( \frac{1-\omega}{\omega} \right) (\Lambda) \left( \frac{\kappa_{fb}}{\kappa_f} \right) \left( \frac{\omega}{\lambda} \right)} \times \tanh \left( \sqrt{3s \left( \frac{1-\omega}{\omega} \right) (\Lambda) \left( \frac{\kappa_{fb}}{\kappa_f} \right) \left( \frac{\omega}{\lambda} \right)} \right) \right] + \left( \frac{\lambda_{aq}}{12 s \kappa_f} \right) \sqrt{s \left( \frac{12(1-\omega_{aq})}{\lambda_{aq}(1-\kappa_f)} \right)} \tanh \left( \sqrt{s \left( \frac{12(1-\omega_{aq})}{\lambda_{aq}(1-\kappa_f)} \right)} \right) \dots\dots\dots (H-39b)$$

Eqn.(H-38) is a homogeneous partial differential equation which is the same as eqn.(A-17). Refer to Appendix A for the rest of the derivation.